Novel Genotoxins that Target Estrogen Receptor- and Androgen Receptor- Positive Cancers: Identification of DNA Adducts, Pharmacokinetics, and Mechanism.

By

Shawn M. Hillier

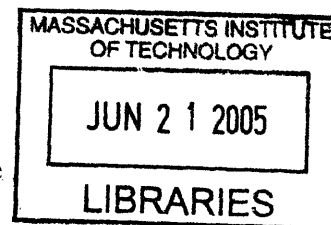B.A. Chemistry
College of the Holy Cross, 1997

SUBMITTED TO THE DEPARTMENT OF CHEMISTRY IN PARTIAL
FULLFILLMENT OF THE REQUIREMENTS FOR THE DEGREE OF

DOCTORATE OF PHILOSOPHY
AT THE
MASSACHUSETTS INSTITUTE OF TECHNOLOGY

June 2005

Signature of Author: _____
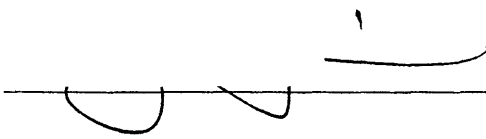Department of Chemistry
April 13, 2005

Certified by: _____
John M. Essigmann
Professor of Chemistry
Thesis Supervisor

Accepted by: _____
Robert W. Field
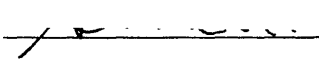Chairman, Departmental Committee on Graduate Students

Thesis Committee:

Reviewed by: _____
John M. Essigmann
Professor of Chemistry
Thesis Advisor

Reviewed by: _____
Steven R. Tannenbaum
Professor of Chemistry
Thesis Committee Chairman

Reviewed by: _____
Catherine L. Drennan
Professor of Chemistry
Thesis Committee Member

Reviewed by: _____
Gerald N. Wogan
Emeritus Professor of Chemistry
Thesis Committee Member

Novel Genotoxins that Target Estrogen Receptor- and Androgen Receptor- Positive Cancers: Identification of DNA Adducts, Pharmacokinetics, and Mechanism.

By

Shawn M. Hillier

Submitted to the Department of Chemistry on April 13, 2005
in Partial Fulfillment of the Requirements for
the Degree of Doctorate of Philosophy in Chemistry.

Abstract

We have designed and synthesized novel molecules capable of selectively killing tumor cells that aberrantly express steroid hormone receptors. Many human breast cancers express high levels of the estrogen receptor (ER), and most prostate cancers express the androgen receptor (AR). We reasoned that the potential genotoxic effect of DNA adducts would be increased in target cells if these adducts were camouflaged by their association with receptor proteins. This association could shield the DNA adducts from repair proteins and thus increase the toxicity towards a tumor cell. Furthermore, these hormone receptors are transcription factors and an interaction between the protein and the DNA adduct could disrupt cellular signaling events, thus leading to further toxicity.

We have synthesized bifunctional agents that contain an aniline mustard linked to ligands for tumor specific hormone receptors. To target ER(+) breast cancers, an aniline mustard was linked to estradiol at the 7α position (E2-7α), and to target AR(+) prostate cancer, the aniline mustard was linked to estradien-3-one at the 11β position (11β). Competitive binding experiments show that E2-7α and 11β compete well with the natural ligands for the ER and AR, respectively. Clonal survival studies have shown that hormone receptor expressing malignant cell lines are more sensitive to our compounds than a corresponding receptor deficient line.

$[^{14}C]$-E2-7α and $[^{14}C]$-11β have been formulated in Cremophor-EL and exhibit good bioavailability and stability when injected into mice intraperitoneally. E2-7α inhibits the growth of ER(+) HeLa cells and 11β inhibits the growth of AR(+) LNCaP cells, both in xenograft mouse models. The compounds are well tolerated by mice after the therapeutic regimens. Stable DNA adducts have been isolated and detected by electrospray mass spectrometry and accelerator mass spectrometry has provided us with a means of quantifying the number of DNA adducts formed *in vivo*. E2-7α DNA adducts are repaired, in part, by nucleotide excision repair but the adducts persist longer in ER(+) cells than in ER(-) ones. Melphalan adducts, however, are repaired with equal rates in

both cell lines. This result provides evidence in support of the repair shielding hypothesis and suggests that it may be a contributing mechanism to the increased toxicity observed for the ER(+) cell line in the clonal survival study.

Supervisor: John M. Essigmann
Title: Professor of Chemistry

Acknowledgements

I would like to thank my advisor, John Essigmann, for his guidance and support during my tenure as a graduate student. He has filled his lab with hard-working, intelligent individuals who are also compassionate, generous, and friendly. I credit these attributes of my labmates to John and am grateful that he has provided an environment well suited for collaborative learning. John's dedication to his classroom teaching has translated into the lab with a zest for perfection in oral and written presentations and my skills have sharpened in these areas as a consequence. Two major life altering events occurred while I was a member of John's lab – my marriage and birth of my first son. I am especially thankful for John's understanding and support, not only in science and my education, but also in my personal life.

I would also like to thank my thesis committee members Steven Tannenbaum, Gerald Wogan, and Catherine Drennan for their advice and insight. I am especially indebted to Steve for finding the holes in my research and suggesting ways of addressing them. Through our collaborations we have discovered a great many details about my project that otherwise would still be unanswered. I would like to thank Pete Wishnok, Paul Skipper, and Rosa Liberman (of the Tannenbaum Laboratory) for their help with the mass spectrometry aspects of my project. I am also grateful to Professor Rick Wood for his assistance and advice in understanding the role that NER plays in the repair of DNA adducts formed by E2-7α. He and Tanaka Kuraoka have kindly supplied XPA protein and XPA antibody, and for that I am very thankful. I am also appreciative for our collaboration with Ram Sasisekharan's Laboratory, especially Shiladitya Sengupta and Sujan Rafiul Kabir, for assisting in our efforts to develop new delivery vehicles for our compounds.

I would like to thank Daniel Nedelcu, a very talented undergraduate, who worked with me in determining the partition coefficient of our molecules. His dedication to the project was unparalleled and his intellectual curiosity kept me on my toes. I wish him the very best in his future endeavors.

I would like to thank the World Champion Boston Red Sox for an amazing come back in the American League Division Series against the loathsome Yankees. My son was only a couple weeks old at the time, and we loved watching the games together. Thank you for breaking the "curse" and making Boston a happier place to live.

After 5 and a half years working towards my doctorate degree, I have worked with over 30 graduate students and post-docs in the Essigmann Laboratory. I am pleased to say they are all my friends and they have all made my graduate career more enjoyable. I am especially indebted to the Fatal Engineering Team. We are a close knit group who must efficiently communicate, collaborate, and design future experiments. We have worked (almost) flawlessly together and have always found time to discuss our endeavors outside the lab. I will miss our interactions. Bob Croy, the leader of the Fatal Engineering Team, has been a wonderful mentor in the laboratory and has guided me with experimental design, troubleshooting, and further understanding of the literature.

John Marquis has been a great friend and colleague, and although I will not necessarily miss our long AMS experiments, I will miss our conversations (and occasional griping) on world affairs, traffic getting into Cambridge, and pretty much anything else. I would like to thank Hyun-Ju Park for teaching me how to set up and run repair reactions and for having a good sense of humor when I too often failed. I would like to thank Kim Bond Schaefer for her patience, kindness, and administrative assistance. I am also grateful for the interactions I had with Kaushik Mitra and Beatrice Zayas and I appreciate their contributions in making my project more successful. I am eternally grateful to Kyle Proffitt and Will Neeley for undergoing the painstaking task of editing my thesis. Your edits were fantastic and I know this work is much better because of you both. Peter Rye was a great classmate, friend, and converted computer geek who I could always rely on for help or a fun night at the Muddy. To Uday, Maryann, Aida, Jim, Zoran, Yuri, Jen, and Charles, I appreciate our conversations about science, but even more so, the ones about life and its amusements that always made the long days pass quickly. I am also proud to point out that Yuri, Charles, and I are members of the reigning champion volleyball team in the Chemistry Department's Summer League.

I would like to thank my friends outside of the lab who have always asked, "When are you going to graduate?" Nel, Ku, and Luke, you challenged me in college to excel and now you continue to keep me on my toes with quick retorts for your sarcastic wits. Jay, Al, Kathy, Kristen, Cory, Chris, Amy, Carey, Katy, Tim, Chris, and Michelle you have encouraged me, supported me, and made me laugh. Tracey, Eric, John, and Donna are the best in-laws I could have ever hoped for. I am especially thankful for the help that Michelle, Donna, Kristina, and Tracey have given me in caring for my son, Ryan, while I was busy writing my thesis.

For teaching me the importance of an education I am especially thankful for my grandparents – Vovô, Vovó, Nana, and Gramps. Your love and constant reminding is the biggest reason I accomplished what I have. I would like to thank my family in Portugal, especially Tía Olga, Tío Jó, Cila, Bela, Mario, Gonçalo, and Inez, not only for Euro Cup 2004 Finals tickets, but for the love and fantastic times we have shared even though we do not always speak the same language. Adam, you were my best man and godfather to Ryan, but you always will be my best friend. Mom and Dad, no words can ever express my undying gratitude for your unconditional love and support throughout the years. Whether it was a little league game when I sat the bench with a broken arm or my college graduation, you have always been there cheering me on. For now, thank you!

Most importantly, I would like to thank my beautiful wife, Kristen, for all of her love and support. You have provided for us financially, emotionally, and a few months ago with the most beautiful baby boy, Ryan. During those middle years when things looked the darkest, you kept my head up, encouraged me to keep at it, and told me that the day would come. Now that the day is almost here, it is as much your day as it is mine. I could not have done it without you and I will forever be grateful. And to our son Ryan, whenever I had a headache from long hours of writing, I could always count on you for that wonderful smile to ease my pain. In your own way, you have made my writing so much easier. I will never be able to thank you both enough!!

This thesis is dedicated to my friends and family who have succumbed to cancer:

Vovó
Nana
Jenny Valente
Nancy Correia
CJ Crooks

And to those who have not given up the fight:

Luke Dunivant
Jasmine Monteiro
Rosemary Domingos
Cecile Oliver

Table of Contents

List of Equations

List of Tables

List of Figures

List of Abbreviations

11β	11β-(17βOH-estradien-Δ4(5),9(10)-3-one)-C6NC2-mustard
AF-1 (-2)	activation function 1 (or 2)
ALT	alanine aminotransferase
AMS	accelerator mass spectrometry
AP	apyrimidinic/apurinic sites
AR	androgen receptor
AST	aspartate aminotransferase
AUC	area under the curve
BER	base excision repair
BRCA 1	breast cancer susceptibility gene 1
BRCA2	breast cancer susceptibility gene 2
BUN	blood urea nitrogen
Cdk	cyclin-dependent kinase
CID	collision induced decay
CL	clearance
Cmax	maximum concentration
CPM	counts per minute
CR-EL	Cremephor-EL
DBD	DNA binding domain
DNA	deoxyribonucleic acid
E2-7α	E2-7α-C6NC2-mustard
EGFR	epidermal growth factor receptor
ELAC2	*Escherichia coli* elaC homolog
ER	estrogen receptor
ER-LBD	estrogen receptor ligand binding domain
ESI-MS	electrospray ionization mass spectrometry
GR	glucocorticoid receptor
Her-2/ErbB2	human epidermal growth factor 2
HMG	high mobility group

HRBC	hormone resistant breast cancer
HRPC	hormone resistant prostate cancer
HRE	hormone response element
hUBF	human upstream binding factor
IL-6	interleukin 6
IP	intraperitoneal
IV	intravenous
kDa	kilodalton
Kd	dissociation constant
LBD	ligand binding domain
LD_{50}	lethal dose at which 50 % of the animals die
Mdm2	murine double minute 2
MPG	3-methyladenine DNA glycosylase
MSR1	macrophage scavenger receptor 1
NCI	National Cancer Institute
NER	nucleotide excision repair
PARP	poly-ADP ribose polymerase
PSA	prostate specific antigen
PTEN	phosphatase and tensin homolog
RBA	relative binding affinity
RNASEL	2'-5'-oligoadnylate-dependent ribonuclease L
siRNA	short interfering ribonucleic acid
SRC-1	steroid receptor coactivator 1
STK11/LKB1	serine/threonine protein kinase 11
Sub-Q	sub-cutaneous
t ½	half-life
TE	Tris-HCl/EDTA buffer
Vd	volume of distribution
VEGF	vascular endothelial growth factor
XPA	xeroderma pigmentosum compliment group A
% ID/g	percent injected dose per gram

Chapter 1

Introduction

Cancer

Cancer is a multifaceted disease with approximately 100 subtypes, all characterized by excessive, uncontrolled growth of abnormal cells that invade and destroy other tissues. (Hanahan and Weinberg 2000). Cancer can develop in almost any organ or tissue of the body and is the second leading cause of death in the U.S. (Cancer Facts and Figures 2005) As a result of better treatment options, over 60% of Americans with the disease live longer than five years. The exact causes of cancer are still unknown, although epidemiological studies have implicated several risk factors including: increased age, obesity, a high salt or fatty diet, and chronic exposure to carcinogens, radiation, environmental or occupational chemicals, and tobacco smoke. Furthermore, exposure to pathogens (certain viruses, bacteria, and parasites), hereditary factors (genetic mutations in proto-oncogenes) and steroid hormones (especially prolonged exposure to estrogen) has also been implicated. The five most common types of cancer in the U.S. are prostate cancer (232,000/yr), breast cancer (212,000 new cases per year), lung cancer (172,000/yr), colorectal cancer (144,000/yr), and lymphoma (64,000/yr) (Cancer Facts and Figures 2005). (Note: Although there are over a million new cases of skin cancer diagnosed each year, the 2005 Cancer Facts and Figures report does not include nonmelanoma skin cancers. There will be an estimated 59,000 new cases of melanoma in 2005.)

After decades of research, a complex body of work has been established revealing cancer to be a disease involving dynamic changes in the genome. The foundation has been set in the discovery of mutations that produce oncogenes with gain of function and inactivate tumor suppressor genes with loss of function (Hanahan and Weinberg 2000). Several lines of evidence indicate that tumorigenesis is a multistep process and that these distinct steps reflect genetic alterations that drive the progression of normal cells to malignant ones. Although the disease can afflict people of all ages, most types are diagnosed with an age-dependent incidence implicating four to seven rate-limiting steps (Renan 1993). Additionally, pathological analyses of a number of organ sites reveal lesions that appear to represent the intermediate steps in a process through which normal cells progressively evolve into malignant invasive cancers (Foulds 1954).

Hanahan and Weinberg suggest that the vast array of cancer cell genotypes is a manifestation of six essential alterations in cell physiology that collectively dictate malignant growth:

1. Self-sufficiency in growth signals: Cancer cells show a reduced dependence on exogenous growth signals for proliferation. The tumor cells generate many of their own growth signals and reduce their dependence on stimulation from the normal tissue microenvironment by overexpressing pro-growth factor receptors, by becoming hyperresponsive to the growth factors, or by altering the downstream cytoplasmic circuitry that responds to ligand activated receptors (Aaronson et al. 1993; Di Fiore et al. 1987).

2. Insensitivity to antigrowth signals: Normal cells use antigrowth signals to maintain cellular quiescence and tissue homeostasis. However, malignant cells acquire insensitivity to the antigrowth signals most likely somewhere along the retinoblastoma protein pathway, thought to be the main antiproliferative signaling pathway (Weinberg 1995).

3. Ability to evade apoptosis: The apoptotic machinery includes sensors which monitor the cellular environment for conditions that influence whether a cell should live or die, and effectors that act on the signals from the sensors. Resistance to apoptosis can be achieved by many mechanisms. Most notably, the DNA damage sensor and proapoptotic regulator, p53, is mutated in more than 50% of human cancers (Harris 1996).

4. Limitless replicative potential: Independent of the cell-cell signaling pathways described above, an intrinsic cellular program limits the ability of many, if not all, cells to multiply. One way cancer cells overcome this limitation is by expressing the protein telomerase, which adds hexanucleotide repeats onto the ends of chromosomes thereby thwarting the cells' natural shortening of telomeres (the ends of chromosomal DNA) (Bryan and Cech 1999). The (normal) progressive shortening of telomeres with each successive replication results in the inability of DNA polymerases to completely replicate the 3' ends of chromosomal DNA during S phase of the cell cycle and eventually in end-to-end fusion of the chromosomes resulting in karyotypic disarray and inevitably cell death.

5. Sustained angiogenesis: Cells within aberrant proliferative lesions initially lack angiogenic (new vascular growth) ability, but in order to further progress, tumors must acquire angiogenic ability to obtain the nutrients and oxygen crucial for cell function and survival (Hanahan and Folkman 1996). Tumors appear to activate blood vessel formation by changing the balance between angiogenesis inducers and repressors. For example, vascular endothelial growth factor (VEGF) has been shown to be upregulated in many tumors and is the target of several anticancer drugs including the recently FDA approved Avastin.

6. Tissue invasion and metastasis: Eventually the primary tumor travels through the blood stream or lymphatic system to settle in a distant site in the body. These metastases are the cause of 90% of cancer deaths (Sporn 1996). Often, alterations in cell-cell adhesion molecules (immunoglobulins and calcium-dependent cadherin proteins) and disruption in cell-environment interactions (by integrins) allow for tumor cells to break free from the extracellular environment and invade normal tissue at distant sites. For example, E-cadherin function is lost in many epithelial cancers by mechanisms involving mutational inactivation of the E-cadherin or β-catenin genes, transcriptional repression, or proteolysis of the extracellular cadherin domain (Christofori and Semb 1999). E-cadherin normally makes intercellular contacts with β-catenin to transmit antigrowth and other signals.

The paths by which cells become malignant are highly variable. Mutations in certain oncogenes and tumor suppressor genes can occur early in some tumor progression pathways, but late in others. A specific genetic mutation may contribute only partially to the acquisition of a single capability, whereas another genetic mutation may aid in the simultaneous acquisition of several distinct capabilities. As a consequence, the acquisition of the six biological alterations described above does not follow a linear sequence, but rather the summation of these events eventually leads to invasive cancer (Hanahan and Weinberg 2000).

Unfortunately for patients, there are few available screens that can readily detect these acquired physiological alterations at the molecular level. However, some cancers

can be screened for specific markers or visual evidence. For example, prostate specific antigen (PSA) is elevated in men with prostate cancer, mammography can visualize breast cancer, and colonoscopy is used to detect polyps and colorectal cancer. Other cancers that have ample space to grow, such as ovarian, are considered silent killers since the tumor usually does not manifest until it is quite large. In many cases, patients only present with cancer at later stages when the malignancies cause some sort of discomfort. Therefore it is imperative that patients are monitored by physicians routinely, especially as they age, and that they inform their physicians of any signs of lethargy or discomfort.

The earlier a patient is diagnosed with cancer, the better the prognostic outcome. There are several options for treatment depending on the disease, but many cancers are at least eradicated with surgical removal of the malignancy. In order to ensure the removal of the entire primary cancer and all micrometastases, oncologists often follow up with radiation therapy, chemotherapy, hormone therapy, and/or immunotherapy. Researchers have shown that combinations of these therapies often results in the best outcome. For example, the chemotherapeutic cisplatin successfully cures 95% of patients afflicted with testicular cancer, typically in combination with etoposide and bleomycin (Feuer, Brown, and Kaplan 1993; Kartalou and Essigmann 2001b). However, the cruel reality is that cancer is a very lethal disease and despite the efforts of thousands of researchers and millions of dollars, much work still needs to be completed in order to better treat cancer patients. The work described here will focus on two novel anticancer agents that target breast and prostate cancers.

Breast Cancer

Breast cancer is the most frequent malignancy among women in the US, accounting for 30% of all cancers diagnosed, (Greenlee et al. 2000) with an incidence of 135 cases per 100,000 women and a death rate of 27.7 per 100,000 women (Weir et al. 2003). The increasing rate of breast cancer incidence and simultaneous decreasing rate in mortality that has been reported in the 1990's can, in part, be attributed to increased mammography screening (Edwards et al. 2002; Howe et al. 2001; Wingo et al. 1998). Screening mammography is currently the best available tool for early detection and reduces mortality rates by 16-30 percent (Kerlikowske 1997).

Screening mammography is especially important in women with a family history of breast cancer. About 10% of breast cancer patients have a familial form of the disease, and of these, about half have inherited mutations in the breast cancer susceptibility genes BRCA1 and BRCA2. BRCA1 and BRCA2 are involved in the repair of oxidative DNA damage and DNA damage from ionizing radiation (Chen et al. 1999; Chen, Lee, and Chew 1999). The remaining half of patients with the familial form of the disease are thought to have mutations in the p53 tumor suppressor (Malkin et al. 1990), the STK/LKB1 protein kinase (Shen et al. 2002), the PTEN phosphatase (Nelen et al. 1996), or other genes as yet undiscovered (Easton 1999). In addition to familial inheritance through genetic mutations, other risk factors include increased hormone exposure with early menarche or late menopause, alcohol consumption, postmenopausal obesity, and hormonal replacement therapy. A decreased risk can be attributed to young age at first pregnancy, prolonged lactation, and physical exercise (Baselga and Norton 2002). Especially for those with a high risk of breast cancer, early detection of the disease is a priority since cure rates are greater the earlier the clinical stage at diagnosis. Clinical signs and symptoms of breast cancer depend largely on whether the disease has metastasized. The most common sites of metastases include the skin, lymph nodes, bone, lung, liver, and central nervous system. The evaluation of a patient at presentation of the disease includes a pathological examination of the tumor and an evaluation of the extent of the disease. The pathological examination includes assessment of histological type, size, and grade of the tumor as well as estrogen receptor (ER) and human epidermal growth factor receptor 2 (Her-2) status (Baselga and Norton 2002).

Her-2, also known as ErbB2, is a transmembrane tyrosine kinase receptor in the epidermal growth factor receptor family and is an essential breast cancer oncogene. Amplification of Her-2 occurs in 30% of early stage breast cancers, and a significant correlation between Her-2 overexpression and reduced survival of breast cancer patients has been found (Lohrisch and Piccart 2001). Her-2 overexpression correlates with a lack of response to endocrine and chemotherapy (Bange, Zwick, and Ullrich 2001). In 1998, the biotechnology company Genentech developed the monoclonal antibody Herceptin (trastuzumab) as a therapy for the 15-30% of patients with metastatic breast cancer whose tumors have gene amplification of Her-2. Herceptin inhibits tumor cell proliferation by

downregulating Her-2 protein receptors upon attaching to the protein on the cell surface and facilitates antibody-dependent cell-mediated cytotoxicity by attracting natural killer cells to the Herceptin/Her-2 complex on the cell surface (Sliwkowski et al. 1999). Additionally, Herceptin is used in combination with conventional chemotherapeutics, especially paclitaxel, and has been shown to improve the duration of response and median survival time by 25% compared to chemotherapy alone (Baselga 2001; Slamon et al. 2001).

Despite the advances in genomics-based therapeutics, most women still undergo surgery, either lumpectomy or mastectomy, followed by radiation as a result of the small portion of the patient population that qualifies for therapies like Herceptin. Systemic adjuvant therapies designed to eradicate clinically undetectable cancer cells that may have spread from the primary tumor are necessary to decrease reoccurrences and improve survival. Adjuvant therapies include endocrine therapy, usually tamoxifen or raloxifene, or chemotherapy, most often as a combination of alkylating agents (e.g. cyclophosphamide), anthracyclins (e.g. doxorubicin), antimetabolites, (e.g. 5-flurouracil), and antimicrotubule agents (e.g. paclitaxel).

The decision to use chemotherapy or hormone therapy depends on the presence or absence of the ER in the primary tumor. Approximately half of breast cancers overexpress the ER (Ferno et al. 1990). The anti-estrogens, tamoxifen and raloxifene, reduce the incidence of cancer relapse in ER-expressing tumors and can even delay or prevent the development of breast cancer in women at high risk (Peto and Mack 2000). These compounds antagonize the effects of estrogen and therefore put tumor cells into a state of stasis, which can eventually lead to apoptosis (programmed cell death) (Lerner and Jordan 1990; Obrero, Yu, and Shapiro 2002). Hormonal therapy can be extended over long periods in which the ER+ tumors are often held in check. However, the long term effectiveness of such therapies is complicated by the development of hormone resistant breast cancer (HRBC) (Katzenellenbogen 1991) and possible carcinogenesis (Jordan 1995; Osborne et al. 1996). Additionally, ovarian tumors that express the ER do not respond well to endocrine therapy. Therefore, a need exists for more effective agents to target ovarian tumors and HRBC.

The current trend in pharmaceutical research is to target smaller patient populations with very specific targets. Herceptin is one such example of a very effective compound that targets only one third of those afflicted with breast cancer. The work described here will discuss the design and efficacy of a compound targeting all breast and ovarian cancers that express the ER.

Prostate Cancer

Prostate cancer is the most frequent cancer among males in the U.S. with an incidence of 170.1 cases per 100,000 men and a death rate of 32.9 per 100,000 men (Weir et al. 2003). Prostate cancer mortality has been declining since 1993 as the frequency of serum testing for PSA has increased. PSA is a glycoprotein secreted into the blood by prostatic epithelial cells and is elevated in most men with prostate cancer. The decline in mortality correlates with the observed decrease in the incidence of late-stage prostate cancer after 1992 and the introduction of PSA screening in a population which had little or no screening (Hankey et al. 1999).

As in the case of breast cancer, early detection is often the best gauge for prognostic outcome. PSA screenings often begin at the age of 40 to establish a baseline level. By the age of 50, the American Cancer Association recommends digital rectal exams and PSA testing annually in an effort to detect prostate cancer at its earliest stage (Smith et al. 2001). Early-stage prostate cancer is often asymptomatic but occasionally causes urethral obstruction leading to difficulty in urination, smaller stream, and frequent and less forceful urination. Although preneoplastic lesions can be found in men in their twenties and are frequent in men by their fifties (Sakr et al. 1993), clinically detectable prostate cancer does not generally manifest until the age of 60 or 70. The morphological changes associated with initiation are relatively common and occur early in life; however, progression to invasive carcinoma is significantly less common and occurs in a more limited population later in life (Abate-Shen and Shen 2000). Therefore, it is not surprising that one of the major risk factors for prostate cancer is aging, although the reason for this is not clearly understood (Sakr et al. 1993).

A positive family history of the disease is also among the strongest epidemiological risk factors (Simard et al. 2003). To date, three familial susceptibility

genes have been described: *Escherichia coli* elaC homolog (ELAC2) (Tavtigian et al. 2001), 2'-5'-oligoadenylate-dependent ribonuclease L (RNASEL) (Carpten et al. 2002), and macrophage scavenger receptor 1 (MSR1) (Xu et al. 2002). Although more has been learned about the function of ELAC2, RNASEL, and MSR1 in recent years, the mechanism linking mutations in these genes to prostate carcinogenesis has yet to be determined. It is also of interest that a significant percentage of men with early-onset prostate cancer (≤ 55) harbor germline mutations in the BRCA2 gene (Edwards et al. 2003; Gayther et al. 2000). Oliveira and Lopes from the beautiful city of Porto, Portugal, have shown that genetic polymorphisms in the androgen receptor (AR) and ER are associated with disease progression and metastasis (Medeiros et al. 2003). While still controversial, there is some evidence that dietary and environmental factors may exert a role in prostate carcinogenesis as the incidence is much higher in the United States than in most other countries, particularly those in Asia (Carter, Carter, and Isaacs 1990; Dhom 1983).

As research continues on the epidemiology and molecular biology of prostate cancer, clinicians still struggle to treat some forms of the disease. In its initial stages, prostate cancer is essentially curable by surgical intervention and/or radiation therapy. In addition, most cases of prostate carcinoma are relatively indolent, such that the majority of men diagnosed with the disease will die instead of other causes. However, if not detected early, or in more aggressive forms of the disease, prostate cancer can advance to stages characterized by local invasion of the seminal vesicles, followed by metastasis primarily to the bone (Abate-Shen and Shen 2000). Metastasis to the lung, lymph nodes, and liver are also common. The transition to metastatic disease is generally followed by a shift from androgen dependence to androgen-independence, which is often provoked by androgen-ablation therapy.

In 1941, Huggins and Hodges published a report in Cancer Research showing that castration, over the short term, caused regression in androgen-dependent prostate cancer (Huggins C and Hodges CV 1941). Since then, clinicians have used surgical castration or chemical castration (lowering of testosterone by using compounds that lower testosterone production and/or by using compounds that block androgens from entering prostate cells) to lower testosterone levels and thereby treat androgen-dependent metastatic prostate

cancer by temporarily arresting tumor growth for several months or even years. Unfortunately, such treatments ultimately result in aggressive and metastatic androgen-independent prostate cancers. This transition to androgen-independence is likely to occur through selection for growth of androgen-independent cells that may already coexist with an androgen-dependent population prior to androgen deprivation therapy (Gingrich et al. 1997; Isaacs and Coffey 1981).

Despite the success and prolonged survival of treating patients with prostatectomy combined with radiation and/or androgen-ablation therapy, many patients eventually progress to hormone-refractory prostate cancer (HRPC) with an increasing PSA level as the only indication of disease. Oncologists adjust the therapeutic regimen by introducing chemotherapeutics alone or in combination to try to stop metastases. Unfortunately, chemotherapeutics are not very effective, in part because several anti-apoptotic factors are present in malignant prostate cells (Lebedeva et al. 2000; Raffo et al. 1995; Vlietstra et al. 1998). Some clinical oncologists debate that doing nothing at all may be the right course of action as some HRPC prostate metastases are slow growing and the quality of life of the patient outweighs the potential benefits of chemotherapy (Bhatnagar et al. 2004; Gulley and Dahut 2003).

Currently pre-clinical and clinical phase research concentrates on new modalities of selectively targeting prostate cancer and its metastases including vaccines to stimulate the body's own immune system to kill the cancer, anti-angiogenesis agents that will suppress neovascular growth and starve off the tumor from necessary nutrients and oxygen, antisense oligonucleotides and siRNA to down regulate specific genes necessary for growth and survival, and novel chemotherapeutic agents and combinations of agents to achieve better selectivity and efficacy. The work here will describe the development of novel chemotherapeutics that selectively target AR expressing prostate cancer cells while sparing non-cancerous cells.

Nuclear Hormone Receptors

Nuclear hormone receptors are ligand-activated transcription factors that regulate gene expression by binding to specific sequences of DNA. This superfamily includes receptors for hydrophobic molecules such as steroids, retinoic acids, thyroid hormones, fatty acids, leukotrienes, prostaglandins and as yet undiscovered ligands. There are currently over 100 nuclear hormone receptors identified and these can be divided into three subfamilies: Class I – ligand dependent and will homodimerize upon ligand binding (includes: ER, AR, progesterone receptor, mineralocorticoid receptor, glucocorticoid receptor), Class II – ligand independent with the potential to homo- or heterodimerize (includes: retinoic acid receptor, vitamin D receptor, thyroid receptor, and peroxisome proliferators activated receptor), and Orphan – unknown ligand or only very recently discovered ligand (includes: pregnane X receptor, constitutive androstane receptor, liver X receptor, benzoate X receptor, and farnesoid X receptor).

Nuclear hormone receptors consist of two domains – a ligand binding domain (LBD) and a DNA binding domain (DBD). Ligand binding allows for the recruitment of coactivator complexes and translocalization into the nucleus (if the unliganded form is in the cytoplasm). The DBD binds DNA, generally as a dimer, with each monomer recognizing a six base pair sequence of DNA known as the hormone response element. The hormone response element lies upstream (5' flanking region) of the gene that will be transcribed into ribonucleic acid (RNA). The binding of the nuclear hormone receptor to the HRE is often in close proximity to the recognition sequences for other transcription factors (TATA box) and interaction between these factors and the receptor play an important role in the rate of transcription (Schule et al. 1988). Nuclear hormone receptors bound to the HRE recruit chromatin remodeling proteins, histone acetylation proteins, and RNA polymerase holoenzyme recruitment proteins to the promoter region of a gene through two activation function areas on the C- and N- terminals known as activation function -1 and -2 (AF-1 and AF-2). Finally, when all of these protein complexes are present an RNA polymerase binds and transcribes a gene. Nuclear hormone receptors regulate genes involved in reproduction, development, and metabolism.

Estrogen Receptor

The ER is a 67 kDa protein belonging to the class I nuclear hormone receptor superfamily and is activated by estrogens (Evans 1988). In 1996, a second isoform of the ER was discovered by a group in Sweden and was termed ERβ (Kuiper et al. 1996). Unlike most nuclear hormone receptors that translocalize from the cytoplasm to the nucleus upon ligand binding, the ER is exclusively localized in the nucleus (King and Greene 1984; Welshons, Krummel, and Gorski 1985). However, recent evidence suggests that ERα also localizes to the plasma membrane where it functionally regulates protein kinase cascades in response to estrogen (Razandi et al. 2003; Xu et al. 2004). While ERα is found mainly in estrogen target tissues (uterus, vagina, and mammary glands), ERβ has been detected in a large variety of tissues (lung, hypothalamus, prostate, and ovary) (Enmark et al. 1997). Interestingly, ERβ is the predominant form in the normal mammary gland, however, in breast cancer ERα predominates (Leclercq 2002).

Although encoded by different genes on different chromosomes, ERα and ERβ have >95% sequence homology in the DBD and >55% in the LBD and have similar binding affinities for many estrogen ligands -- ERα binds estradiol with a Kd of 0.35 nM whereas ERβ binds it with a Kd of 0.6 nM (Kuiper et al. 1998). With such high sequence homology in the DBD, the two receptors bind a largely overlapping set of HREs. They differ, however, in their ligand binding and transcriptional activation regions (AF-1 and AF-2) (Barkhem et al. 1998). AF-1 is located in the N-terminus of the ER while AF-2 is in the C-terminus. Although AF-2 function is dependent upon ligand binding, AF-1 functions independently of ligand binding but synergizes with AF-2 in the promotion of ligand-dependent transcriptional activation (Tsai and O'Malley 1994). Alternatively, AF-1 and -2 can function independently, depending on the cellular context (McInerney and Katzenellenbogen 1996). Ligand binding produces a conformational change in AF-2 that allows for the recruitment of transcriptional co-regulatory proteins. Since the amino acid identity of ERα and β is relatively low in the AF region, it is not surprising that the same ligand can and does have different levels of potency and efficacy towards the different receptor subtypes. This allows for selective stimulation of diverse estrogen-regulated genes (Makela et al. 1999).

Upon ligand binding the ER undergoes conformational changes and is released from inactive complexes containing heat shock proteins (hsp90, hsp70) and immunophilins (Klinge et al. 1997; Ylikomi et al. 1998). The ER then dimerizes and binds to its HRE in order to stimulate transcription. The consensus sequence for ERα and ERβ is a palindromic inverted repeat: (A/G)GGTCAnnnTGACC(T/C) (where n is any nucleotide) (Klein-Hitpass et al. 1988; Sanchez et al. 2002). The ER contains a zinc finger in the DBD that makes sequence specific contacts with DNA allowing for AF-1 and AF-2 to recruit the cellular transcription machinery. The ER may also regulate transcription through protein-protein interactions in the absence of DNA and ligand. This subject is the focus of several reviews (Katzenellenbogen and Katzenellenbogen 2000; Klinge 2000; Sanchez et al. 2002).

In order for the ER to act as a transcription factor, it must first be activated. The phosphorylation of a serine residue at position 118 (Ser118) is required for full activity of the ER. Ser118 is phosphorylated by mitogen-activated protein kinase (MAPK) in the Ras-MAPK signaling pathway (Kato et al. 1995). Recently, protein phosphatase 5 was shown to inhibit the phosphorylation of Ser118 and thereby act as a negative regulator of transcription *in vivo* (Ikeda et al. 2004). Additional sites of phosphorylation include: Ser-104, 106, 126, 167 and Tyrosine-537. They are phosphorylated by various protein kinases and all seem to play a role in ER activation (Arnold et al. 1994; Arnold et al. 1995a; Arnold et al. 1995b; Auricchio et al. 1984; Le Goff et al. 1994). The ER is also activated by glycosylation at Ser-10, Threonine-50 and -575 and these glycosylations, particularly Thr-575, may help regulate transcription by inhibiting degradation (Cheng et al. 2000; Cheng and Hart 2000; Jiang and Hart 1997; Rechsteiner and Rogers 1996). Even though ligand binding is required for transcriptional activation, estradiol binding actually induces the degradation of the ER by the ubiquitin-proteasome pathway (Nawaz et al. 1999) and reduces its half-life from ~5 days to 3-4 hours (Pakdel, Le Goff, and Katzenellenbogen 1993). Therefore, the cell has evolved a clever way to respond to a stimulus, activate a necessary response gene, and quickly degrade the activation signal so as not to overcompensate for the initial stimulus.

The ER is expressed at low levels in normal breast epithelial cells, averaging only 10-20% of cells depending on the menstrual cycle (Ricketts et al. 1991). However, in

early non-invasive breast cancer approximately 75% of cells express the ER (Harvey et al. 1999; Karayiannakis et al. 1996) and 50% express the ER at high levels (Ferno et al. 1990; Pallis et al. 1992). Although there are two isoforms of the ER, it appears that ERα is the predominate player in early breast cancer (Leclercq 2002). However, ERβ was more recently discovered and despite its low abundance in early breast cancer tissue, could in fact play a very important role in disease progression. Additionally, it has been estimated that about 75% of invasive breast cancers express ERα (Harvey et al. 1999) and about 50% express ERβ (Speirs et al. 1999). As in the case of early breast cancer, the role of ERβ in invasive breast cancer growth and progression is not clearly understood.

Since many breast cancers are initially positive for the ER, their growth is stimulated by estrogens and inhibited by antiestrogens. This is evident in the fact that the benefit from tamoxifen therapy (reduction in recurrence and mortality) was directly related to ER expression levels in breast cancers (Rutqvist et al. 1989). However, tamoxifen-sensitive tumors invariably become resistant after prolonged treatment. Although ER expression is generally maintained during metastasis, other genetic and nongenomic events must override hormone responsiveness and contribute to the evolution of resistance to antiestrogen therapies. Alterations in ER expression, function, and estrogen responsiveness could play a role in breast cancer progression. Therefore a considerable effort has been devoted to the investigation of the ER in breast cancer progression and in the transition to HRBC.

Gene mutations of the ER could be responsible for deviations from its normal role. In fact, mutations in the ER gene have been shown to elicit changes in receptor activation by conferring constitutive activity, presumably through conformational changes, (Weis et al. 1996; Zhang et al. 1997) modulating ER activity due to abrogation of phosphorylation sites, (Le Goff et al. 1994) interfering with cofactor binding, (Henttu, Kalkhoven, and Parker 1997; Weis et al. 1996) and/or by modulating the agonist/antagonist activity ratio of antiestrogens (Montano et al. 1996). For example, a clinically observed tyrosine 537 to asparagine mutation affects a major site of phosphorylation in the LBD and results in a constitutively active receptor (Karnik et al. 1994). Mutational analysis of this site has shown that alanine, serine, aspartic acid, and glutamic acid can also cause the receptor to be constitutively active. However, these ER

mutants are capable of binding the co-activator, steroid receptor coactivator 1 (SRC-1), even in the absence of ligand. This illustrates that the mechanisms above are non-mutually exclusive. Although missense mutations have been estimated to be present in only 1% of primary breast cancers, (Roodi et al. 1995) the frequency may be higher in metastatic malignancies (Karnik et al. 1994; Zhang et al. 1997). Mutations in the ER may affect any one of the various functions of the ER – recruitment of coactivators/repressors, ligand binding, DNA binding, etc.

Either through mutations or some other unknown mechanism, the ER in a cancerous cell may be a more (or less) active form of the protein. In a normal cell, the ER regulates many genes necessary for growth and survival. The overexpression of the ER in malignant cells, therefore, induces the proliferation of many proto-oncogenes and growth factors that promote tumor survival. For example, the nuclear proto-oncogenes, c-fos, c-jun, and c-myc, are regulated by the ER. An increase in ER expression could lead to tumor progression. Likewise, key factors necessary for the development of new blood vessels to provide nutrients to the growing tumor, such as VEGF, are regulated by the ER. VEGF is induced by both estrogen and the antiestrogen tamoxifen. Continued ER expression may promote new vessel formation and contribute to the early phases of tumor growth and metastatic dispersal into the vasculature (Hyder et al. 2000; Ruohola et al. 1999).

Although the ER is known to be involved in breast caner initiation, progression, and possibly the transition to HRBC, its exact role in the proliferation and survival of malignant cells is still unknown. Since the ER is involved in cellular proliferation, stress response, and signaling pathways, an alteration in the expression or function of the protein has a drastic effect on the fate of a cell. Evidence has shown that genetic mutations in the ER can lead to increased transcriptional activation. Although not discussed here, a recent review presents evidence from tissue culture, animal, and clinical studies supporting the hypothesis that corepressors are crucial regulators of ERα-mediated action, and that their loss could promote breast cancer development and resistance to antiestrogen therapy (Dobrzycka et al. 2003). Thus, the role of the ER in breast cancer is complex and further research is needed to better elucidate its actions.

The most likely scenario is that there is no one mechanism by which the ER initiates breast cancer or aids in its progression. While many researchers focus on the biochemical aspects of this problem, the fact remains that current therapies do not effectively cure most breast cancer cases. Therefore, new therapies are required to combat the different stages of the disease. The work here will describe novel genotoxins that take advantage of the overexpression of the ER in breast cancers and other malignancies, such as epithelial ovarian tumors, to achieve selective killing of malignant cells.

Androgen Receptor

The androgen receptor is a 110 kDa protein that acts as a transcription factor in response to androgen binding and plays a major role in sexual development and sexual function in males. It is a member of the Class I nuclear receptor superfamily and will usually homodimerize upon ligand binding. The AR has high affinity for both testosterone and 5α-dihydrotestosterone with a Kd of 1 nM and 0.1 nM, respectively. The tissue specific actions of testosterone and dihydrotestosterone mediated by the same receptor suggest ligand specific recruitment of transcription intermediary factors (Brinkmann 2001). However, no such experimental evidence has been provided. The AR has two variable-length amino acid repeats in the N-terminal domain that result from trinucletotide repeats in the AR gene: polyglutamine (CAG) and polyglycine (GGN). Several reports have shown that shorter repeats (for example, ≤ 19 versus ≥25 polyglutamines) correlate with a higher transactivational function or expression level of AR, which is associated with an increased risk of prostate cancer (Giovannucci et al. 1999). Although trinucleotide repeat expansion has been implicated in prostate cancer disease progression, there are conflicting reports on their actual involvement (Montgomery, Price, and Figg 2001).

Most of the unliganded AR is localized in the cytoplasm (Tyagi et al. 2000), where it is sequestered as a multiprotein complex with heat shock proteins (Hsp90) and immunophilins (DeFranco 1999). Upon ligand binding, the AR dissociates from the heat shock proteins, dimerizes, and translocates into the nucleus. Dimerization allows for a conformational change in the protein exposing a nuclear localization signal. The exposed

nuclear localization signal is then capable of binding to importins, which serve as chaperones for the transport of the ligand-activated AR into the nucleus. Once in the nucleus, the AR recognizes and binds to its HRE, typically in the promoter region of target genes, through sequence specific contacts between DNA and zinc fingers in the protein. The consensus DNA binding sequence for the AR is comprised of two imperfect palindromic 6-base pair elements separated by a three base pair spacer, GG(A/T)ACAnnnTGTTCT (where n is three nucleotides) (Roche, Hoare, and Parker 1992), although more specific AR response element sequences have been identified (Claessens et al. 1996; Rundlett and Miesfeld 1995). Upon binding to the HRE, the AR signals for the cellular transcription machinery to express a gene through its activation functions.

The AR contains two amino-terminal activation functions AF-1 (ligand dependent) and AF-5 (ligand independent), and one carboxy-terminal activation function, AF-2 (ligand dependent). Since AF-5 is ligand independent, the AR has transcriptional activity even in the absence of ligand binding. Mutations in the AF-2 region result in a decrease in activation function without affecting the ligand-binding capability despite the close proximity to the LBD. This indicates that the amino acid residues in the AF-2 region are not directly involved in ligand binding, but rather, determine the interaction surface (Berrevoets et al. 1998; Feng et al. 1998). The interaction between AF-2 and either of the activation functions in the amino-terminus reduces the dissociation rate of the bound androgen and stabilizes the receptor (He et al. 2001). The interaction of the activation functions aids in the recruitment of coactivator and/or corepressor proteins for the transcription of an AR response gene.

Like the ER, the AR is activated by post-translational modifications including phosphorylation, acetylation, and sumoylation. The phosphorylation occurs within minutes after translation and results in a shift from a 110 kDa band on a sodium dodecyl sulfate (SDS) – polyacrylamide gel to a 112 kDa band indicative of a phosphoisoform of the AR (Jenster et al. 1994). Several phosphorylation sites have been identified, including: Ser-81, -94, -515, -650, and -662, (Blok, de Ruiter, and Brinkmann 1998; Jenster et al. 1994; Zhou, Kemppainen, and Wilson 1995) although as many as 21 potential phosphorylation sites have been identified (Kuiper et al. 1993). Ser-650 seems

to be a key phosphorylation site since mutating the AR by substituting an alanine for the serine reduced AR activity by 30% (substitution for the other serines showed no difference in activity). (Zhou, Kemppainen, and Wilson 1995) A third isoform has been identified with a molecular weight of 114 kDa and is thought to involve an addition and redistribution of phosphorylation sites, but only after ligand binding (Jenster et al. 1994; Kuiper et al. 1993; Zhou, Kemppainen, and Wilson 1995). The ligand-bound AR is acetylated at lysines (K) within the 630-633 region (KxKK) (Fu et al. 2003; Fu et al. 2000). Recently, work from the Pestell group showed that the acetylation of the AR regulates coactivator complex binding and, therefore, the expression of genes that are transcriptionally activated by the AR. Furthermore, AR acetylation promoted cell survival and growth of prostate cancer cells in soft agar and in nude mice suggesting that acetylation alters the expression of specific growth control genes (cyclin D1, cyclin E, and cyclin A) and may promote aberrant cellular growth in prostate cancer (Fu et al. 2003). Finally, the AR is modified in an androgen-dependent factor by sumoylation at Lys-386 and -520. The sumoylated lysine residues enhance transcriptional activity of the AR and it has been suggested that reversible sumoylation is a mechanism for regulation of the steroid receptor function (Poukka et al. 2000).

Ligand binding of the AR induces a conformational change that exposes a nuclear localization signal, which leads to the translocation of the AR from the cytoplasm into the nucleus. Not only does the AR require ligand binding to translocate into the nucleus, but ligand binding seems essential for its retention in the nucleus. This is evidenced by the fact that after its androgen-mediated nuclear import, androgen withdrawal (by transferring cells to a DHT-free medium) results in the export of the receptor back into the cytoplasm. In fact, the AR has been reported to undergo up to four rounds of cycling into and back out of the nucleus (Roy et al. 2001). The ability of one molecule of AR to undergo multiple rounds of signaling indicates that, unlike the ER which is tagged for degradation upon ligand binding, ligand dissociation and/or inactivation may play a more critical role in the termination of androgen signaling.

Although androgen binding stabilizes the AR, the receptor is eventually degraded by the ubiquitin-proteasome pathway. Initial evidence stemmed from the fact that a highly conserved proline-, glutamate-, serine-, threonine-rich sequence in the AR which

is thought to target proteins for ubiquitination and proteasomal degradation was found. Additionally, AR protein levels were elevated under proteasome inhibitor treatment (Sheflin et al. 2000). More recently a group from the University of Rochester demonstrated that Akt and Mdm2 formed a complex with the AR and promoted phosphorylation-dependent AR ubiquitination and subsequent degradation by the proteasome (Lin et al. 2002).

The AR is expressed in both androgen-dependent and –independent cancers at both the primary and metastatic sites and in HRPC (Hobisch et al. 1995; Marcelli and Cunningham 1999). Most patients with prostate cancer initially respond to androgen ablation therapy, but the recurrence of the cancer with its hormone independent status makes it difficult to treat. Thus the progression from androgen-dependence to – independence is a critical step in the development of prostate cancer, although the molecular mechanisms are poorly understood. Loss of androgen sensitivity is generally considered to have four causes: selection of cancer clones, adaptation of cells to an environment without androgen, an alternative pathway of signal transduction, and involvement of the AR (Suzuki et al. 2003).

There are three central mechanisms that describe the role of the AR in tumor progression: mutations, activation and upregualtion of receptor activity by androgens, and ligand-independent activation. The AR is frequently mutated within the LBD in both cell lines and primary tumors, rendering the AR permissive for binding of other steroid hormones (Elo et al. 1995; Gaddipati et al. 1994; Trapman et al. 1990). AR mutations have also been found in other regions of the protein including the coding region (Taplin et al. 1995; Tilley et al. 1996) and in the polyglutamine and polyglycine repeats (Montgomery, Price, and Figg 2001) which may increase the risk of cancer.

Through these mutations or other unknown mechanisms, AR function may become highly sensitized to low levels of residual androgens. The AR in normal prostate and in prostate cancer is involved in cellular proliferation, apoptosis, and angiogenic events. Androgens enhance the expression of cyclin-dependent kinases 2 and 4 (cdk-2/-4), as well as induce the down regulation of the cell cycle inhibitor p16 in cells expressing the AR, whereas in androgen-independent cells, there is no difference in expression of these proteins upon androgen stimulation (Lu, Tsai, and Tsai 1997).

Therefore in cells expressing the AR, there is an overall increase in Cdk activity and stimulation of the cells to enter S phase of the cell cycle and thus an enhancement of cellular proliferation. Androgens also upregulate the anti-apoptotic factor, p21, suggesting that androgens may induce anti-apoptotic activity (Lu et al. 1999). Data has shown that patients with advanced prostate cancer do in fact have increased p21 expression (Aaltomaa et al. 1999). Therefore, upregulation or increased activity of the AR could lead to increased cell proliferation and cancer progression. In fact, most prostate cancers express the AR and a high proportion of HRPC overexpress it (Hobisch et al. 1995).

The AR can also be activated in a steroid-independent manner by various growth factors, cytokines, Her-2, peptide hormones, and neurotransmitters (Craft et al. 1999; Culig et al. 1994; Hobisch et al. 1998; Nazareth and Weigel 1996). For example, insulin growth factor 1 and keratinocyte growth factor are able to promote AR transcriptional activity *in vitro* in the absence of androgens (Culig et al. 1994). The plasma concentration of the cytokine, interleukin 6 (IL-6), is elevated in patients with HPRC and seems to correlate with increased PSA level (Adler et al. 1999). IL-6 can enhance AR transactivation via the STAT3 or MAPK pathways and can suppress transactivation via the PI3K/Akt pathway (Yang et al. 2003). However, the mechanism of IL-6 induction of AR transactivation is still unknown; as is the physiological role each of these pathways play in the promotion of AR induced transcription.

These data suggest that the AR plays an important role in the progression of prostate cancer. Since the AR is overexpressed in many prostate cancers, it provides an obvious target for therapeutics (Hobisch et al. 1995; Marcelli and Cunningham 1999). However, current androgen ablation therapies are limited in scope by the transition from androgen-dependent to –independent status (Gingrich et al. 1997; Isaacs and Coffey 1981). Therefore, a need exists to treat prostate cancer before and after it becomes refractory to androgen ablation therapy. The work described here will discuss novel DNA damaging agents that take advantage of the expression of the AR in order to achieve selective killing of prostate malignancies.

Design of Novel Anticancer Agents

Current therapy for most cancers includes the surgical removal of the tumor followed by adjuvant therapy to rid the body of any micrometastases or cancerous cells not removed by the surgeon. The adjuvant therapy often includes hormones, radiation, and chemotherapeutics either alone or in combination. The drawback of current chemotherapies is the severe toxic side effects experienced by non-cancerous tissues resulting in a painful and arduous course for the patient. Moreover, these treatments usually do not fully cure the cancer, but rather only prolong the patient's life expectancy by placing the tumor into a temporary state of stasis. Cisplatin is somewhat unusual in this regard as it is extremely effective against testicular tumors and is capable of curing 95% of men with the disease (Feuer, Brown, and Kaplan 1993). Although the exact biological mechanism of cisplatin is unknown, it is well-established that the cellular toxicity derives from processes triggered by its reaction with DNA. From the lessons learned about the mechanism of action of cisplatin, we have rationally designed chemotherapeutics that produce DNA damage and exploit molecular changes in tumor cells.

Lessons Learned from Cisplatin

cis-Diamminedichloroplatinum (II) (cisplatin) (Fig 1.1A), typically in combination with etoposide and bleomycin, displays significant antitumor activity against cancers of the testis, ovary, head, neck, and lung (Masters and Koberle 2003). Once cisplatin enters a cell, its chloride ligands are displaced by water molecules generating a positively charged species that is capable of reacting with nucleophilic sites on DNA, RNA and proteins. Despite the chemical feasibility of cisplatin to form adducts with RNA and proteins, the level of adduction to these macromolecules are too low to be physiologically relevant (Akaboshi et al. 1992; Pascoe and Roberts 1974). All evidence points to the interaction of cisplatin with DNA as the key step underlying its toxicity: *Escherichia coli* and eukaryotic cells deficient in DNA repair enzymes are more sensitive to cisplatin than the corresponding wild type cells; there is an inverse correlation between DNA adduct levels and cell survival in culture; and there is a direct correlation between

cisplatin adduct levels in blood cells of cancer patients and clinical response (Kartalou and Essigmann 2001a; Kartalou and Essigmann 2001b).

Cisplatin is injected intravenously and remains coordinated to its chloride ligands while circulating in the blood where the chloride concentration is high (100 mM). Upon entering the cell where the chloride concentration is low (4 mM), the chloride ligands are rapidly substituted by water molecules ($t_{1/2}$ = 2 hr. for substitution of the first chloride ligand with water) (Bancroft, Lepre, and Lippard 1990; Johnson, Hoeschele, and Rahn 1980). The aquated species of cisplatin is capable of reacting with nucleophilic sites on the various macromolecules in the cell, such as DNA, RNA, and proteins. The water molecule of the singly aquated species is far more easily displaced than the chloride ligand, and is

susceptible to nucleophilic attack by the N7 position of guanine (or by adenine) forming a monofunctional DNA adduct ($t_{1/2}$ = 0.1 hr) (Bancroft, Lepre, and Lippard 1990). If there is another potentially reactive site nearby, the monofunctional adduct can react further to form an inter- or intra-strand crosslink ($t_{1/2}$ = 2.1 hr) (Bancroft, Lepre, and Lippard 1990). Cisplatin reacts with DNA to form approximately 65% 1,2-d(GpG), 25% 1,2-d(ApG), and 5-10% 1,3-d(GpNpG) intrastrand crosslinks and only a small percentage of monoadducts and interstrand crosslinks (Kartalou and Essigmann 2001b). These adducts result in the bending of DNA towards the major groove and an unwinding in the helical nature of DNA (reviewed in (Kartalou and Essigmann 2001a)). Cisplatin treatment results in inhibition of DNA replication (Ciccarelli et al. 1985; Uchida et al. 1986), inhibition of RNA transcription (Mello, Lippard, and Essigmann 1995), arrest at the G2 phase of the cell cycle and/or programmed cell death (Sorenson and Eastman 1988a; Sorenson and Eastman 1988b). The molecular mechanisms that link these physiological events with the initial formation of DNA adducts are not entirely understood.

One possible link between the physiological toxicity and DNA adduct formation may stem from the fact that certain proteins bind to cisplatin-DNA adducts (Pil and Lippard 1992; Toney et al. 1989). Partially through work in the Essigmann laboratory, several nuclear proteins, most containing a high mobility group (HMG) domain, have been identified with very high affinity for the therapeutically active cisplatin DNA adducts (Brown, Kellett, and Lippard 1993; Bruhn et al. 1992; Donahue et al. 1990; Pil

and Lippard 1992; Toney et al. 1989). On the surface, this may not be surprising as the structure of cisplatin DNA adducts is very similar to the structure of HMG box proteins bound to DNA – upon binding, HMG proteins bend and unwind DNA to a degree similar to that of a cisplatin adduct. However, other proteins, such as the ER, also bend DNA upon binding to its response element, but the affinity of the ER is lost when cisplatin is adducted to a base within this region (Massaad-Massade et al. 2000). Therefore, the interaction between the HMG proteins and the cisplatin adducts is specific. The stability of the unnatural bent DNA structure is further enhanced by the intercalation of an amino acid side chain (from HMG) into the duplex at the site of the bend (Kartalou and Essigmann 2001a).

Several models have been proposed to explain the involvement of HMG proteins in the cellular toxicity of cisplatin (Fig 1.2). One model suggests that the binding of these proteins to the cisplatin-DNA adduct is so tight that repair enzymes are inhibited from accessing the lesion (Fig 1.2A). Evidence has illustrated that HMG proteins sensitize cells to cisplatin toxicity by shielding DNA adducts from repair (Brown, Kellett, and Lippard 1993; Huang et al. 1994; McA'Nulty and Lippard 1996). A second model (Fig 1.2B) stems from the discovery that human upstream binding factor (hUBF), a transcription factor that plays a key role in the regulation of ribosomal RNA synthesis, binds to cisplatin adducts with a similar affinity to its cognate promoter sequence (Kd = 60 pM and 18 pM, respectively) (Treiber et al. 1994). Since hUBF is essential for proliferating cells, cisplatin adducts may hijack the transcription factor and deplete the cells of a necessary resource to grow (Treiber et al. 1994). The "repair shielding" and "transcription factor hijacking" mechanisms, although not mutually exclusive, may help explain the unusual effectiveness of cisplatin against malignant cells (Kartalou and Essigmann 2001a). The main drawback of cisplatin is its relatively limited applicability to only a small handful of cancers.

Applying the Lessons Learned from Cisplatin to Novel Anticancer Agents

The toxicity of cisplatin can, in part, be attributed to the repair shielding and transcription factor hijacking mechanisms. The work here describes the use of synthetic chemistry to create *de novo* molecules that are capable of killing malignant cells through

these two mechanisms. In order to achieve this goal, the new compound must be capable of adducting DNA and attracting specific proteins present only (or predominantly) in cancer cells. The salient features of the compounds that were designed and their intended mechanism of action are shown in Figure 1.3. The compounds are bifunctional molecules containing a DNA reactive warhead and a protein recognition domain capable of attracting tumor specific proteins. In normal cells where the repair blocking protein is absent (or at concentrations too low to be physiologically relevant), the adduct is unshielded and hence more readily accessible to repair enzymes (Fig 1.3 lower left). However, in cancerous cells where the protein is aberrantly expressed, the protein would be attracted to the DNA lesion. A tight interaction between the tumor specific protein and the drug's protein recognition domain would inhibit repair enzymes from accessing the lesion (Fig 1.3 lower right). The adduct would persist and thus cause the cell to enter the apoptotic cascade. Additionally, if the tumor specific protein were a transcription factor, the DNA adduct could hijack the protein and disrupt necessary cellular transcriptional events. Moreover, if the protein was overexpressed in tumor cells, those cells would be selectively more sensitive than normal cells, resulting in a favorable therapeutic index.

Examples of the types of molecules we have studied are shown in Figure 1.1B-D. Aromatic nitrogen mustards were chosen as the DNA damaging warhead because they react slowly (they have comparatively low toxicity when compared to more reactive alkyl mustards), and they form DNA adducts that are readily repaired. Furthermore, repair deficient cell lines are more sensitive to mustard compounds (De Silva et al. 2000; Frankfurt 1991). We therefore reasoned that inhibiting the repair of these DNA adducts in tumor cells should increase lethality. The nitrogen mustard, which is based on the FDA approved drugs chlorambucil and melphalan, was linked to a protein recognition domain. The ER was a logical protein to target since it is both a transcription factor and is overexpressed in approximately 50% of all breast cancers (Ferno et al. 1990; Pallis et al. 1992). Initial studies were conducted with a phenyl-indole linked to a nitrogen mustard and served as a relatively uncomplicated synthetic molecule that could be used to test the overall strategy (Fig 1.1B). The phenyl-indole moiety was later substituted for estradiol linked at the 7α position (Fig 1.1C) to provide a molecule with increased affinity

for the ER. Lastly, this platform has been expanded to treat prostate cancers by tethering a testosterone-like moiety to the nitrogen mustard (Fig 1.1D). As in the case of breast cancer, many prostate cancers also overexpress the AR and the AR is also a transcription factor (Hobisch et al. 1995; Marcelli and Cunningham 1999).

Although seemingly functionally silent in the repair shielding and transcription factor hijacking mechanisms, great care went into devising the region linking the warhead to the protein recognition domain. The linker was optimized based on several factors: 1. ease and simplicity of chemical synthesis, 2. stability from enzymatic degradation, 3. enhanced solubility of the overall compound, 4. binding to the tumor specific protein, 5. formation of DNA adducts. Several iterations were synthesized before proceeding with the compounds shown in Fig 1.1B-D. This will be discussed in brief below.

2-Phenyl-indole-C6NC2-mustard – A Rationally Designed Drug Candidate

The main drawback of conventional chemotherapeutics is the toxic side effects suffered by non-target tissues. Using the lessons learned from cisplatin, the Essigmann laboratory initially sought out to improve the therapeutic index of chemotherapeutics targeting breast and ovarian cancers that aberrantly expressed the ER (Rink et al. 1996). The rationale was to form DNA adducts that were capable of attracting tumor specific proteins, such as the ER. If the ER is attracted to DNA adducts, the adduct-protein complex could inhibit repair enzymes from accessing the lesion and rendering it nontoxic. The lesion would persist and the cell would enter into apoptosis. Alternatively, a malignant cell could also enter programmed cell death if the DNA adduct disrupts necessary transcriptional events by hijacking the ER from its response element. As a proof of concept 2-(4'-hydroxyphenyl)-3-methyl-5-hydroxy-indole was linked to 4-(3-aminopropyl)-N,N-(2-chloroethyl)-aniline (Fig 1.4). The former is a molecule that interacts well with the ER in competitive binding experiments with estradiol and the latter is the DNA reactive warhead (von Angerer, Prekajac, and Strohmeier 1984).

Rink et al. synthesized a series of bifunctional alkylating agents capable of damaging DNA and attracting the ER. The linkage between the warhead and the protein recognition domain was designed to permit DNA damage while preserving the ability of

the phenylindole group to interact with the ER. Therefore, the number of carbon atoms between the phenylindole and the secondary amine and between the secondary amine and the carbamate was systematically varied to optimize both DNA adduction and protein binding (Fig 1.4). A fourth compound, 2PI(OH)-C6NC2, was synthesized as a control compound that has poor affinity for the ER as a result of only a monohydroxylation of the phenylindole (von Angerer, Prekajac, and Strohmeier 1984). A carbamate was chosen to join the two halves of the molecules together because it is resistant to enzymatic degradation *in vivo* (Cho et al. 1993), and it provides a stable synthetic handle. Additionally, a secondary amino group was incorporated into the linker to enhance solubility. Since the pKa of the secondary amino group is ~10, these compounds are anticipated to have a positive charge which may promote association with DNA.

The relative binding affinities (RBA) of the four molecules illustrated that the 2PI-C6NC2 mustard interacted the best with the ER (Fig 1.4). An RBA of 7.1 indicates that 2PI-C6NC2 binds to the ER with an affinity that is 7.1% of that for estradiol, the natural ligand for the ER. As expected, the monohydroxylated 2PI(OH)-C6NC2-mustard showed poor binding to the ER. The C3NC3 and C5NC3 linkers also displayed relatively disappointing binding affinities to the ER. The solving of the ER crystal structure in 1997 now sheds light as to why the C6NC2 linker had the highest affinity for the ER (Brzozowski et al. 1997). Due to the depth of the ligand binding pocket, a six carbon chain is necessary to provide optimal binding and minimize steric clashes from the secondary amine. Figure 1.5 depicts a molecular docking model of a second generation nitrogen mustard (E2-7α) DNA adduct with the ER-LBD. This model illustrates two points: 1. although not easily seen in the figure shown, a six carbon chain is optimal for efficient binding of the ER to the nitrogen mustard, and 2. the linker is of sufficient overall length to allow for the binding of the mustard even when adducted to DNA. The second point is of particular importance since the compounds were designed to hijack transcription factors and shield DNA adducts from repair enzymes. These two mechanisms can only be effective if the ER has a high affinity for the drug-DNA adducts and not just for the compounds alone.

The compounds in Figure 1.4 were allowed to react with a 16-mer oligonucleotide. The overall reactivity of the compounds tested was 2PI-C3NC3 > 2PI-

5NC3 > 2PI-C6NC2 > chlorambucil > 2PI(OH)-C6NC2. Based upon chemical fragmentation analysis of the alkylated products, guanine was the primary base alkylated by these compounds, followed by adenine. It is likely that the adducts were mainly at the N7 position of guanine (Lawley 1966; Singer 1975) and the N3 position of the adenine residues (Pieper, Futscher, and Erickson 1989). Additionally, the DNA adducts of the 2PI-C6NC2-mustard were able to compete with estradiol for the ER ligand binding site (RBA ~ 0.5). Furthermore, this result provides experimental evidence for the molecular docking model indicating that 2PI-C6NC2-mustard DNA adducts can act as a molecular decoy binding site for the ER.

Finally, Rink et al. evaluated the phenylindole mustard compounds for their selective toxicity towards ER expressing cells, MCF-7, versus ER deficient cells, MDA-MB231. Both cell lines were treated for a brief, 2 hr period to minimize ER antagonistic effects in a clonogenic survival assay. Figure 1.6 illustrates the survival curves for the MCF-7 and MDA-MB231 cells treated with the mustard compounds. The overall toxicity of the compounds tested in either cell line were consistent with their abilities to adduct DNA *in vitro* -- 2PI-C3NC3 > 2PI-5NC3 > 2PI-C6NC2 > 2PI(OH)-C6NC2 > chlorambucil. However, the two compounds that interacted best with the ER, 2PI-C5NC3- and 2PI-C6NC2-mustard, were more toxic to the ER(+) MCF-7 cells than they were to the ER(-) MDA-MB231 cells (Fig 1.6 C and D). Chlorambucil, 2PI-C3NC3-mustard, and 2PI(OH)-C6NC2-mustard did not exhibit selective toxicity toward either cell line (Fig 1.6 A and B). The results with the control compounds made it unlikely that the selective toxicity towards the MCF-7 cells by 2PI-C5NC2-mustard and 2PI-C6NC2-mustard were due to cell line specific variation in the detoxification of the mustards or in their DNA repair capability. Instead, these results suggest that the difference in sensitivity between the two cell lines is due, in part, to their ER status.

These data illustrate that the compounds that interact the best with the ER, both alone and as DNA adducts, are more toxic to ER(+) MCF-7 cells than to ER(-) MDA-MB231 cells. Several mechanisms could explain the selective toxicity including ER antagonism, selective delivery to ER(+) cells, or the repair shielding/transcription factor hijacking models. Since the cells were treated for a very short period (2 hr), it is unlikely that the primary source of toxicity of the phenylindole mustards resulted from ER

antagonism. As a control experiment, 2PI-C6NC2-mustard was inactivated by hydrolyzing the bis-chloroethyl arms of the nitrogen mustard. Only after extended periods of exposure to cells (when the inactivated 2PI-C6NC2-mustard was continuously present in the cell growth medium) were some signs of toxicity evident. A 2 hr exposure to the inactivated drug showed minimal effect on survival – approximately a 10% reduction in survival. This ruled out the possibility that the toxicity of the phenylindole mustards was due strictly to ER antagonism. Furthermore, it is unlikely that the mustards were selectively delivered to the ER(+) cells based on the fact that the levels of interstrand crosslinks of 2PI-C6NC2-mustard in the ER(+) MCF-7 and ER(-) MDA-MB231 cells are identical shortly after dosing. This is compounded by the fact that Rink et al. calculated that 20-25% of the DNA adducts formed by 2PI-C6NC2-mustard are likely to be associated with the ER (Rink et al. 1996). Therefore it is quite possible that the repair shielding and transcription factor hijacking mechanisms are responsible for the selective toxicity.

Based on the initial findings linking the repair shielding and transcription factor hijacking mechanisms with the selective toxicity of these compounds, future iterations have continued to use many of the key features from the preliminary work of Rink et al. The work described here will focus on two new molecules with higher specificity for their respective nuclear hormone receptors. In the case of breast cancer, a new agent incorporates into its design the warhead and the linker of the 2PI-C6NC2-mustard molecule, but has substituted the phenylindole moiety with 17β-estradiol to increase the affinity for the ER. In the case of prostate cancer, the same warhead and linker have been tethered to a testosterone-like moiety. In the subsequent chapters, I have treated these two molecules separately since they target different cancers and seem to have slightly different mechanisms of action. The next 4 chapters will focus on work with the compounds that we have used to target ER(+) breast cancer. Chapters 6-8 will focus on the work I have completed with a molecule that targets prostate cancer. For both compounds, I will initially discuss the results from various *in vitro* experiments which illustrate their potential as chemotherapeutic agents – ability to form DNA adducts, bind to their respective receptors, and selectively destroy receptor expressing cancer cell lines. I will then discuss the results of *in vivo* experiments, including pharmacokinetics, toxicity

and efficacy against xenograft tumor models. I will conclude by hypothesizing on the mechanism of action of these compounds. Although I will focus on the experiments that I have done during my graduate career, I will occasionally introduce work from my colleagues, as it makes for a much more interesting and complete story.

Reference List

Cancer Facts and Figures. American Cancer Society, 1-60 (2005)

Aaltomaa, S., Lipponen, P., Eskelinen, M. et al. Prognostic value and expression of p21(waf1/cip1) protein in prostate cancer. *Prostate* **39**, 8-15 (1999)

Aaronson, S.A., Miki, T., Meyers, K., and Chan, A. Growth factors and malignant transformation. *Adv. Exp. Med. Biol.* **348**, 7-22 (1993)

Abate-Shen, C. and Shen, M.M. Molecular genetics of prostate cancer. *Genes Dev.* **14**, 2410-2434 (2000)

Adler, H.L., McCurdy, M.A., Kattan, M.W. et al. Elevated levels of circulating interleukin-6 and transforming growth factor-beta1 in patients with metastatic prostatic carcinoma. *J. Urol.* **161**, 182-187 (1999)

Akaboshi, M., Kawai, K., Maki, H. et al. The number of platinum atoms binding to DNA, RNA and protein molecules of HeLa cells treated with cisplatin at its mean lethal concentration. *Jpn. J. Cancer Res.* **83**, 522-526 (1992)

Arnold, S.F., Obourn, J.D., Jaffe, H., and Notides, A.C. Serine 167 is the major estradiol-induced phosphorylation site on the human estrogen receptor. *Mol. Endocrinol.* **8**, 1208-1214 (1994)

Arnold, S.F., Obourn, J.D., Jaffe, H., and Notides, A.C. Phosphorylation of the human estrogen receptor by mitogen-activated protein kinase and casein kinase II: consequence on DNA binding. *J. Steroid Biochem. Mol. Biol.* **55**, 163-172 (1995a)

Arnold, S.F., Obourn, J.D., Jaffe, H., and Notides, A.C. Phosphorylation of the human estrogen receptor on tyrosine 537 in vivo and by src family tyrosine kinases in vitro. *Mol. Endocrinol.* **9**, 24-33 (1995b)

Auricchio, F., Migliaccio, A., Castoria, G. et al. Direct evidence of in vitro phosphorylation-dephosphorylation of the estradiol-17 beta receptor. Role of Ca2+-calmodulin in the activation of hormone binding sites. *J. Steroid Biochem.* **20**, 31-35 (1984)

Bancroft, D.P., Lepre, C.A., and Lippard, S.J. Platinum-195 NMR kinetic and mechanistic studies of cis- and trans-diamminedichloroplatinum(II) binding to DNA. *Journal of the American Chemical Society* **112**, 6860-6871 (1990)

Bange, J., Zwick, E., and Ullrich, A. Molecular targets for breast cancer therapy and prevention. *Nat. Med.* **7**, 548-552 (2001)

Barkhem, T., Carlsson, B., Nilsson, Y. et al. Differential response of estrogen receptor alpha and estrogen receptor beta to partial estrogen agonists/antagonists. *Mol. Pharmacol.* **54**, 105-112 (1998)

Baselga, J. Clinical trials of Herceptin(R) (trastuzumab). *Eur. J. Cancer* **37 (Suppl 1)**, 18-24 (2001)

Baselga, J. and Norton, L. Focus on breast cancer. *Cancer Cell* **1**, 319-322 (2002)

Berrevoets, C.A., Doesburg, P., Steketee, K. et al. Functional interactions of the AF-2 activation domain core region of the human androgen receptor with the amino-terminal domain and with the transcriptional coactivator TIF2 (transcriptional intermediary factor2). *Mol. Endocrinol.* **12**, 1172-1183 (1998)

Bhatnagar, V., Stewart, S.T., Bonney, W.W., and Kaplan, R.M. Treatment options for localized prostate cancer: quality-adjusted life years and the effects of lead-time. *Urology* **63**, 103-109 (2004)

Blok, L.J., de Ruiter, P.E., and Brinkmann, A.O. Forskolin-induced dephosphorylation of the androgen receptor impairs ligand binding. *Biochemistry* **37**, 3850-3857 (1998)

Brinkmann, A.O. Lessons to be learned from the androgen receptor. *Eur. J. Dermatol.* **11**, 301-303 (2001)

Brown, S.J., Kellett, P.J., and Lippard, S.J. Ixr1, a yeast protein that binds to platinated DNA and confers sensitivity to cisplatin. *Science* **261**, 603-605 (1993)

Bruhn, S.L., Pil, P.M., Essigmann, J.M. et al. Isolation and characterization of human cDNA clones encoding a high mobility group box protein that recognizes structural distortions to DNA caused by binding of the anticancer agent cisplatin. *Proc. Natl. Acad. Sci. U. S. A* **89**, 2307-2311 (1992)

Bryan, T.M. and Cech, T.R. Telomerase and the maintenance of chromosome ends. *Curr. Opin. Cell Biol.* **11**, 318-324 (1999)

Brzozowski, A.M., Pike, A.C., Dauter, Z. et al. Molecular basis of agonism and antagonism in the oestrogen receptor. *Nature* **389**, 753-758 (1997)

Carpten, J., Nupponen, N., Isaacs, S. et al. Germline mutations in the ribonuclease L gene in families showing linkage with HPC1. *Nat. Genet.* **30**, 181-184 (2002)

Carter, B.S., Carter, H.B., and Isaacs, J.T. Epidemiologic evidence regarding predisposing factors to prostate cancer. *Prostate* **16**, 187-197 (1990)

Chen, J.J., Silver, D., Cantor, S. et al. BRCA1, BRCA2, and Rad51 operate in a common DNA damage response pathway. *Cancer Res.* **59**, 1752s-1756s (1999)

Chen, Y., Lee, W.H., and Chew, H.K. Emerging roles of BRCA1 in transcriptional regulation and DNA repair. *J. Cell Physiol* **181**, 385-392 (1999)

Cheng, X., Cole, R.N., Zaia, J., and Hart, G.W. Alternative O-glycosylation/O-phosphorylation of the murine estrogen receptor beta. *Biochemistry* **39**, 11609-11620 (2000)

Cheng, X. and Hart, G.W. Glycosylation of the murine estrogen receptor-alpha. *J. Steroid Biochem. Mol. Biol.* **75**, 147-158 (2000)

Cho, C.Y., Moran, E.J., Cherry, S.R. et al. An unnatural biopolymer. *Science* **261**, 1303-1305 (1993)

Christofori, G. and Semb, H. The role of the cell-adhesion molecule E-cadherin as a tumour-suppressor gene. *Trends Biochem. Sci.* **24**, 73-76 (1999)

Ciccarelli, R.B., Solomon, M.J., Varshavsky, A., and Lippard, S.J. In vivo effects of cis- and trans-diamminedichloroplatinum(II) on SV40 chromosomes: differential repair, DNA-protein cross-linking, and inhibition of replication. *Biochemistry* **24**, 7533-7540 (1985)

Claessens, F., Alen, P., Devos, A. et al. The androgen-specific probasin response element 2 interacts differentially with androgen and glucocorticoid receptors. *J. Biol. Chem.* **271**, 19013-19016 (1996)

Craft, N., Shostak, Y., Carey, M., and Sawyers, C.L. A mechanism for hormone-independent prostate cancer through modulation of androgen receptor signaling by the HER-2/neu tyrosine kinase. *Nat. Med.* **5**, 280-285 (1999)

Culig, Z., Hobisch, A., Cronauer, M.V. et al. Androgen receptor activation in prostatic tumor cell lines by insulin-like growth factor-I, keratinocyte growth factor, and epidermal growth factor. *Cancer Res.* **54**, 5474-5478 (1994)

De Silva, I.U., McHugh, P.J., Clingen, P.H., and Hartley, J.A. Defining the roles of nucleotide excision repair and recombination in the repair of DNA interstrand cross-links in mammalian cells. *Mol. Cell Biol.* **20**, 7980-7990 (2000)

DeFranco, D.B. Regulation of steroid receptor subcellular trafficking. *Cell Biochem. Biophys.* **30**, 1-24 (1999)

Dhom, G. Epidemiologic aspects of latent and clinically manifest carcinoma of the prostate. *J. Cancer Res. Clin. Oncol.* **106**, 210-218 (1983)

Di Fiore, P.P., Pierce, J.H., Kraus, M.H. et al. erbB-2 is a potent oncogene when overexpressed in NIH/3T3 cells. *Science* **237**, 178-182 (1987)

Dobrzycka, K.M., Townson, S.M., Jiang, S., and Oesterreich, S. Estrogen receptor corepressors -- a role in human breast cancer? *Endocr. Relat Cancer* **10**, 517-536 (2003)

Donahue, B.A., Augot, M., Bellon, S.F. et al. Characterization of a DNA damage-recognition protein from mammalian cells that binds specifically to intrastrand d(GpG) and d(ApG) DNA adducts of the anticancer drug cisplatin. *Biochemistry* **29**, 5872-5880 (1990)

Easton, D.F. How many more breast cancer predisposition genes are there? *Breast Cancer Res.* **1**, 14-17 (1999)

Edwards, B.K., Howe, H.L., Ries, L.A. et al. Annual report to the nation on the status of cancer, 1973-1999, featuring implications of age and aging on U.S. cancer burden. *Cancer* **94**, 2766-2792 (2002)

Edwards, S.M., Kote-Jarai, Z., Meitz, J. et al. Two percent of men with early-onset prostate cancer harbor germline mutations in the BRCA2 gene. *Am. J. Hum. Genet.* **72**, 1-12 (2003)

Elo, J.P., Kvist, L., Leinonen, K. et al. Mutated human androgen receptor gene detected in a prostatic cancer patient is also activated by estradiol. *J. Clin. Endocrinol. Metab* **80**, 3494-3500 (1995)

Enmark, E., Pelto-Huikko, M., Grandien, K. et al. Human estrogen receptor beta-gene structure, chromosomal localization, and expression pattern. *J. Clin. Endocrinol. Metab* **82**, 4258-4265 (1997)

Evans, R.M. The steroid and thyroid hormone receptor superfamily. *Science* **240**, 889-895 (1988)

Feng, W., Ribeiro, R.C., Wagner, R.L. et al. Hormone-dependent coactivator binding to a hydrophobic cleft on nuclear receptors. *Science* **280**, 1747-1749 (1998)

Ferno, M., Borg, A., Johansson, U. et al. Estrogen and progesterone receptor analyses in more than 4,000 human breast cancer samples. A study with special reference to age at diagnosis and stability of analyses. Southern Swedish Breast Cancer Study Group. *Acta Oncol.* **29**, 129-135 (1990)

Feuer, E.J., Brown, L.M., and Kaplan, R.S. SEER Cancer Statistics Review 1973-1990. XXIV. 1-XXIV. 13 (1993)

Foulds, L. The experimental study of tumor progression: a review. *Cancer Res* **14**, 327-339 (1954)

Frankfurt, O.S. Inhibition of DNA repair and the enhancement of cytotoxicity of alkylating agents. *Int. J. Cancer* **48**, 916-923 (1991)

Fu, M., Rao, M., Wang, C. et al. Acetylation of androgen receptor enhances coactivator binding and promotes prostate cancer cell growth. *Mol. Cell Biol.* **23**, 8563-8575 (2003)

Fu, M., Wang, C., Reutens, A.T. et al. p300 and p300/cAMP-response element-binding protein-associated factor acetylate the androgen receptor at sites governing hormone-dependent transactivation. *J. Biol. Chem.* **275**, 20853-20860 (2000)

Gaddipati, J.P., McLeod, D.G., Heidenberg, H.B. et al. Frequent detection of codon 877 mutation in the androgen receptor gene in advanced prostate cancers. *Cancer Res.* **54**, 2861-2864 (1994)

Gayther, S.A., de Foy, K.A., Harrington, P. et al. The frequency of germ-line mutations in the breast cancer predisposition genes BRCA1 and BRCA2 in familial prostate cancer. The Cancer Research Campaign/British Prostate Group United Kingdom Familial Prostate Cancer Study Collaborators. *Cancer Res.* **60**, 4513-4518 (2000)

Gingrich, J.R., Barrios, R.J., Kattan, M.W. et al. Androgen-independent prostate cancer progression in the TRAMP model. *Cancer Res.* **57**, 4687-4691 (1997)

Giovannucci, E., Platz, E.A., Stampfer, M.J. et al. The CAG repeat within the androgen receptor gene and benign prostatic hyperplasia. *Urology* **53**, 121-125 (1999)

Greenlee, R.T., Murray, T., Bolden, S., and Wingo, P.A. Cancer statistics, 2000. *CA Cancer J. Clin.* **50**, 7-33 (2000)

Gulley, J. and Dahut, W.L. Novel approaches to treating the asymptomatic hormone-refractory prostate cancer patient. *Urology* **62**, 147-154 (2003)

Hanahan, D. and Folkman, J. Patterns and emerging mechanisms of the angiogenic switch during tumorigenesis. *Cell* **86**, 353-364 (1996)

Hanahan, D. and Weinberg, R.A. The hallmarks of cancer. *Cell* **100**, 57-70 (2000)

Hankey, B.F., Feuer, E.J., Clegg, L.X. et al. Cancer surveillance series: interpreting trends in prostate cancer--part I: Evidence of the effects of screening in recent prostate cancer incidence, mortality, and survival rates. *J. Natl. Cancer Inst.* **91**, 1017-1024 (1999)

Harris, C.C. p53 tumor suppressor gene: from the basic research laboratory to the clinic--an abridged historical perspective. *Carcinogenesis* **17**, 1187-1198 (1996)

Harvey, J.M., Clark, G.M., Osborne, C.K., and Allred, D.C. Estrogen receptor status by immunohistochemistry is superior to the ligand-binding assay for predicting response to adjuvant endocrine therapy in breast cancer. *J. Clin. Oncol.* **17**, 1474-1481 (1999)

He, B., Bowen, N.T., Minges, J.T., and Wilson, E.M. Androgen-induced NH2- and COOH-terminal Interaction Inhibits p160 coactivator recruitment by activation function 2. *J. Biol. Chem.* **276**, 42293-42301 (2001)

Henttu, P.M., Kalkhoven, E., and Parker, M.G. AF-2 activity and recruitment of steroid receptor coactivator 1 to the estrogen receptor depend on a lysine residue conserved in nuclear receptors. *Mol. Cell Biol.* **17**, 1832-1839 (1997)

Hobisch, A., Culig, Z., Radmayr, C. et al. Distant metastases from prostatic carcinoma express androgen receptor protein. *Cancer Res.* **55**, 3068-3072 (1995)

Hobisch, A., Eder, I.E., Putz, T. et al. Interleukin-6 regulates prostate-specific protein expression in prostate carcinoma cells by activation of the androgen receptor. *Cancer Res.* **58**, 4640-4645 (1998)

Howe, H.L., Wingo, P.A., Thun, M.J. et al. Annual report to the nation on the status of cancer (1973 through 1998), featuring cancers with recent increasing trends. *J. Natl. Cancer Inst.* **93**, 824-842 (2001)

Huang, J.C., Zamble, D.B., Reardon, J.T. et al. HMG-domain proteins specifically inhibit the repair of the major DNA adduct of the anticancer drug cisplatin by human excision nuclease. *Proc. Natl. Acad. Sci. U. S. A* **91**, 10394-10398 (1994)

Huggins C and Hodges CV. Studies in prostatic cancer. I. The effects of castration, of estrogen, and of androgen injection of serum phosphatases in metastatic carcinoma of the prostate. *Cancer Research* **1**, 293-302 (1941)

Hyder, S.M., Nawaz, Z., Chiappetta, C., and Stancel, G.M. Identification of functional estrogen response elements in the gene coding for the potent angiogenic factor vascular endothelial growth factor. *Cancer Res.* **60**, 3183-3190 (2000)

Ikeda, K., Ogawa, S., Tsukui, T. et al. Protein Phosphatase 5 Is a Negative Regulator of Estrogen Receptor-mediated Transcription. *Mol. Endocrinol.* **18**, 1131-1143 (2004)

Isaacs, J.T. and Coffey, D.S. Adaptation versus selection as the mechanism responsible for the relapse of prostatic cancer to androgen ablation therapy as studied in the Dunning R-3327-H adenocarcinoma. *Cancer Res.* **41**, 5070-5075 (1981)

Jenster, G., de Ruiter, P.E., van der Korput, H.A. et al. Changes in the abundance of androgen receptor isotypes: effects of ligand treatment, glutamine-stretch variation, and mutation of putative phosphorylation sites. *Biochemistry* **33**, 14064-14072 (1994)

Jiang, M.S. and Hart, G.W. A subpopulation of estrogen receptors are modified by O-linked N-acetylglucosamine. *J. Biol. Chem.* **272**, 2421-2428 (1997)

Johnson, N.P., Hoeschele, J.D., and Rahn, R.O. Kinetic analysis of the in vitro binding of radioactive cis- and trans-dichlorodiammineplatinum(II) to DNA. *Chem. Biol. Interact.* **30**, 151-169 (1980)

Jordan, V.C. Tamoxifen and tumorigenicity: a predictable concern. *J. Natl. Cancer Inst.* **87**, 623-626 (1995)

Karayiannakis, A.J., Bastounis, E.A., Chatzigianni, E.B. et al. Immunohistochemical detection of oestrogen receptors in ductal carcinoma in situ of the breast. *Eur. J. Surg. Oncol.* **22**, 578-582 (1996)

Karnik, P.S., Kulkarni, S., Liu, X.P. et al. Estrogen receptor mutations in tamoxifen-resistant breast cancer. *Cancer Res.* **54**, 349-353 (1994)

Kartalou, M. and Essigmann, J.M. Recognition of cisplatin adducts by cellular proteins. *Mutat. Res.* **478**, 1-21 (2001a)

Kartalou, M. and Essigmann, J.M. Mechanisms of resistance to cisplatin. *Mutat. Res.* **478**, 23-43 (2001b)

Kato, S., Endoh, H., Masuhiro, Y. et al. Activation of the estrogen receptor through phosphorylation by mitogen-activated protein kinase. *Science* **270**, 1491-1494 (1995)

Katzenellenbogen, B.S. Antiestrogen resistance: mechanisms by which breast cancer cells undermine the effectiveness of endocrine therapy. *J. Natl. Cancer Inst.* **83**, 1434-1435 (1991)

Katzenellenbogen, B.S. and Katzenellenbogen, J.A. Estrogen receptor transcription and transactivation: Estrogen receptor alpha and estrogen receptor beta: regulation by selective estrogen receptor modulators and importance in breast cancer. *Breast Cancer Res.* **2**, 335-344 (2000)

Kerlikowske, K. Efficacy of screening mammography among women aged 40 to 49 years and 50 to 69 years: comparison of relative and absolute benefit. *J Natl. Cancer Inst. Monogr* 79-86 (1997)

King, W.J. and Greene, G.L. Monoclonal antibodies localize oestrogen receptor in the nuclei of target cells. *Nature* **307**, 745-747 (1984)

Klein-Hitpass, L., Ryffel, G.U., Heitlinger, E., and Cato, A.C. A 13 bp palindrome is a functional estrogen responsive element and interacts specifically with estrogen receptor. *Nucleic Acids Res.* **16**, 647-663 (1988)

Klinge, C.M. Estrogen receptor interaction with co-activators and co-repressors. *Steroids* **65**, 227-251 (2000)

Klinge, C.M., Brolly, C.L., Bambara, R.A., and Hilf, R. hsp70 is not required for high affinity binding of purified calf uterine estrogen receptor to estrogen response element DNA in vitro. *J. Steroid Biochem. Mol. Biol.* **63**, 283-301 (1997)

Kuiper, G.G., de Ruiter, P.E., Trapman, J. et al. Localization and hormonal stimulation of phosphorylation sites in the LNCaP-cell androgen receptor. *Biochem. J.* **291**, 95-101 (1993)

Kuiper, G.G., Enmark, E., Pelto-Huikko, M. et al. Cloning of a novel receptor expressed in rat prostate and ovary. *Proc. Natl. Acad. Sci. U. S. A* **93**, 5925-5930 (1996)

Kuiper, G.G., Lemmen, J.G., Carlsson, B. et al. Interaction of estrogenic chemicals and phytoestrogens with estrogen receptor beta. *Endocrinology* **139**, 4252-4263 (1998)

Lawley, P.D. Effects of some chemical mutagens and carcinogens on nucleic acids. *Prog. Nucleic Acid Res. Mol. Biol.* **5:89-131.**, 89-131 (1966)

Le Goff, P., Montano, M.M., Schodin, D.J., and Katzenellenbogen, B.S. Phosphorylation of the human estrogen receptor. Identification of hormone-regulated sites and

examination of their influence on transcriptional activity. *J. Biol. Chem.* **269**, 4458-4466 (1994)

Lebedeva, I., Rando, R., Ojwang, J. et al. Bcl-xL in prostate cancer cells: effects of overexpression and down- regulation on chemosensitivity. *Cancer Res.* **60**, 6052-6060 (2000)

Leclercq, G. Molecular forms of the estrogen receptor in breast cancer. *J. Steroid Biochem. Mol. Biol.* **80**, 259-272 (2002)

Lerner, L.J. and Jordan, V.C. Development of antiestrogens and their use in breast cancer: eighth Cain memorial award lecture. *Cancer Res.* **50**, 4177-4189 (1990)

Lin, H.K., Wang, L., Hu, Y.C. et al. Phosphorylation-dependent ubiquitylation and degradation of androgen receptor by Akt require Mdm2 E3 ligase. *EMBO J.* **21**, 4037-4048 (2002)

Lohrisch, C. and Piccart, M. HER2/neu as a predictive factor in breast cancer. *Clin. Breast Cancer* **2**, 129-135 (2001)

Lu, S., Liu, M., Epner, D.E. et al. Androgen regulation of the cyclin-dependent kinase inhibitor p21 gene through an androgen response element in the proximal promoter. *Mol. Endocrinol.* **13**, 376-384 (1999)

Lu, S., Tsai, S.Y., and Tsai, M.J. Regulation of androgen-dependent prostatic cancer cell growth: androgen regulation of CDK2, CDK4, and CKI p16 genes. *Cancer Res.* **57**, 4511-4516 (1997)

Makela, S., Savolainen, H., Aavik, E. et al. Differentiation between vasculoprotective and uterotrophic effects of ligands with different binding affinities to estrogen receptors alpha and beta. *Proc. Natl. Acad. Sci. U. S. A* **96**, 7077-7082 (1999)

Malkin, D., Li, F.P., Strong, L.C. et al. Germ line p53 mutations in a familial syndrome of breast cancer, sarcomas, and other neoplasms. *Science* **250**, 1233-1238 (1990)

Marcelli, M. and Cunningham, G.R. Hormonal signaling in prostatic hyperplasia and
neoplasia. *J. Clin. Endocrinol. Metab* **84**, 3463-3468 (1999)

Massaad-Massade, L., Massaad, C., Legendre, F. et al. A single d(GpG) cisplatin adduct
on the estrogen response element decreases the binding of the estrogen receptor.
FEBS Lett. **466**, 49-53 (2000)

Masters, J.R. and Koberle, B. Curing metastatic cancer: lessons from testicular germ-cell
tumours. *Nat. Rev. Cancer* **3**, 517-525 (2003)

McA'Nulty, M.M. and Lippard, S.J. The HMG-domain protein Ixr1 blocks excision
repair of cisplatin-DNA adducts in yeast. *Mutat. Res.* **362**, 75-86 (1996)

McInerney, E.M. and Katzenellenbogen, B.S. Different regions in activation function-1
of the human estrogen receptor required for antiestrogen- and estradiol-dependent
transcription activation. *J. Biol. Chem.* **271**, 24172-24178 (1996)

Medeiros, R., Vasconcelos, A., Costa, S. et al. Steroid hormone genotypes ARStuI and
ER325 are linked to the progression of human prostate cancer. *Cancer Genet.
Cytogenet.* **141**, 91-96 (2003)

Mello, J.A., Lippard, S.J., and Essigmann, J.M. DNA adducts of cis-
diamminedichloroplatinum(II) and its trans isomer inhibit RNA polymerase II
differentially in vivo. *Biochemistry* **34**, 14783-14791 (1995)

Montano, M.M., Ekena, K., Krueger, K.D. et al. Human estrogen receptor ligand activity
inversion mutants: receptors that interpret antiestrogens as estrogens and
estrogens as antiestrogens and discriminate among different antiestrogens. *Mol.
Endocrinol.* **10**, 230-242 (1996)

Montgomery, J.S., Price, D.K., and Figg, W.D. The androgen receptor gene and its
influence on the development and progression of prostate cancer. *J. Pathol.* **195**,
138-146 (2001)

Nawaz, Z., Lonard, D.M., Dennis, A.P. et al. Proteasome-dependent degradation of the human estrogen receptor. *Proc. Natl. Acad. Sci. U. S. A* **96**, 1858-1862 (1999)

Nazareth, L.V. and Weigel, N.L. Activation of the human androgen receptor through a protein kinase A signaling pathway. *J. Biol. Chem.* **271**, 19900-19907 (1996)

Nelen, M.R., Padberg, G.W., Peeters, E.A. et al. Localization of the gene for Cowden disease to chromosome 10q22-23. *Nat. Genet.* **13**, 114-116 (1996)

Obrero, M., Yu, D.V., and Shapiro, D.J. Estrogen receptor-dependent and estrogen receptor-independent pathways for tamoxifen and 4-hydroxytamoxifen-induced programmed cell death. *J. Biol. Chem.* **277**, 45695-45703 (2002)

Osborne, M.R., Hewer, A., Hardcastle, I.R. et al. Identification of the major tamoxifen-deoxyguanosine adduct formed in the liver DNA of rats treated with tamoxifen. *Cancer Res.* **56**, 66-71 (1996)

Pakdel, F., Le Goff, P., and Katzenellenbogen, B.S. An assessment of the role of domain F and PEST sequences in estrogen receptor half-life and bioactivity. *J. Steroid Biochem. Mol. Biol.* **46**, 663-672 (1993)

Pallis, L., Wilking, N., Cedermark, B. et al. Receptors for estrogen and progesterone in breast carcinoma in situ. *Anticancer Res.* **12**, 2113-2115 (1992)

Pascoe, J.M. and Roberts, J.J. Interactions between mammalian cell DNA and inorganic platinum compounds. I. DNA interstrand cross-linking and cytotoxic properties of platinum(II) compounds. *Biochem. Pharmacol.* **23**, 1359-1365 (1974)

Peto, J. and Mack, T.M. High constant incidence in twins and other relatives of women with breast cancer. *Nat. Genet.* **26**, 411-414 (2000)

Pieper, R.O., Futscher, B.W., and Erickson, L.C. Transcription-terminating lesions induced by bifunctional alkylating agents in vitro. *Carcinogenesis* **10**, 1307-1314 (1989)

Pil, P.M. and Lippard, S.J. Specific binding of chromosomal protein HMG1 to DNA damaged by the anticancer drug cisplatin. *Science* **256**, 234-237 (1992)

Poukka, H., Karvonen, U., Janne, O.A., and Palvimo, J.J. Covalent modification of the androgen receptor by small ubiquitin-like modifier 1 (SUMO-1). *Proc. Natl. Acad. Sci. U. S. A* **97**, 14145-14150 (2000)

Raffo, A.J., Perlman, H., Chen, M.W. et al. Overexpression of bcl-2 protects prostate cancer cells from apoptosis in vitro and confers resistance to androgen depletion in vivo. *Cancer Res.* **55**, 4438-4445 (1995)

Razandi, M., Alton, G., Pedram, A. et al. Identification of a structural determinant necessary for the localization and function of estrogen receptor alpha at the plasma membrane. *Mol. Cell Biol.* **23**, 1633-1646 (2003)

Rechsteiner, M. and Rogers, S.W. PEST sequences and regulation by proteolysis. *Trends Biochem. Sci.* **21**, 267-271 (1996)

Renan, M.J. How many mutations are required for tumorigenesis? Implications from human cancer data. *Mol. Carcinog.* **7**, 139-146 (1993)

Ricketts, D., Turnbull, L., Ryall, G. et al. Estrogen and progesterone receptors in the normal female breast. *Cancer Res.* **51**, 1817-1822 (1991)

Rink, S.M., Yarema, K.J., Solomon, M.S. et al. Synthesis and biological activity of DNA damaging agents that form decoy binding sites for the estrogen receptor. *Proc. Natl. Acad. Sci. U. S. A* **93**, 15063-15068 (1996)

Roche, P.J., Hoare, S.A., and Parker, M.G. A consensus DNA-binding site for the androgen receptor. *Mol. Endocrinol.* **6**, 2229-2235 (1992)

Roodi, N., Bailey, L.R., Kao, W.Y. et al. Estrogen receptor gene analysis in estrogen receptor-positive and receptor-negative primary breast cancer. *J. Natl. Cancer Inst.* **87**, 446-451 (1995)

Roy, A.K., Tyagi, R.K., Song, C.S. et al. Androgen receptor: structural domains and functional dynamics after ligand-receptor interaction. *Ann. N. Y. Acad. Sci.* **949**, 44-57 (2001)

Rundlett, S.E. and Miesfeld, R.L. Quantitative differences in androgen and glucocorticoid receptor DNA binding properties contribute to receptor-selective transcriptional regulation. *Mol. Cell Endocrinol.* **109**, 1-10 (1995)

Ruohola, J.K., Valve, E.M., Karkkainen, M.J. et al. Vascular endothelial growth factors are differentially regulated by steroid hormones and antiestrogens in breast cancer cells. *Mol. Cell Endocrinol.* **149**, 29-40 (1999)

Rutqvist, L.E., Cedermark, B., Fornander, T. et al. The relationship between hormone receptor content and the effect of adjuvant tamoxifen in operable breast cancer. *J. Clin. Oncol.* **7**, 1474-1484 (1989)

Sakr, W.A., Haas, G.P., Cassin, B.F. et al. The frequency of carcinoma and intraepithelial neoplasia of the prostate in young male patients. *J. Urol.* **150**, 379-385 (1993)

Sanchez, R., Nguyen, D., Rocha, W. et al. Diversity in the mechanisms of gene regulation by estrogen receptors. *Bioessays* **24**, 244-254 (2002)

Schule, R., Muller, M., Kaltschmidt, C., and Renkawitz, R. Many transcription factors interact synergistically with steroid receptors. *Science* **242**, 1418-1420 (1988)

Sheflin, L., Keegan, B., Zhang, W., and Spaulding, S.W. Inhibiting proteasomes in human HepG2 and LNCaP cells increases endogenous androgen receptor levels. *Biochem. Biophys. Res. Commun.* **276**, 144-150 (2000)

Shen, Z., Wen, X.F., Lan, F. et al. The tumor suppressor gene LKB1 is associated with prognosis in human breast carcinoma. *Clin. Cancer Res.* **8**, 2085-2090 (2002)

Simard, J., Dumont, M., Labuda, D. et al. Prostate cancer susceptibility genes: lessons learned and challenges posed. *Endocr. Relat Cancer* **10**, 225-259 (2003)

Singer, B. The chemical effects of nucleic acid alkylation and their relation to mutagenesis and carcinogenesis. *Prog. Nucleic Acid Res. Mol. Biol.* **15**, 219-284 (1975)

Slamon, D.J., Leyland-Jones, B., Shak, S. et al. Use of chemotherapy plus a monoclonal antibody against HER2 for metastatic breast cancer that overexpresses HER2. *N. Engl. J. Med.* **344**, 783-792 (2001)

Sliwkowski, M.X., Lofgren, J.A., Lewis, G.D. et al. Nonclinical studies addressing the mechanism of action of trastuzumab (Herceptin). *Semin. Oncol.* **26**, 60-70 (1999)

Smith, R.A., von Eschenbach, A.C., Wender, R. et al. American Cancer Society guidelines for the early detection of cancer: update of early detection guidelines for prostate, colorectal, and endometrial cancers. Also: update 2001--testing for early lung cancer detection. *CA Cancer J. Clin.* **51**, 38-75 (2001)

Sorenson, C.M. and Eastman, A. Influence of cis-diamminedichloroplatinum(II) on DNA synthesis and cell cycle progression in excision repair proficient and deficient Chinese hamster ovary cells. *Cancer Res.* **48**, 6703-6707 (1988a)

Sorenson, C.M. and Eastman, A. Mechanism of cis-diamminedichloroplatinum(II)-induced cytotoxicity: role of G2 arrest and DNA double-strand breaks. *Cancer Res.* **48**, 4484-4488 (1988b)

Speirs, V., Parkes, A.T., Kerin, M.J. et al. Coexpression of estrogen receptor alpha and beta: poor prognostic factors in human breast cancer? *Cancer Res.* **59**, 525-528 (1999)

Sporn, M.B. The war on cancer. *Lancet* **347**, 1377-1381 (1996)

Suzuki, H., Ueda, T., Ichikawa, T., and Ito, H. Androgen receptor involvement in the progression of prostate cancer. *Endocr. Relat Cancer* **10**, 209-216 (2003)

Taplin, M.E., Bubley, G.J., Shuster, T.D. et al. Mutation of the androgen-receptor gene in metastatic androgen-independent prostate cancer. *N. Engl. J. Med.* **332**, 1393-1398 (1995)

Tavtigian, S.V., Simard, J., Teng, D.H. et al. A candidate prostate cancer susceptibility gene at chromosome 17p. *Nat. Genet.* **27**, 172-180 (2001)

Tilley, W.D., Buchanan, G., Hickey, T.E., and Bentel, J.M. Mutations in the androgen receptor gene are associated with progression of human prostate cancer to androgen independence. *Clin. Cancer Res.* **2**, 277-285 (1996)

Toney, J.H., Donahue, B.A., Kellett, P.J. et al. Isolation of cDNAs encoding a human protein that binds selectively to DNA modified by the anticancer drug cis-diamminedichloroplatinum(II). *Proc. Natl. Acad. Sci. U. S. A* **86**, 8328-8332 (1989)

Trapman, J., Ris-Stalpers, C., van der Korput, J.A. et al. The androgen receptor: functional structure and expression in transplanted human prostate tumors and prostate tumor cell lines. *J. Steroid Biochem. Mol. Biol.* **37**, 837-842 (1990)

Treiber, D.K., Zhai, X., Jantzen, H.M., and Essigmann, J.M. Cisplatin-DNA adducts are molecular decoys for the ribosomal RNA transcription factor hUBF (human upstream binding factor). *Proc. Natl. Acad. Sci. U. S. A* **91**, 5672-5676 (1994)

Tsai, M.J. and O'Malley, B.W. Molecular mechanisms of action of steroid/thyroid receptor superfamily members. *Annu. Rev. Biochem.* **63**, 451-486 (1994)

Tyagi, R.K., Lavrovsky, Y., Ahn, S.C. et al. Dynamics of intracellular movement and nucleocytoplasmic recycling of the ligand-activated androgen receptor in living cells. *Mol. Endocrinol.* **14**, 1162-1174 (2000)

Uchida, K., Tanaka, Y., Nishimura, T. et al. Effect of serum on inhibition of DNA synthesis in leukemia cells by cis- and trans-(Pt (NH3) 2C1(2)). *Biochem. Biophys. Res. Commun.* **138**, 631-637 (1986)

Vlietstra, R.J., van Alewijk, D.C., Hermans, K.G. et al. Frequent inactivation of PTEN in prostate cancer cell lines and xenografts. *Cancer Res.* **58**, 2720-2723 (1998)

von Angerer, E., Prekajac, J., and Strohmeier, J. 2-Phenylindoles. Relationship between structure, estrogen receptor affinity, and mammary tumor inhibiting activity in the rat. *J. Med. Chem.* **27**, 1439-1447 (1984)

Weinberg, R.A. The retinoblastoma protein and cell cycle control. *Cell* **81**, 323-330 (1995)

Weir, H.K., Thun, M.J., Hankey, B.F. et al. Annual report to the nation on the status of cancer, 1975-2000, featuring the uses of surveillance data for cancer prevention and control. *J. Natl. Cancer Inst.* **95**, 1276-1299 (2003)

Weis, K.E., Ekena, K., Thomas, J.A. et al. Constitutively active human estrogen receptors containing amino acid substitutions for tyrosine 537 in the receptor protein. *Mol. Endocrinol.* **10**, 1388-1398 (1996)

Welshons, W.V., Krummel, B.M., and Gorski, J. Nuclear localization of unoccupied receptors for glucocorticoids, estrogens, and progesterone in GH3 cells. *Endocrinology* **117**, 2140-2147 (1985)

Wingo, P.A., Ries, L.A., Rosenberg, H.M. et al. Cancer incidence and mortality, 1973-1995: a report card for the U.S. *Cancer* **82**, 1197-1207 (1998)

Xu, J., Zheng, S.L., Komiya, A. et al. Germline mutations and sequence variants of the macrophage scavenger receptor 1 gene are associated with prostate cancer risk. *Nat. Genet.* **32**, 321-325 (2002)

Xu, Y., Traystman, R.J., Hurn, P.D., and Wang, M.M. Membrane restraint of estrogen receptor alpha enhances estrogen-dependent nuclear localization and genomic function. *Mol. Endocrinol.* **18**, 86-96 (2004)

Yang, L., Wang, L., Lin, H.K. et al. Interleukin-6 differentially regulates androgen receptor transactivation via PI3K-Akt, STAT3, and MAPK, three distinct signal

pathways in prostate cancer cells. *Biochem. Biophys. Res. Commun.* **305**, 462-469 (2003)

Ylikomi, T., Wurtz, J.M., Syvala, H. et al. Reappraisal of the role of heat shock proteins as regulators of steroid receptor activity. *Crit Rev. Biochem. Mol. Biol.* **33**, 437-466 (1998)

Zhang, Q.X., Borg, A., Wolf, D.M. et al. An estrogen receptor mutant with strong hormone-independent activity from a metastatic breast cancer. *Cancer Res.* **57**, 1244-1249 (1997)

Zhou, Z.X., Kemppainen, J.A., and Wilson, E.M. Identification of three proline-directed phosphorylation sites in the human androgen receptor. *Mol. Endocrinol.* **9**, 605-615 (1995)

Relevant Structures
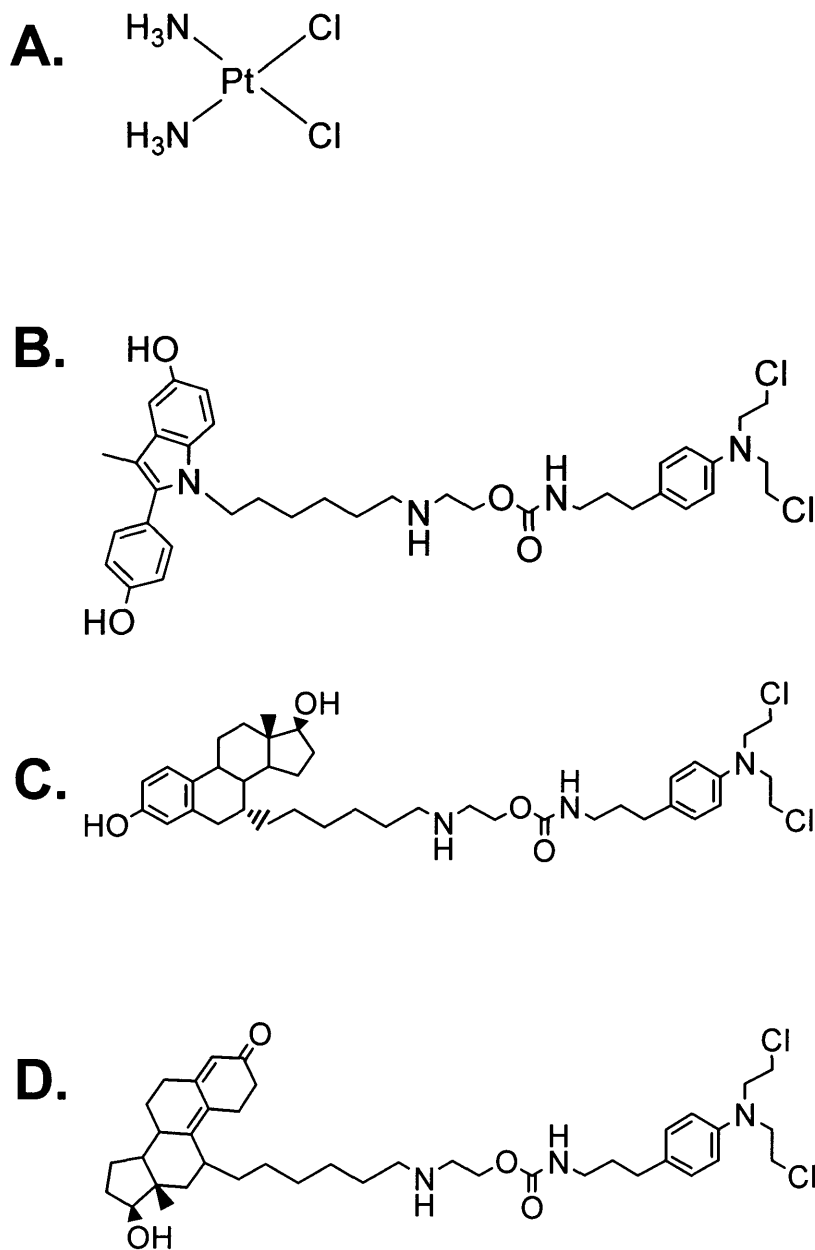
Fig 1.1 Structures of interest. **A.** *cis*-Diamminedichloroplatinum (II) (cisplatin) **B.** 2PI-C6NC2-mustard (2PI) **C.** E2-7α-C6NC2-mustard (E2-7α) **D.** 11β-C6NC2-mustard (11β)

Possible Mechanisms for the Toxicity of Cisplatin

Cell About to Experience
DNA Damage by
Cisplatin

Nuclear Protein
(hUBF, ER, AR, tsHMG)

Promoter

Genome

Expression of
Essential Gene

A. *Adduct Shielded From Repair*

DNA Repair
Complex

Adduct Persists

B. *Adduct Hijacks Transcription Factor*

Cell Death

Diminished Expression
of Essential Gene
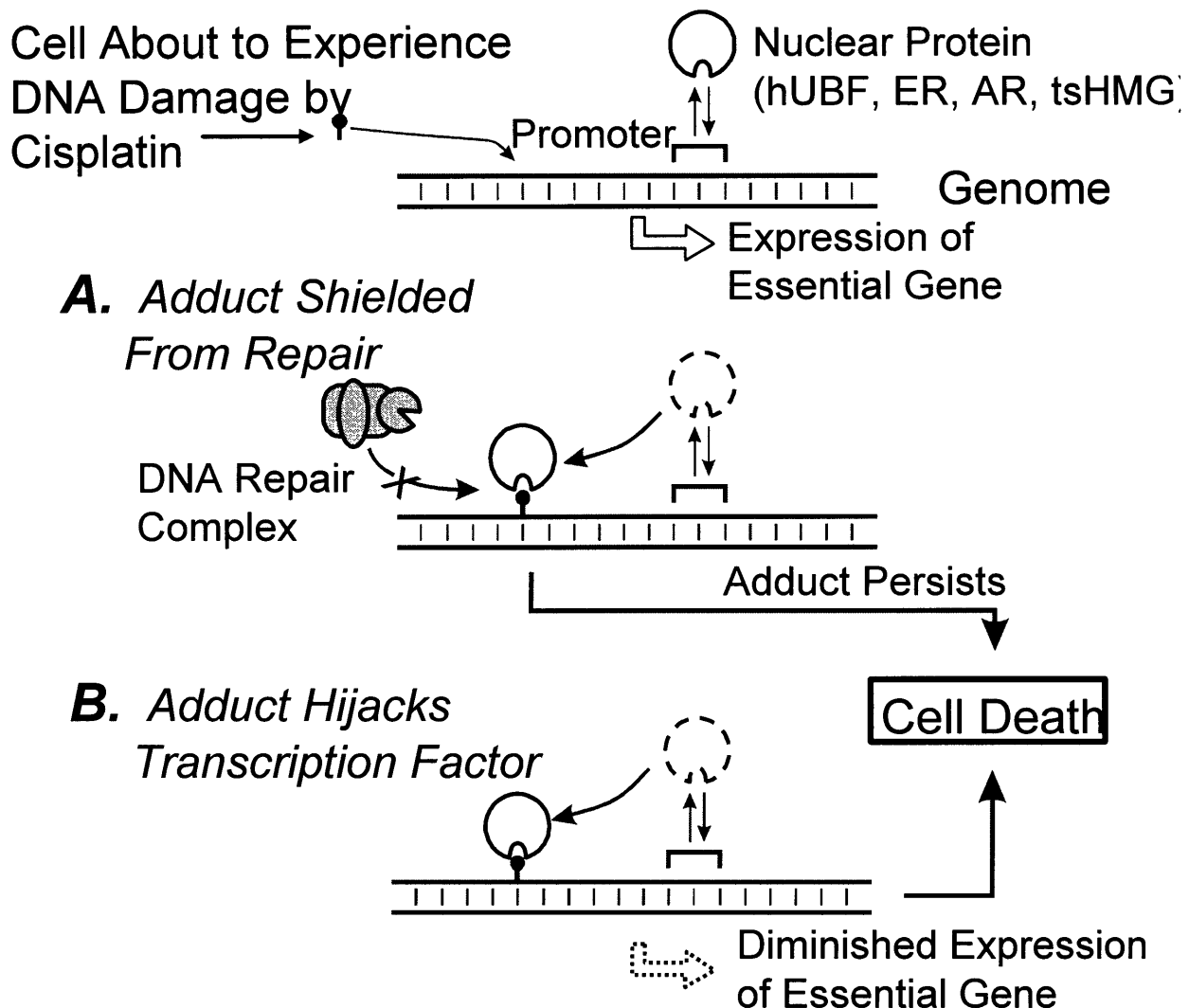
Fig 1.2 The cellular toxicity of cisplatin may be explained by the extremely tight interaction between DNA adducts and cellular proteins, such as HMG and hUBF. **A.** The interaction between a cisplatin-DNA adduct and a cellular protein may inhibit repair enzymes from accessing the damaged base, resulting in persistence of the adduct and thus toxicity to the cell. This has been coined the "repair shielding" mechanism. **B.** hUBF, a cellular transcription factor, binds to cisplatin adducts with a similar affinity to its cognate promoter sequence (Kd = 60 pM and 18 pM respectively). Therefore, a cisplatin-DNA adduct could hijack a transcription factor from expressing an essential gene and result in cell death. This has been coined the "transcription factor hijacking" mechanism.

A Novel Agent Designed to Inhibit Repair Processes in a Cancer Cell

Protein Recognition Domain

Warhead

Compound reacts with DNA

NON-CANCEROUS CELL

Repair Enzyme

BREAST CANCER CELL

Estrogen Receptor

Adduct is Repaired and Rendered Non-Toxic

Complex is Toxic to Cell
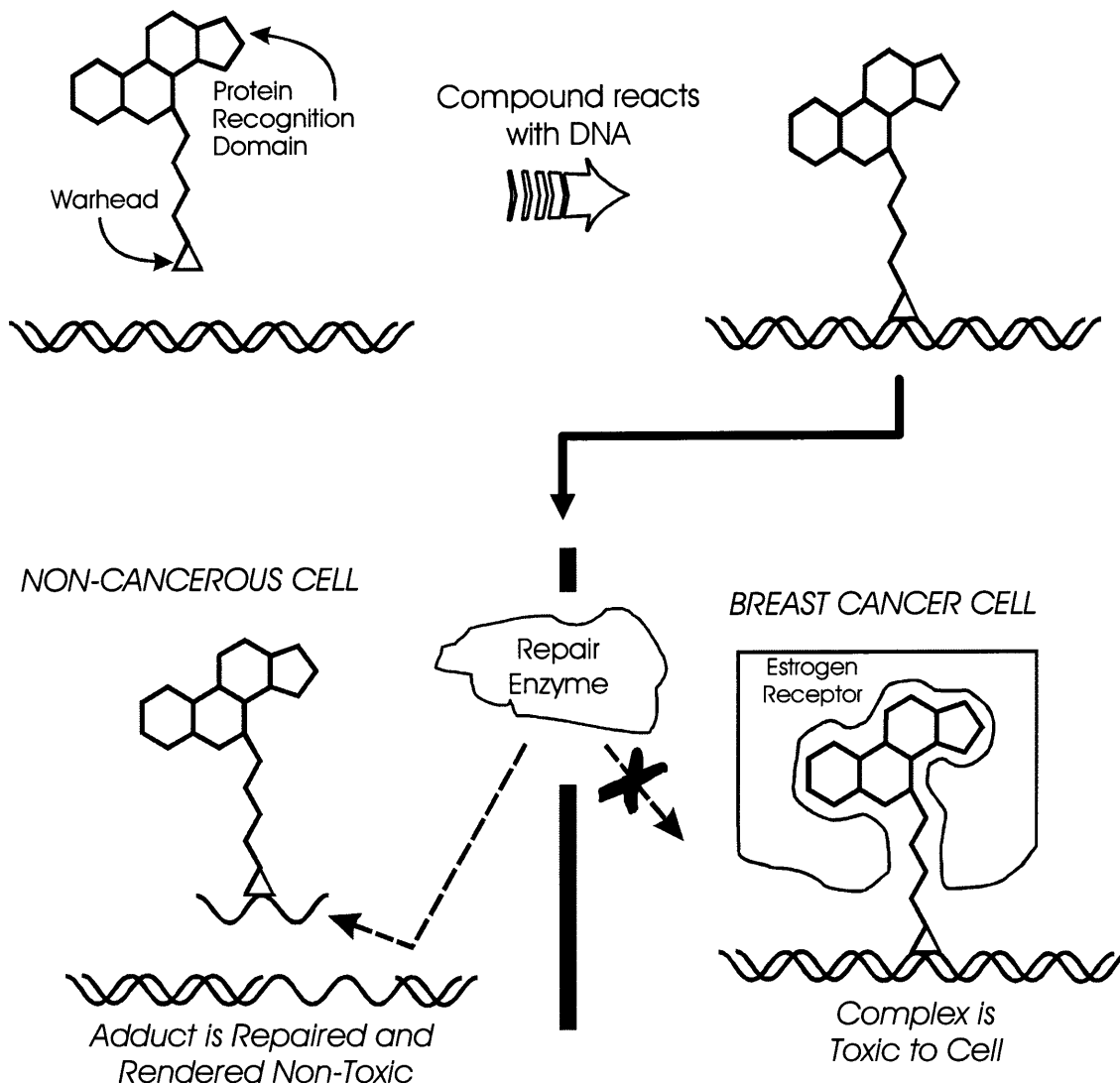
Fig 1.3 The compounds we designed consist of a protein recognition domain linked to a DNA damaging warhead (top left). This compound can covalently modify DNA within a cell (top right). In non-cancerous cells, the adduct is repaired and rendered non-toxic (lower left). In many cancer cells a tumor specific protein is aberrantly expressed, as is the case with the estrogen receptor (ER) in many breast cancers. An interaction between the ER and the protein recognition domain of the designed molecules could inhibit the repair of the adduct, render the complex toxic to the cancer cell and cause it to undergo apoptosis (lower right).

Structure and Binding Affinity for the Estrogen Receptor of 2-Phenyl-Indole Derivatives
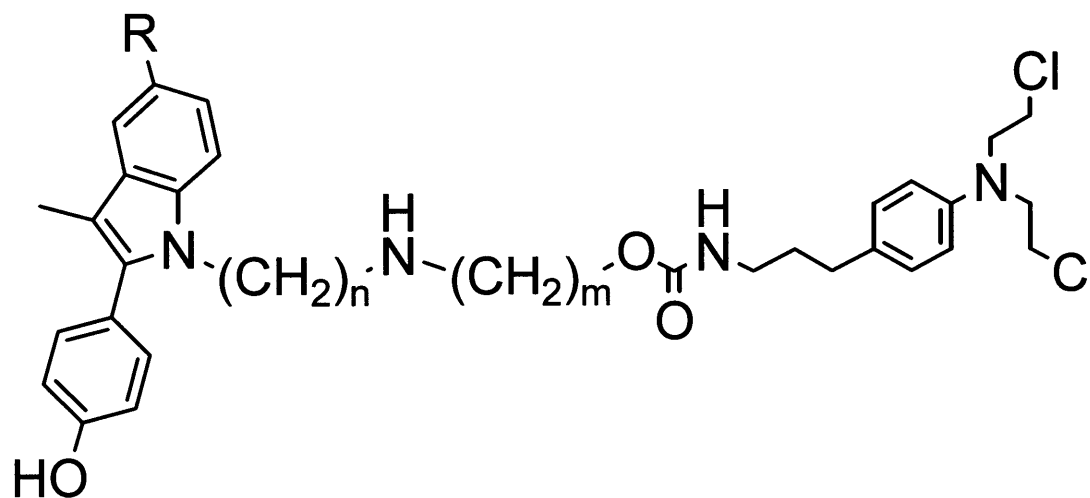
Mustard	m	n	R	RBA
2PI-C3NC3	3	3	OH	0
2PI-C5-NC3	3	5	OH	0.6
2PI-C6NC2	2	6	OH	7.1
2PI(OH)-C6NC2	2	6	H	0.1

Fig 1.4 Structures of aniline mustard conjugates and their corresponding relative binding affinity (RBA) for the ER.

Molecular Model of E2-7α Bound to the Estrogen Receptor-Ligand Binding Domain

E2-7α
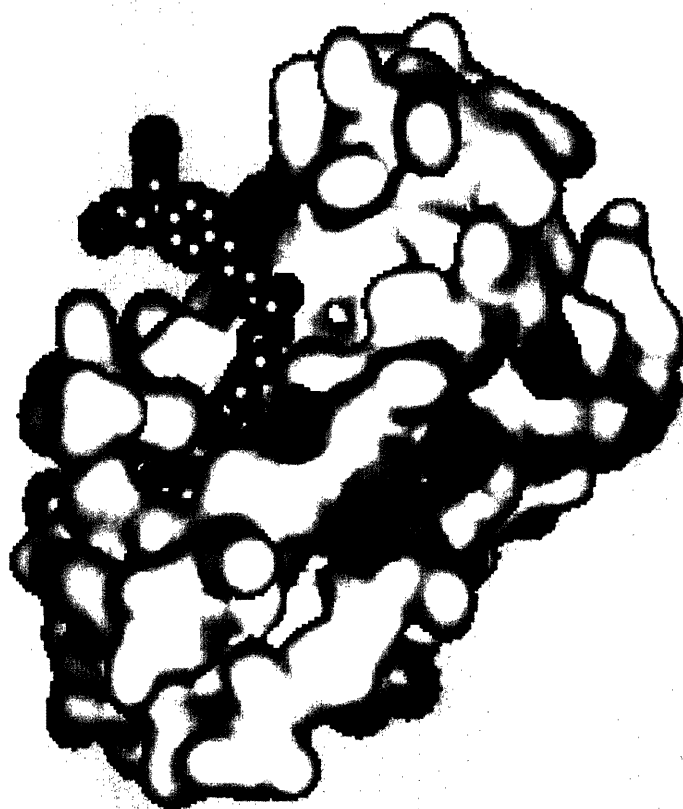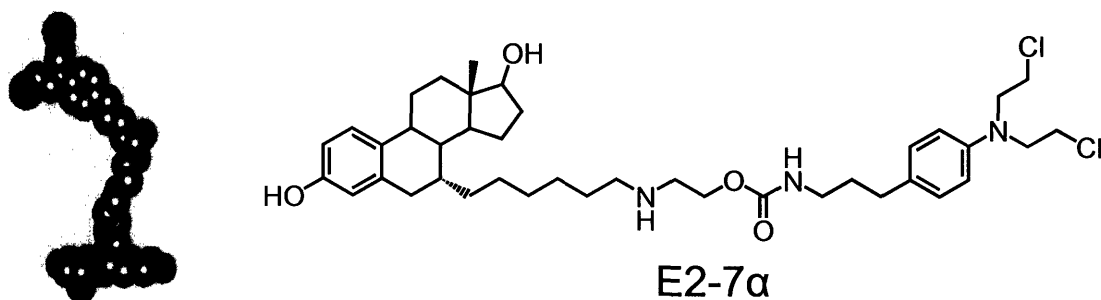
Fig 1.5 A molecular model of E2-7α with the ER-LBD. The 7α-hexanyl linkage is of sufficient length to transcend the hydrophobic binding pocket of the ER-LBD and the reactive aniline mustard is capable of forming an adduct with DNA when bound to the ER-LBD. (based on Pike et al. 2001 Structure 9, 145-153.)

Differential Toxicity of 2-Phenyl-Indole Derivatives in Estrogen Receptor (+/-) Cells
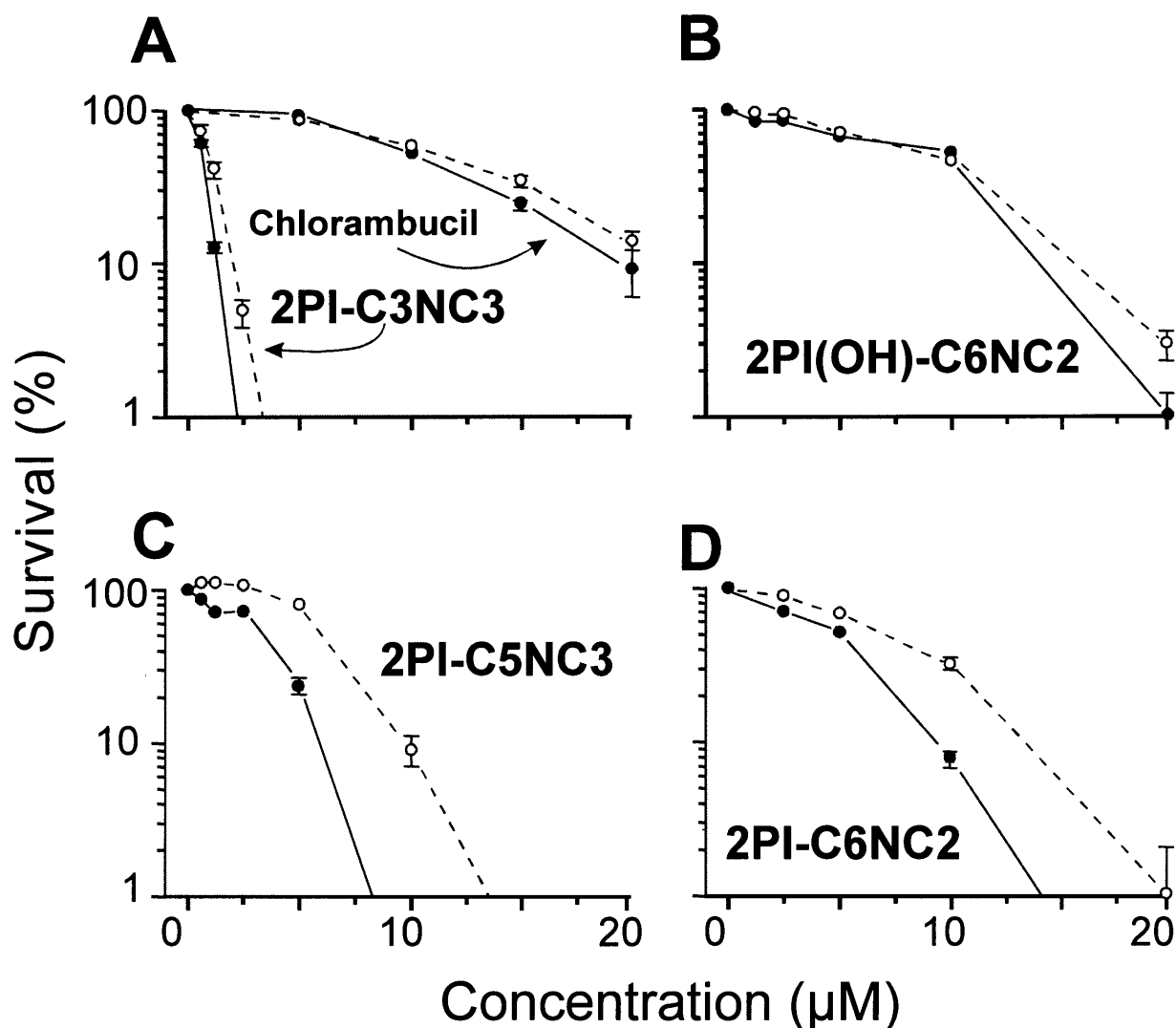
Fig 1.6 Survival curves for ER (+) MCF-7 (solid line) and ER (-) MDA-MB231 (dashed line) cells treated with various compounds. 2PI-C3NC3 **(A)**, chlorambucil **(A)**, and the monohydroxylated 2PI(OH)-C6NC2 **(B)**, which does not interact well with the ER, were equally toxic to both ER cell lines. Only the compounds that had the greatest affinity for the ER-LBD (those with the highest RBA in Fig 4), 2PI-C5NC3 **(C)** and 2PI-C6NC2 **(D)**, were selectively more toxic to the ER expressing MCF-7 cell line.

Chapter 2

Biophysical Properties of a Series of Compounds Designed to Selectively Target Estrogen Receptor Expressing Cancers

The work discussed in this chapter pertains to my contribution to the following publications:

1. Mitra K, Marquis JC, **Hillier SM,** Rye PT, Zayas B, Lee AS, Essigmann JM, Croy RG. A rationally designed genotoxin that selectively destroys estrogen receptor-positive breast cancer cells. J Am. Chem. Soc. 2002 Mar 6;124(9):1862-3.

2. Sharma U, Marquis JC, Nicole Dinaut A, **Hillier SM**, Fedeles B, Rye PT, Essigmann JM, Croy RG. Design, synthesis, and evaluation of estradiol-linked genotoxicants as anti-cancer agents. Bioorg. Med. Chem. Lett. 2004 Jul 16;14(14):3829-3833.

Although these publications contain work by several people, I shall focus on the experiments that I conducted. The results of others will be discussed (and referenced accordingly) to provide a complete story. The work from these two publications has established a ground work from which my subsequent experiments have been designed.

Introduction

Many antitumor agents produce their cytotoxic effect by covalently modifying DNA (Hurley 2002; Teicher 1997). The persistence of DNA damage produced by alkylating agents has lethal consequences for malignant cells. DNA repair enzymes that remove these lesions restore the integrity of the genome but limit the effectiveness of these drugs. Therefore, inhibition of the DNA repair machinery specifically in cancer cells is an attractive strategy to potentiate the therapeutic effects of alkylating chemotherapeutics (Barret and Hill 1998; Dolan 1997). Early work in the Essigmann laboratory has helped to illustrate this principle through studies on the effectiveness of the chemotherapeutic cisplatin.

cis-Diamminedichloroplatinum (II) (cisplatin) is a strikingly effective treatment for testicular and ovarian malignancies. It has a high cure rate of 95% in men treated for testicular cancer and is an effective initial treatment for ovarian cancer but is typically not curative. Investigations in our laboratory and others demonstrate that cisplatin forms DNA adducts that attract certain nuclear proteins and bind them with very high affinity (K_d values in the 60 pM range have been observed) (Donahue et al. 1990; Pil and Lippard 1992). These protein-adduct complexes are so tight that DNA repair enzymes are unable to gain access to the lesion for repair (Huang et al. 1994), leading to retention of the cytotoxic adducts and increased lethality. A second, non-mutually exclusive mechanism stems from the observation that the proteins that bind the most tightly to cisplatin adducts are often critical transcription factors. We have proposed (and found in one case) that the regulation of the genes controlled by these transcription factors is disrupted in the presence of cisplatin adducts (Treiber et al. 1994; Zhai et al. 1998). These two mechanisms, DNA adduct repair shielding and transcription factor hijacking, may explain the unusual effectiveness of cisplatin against germ cell malignancies (Kartalou and Essigmann 2001).

The repair shielding and transcription factor hijacking mechanisms discovered for cisplatin have become the basis for our design of novel anticancer agents targeted against breast and prostate cancers. Our drug design strategy takes advantage of the fact that these tumors selectively express certain proteins. For example, over half of human breast cancers express the estrogen receptor (ER) (Ferno et al. 1990), and most prostate cancers express the androgen receptor (AR) (Hobisch et al. 1995; Marcelli and Cunningham

78

1999) and progesterone receptor (PR)(Bonkhoff et al. 2001). We reasoned that if these abundant tumor specific proteins could be attracted to the sites of DNA adducts, then increased toxicity could be achieved in tumor cells by the repair shielding mechanism. In addition, since all three of these hormone receptors are transcription factors, their association with DNA lesions could disrupt the genes critical for growth and survival as is the case with current antihormonal therapies for breast and prostate malignancies (Bruckheimer, Gjertsen, and McDonnell 1999; Kozlowski, Ellis, and Grayhack 1991; Kreis 1995; Peto and Mack 2000; Santen 1992).

As a proof of concept and in an effort to design novel anticancer agents rationally, a series of compounds containing a protein recognition domain that could attract tumor specific proteins was linked to a DNA damaging warhead that could covalently modify DNA. These compounds initially consisted of *N,N*-bis-chloroethylaniline connected to a 2-phenylindole group by alkyl-amino-carbamate linkers of various lengths (Rink et al. 1996). 2-Phenylindole was chosen for the protein recognition domain of the molecule because studies have shown it interacts well with the ER in competitive binding experiments with estradiol (von Angerer, Prekajac, and Strohmeier 1984). *N,N-bis*-Chloroethylaniline is a nitrogen mustard that is capable of covalently modifying DNA, most commonly at the N7 position of guanine. Investigations with these derivatives identified several molecular characteristics of the linker that were important for the compound to react with DNA and bind to the ER. These features were discussed in Chapter 1.

Of all the compounds tested by Rink, et al., 2PI-C6NC2-mustard was determined to have an optimal balance of properties suitable for an agent designed to shield adducts from repair and to hijack the ER from its role as a transcription factor, these being affinity for the ER both alone and when covalently adducted to DNA, reactivity with DNA, lethality towards breast cancer cell lines, and selective toxicity in favor of ER(+) cell lines over ER(−). 2PI-C6NC2-mustard served as a proof of concept that it is possible to rationally design an agent that could form DNA adducts and that these adducts could serve as molecular decoys capable of hijacking the ER from its natural targets. The results implicated the transcription factor hijacking and repair shielding mechanisms as possible explanations for the observed selective toxicity (Rink et al. 1996).

Despite the promising results with these initial findings, we reasoned that an agent with a higher affinity for the ER may be more potent in selectively killing ER(+) breast cancer. In this effort, the 2-phenylindole group was replaced by 17β-estradiol at the 7α position. The site of substitution of estradiol in E2-7α was based on reports that relatively large alkyl groups can be attached at the 7α position with retention of high affinity for the ER (Bowler et al. 1989; Bucourt, Vignau, and Torelli 1978; DaSilva and van Lier 1990). The work by Mitra, et al., utilized the same C6NC2 linker as by Rink, et al., described in Chapter 1. However, Sharma, et al. systematically studied the linker by substituting C6NC2 with seven other novel linkers. The modified linkers retain the six carbon chain that appears to be essential for the attached ligand to fit into the estradiol binding pocket of the ER (Brzozowski et al. 1997; Rink et al. 1996). Amino, amido, and guanidino groups were incorporated into the region connecting the hexanyl-substituted estradiol and the aniline mustard. These changes were designed to probe linker variations that could provide a less complex synthesis, improved DNA adduction, enhanced ER binding, increased water solubility, and/or increased selective toxicity towards ER(+) breast cancer cells.

The work described in this chapter will focus on E2-7α and its derivatives. The synthesis of these molecules will not be covered as their syntheses have been previously documented (Mitra et al. 2002; Sharma et al. 2004). However, the reactivity of E2-7α with DNA and the identification of these DNA adducts by mass spectrometry will be given considerable attention. The kinetics of DNA adduction by E2-7α over time will also be described.

Additionally, the partition coefficient (log P) for E2-7α and its derivatives will be discussed in some detail. The log P can be predictive of aqueous solubility, absorption, and permeability (Hansch and Fujita 1964; Leo, Hansch, and Elkins 1971). Octanol is used to mimic the phospholipid cellular membrane and water is used to mimic the cytosol. Therefore, the amount of drug that partitions between the two solvents helps describe the potential of a drug to enter a cell. Lipinski, in 1997, coined the "rule of five" to describe a compounds "drugability" (Lipinski et al. 1997). Lipinski claimed an ideal drug has the following properties: a log P < 5, the # of H bond acceptors < 10, the # of H bond donors < 5, and a molecular weight < 500. Additionally, the log P of a compound can provide an estimate of how the drug will be excreted and what routes of

administration would most likely be used: log P < 0: injectable, log P 0-3: oral, log P 3-4: transdermal, log P 4-7: not ideal because of a toxic buildup in fatty tissues.

There are several ways to measure a log P, the most common of which is the shake-flask method. In this method, the drug of interest is placed in a mixture of octanol and water, and this mixture is quickly shaken. The concentration of drug in the octanol phase and in the aqueous phase is measured. The Log P value is calculated by taking the log of the ratio of the concentration of drug in the octanol phase divided by the concentration in the aqueous phase. Alternative means of calculating a log P are by computer simulation, slow stir-flask, generator column, and HPLC. I shall discuss my results with several of these methods and some of their limitations. The log D, the log P at physiological pH of 7.4, was then calculated based on the experimentally determined log P (Donovan and Pescatore 2002).

Finally, I will provide reference to the remaining experiments in Mitra, et al. and Sharma, et al. (Mitra et al. 2002; Sharma et al. 2004). Specifically, I shall discuss the RBA, the amount of DNA adduction as assessed by piperidine cleavage, the ability of DNA adducts to interact with the ER-LBD, and the selective toxicity towards ER(+) cell lines for E2-7α and its derivatives. Although I did not directly conduct these experiments, I believe it is important to discuss them in brief as they have provided the groundwork for the remainder of my research.

Materials and Methods

Synthesis. The complete chemical synthesis of all estradiol-linked genotoxicants has been conducted by various members of the Essigmann laboratory. The work was described in Mitra, et al.(Mitra et al. 2002) and Sharma, et al. (Sharma et al. 2004).

Covalent Modification of DNA by E2-7α. pGEM-7fz plasmid DNA (150 μg, Promega) was dissolved in 270 μL of 10mM Tris-HCl/1 mM EDTA (pH 8). [^{14}C]-E2-7α (specific activity 53 mCi/mmol, dissolved in DMSO) was added to this solution to obtain a final concentration of 100 μM E2-7α, 10% DMSO by volume. This mixture was incubated at 37°C and 50 μL aliquots were removed at 0, 0.5, 1, 2, 4, 6, and 24 hours. Non-covalently bound E2-7α was removed by extraction with phenol:chloroform:isoamyl alcohol (25:24:1) and subsequent ethanol precipitation. The DNA was dried *in vacuo* and

redissolved in 100 μL of 10 mM Tris-HCl/1 mM EDTA (pH 8). DNA concentration was determined by absorbance at 260 nm and radioactivity was measured by scintillation counting.

Mass Spectrometric Analysis of E2-7α DNA Adducts. Reaction of DNA with E2-7α was performed on a larger scale to obtain sufficient material for structural analysis of covalent products. Salmon testes DNA (20 mg, Sigma-Aldrich) was dissolved in 20 mL of 5 mM sodium cacodylate, 25% *N,N*-dimethlyformamide. To the DNA solution was added 100 μL of 10 mM E2-7α in DMSO, and the final concentration of E2-7α was 50 μM. After incubation for 16 hours at 37 °C, unbound E2-7α was removed by extraction with phenol:chloroform:isoamyl alcohol (25:24:1) and subsequent ethanol precipitation. The DNA was then reconstituted in water and subsequently hydrolyzed in 0.1 N HCl for 30 min at 70°C. The solution was then neutralized with 1N NaOH and adjusted to 20 mM Tris-HCl (pH 7.4), 10% methanol. The hydrolyzed DNA was loaded onto a C18 Sep-Pak® (Waters Co.) column and eluted sequentially with 10 mL of 10% and 50% aqueous methanol solutions and finally with 100% methanol. The 100% methanol fraction was reduced *in vacuo* and analyzed by HPLC and mass spectrometry. HPLC analyses were performed using a Beckman ODS 4.6 x 250 mm Ultrasphere column eluted at 1 mL/min with a 20 min linear gradient of 50% 0.1 M ammonium acetate/10% acetonitrile, 50% methanol to 100% methanol. Aliquots of samples obtained from HPLC fractionation were analyzed by electrospray ionization mass spectrometry (ESI-MS) using flow injection (0.2 mL/min) in methanol:water:acetontrile (50:45:5) in positive ion mode. The mass spectrometric analysis was conducted with the help of John Wishnok and Beatrice Zayas.

Determination of the Partition Coefficient (log P):

Computer Simulation: The structure of various reference compounds and the E2-7α derivatives were entered into the following web sites: 1. www.logp.com and 2. www.molinspiration.com. The log P of the reference compounds determined by the

computer simulations were compared to experimentally derived log P values found in the literature to test the accuracy of these simulations.

HPLC: The log P of all compounds was determined by the HPLC method of Donovan and Pescatore. (Donovan and Pescatore 2002) Briefly, 1 mg of the test compound was dissolved in 1 mL internal standard solution, which consisted of 2 mL toluene and 20 mg triphenylene dissolved in 200 mL of methanol. The compound/internal standard solution (2 μL) was injected into a Rainin HPLC with an octadecyl poly(vinyl alcohol) (ODP-50) 20x4 mm, 5 μm, 250 Å pore size column (Supelco), 10-100% 0.01 M sodium phosphate(pH 7)/methanol gradient over 9.4 min, and a flow rate of 1.5 mL. The compounds were detected at 260 nm by a Dynamax UV-1 detector. The log P of the test compound is calculated by Equation 2.1. The log D at physiological pH was calculated based on the equation derived by Horvath, Equation 2.2 (Horváth, Melánder, and Molnár 1977).

Results

E2-7α Modifies DNA Covalently. In order to achieve selective toxicity towards ER(+) cancer cells, E2-7α must be capable of forming DNA adducts and attracting tumor specific proteins. ^{14}C-E2-7α was incubated with pGEM-7fz plasmid and aliquots were removed at various intervals to test the ability of E2-7α to form stable DNA adducts. E2-7α covalently modifies DNA at a rate of 13.1 DNA adducts per plasmid per hour during the first 6 hours (Fig 2.1A). This rate of adduction eventually diminishes, as evident by Figure 2.1B. Between 6 and 24 hours E2-7α covalently modifies DNA at a much slower rate of 3.4 adducts per plasmid per hour.

E2-7α Forms DNA Adducts with Guanine Residues. The reaction of E2-7α with DNA was then performed on a larger scale in order to analyze the nature of the covalently modified DNA. Full scan ESI-MS analysis of the material that eluted at 14.5 min by HPLC (Fig 2.2A) revealed a prominent signal at m/z 813.5 (Fig 2.2B). A separate high resolution mass spectrometric analysis (not shown) provided an m/z of 813.5051 (812.4949 calculated). Collision induced decay (CID) on the 813.5 molecular ion yielded prominent fragment ions at m/z 662.3 and 372.1 (Fig 2.3). The 813.5 mass and the resulting CID are consistent with a chemical structure in which one ethylene arm of the

mustard of E2-7α is attached to guanine and the other has a substituted hydroxyl group for the chlorine atom (Fig 2.4, left panel). As shown in Figure 2.4 (left), these ions are consistent with the loss of the guanine fragment from the adduct (m/z 662.3) and from the fragmentation of the proposed structure at the secondary amino group in the linker (m/z 372.1). Confirmation of these structures and of the 813.5 molecular ion resulting from an E2-7α-Guanine adduct was provided by analysis of covalent products from a tetradeuterated analog of E2-7α (d_4-E2-7α). HPLC and ESI-MS analysis of the hydrolysis products of d_4-E2-7α under identical conditions identified a compound that formed a molecular ion of 817.5 (a separate high resolution mass spectrometric analysis, not shown, provided an m/z of 817.4120, 816.5200 calculated) with the same retention time as the compound that produced the m/z 813.5 ion. This result is consistent with a d_4-E2-7α-Guanine adduct (Figure 2.4, right panel). CID on the 817.5 molecular ion yielded fragment ions of m/z 666.5 and 372.1, indicating that the m/z 666.5 ion contained the deuterated portion of the molecule while the m/z 372.1 did not (Fig 2.5). These results support the proposed structure for the E2-7α-Guanine adduct and the proposed fragmentation pattern.

The Log P of the E2-7α Derivatives Encompass a Wide Range of Values. The log P of a compound can be predictive of aqueous solubility, absorption, and permeability (Lipinski et al. 1997). The lipophilicity of E2-7α and its derivatives were assessed by the HPLC method of Donovan and Pescatore (Donovan and Pescatore 2002). Prior to settling on the HPLC methodology, computer simulations were employed in an effort to narrow the potential log P range of our series of compounds so a suitable methodology could be used. The structures of a series of reference compounds (including estradiol, testosterone, progesterone, chlorambucil, and decachlorobiphenyl) (Fig 2.6) and the E2-7α homologues (Fig 2.7) were entered into two websites, www.logP.com and www.molinspiration.com. The reference compounds were chosen because they are structurally related to our compounds – estradiol is the protein recognition domain and chlorambucil is a nitrogen mustard similar to the warhead of our compounds. Decachlorobiphenyl has the highest experimentally determined log P and was used as an upper limit on hydrophobicity. Unfortunately, the values obtained from the websites did not correlate well with the values published in the literature (Table 2.1) (De Bruijn et al.

1989; Donovan and Pescatore 2002; Greig et al. 1990). In fact, the computer simulations seemed to overestimate the log P in nearly every case.

Nonetheless, these results suggested that our compounds were relatively lipophilic and therefore the best methodology of determining the log P of our series of compounds was to use HPLC. The reference compounds (mentioned above) were first used to test the HPLC methodology of Donovan and Pescatore (Donovan and Pescatore 2002). As seen in Table 2.2 the HPLC derived log P values of the reference compounds correlated very well with the values found in the literature. This gave confidence in the HPLC methodology, so the log P of the neutral form of E2-7α and its derivatives were determined using this approach. A representative HPLC chromatogram is shown in Figure 2.8. E2-7α (11.52 min) is bracketed by toluene (8.53 min) and triphenylene (12.72 min). The log D at pH 7.4 was estimated using an equation derived by Horvath et al (Horváth, Melánder, and Molnár 1977). Table 2.3 displays the log P and log D values of the 8 compounds. In all cases the computer simulations grossly overestimated the log P values obtained by HPLC. The log D values in Table 2.3 indicate that the aqueous solubility of the eight compounds span approximately a 2500-fold range under physiological conditions.

Discussion

Covalent Modification of DNA by E2-7α and Identification of Adducts by Mass Spectrometric Analysis. The ability of E2-7α to modify DNA covalently was investigated by incubating the compound with pGEM-7zf plasmid and removing aliquots at various time intervals. The amount of radioactivity bound to DNA increased at an apparent zero order rate of 13.1 adducts/plasmid/hour for the first 6 hours, indicative of the formation of covalently bound E2-7α DNA adducts. However, between 6 and 24 hours, the rate of DNA adduction dramatically decreased to 3.4 adducts/plasmid/hour indicating a pseudo-first order rate as the reactant, E2-7α, was consumed. This perhaps is not surprising as the effective concentration of E2-7α would diminish over time as a result of DNA adduct formation and decomposition (through hydrolysis) of the reactive aniline mustard.

The clinically used nitrogen mustard, chlorambucil, has a half-life of only 18 minutes in a non-nucleophilic 0.2 M cacodylic acid solution at 37°C. The predominant

decomposition product is the inactivation of the *N,N-bis*(2-chloroethyl) arms of the mustard through hydrolysis yielding an *N,N*-bis(2-hydroxyethyl) substituted product (Haapala et al. 2001). The rapid decomposition of chlorambucil is a result of an intramolecular, rate-determining attack of the deprotonated nitrogen atom to form an aziridinium ion intermediate followed by attack of an external nucleophile (such as water) (Chatterji, Yeager, and Gallelli 1982; Kundu, Schullek, and Wilson 1994; Owen and Stewart 1979). Hence, chlorambucil (and other nitrogen mustards) is a reactive compound that decomposes rapidly in aqueous solutions and forms covalent bonds with other nucleophiles. When chlorambucil does react with DNA, the most common stable end product is at the N7 position of guanine (Haapala et al. 2001). It has been well-documented in the literature that alkylating agents typically form covalent adducts with the N7 position of guanine (and the N3 position of adenine) because of the highly nucleophilic nature of the nitrogen atom (Roberts 1978; Singer and Grunberger 1983; Singer and Kusmierek 1982).

Since we had shown that E2-7α is capable of adducting DNA, we investigated whether it would act analogously to chlorambucil and predominantly adduct the N7 position of guanine. E2-7α was incubated with DNA to form covalent adducts. These adducts were isolated and analyzed by ESI-MS. A molecular ion of 813.5 m/z was obtained which is consistent with one arm of the nitrogen mustard adducted to guanine and the other arm being hydroxylated. Furthermore d_4-E2-7α yielded a molecular ion of 817.5 m/z with the same retention time as the 813.5 m/z and the CID of both molecules are identical with the exception that the tetradeuterated molecule had one breakdown product with a + 4 m/z. These ESI-MS results illustrate that E2-7α forms DNA adducts with guanine in a similar manner as to what has previously been reported with chlorambucil (Haapala et al. 2001).

The Partition Coefficient (log P): In an effort to predict the toxicological and pharmacokinetic properties of a substance, Hansch and Fujita implemented a method for correlating the lipophilicity of a molecule with biological activity (Hansch et al. 1962; Hansch and Fujita 1964). They used a simple biphasic solution consisting of equal parts octanol and water. A test compound is added to the solution and briefly shaken; hence the procedure is termed the "shake-flask" method. The log P is calculated as the log of

the ratio of the concentration of compound in the octanol phase divided by the concentration in the aqueous phase. Octanol is now the most widely accepted reference system because of its high correlation of physicochemical properties with biomembranes (Leo, Hansch, and Elkins 1971; Walter, Brooks, and Fisher 1985). Despite the foresight of Hansch and Fujita, their methodology has a major drawback: the log P of the test compound is only accurate if it is < 5. Therefore, alternative means of determining the partition coefficient have been established.

In an effort to estimate the log P of our compounds and focus on an experimental methodology, computer simulation was initially incorporated to provide an initial, albeit crude, value. Two websites were used: www.logp.com and www.molinspiration.com. Reference compounds were chosen because they resemble the E2-7α derivatives and have experimentally determined values: chlorambucil is a nitrogen mustard similar to the warhead in E2-7α, estradiol is the protein recognition domain of E2-7α, progesterone and testosterone are other steroids similar in structure to estradiol, and decachlorobiphenyl has the highest experimentally determined log P. These compounds give a range of log P values and are very representative of our series of compounds. Unfortunately, the calculations for the reference compounds did not correlate very well with their experimentally derived values (De Bruijn et al. 1989; Donovan and Pescatore 2002) (Table 2.1). In all cases, the computer simulations resulted in higher log P values than those determined experimentally (note the good correlation found between the literature values and the HPLC methodology that was eventually employed, as seen in Table 2.2). Calculated Log P values are typically estimated by the hydrophobic fragment approach of Rekker (Rekker 1976) or by the approach of Leo and Hansch (Leo 1993; Leo et al. 1975). Significant deviations between predicted and experimental log P values occur when the pattern of connectivity and non-bonded intramolecular interactions are unfamiliar to the database upon which these methodologies rely (Bodor, Gabanyi, and Wong 1989). Neither www.molinspiration.com nor www.logp.com provided information on which methodology they use (although molinspiration.com did indicate that their calculations were likely to be less accurate than the CLogP program available through ACD Labs).

Despite the inherent error found in the computer calculated log P values for the reference compounds, E2-7α and its derivatives were still entered into the websites in an effort to provide a crude estimate of their log P. This data was then used to decide upon

an experimental methodology. The log P of E2-7α and its derivatives were estimated to be between 5 and 9 with the majority of the derivatives > 8 (Table 2.1). Starting with such lipophilic compounds ruled out the traditional shake-flask method of Hansch and Fujita. However, the slow-stir flask method was initially considered as an option. The slow-stir method has been used to experimentally determine the log P of decachlorobiphenyl (8.23) (De Bruijn et al. 1989). This methodology uses a small volume of octanol (i.e. 1-50 mL) and a much larger volume of water (i.e. 950-999 mL) buffered with 0.1 M sodium phosphate and pH adjusted to 7.4 (similar salt concentration and pH as found in human blood). The solutions are pre-saturated in order to account for the small mutual miscibility of the two solvents. The compound is added to the octanol and the biphasic solution is stirred for several hours (or days) with aliquots removed until equilibrium is reached (for highly lipophilic compounds often 3-7 days later). The log P is calculated based on the concentration in each layer. Although this method was initially tested, it was soon proved to be inadequate due to the large volumes that would have been necessary to obtain a valid log P value. Additionally, it is very time consuming and would have required extremely precise measurements of test compound concentrations.

Therefore, the HPLC method of Donovan and Pescatore was tested. The main advantages of this method are speed, simplicity, and theoretically any log P value can be obtained. Methanol is used as the organic mobile phase, instead of acetonitrile, because of its hydrogen bonding capability and better correlations to traditional log P methodologies (Cimpan et al. 1998; Cole, Dorsey, and Dill 1992). Vallat et al. have shown that the ODP-50 columns measure the log P with good accuracy (Vallat et al. 1992) and these columns can accommodate a wide range of pH buffers (2-13). The internal standards allowed for corrections in the subtle differences in flow-rate and percent composition from run to run. Additionally, toluene and triphenylene are easily monitored at 260 nm.

As shown in Table 2.2, this HPLC methodology provides accurate analysis of the log P of a wide variety of compounds. The results in Table 2.3 illustrate the range of log D values of the E2-7α derivatives. Three compounds, the diamide, amide, and carbamate, have log D values of 4.85, 5.07 and 5.61 respectively. With such high log D values it is unlikely these molecules would make good drug candidates as a result of the likely toxicity to fat tissue and poor bioavailability. However, the diamine, E2-7α (amine

carbamate), guanidine, amine, and amine guanidine had log D of 2.22, 2.22, 2.52, 2.87, and 3.12, respectively, all of which could potentially be formulated for oral administration and have favorable bioavailability.

Despite the favorable log D values obtained for many of the E2-7α derivatives, further research is required prior to claiming to have a successful drug candidate. Our series of molecules has been designed with two key features in mind: (1) the ability to covalently modify DNA and (2) the ability to interact with the ER in order to inhibit the repair of DNA adducts and to titrate the ER from its necessary cellular role as a transcription factor. A successful drug candidate would have the ability to accomplish both of these feats in order to achieve selective toxicity in ER expressing cells or tumors. I have shown that E2-7α covalently modifies DNA, but, as of yet, I have not mentioned its ability to interact with the ER. Below I shall briefly summarize the experiments conducted by several members of the Essigmann laboratory who have shown the extent to which the E2-7α derivatives can modify DNA, bind to the ER both free in solution and when adducted to DNA, and achieve selective toxicity in favor of ER expressing cells. I shall not discuss experimental detail as it can be found in Mitra, et al. and Sharma, et al. (Mitra et al. 2002; Sharma et al. 2004). I shall however, provide a summary of the findings, their implications and the relationship with the log D values I have determined.

Covalent modification of DNA by the E2-7α derivatives. The reactivity of each compound with DNA was assessed by its ability to produce piperidine-labile sites in the self complimentary deoxyoligonucleotide 5'-d(AATATTGGCCAATATT) by Bogdan Fedeles. The results in Table 2.4, column 3 (% DNA Adduction) indicate the percent of the oligonucleotide that was cleaved by piperidine. The diamine produced the greatest number of DNA adducts, with 79% of the oligonucleotide cleaved by piperidine, whereas the carbamate produced the least number of adducts with only 3% of the oligonucleotide cleaved. Modification of the carbamate to an amido resulted in a 5-fold increase in adduction to 14%. The presence of a cationic species within the linker tended to increase the formation of DNA adducts, for example, adding an amine to the carbamate linker increased the adduction by over 10-fold (carbamate 3%, amine carbamate 45%). Additionally, the amine (44%), guanidine (58%), and the amine guanidine (29%), which would all be cationic under experimental conditions, illustrated significant levels of

adduction. It is likely that the presence of a cationic species within the linker would localize the reactive alkylating group in the vicinity of nucleophilic atoms within (anionic) DNA. A similar result has been reported for a conjugate of chlorambucil with the polyamine spermidine (Holley et al. 1992).

Affinity of the E2-7α derivatives for the estrogen receptor. The affinity of our compounds for the ER was assessed both when free in solution and when adducted to DNA. Nicole Dinaut used a radiometric competitive binding assay (Pike et al. 2001) with rabbit uterine ER to determine the RBA of each compound for the ER as compared with estradiol (by definition the RBA of estradiol = 100%). (See Figure 2.9 for RBA curve of E2-7α). Each of the 8 derivatives has some affinity for the ER as illustrated in Table 2.4, column 4. The amine carbamate (E2-7α) has the highest RBA of 46 (this means that E2-7α binds to the ER 46% as tightly as estradiol), whereas the carbamate has the lowest (6). The amine, guanidine, diamine, and diamide also had RBA's > 28 which is a considerable feat considering the amount of extraneous mass that is connected to the estradiol moiety in our derivatives. Previous work by Rink, et al. implied a 6 carbon chain was necessary to pass through the hydrophobic binding pocket of the ER active site (Rink et al. 1996). The explanation of this result has been made clearer through work in the Carlquist laboratory (Brzozowski et al. 1997; Pike et al. 2001; Rink et al. 1996). A co-crystal structure using a 7α-undecylamide estradiol analog (ICI 164,384) reveals that the positioning and orientation of the estradiol moiety of ICI 164,384 within the hydrophobic binding cavity of the ER is directed by its 7α side chain which protrudes out of a hydrophobic channel extending from the binding pocket. At the surface of the ER-LBD, a 90° flexion of the undecyl chain enables the remainder of the linker to track closely with the surface contours of the LBD (Pike et al. 2001). The low RBAs of the amine guanidine, amide, and carbamate may result from surface interactions adopted by the linkers in these molecules that do not permit optimal alignment of the estradiol moiety within the binding cavity.

Using an electrophoretic gel mobility shift assay (Mitra et al. 2002), Kaushik Mitra, Bogdan Fedeles, and Peter Rye observed that covalent DNA adducts of the amine carbamate, amine, diamine, amine guanidine, and guanidine form complexes with the ER-LBD (Table 2.4, column 5). The extent of complex formation generally correlated

with the RBAs of the unreacted compounds. The exception was the amine guanidine where virtually all of the modified oligonucleotide formed a slowly moving band, despite its relatively low RBA of 10. We do not know the basis for this unexpected finding (see Fig 2.10A for the gel shift produced by E2-7α). (Note: Figure 2.10A also illustrates some control compounds, which are truncated versions of E2-7α that lack the steroid binding domain. None of these control compounds result in a band shift indicating that the shift observed with E2-7α is specific.)

Bob Croy confirmed the specificity of the interaction between the ER and the E2-7α derivatives by adding the competitor, estradiol. Under conditions that allowed complex formation, addition of the ER to the modified oligomer resulted in the appearance of a slowly migrating band that was eliminated by addition of excess competitor, estradiol. Fig. 2.10B illustrates the competition between estradiol and an E2-7α modified oligonucleotide. Increasing concentrations of estradiol diminishes the ability of the E2-7α adducted oligomer to interact with the ER and result in a band shift. This result, as well as the result with the control compounds in Fig 2.10A, indicates that the interaction between the ER and our series of molecules is specific to the ability of the molecule to interact with the ER and is not the results of other, nonspecific interactions.

Differential Toxicity towards estrogen receptor expressing cells. The lethal effects of the E2-7α derivatives were investigated in the ER(+) MCF-7 and ER(-) MDA-MB231 breast cancer cell lines. John Marquis dosed the cells for two hours and assessed the toxicity by a colony forming assay. Table 2.4 columns 6 and 7 indicate that many of the modifications in the linker resulted in decreased toxicity toward both cell lines. Despite showing reactivity toward DNA *in vitro*, the guanidine and amine guanidine compounds did not show any significant toxicity at the highest dose of 20 μM. The low toxicity of the guanidinium-containing linkers may be related to either poor uptake by cells or their rapid excretion once absorbed (Brown and Heim 1973). Lack of uptake by the cells may also be responsible for the low toxicity of the carbamate, diamide, and amide compounds that have high log D values indicative of poor absorption (Lipinski et al. 1997). Further work is warranted in order to definitively determine if cellular uptake is indeed limiting for these compounds.

Future Work

The results described in this chapter have illustrated the importance of the linker moiety of our compounds. Slight modifications in the linker, such as the addition of a secondary amine (i.e., amine carbamate vs. carbamate), result in drastically different biochemical properties and toxicological profiles. E2-7α was found to have an optimal balance of properties which enabled it to have the greatest differential toxicity in favor of ER(+) cells. Therefore, all future work targeting ER expressing cancers was conducted with the E2-7α molecule. With the help of a great many individuals, these studies have provided the foundation of my work.

In the next chapter, I will test the results I obtained in determining the log P and log D values by injecting E2-7α into mice and observing the bioavailability, distribution in tissues, acute toxicity, and ability of E2-7α to remain intact and form DNA adducts *in vivo*. The subsequent chapter will address the efficacy of E2-7α as an anti-cancer agent by treating human xenografts that have been implanted into nude mice. Finally, I will address current evidence for the mechanism of action of E2-7α in support of the repair shielding and transcription factor hijacking hypothesis. (Singer and Kusmierek 1982; Tsai and O'Malley 1994)

As previously reported, E2-7α was significantly more toxic toward MCF-7 cells than MDA-MB231 cells (Mitra et al. 2002). The amine and diamine compounds also showed toxicity similar to that of E2-7α (amine-carbamate) and were selectively more toxic to the ER expressing MCF-7 cells. This result was consistent with our intended mechanism in that these two compounds, like E2-7α, had low log D values, high RBA's, and high reactivity with DNA. The compound with the greatest differential toxicity, E2-7α, also had DNA adducts with the greatest affinity for the ER-LBD as assessed by the electrophoretic gel mobility shift assay. A balance between reactivity with DNA, affinity for the ER, and solubility seemed to confer to E2-7α optimal properties as a selectively cytotoxic agent.

Conclusion

We have rationally designed and synthesized a series of bifunctional molecules capable of attracting the ER and adducting DNA. Previously, we have reported on the synthesis of a series of compounds using 2-phenyl-indole as the protein recognition domain of our molecules (Rink et al. 1996). Using the lessons learned from those studies we have maintained the 7α-hexanyl linker to ensure optimal binding to the ER and transitioning out of the hydrophobic binding pocket. The work described here illustrates the use of structure-activity relationships to further modify the linker and achieve selective toxicity towards ER expressing cell lines. Interestingly, the parent compound, E2-7α, seemed to contain an optimal balance of properties as it had the greatest differential toxicity towards the ER(+) MCF-7 cells as compared to the ER(-) MDA-MB231 cells. E2-7α ranked first in RBA, first in ability to interact with the ER when covalently adducted to DNA, third in ability to covalently modify DNA, and had the lowest log D which would indicate it should have good absorption. Likewise, the only two other compounds that illustrated differential toxicity, the amine and diamine, were also among the highest ranking compounds in each of these categories. Although no one biochemical property clearly indicated therapeutic effectiveness, a combination and good overall balance of them did.

Reference List

Barret, J.M. and Hill, B.T. DNA repair mechanisms associated with cellular resistance to antitumor drugs: potential novel targets. *Anticancer Drugs* **9**, 105-123 (1998)

Bodor, N., Gabanyi, Z., and Wong, C. A new method for the estimation of partition coefficient. *J. Amer. Chem. Soc.* **111**, 3783-3786 (1989)

Bonkhoff, H., Fixemer, T., Hunsicker, I., and Remberger, K. Progesterone receptor expression in human prostate cancer: correlation with tumor progression. *Prostate* **48**, 285-291 (2001)

Bowler, J., Lilley, T.J., Pittam, J.D., and Wakeling, A.E. Novel steroidal pure antiestrogens. *Steroids* **54**, 71-99 (1989)

Brown, H.C. and Heim, P. Selective reductions XVIII. Fast reaction of primary, secondary and tertiary amides with diborane. Simple, convenient procedure for the conversion of amides to the corresponding amines. *J. Org. Chem.* **38**, 912-916 (1973)

Bruckheimer, E.M., Gjertsen, B.T., and McDonnell, T.J. Implications of cell death regulation in the pathogenesis and treatment of prostate cancer. *Semin. Oncol.* **26**, 382-398 (1999)

Brzozowski, A.M., Pike, A.C., Dauter, Z. et al. Molecular basis of agonism and antagonism in the oestrogen receptor. *Nature* **389**, 753-758 (1997)

Bucourt, R., Vignau, M., and Torelli, V. New biospecific adsorbents for the purification of estradiol receptor. *J. Biol. Chem.* **253**, 8221-8228 (1978)

Chatterji, D.C., Yeager, R.L., and Gallelli, J.F. Kinetics of chlorambucil hydrolysis using high-pressure liquid chromatography. *J. Pharm. Sci.* **71**, 50-54 (1982)

Cimpan, G., Irimie, F., Gocan, S., and Claessens, H.A. Role of stationary phase and eluent composition on the determination of log P values of N-hydroxyethylamide of aryloxyalkylen and pyridine carboxylic acids by reversed-phase high-performance liquid chromatography. *J. Chromatogr. B Biomed. Sci. Appl.* **714**, 247-261 (1998)

Cole, L.A., Dorsey, J.G., and Dill, K.A. Temperature dependence of retention in reversed-phase liquid chromatography. 2. Mobile-phase considerations. *Anal. Chem.* **64**, 1324-1327 (1992)

DaSilva, J.N. and van Lier, J.E. Synthesis and structure-affinity of a series of 7 alpha-undecylestradiol derivatives: a potential vector for therapy and imaging of estrogen-receptor-positive cancers. *J. Med. Chem.* **33**, 430-434 (1990)

De Bruijn, J., Busser, F., Seinen, W., and Hermens, J. Determination of Octanol/Water Patition Coefficients for Hydrophobic Organic Chemicals with the "Slow-Stirring" Method. *Environmental Toxicology and Chemistry* **8**, 499-512 (1989)

Dolan, M.E. Inhibition of DNA repair as a means of increasing the antitumor activity of DNA reactive agents. *Adv. Drug Del. Rev.* **26**, 105-118 (1997)

Donahue, B.A., Augot, M., Bellon, S.F. et al. Characterization of a DNA damage-recognition protein from mammalian cells that binds specifically to intrastrand d(GpG) and d(ApG) DNA adducts of the anticancer drug cisplatin. *Biochemistry* **29**, 5872-5880 (1990)

Donovan, S.F. and Pescatore, M.C. Method for measuring the logarithm of the octanol-water partition coefficient by using short octadecyl-poly(vinyl alcohol) high-performance liquid chromatography columns. *J. Chromatogr. A* **952**, 47-61 (2002)

Ferno, M., Borg, A., Johansson, U. et al. Estrogen and progesterone receptor analyses in more than 4,000 human breast cancer samples. A study with special reference to age at diagnosis and stability of analyses. Southern Swedish Breast Cancer Study Group. *Acta Oncol.* **29**, 129-135 (1990)

Greig, N.H., Genka, S., Daly, E.M. et al. Physicochemical and pharmacokinetic parameters of seven lipophilic chlorambucil esters designed for brain penetration. *Cancer Chemother. Pharmacol.* **25**, 311-319 (1990)

Haapala, E., Hakala, K., Jokipelto, E. et al. Reactions of N,N-bis(2-chloroethyl)-p-aminophenylbutyric acid (chlorambucil) with 2'-deoxyguanosine. *Chem. Res. Toxicol.* **14**, 988-995 (2001)

Hansch, C. and Fujita, T. A method for the correlation of biological activty and chemical structure. *Journal of the American Chemical Society* **86**, 1616-1627 (1964)

Hansch, C., Maloney, P., Fujita, T., and Muir, R. Correlation of biological activity of phenoxyacetic acids with Hammett substituent constants and partition coefficients. *Nature* **194**, 178-80 (1962)

Hobisch, A., Culig, Z., Radmayr, C. et al. Distant metastases from prostatic carcinoma express androgen receptor protein. *Cancer Res.* **55**, 3068-3072 (1995)

Holley, J.L., Mather, A., Wheelhouse, R.T. et al. Targeting of tumor cells and DNA by a chlorambucil-spermidine conjugate. *Cancer Res.* **52**, 4190-4195 (1992)

Horváth, Cs., Melánder, W., and Molnár, I. Liquid chromatography of ionogenic substances with nonpolar stationary phases. *Anal. Chem.* **49**, 142-154 (1977)

Huang, J.C., Zamble, D.B., Reardon, J.T. et al. HMG-domain proteins specifically inhibit the repair of the major DNA adduct of the anticancer drug cisplatin by human excision nuclease. *Proc. Natl. Acad. Sci. U. S. A* **91**, 10394-10398 (1994)

Hurley, L.H. DNA and its associated processes as targets for cancer therapy. *Nature Rev. Cancer* **2**, 188-200 (2002)

Kartalou, M. and Essigmann, J.M. Mechanisms of resistance to cisplatin. *Mutat. Res.* **478**, 23-43 (2001)

Kozlowski, J.M., Ellis, W.J., and Grayhack, J.T. Advanced prostatic carcinoma. Early versus late endocrine therapy. *Urol. Clin. North Am.* **18**, 15-24 (1991)

Kreis, W. Current chemotherapy and future directions in research for the treatment of advanced hormone-refractory prostate cancer. *Cancer Invest* **13**, 296-312 (1995)

Kundu, G.C., Schullek, J.R., and Wilson, I.B. The alkylating properties of chlorambucil. *Pharmacol. Biochem. Behav.* **49**, 621-624 (1994)

Leo, A. Calculating log Poct from structures. *Chemical Reviews* **93**, 1281-1306 (1993)

Leo, A., Hansch, C., and Elkins, D. Partition coefficients and their uses. *Chemical Reviews* **71**, 525-616 (1971)

Leo, A., Jow, P.Y., Silipo, C., and Hansch, C. Calculation of hydrophobic constant (log P) from pi and f constants. *J. Med. Chem.* **18**, 865-868 (1975)

Lipinski, C.A., Lombardo, F., Dominy, B.W., and Feeney, P.J. Experimental and computational approaches to estimate solubility and permeability in drug discovery and developmental settings. *Adv. Drug Del. Rev.* **23**, 3-25 (1997)

Marcelli, M. and Cunningham, G.R. Hormonal signaling in prostatic hyperplasia and neoplasia. *J. Clin. Endocrinol. Metab* **84**, 3463-3468 (1999)

Mitra, K., Marquis, J.C., Hillier, S.M. et al. A rationally designed genotoxin that selectively destroys estrogen receptor-positive breast cancer cells. *J. Amer. Chem. Soc.* **124**, 1862-1863 (2002)

Owen, W.R. and Stewart, P.J. Kinetics and mechanism of chlorambucil hydrolysis. *J. Pharm. Sci.* **68**, 992-996 (1979)

Peto, J. and Mack, T.M. High constant incidence in twins and other relatives of women with breast cancer. *Nat. Genet.* **26**, 411-414 (2000)

Pike, A.C.W., Brzozowski, A.M., Walton, J. et al. Structural insights into the mode of action of a pure antiestrogen. *Structure* **9**, 145-153 (2001)

Pil, P.M. and Lippard, S.J. Specific binding of chromosomal protein HMG1 to DNA damaged by the anticancer drug cisplatin. *Science* **256**, 234-237 (1992)

Rekker, R. The Hydrophobic Fragment Constant. Elsevier Amsterdam (1976)

Rink, S.M., Yarema, K.J., Solomon, M.S. et al. Synthesis and biological activity of DNA damaging agents that form decoy binding sites for the estrogen receptor. *Proc. Natl. Acad. Sci. U. S. A* **93**, 15063-15068 (1996)

Roberts, J.J. The repair of DNA modified by cytotoxic, mutagenic, and carcinogenic chemicals. *Adv. Radiat. Biol.* **7**, 211-435 (1978)

Santen, R.J. Clinical review 37: Endocrine treatment of prostate cancer. *J. Clin. Endocrinol. Metab* **75**, 685-689 (1992)

Sharma, U., Marquis, J.C., Nicole, D.A. et al. Design, synthesis, and evaluation of estradiol-linked genotoxicants as anti-cancer agents. *Bioorg. Med. Chem. Lett.* **14**, 3829-3833 (2004)

Singer, B. and Grunberger, D. Molecular Biology of Mutagens and Carcinogens. Plenum Publishing Corp. New York (1983)

Singer, B. and Kusmierek, J.T. Chemical mutagenesis. *Annu. Rev. Biochem.* **51**, 655-693 (1982)

Teicher, B.A. Cancer Principles and Practice. <u>Antitumor alkylating agents</u> 5, 405-417 (1997)

Treiber, D.K., Zhai, X., Jantzen, H.M., and Essigmann, J.M. Cisplatin-DNA adducts are molecular decoys for the ribosomal RNA transcription factor hUBF (human upstream binding factor). *Proc. Natl. Acad. Sci. U. S. A* **91**, 5672-5676 (1994)

Tsai, M.J. and O'Malley, B.W. Molecular mechanisms of action of steroid/thyroid receptor superfamily members. *Annu. Rev. Biochem.* **63**, 451-486 (1994)

Vallat, P., Fan, W., El Tayar, N. et al. *Journal of Liquid Chromatography* 2133-1992)

von Angerer, E., Prekajac, J., and Strohmeier, J. 2-Phenylindoles. Relationship between structure, estrogen receptor affinity, and mammary tumor inhibiting activity in the rat. *J. Med. Chem.* **27**, 1439-1447 (1984)

Walter, H., Brooks, D., and Fisher, D. Partitioning in Aqueous Two Phase Systems. Academic Press London (1985)

Zhai, X., Beckmann, H., Jantzen, H.M., and Essigmann, J.M. Cisplatin-DNA adducts inhibit ribosomal RNA synthesis by hijacking the transcription factor human upstream binding factor. *Biochemistry* **37**, 16307-16315 (1998)

Equations used to Calculate
the Log P and Log D

$$\log P_{unk} = \frac{(\log P_{tol} - \log P_{triph})*t_{unk} + t_{tol}*\log P_{triph} - t_{triph}*\log P_{tol}}{t_{tol} - t_{triph}}$$

Equation 2.1. t is the retention time as determined by HPLC (tol = toluene, triph = triphenylene, unk = unknown). The log P of toluene and triphenylene were 2.61 and 6.27 respectively as previously reported.

$$\log D = \log (P * 10^{pKa} + P_i * 10^{pH}) - \log(10^{pKa} + 10^{pH})$$

Equation 2.2. P is the partition coefficient for the neutral molecule (as determined by HPLC), P_i is the partition coefficient for the ion (not measured but assumed the log P_i was 3.15 less than the log P of the neutral molecule), K_a is the equilibrium constant for acids.

Calculated Log P Values of Reference Compounds and E2-7α Derivatives

Reference Compounds	molinspiration.com	logP.com	Lit. logP
Decachlorbiphenyl	9.89	8.44	8.23
Chlorambucil	3.05	3.36	-0.66
Progesterone	4.30	3.74	3.56
Testosterone	3.77	3.24	2.79-3.29
Estradiol	4.50	3.50	3.34-4.01

E2-7α Derivatives	molinspiration.com	logP.com
amine guanidine	8.60	4.84
monoamine	9.25	8.79
guanidine	8.93	4.92
carbamate	8.96	6.82
E2-7a (amine carbamate)	9.06	7.26
diamine	8.50	8.80
amide	9.19	7.66
diamide	9.24	6.08

Table 2.1 Comparison of the log P values obtained from the two free website. The values obtained for the reference compounds did not agree very well with previously published literature values.

Note: The literature value obtained for chlorambucil was calculated by the method of Leo and Hansch for the ionized molecule. The values for the other reference compounds were obtained experimentally. (Leo, Hansch, and Elkins; De Bruijn et al.;Donovan and Pescatore;Greig et al.)

A Comparison of the Log P of the Reference Compounds by Different Methodologies

Compound	HPLC LogP	Literature LogP	molinspiration.com LogP	logP.com LogP
Decachlorobiphenyl	7.35	8.23	9.89	8.44
Chlorambucil	1.44	-0.66	3.05	3.36
Progesterone	3.69	3.56	4.30	3.24
Testosterone	2.61	2.79-3.29	3.77	3.24
Estradiol	3.53	3.34-4.01	4.50	3.50

Table 2.2 A comparison of the HPLC derived log P values with the computer simulation and literature values. The HPLC values corresponded to the literature values better than the computer simulations.

A Comparison of the Log P of the E2-7α Derivatives Obtained by Different Methodologies

Compound	HPLC logP	HPLC logD pH 7.4	Molinspiration logP	logP.com logP
amine guanidine	6.27	3.12	8.6	4.84
amine	5.96	2.87	9.25	8.79
guanidine	5.67	2.52	8.93	4.92
carbamate	5.61	5.61	8.96	6.82
E2-7a (amine carbamate)	5.32	2.22	9.06	7.26
diamine	5.32	2.22	8.5	8.8
amide	5.07	5.07	9.19	7.66
diamide	4.85	4.85	9.24	6.08

Table 2.3 The log P and log D values obtained for the E2-7α derivatives. The log D values of the series span a range of approximately 2500-fold in lipophilicity. Since blood is at the physiological pH of 7.4, the log D values best estimate the fate of the compounds *in vivo*.

Physical Properties of the E2-7α Derivatives

Linker	Log D	% DNA Adduction	RBA	% Oligo Shifted	EC30 (μM) MDA-MB231	MCF-7
Amine-Carbamate	2.22	45	46	93	9.6	5.1
Amine	2.87	44	40	67	8.6	5.1
Diamine	3.17	79	29	38	7.9	5.1
Diamide	4.85	39	29	n.d.	>20	>20
Guanidine	2.52	58	28	38	>20	>20
Amide	5.07	14	13	n.d.	>20	>20
Amine-Guanidine	3.12	29	10	93	>20	>20
Carbamate	5.61	3	6	n.d.	>20	>20

Table 2.4 Summary of the results obtained for the E2-7α derivatives. The log D, % DNA adduction, RBA, % oligo shifted, and the EC_{30} for each compound is shown.

E2-7α Forms Adducts in DNA with Apparent Zero-Order Kinetics
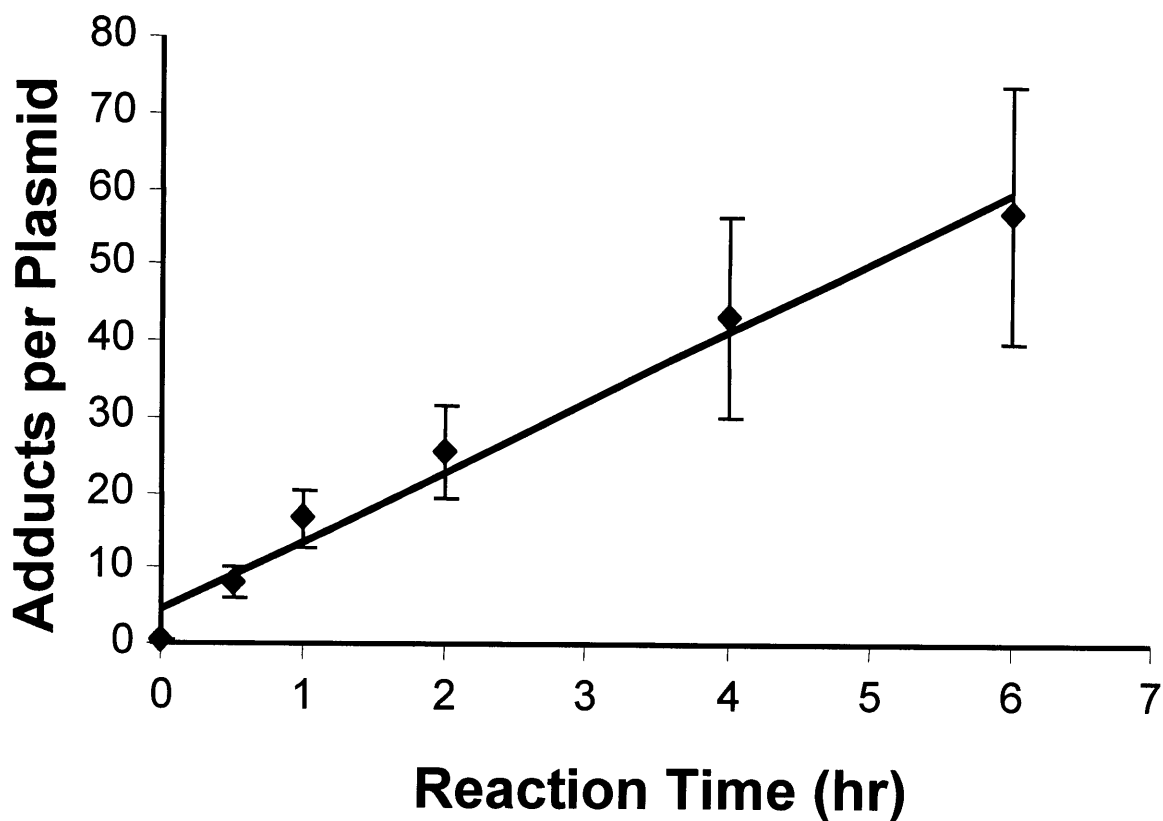
Fig 2.1A E2-7α forms 13.1DNA adducts per plasmid per hour in a seemingly linear manner.

As time Progresses, E2-7α Forms Adducts in DNA with Pseudo First-Order Kinetics
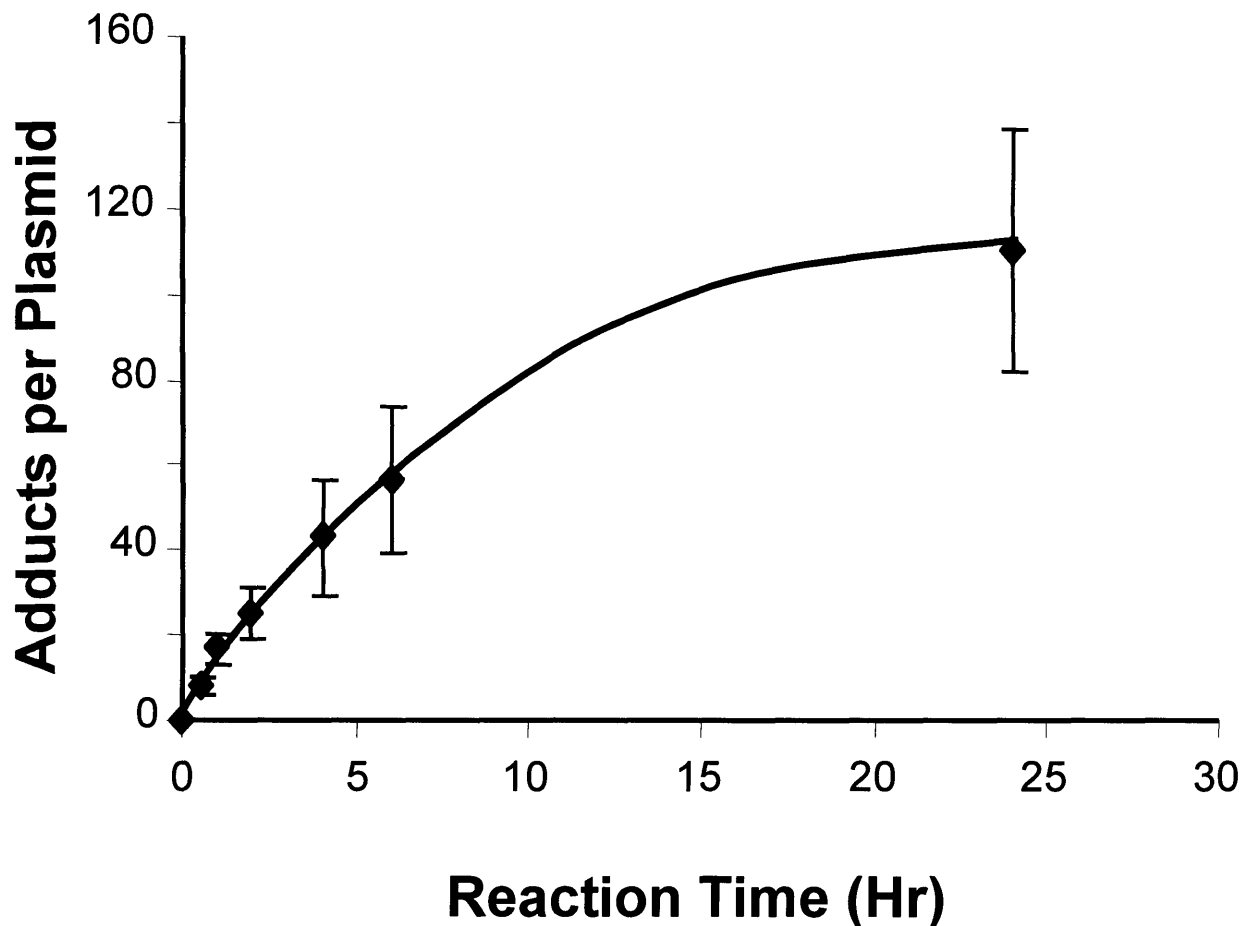
Fig 2.1B The rate of adduction of DNA by E2-7α slows over time. An initial rate of 13.4 adducts per plasmid per hour over the first 6 hours decreases to 3.4 adducts per plasmid per hour between 6 and 24 hours.

The Identification of E2-7α DNA Adducts

A
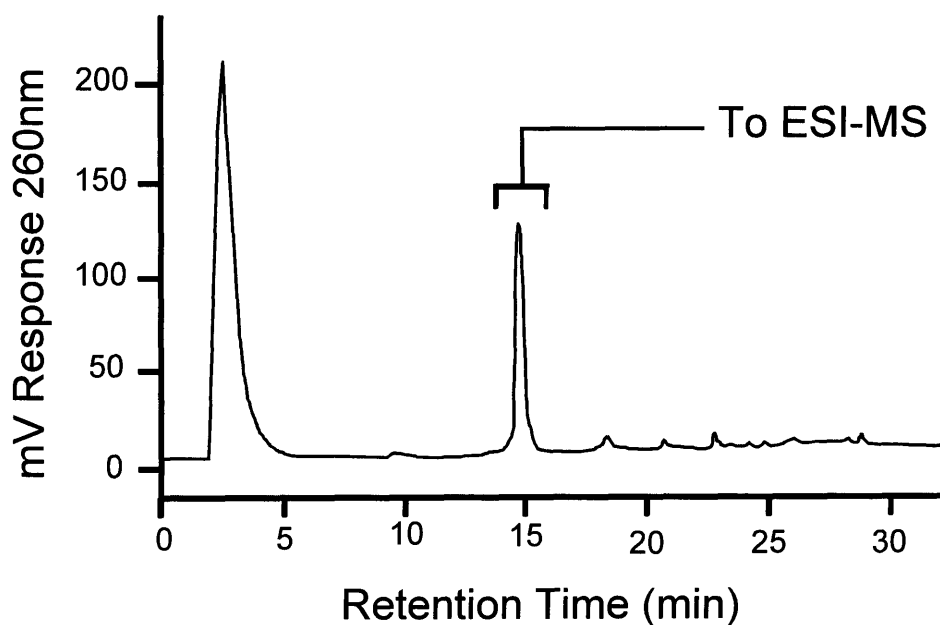
B
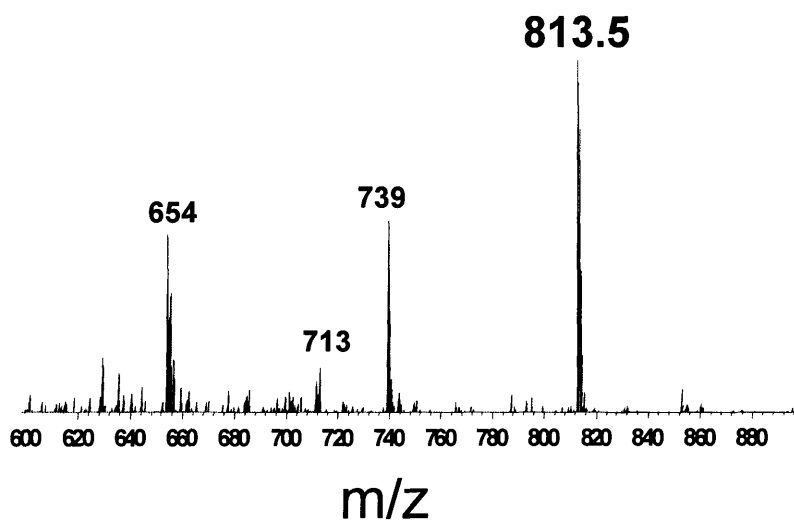
Fig 2.2 A. HPLC chromatogram of the hydrolysis products after E2-7α reacted with DNA. **B.** The ESI-MS chromatogram of the 14.5 min peak isolated by HPLC. The 813.5 m/z ion corresponds to an E2-7α guanine monoadduct where the second arm of the nitrogen mustard has become hydroxylated.

Characterization of E2-7α DNA Adducts by Collision Induced Decay Mass Spectrometry

A

B
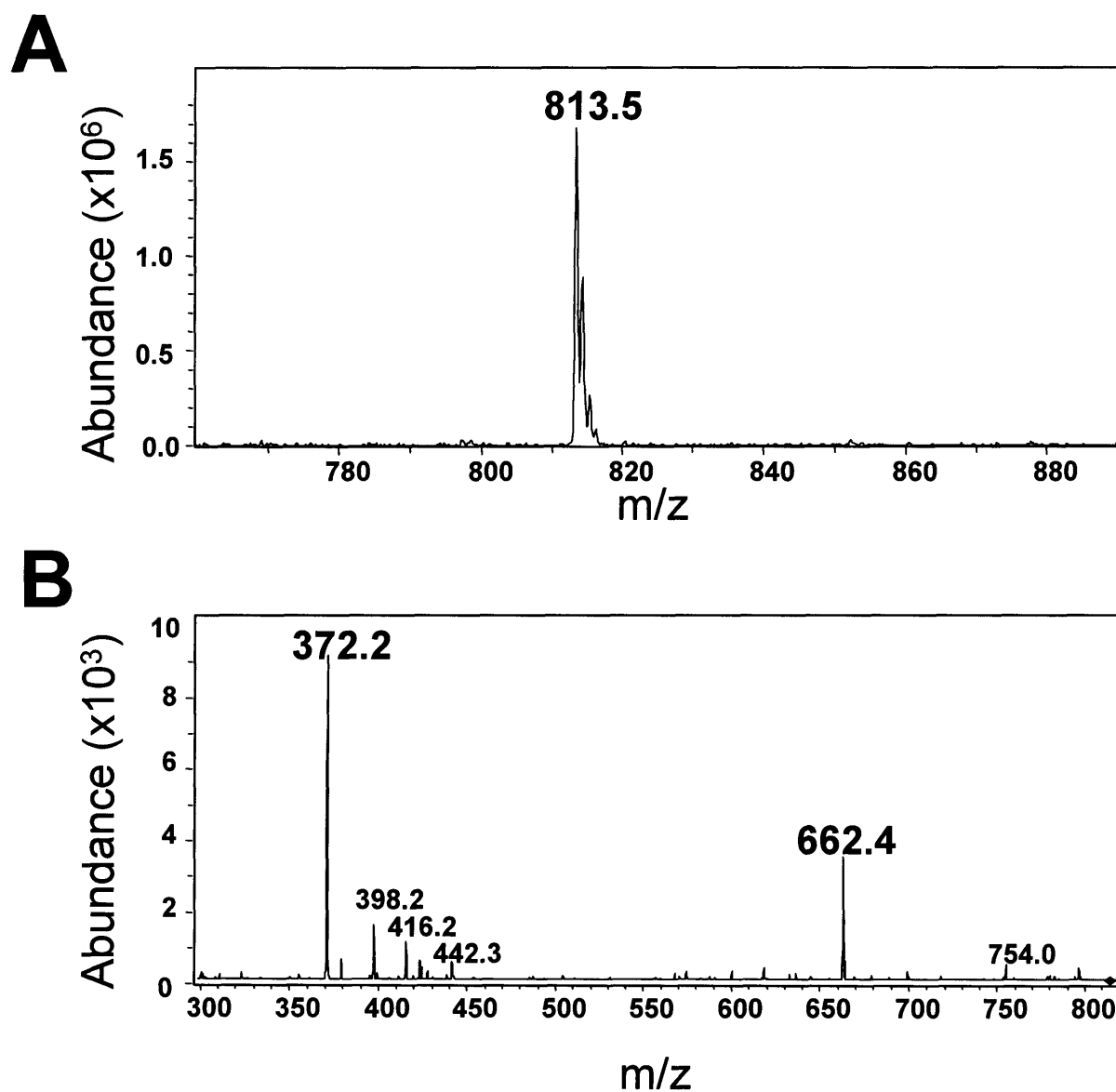
Fig 2.3 A. ESI-MS analysis of the 14.5 min peak on HPLC produces a molecular ion of 813.5 m/z. **B.** CID of the 813.5 m/z ion produces two daughter ions of 372.2 m/z and 662.4 m/z.

Structures of E2-7α Fragmentation Pattern after Collision Induced Decay Mass Spectrometry
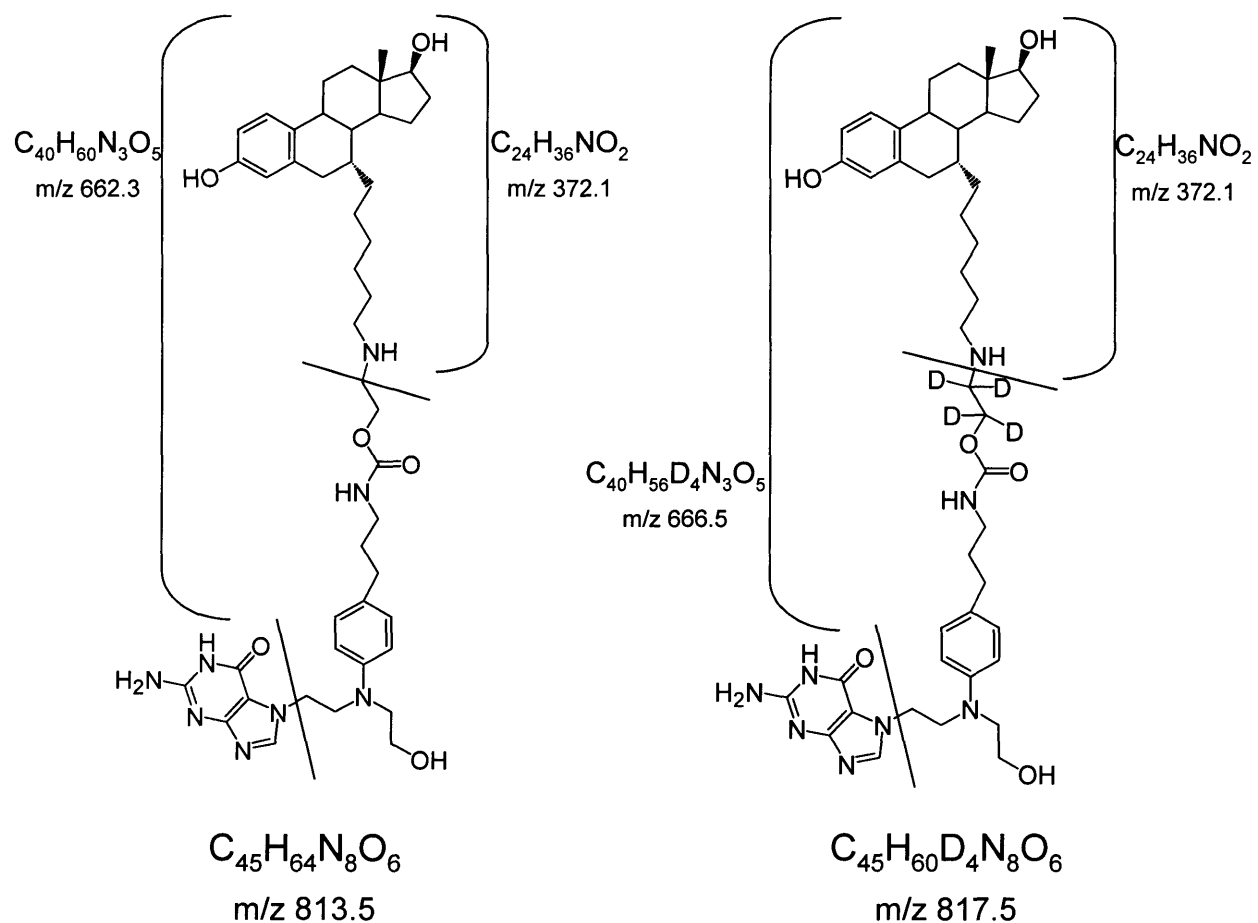
Fig 2.4 CID of the 813.5 m/z ion produced by the reaction of E2-7α with DNA (left). d4-E2-7α was reacted with DNA and produced a similar CID fragmentation pattern (right). The notable difference is in the 662.4 / 666.4 m/z molecular ion in which the latter contains the tetradeuterated linker. This result supports the structure and fragmentation pattern proposed for the undeuterated compound.

A Tetradeuterated-E2-7α Produces a Similar Fragmentation Pattern as E2-7α

A
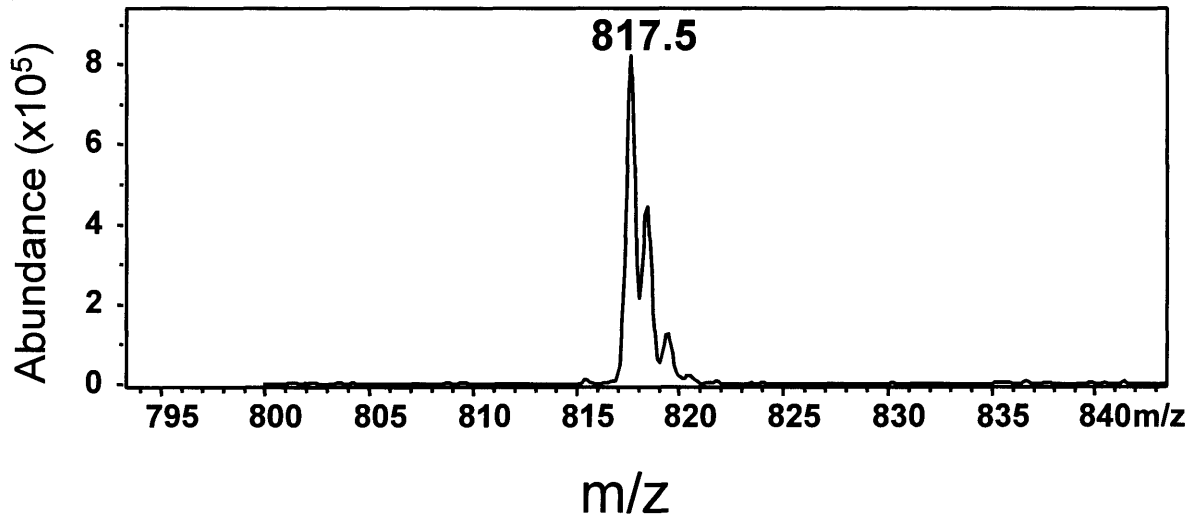
B
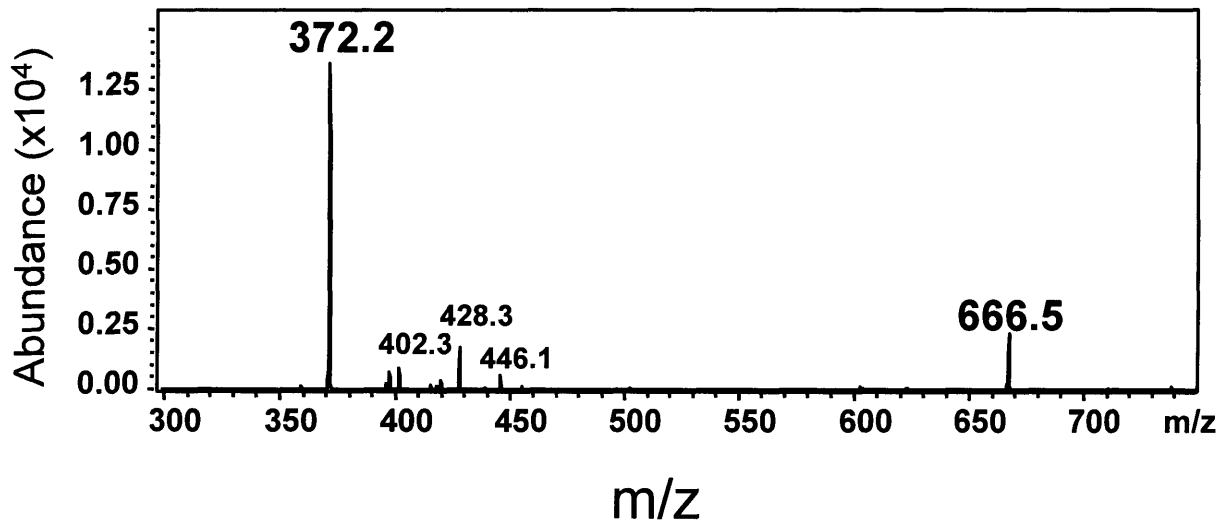
Fig 2.5 A. ESI-MS analysis of the 14.5 min peak on HPLC (after d4-E2-7α was allowed to react with DNA) produces a molecular ion of 817.5 m/z. B. CID of the 813.5 m/z ion produces two daughter ions of 372.2 m/z and 666.4 m/z.

Chemical Structures of Log P Reference Compounds
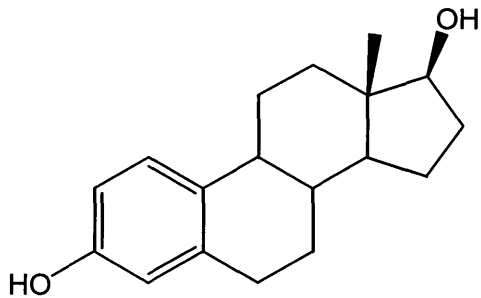
Estradiol
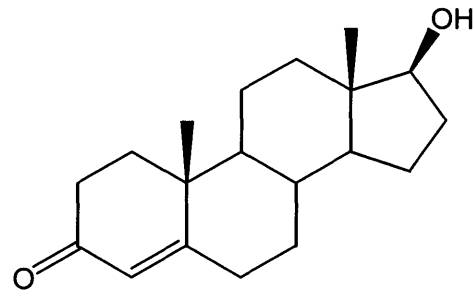
Testosterone
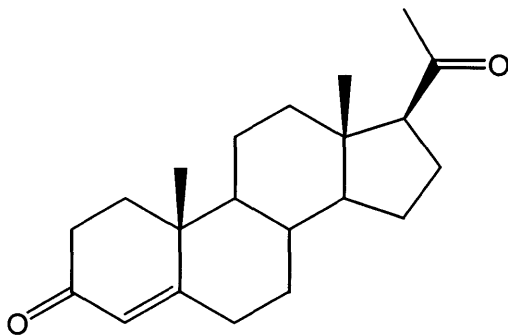
Progesterone
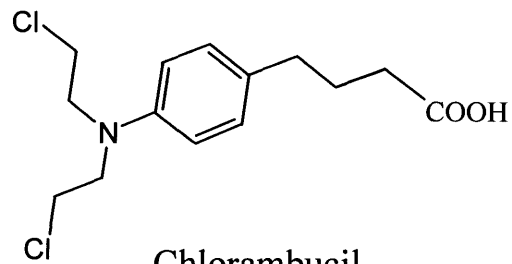
Chlorambucil
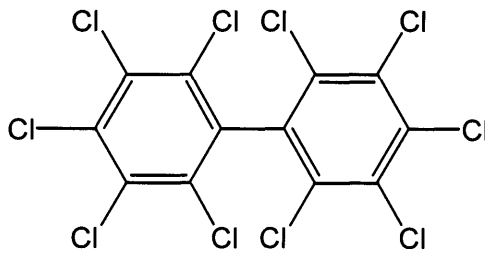
Decachlorobiphenyl

Fig 2.6 The chemical structures of the reference compounds used to validate the log P values obtained by computer simulation .

Chemical Structures of E2-7α Derivatives
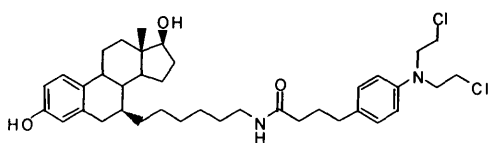
Amide
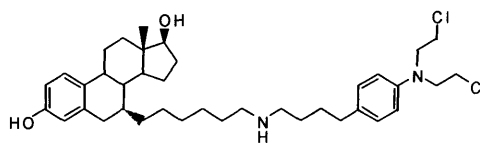
Amine
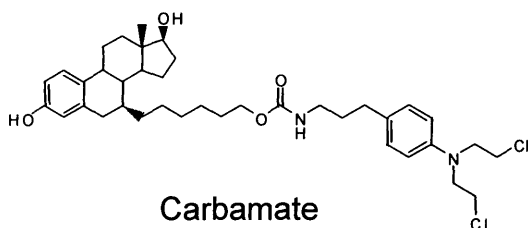
Carbamate
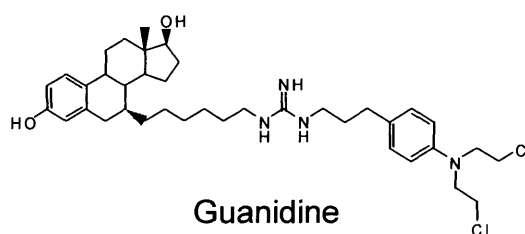
Guanidine
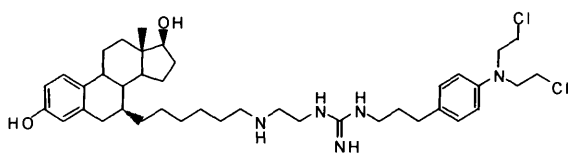
Amine Guanidine
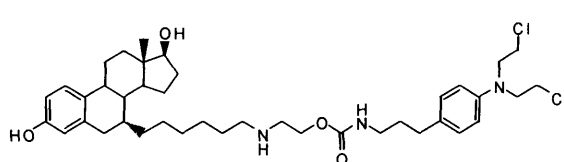
E2-7α (Amine Carbamte)
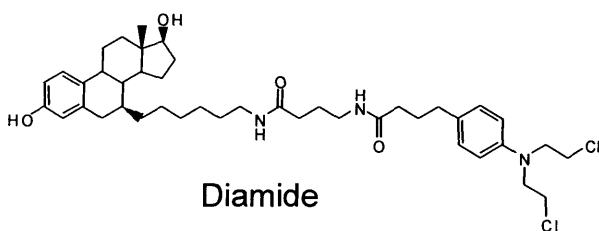
Diamide
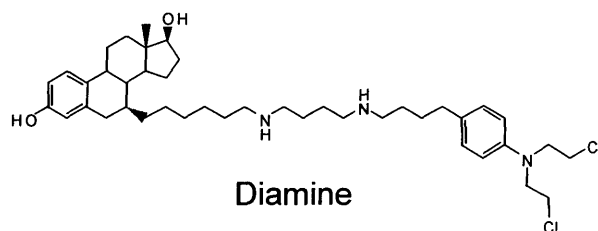
Diamine

Fig 2.7 The chemical structures for the E2-7α derivatives.

HPLC Chromatogram used to Determine the Log P of E2-7α
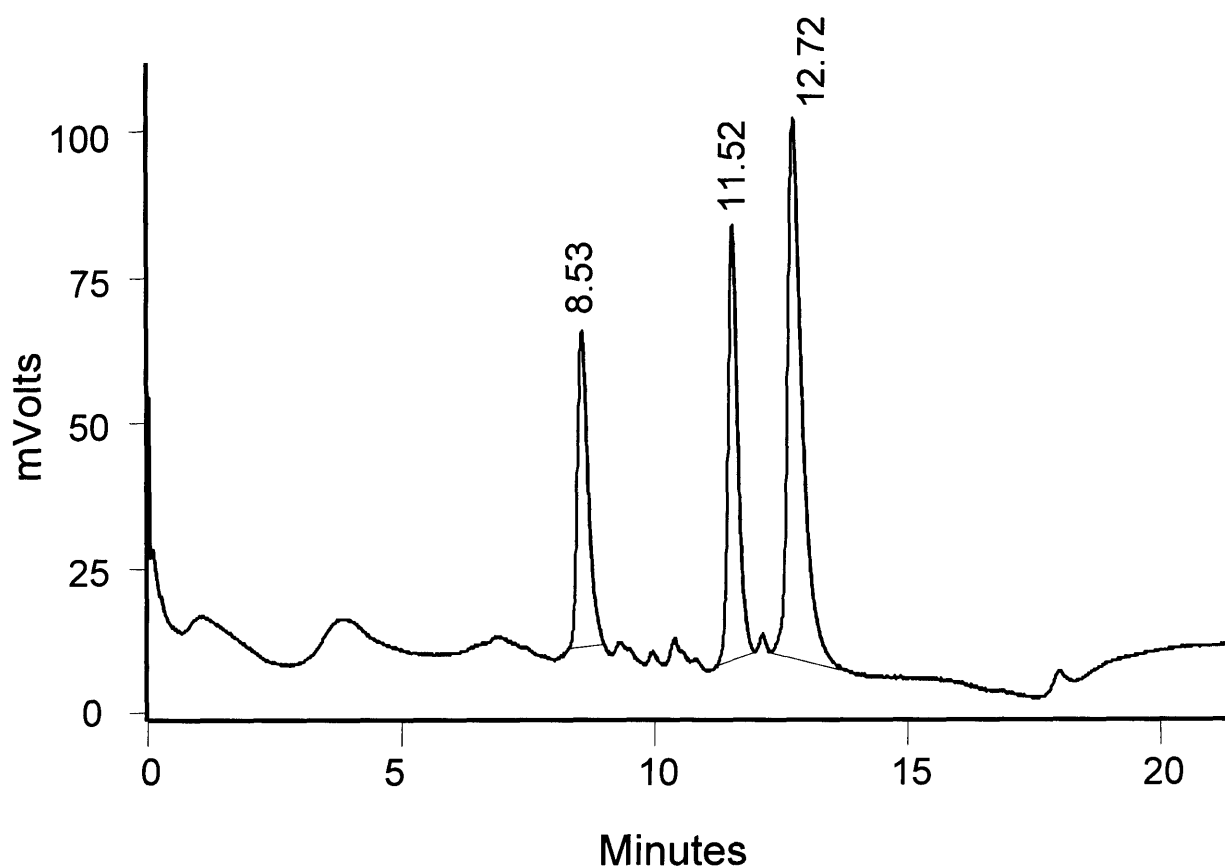
Fig 2.8 HPLC Chromatogram of E2-7α co-injected with the Log P standard. The peak at 8.53 min. is toluene, 11.52 min. is E2-7α, and at 12.72 min. is triphenylene.

Chapter 3

Probing the Biochemical Mechanisms of
E2-7α *in Vivo:*

Pharmacokinetics, Toxicity, and Adduct Identification

Introduction

Cytotoxic alkylating agents have been used for decades to treat cancer. While they usually cause an initial antitumor response, they cure cancers with only modest success. These agents, such as chlorambucil and melphalan, react with DNA in all cells, but the majority of the adducts are readily repaired. Persistent DNA damage by alkylating agents has lethal consequences for malignant cells (Dolan 1997; Frankfurt 1991; Hurley 2002; Teicher 1997). Therefore, inhibition of the DNA repair machinery, specifically in cancer cells, is an attractive strategy to potentiate the therapeutic effects of alkylating chemotherapeutics (Barret and Hill 1998; Dolan 1997). In line with this goal, we have described the rational design of compounds capable of covalently modifying DNA and attracting tumor specific proteins to the site of the modification (Mitra et al. 2002; Rink et al. 1996; Sharma et al. 2004).

As a proof of concept, Rink et al. linked an aniline mustard with a 2-phenylindole moiety, which is capable of attracting the estrogen receptor (ER). The ER is an attractive target because approximately 50% of breast cancers overexpress this protein (Ferno et al. 1990). Rink et al., were able to show that the newly synthesized molecules were capable of forming adducts with DNA that attract the ER with modest binding affinity (Rink et al. 1996). Therefore, it is possible that in a malignant cell in which the ER is overexpressed, a drug-DNA adduct complex could be inhibited from repair if the ER were bound tightly to the adducted site and it shielded the repair enzymes from accessing the lesion. If the ER were attracted to the site of adduction, an interaction between the ER and the DNA adduct could disrupt necessary cellular signaling events since the ER is also a transcription factor.

Subsequent synthetic work in the Essigmann Laboratory has improved the lead compound by substituting an estradiol moiety for the 2-phenylindole, while maintaining the key molecular characteristics of the linker that were important for the compound to react with DNA and bind to the ER. The new compound, E2-7α, was a dramatically improved version of 2PI since the RBA for E2-7α was 7-fold higher. In an effort to improve E2-7α further, a series of derivatives were synthesized and evaluated as potential new drug candidates. The results were discussed in Chapter 2. The compounds had a varied range in affinity for the ER and differential toxicity towards ER-expressing cells.

No new derivative was a significant improvement over E2-7α so subsequent studies were conducted with E2-7α.

The results discussed in Chapter 2 gave us confidence in E2-7α as a potential drug candidate because of its high RBA (46), ability to form adducts with DNA, low log D (2.22), and differential toxicity in favor of killing the ER(+) MCF-7 cell line over the ER(-) MDA-MB231 line. We therefore believed it was necessary to take the compound forward by injecting it into animals and studying its pharmacological properties. E2-7α was initially formulated in DMSO and injected intravenously (IV), but a Cremophor-EL (CR-EL) formulation injected intraperitoneally (IP) was later shown to be superior. (Note: CR-EL is currently part of the formulation for the clinically used Taxol (paclitaxel) in the therapy of ovarian cancer, breast cancer, Kaposi 's sarcoma, and non-small cell lung cancer.) The distribution in mice injected with E2-7α by either of these vehicles will be discussed as will the pharmacokinetic parameters derived from these studies.

Additionally, a dose range finding study was performed to address the acute toxicity of E2-7α dissolved in the CR-EL vehicle administered IP. Blood chemistry and hematology reports provided a means of addressing organ specific toxicity. This information is critical in deciding upon a therapeutic dose when initiating a tumor ablation study and in more focused monitoring of the side-effect profile of the treated mice (to be discussed in Chapter 4). I shall also discuss the identification of E2-7α DNA adducts isolated from tissue *in vivo*. These results parallel the *in vitro* work discussed in Chapter 2.

Materials and Methods

Animals. Four to six week old NIH Swiss Webster mice were purchased from Charles River Laboratories, Wilmington, MA. NIH Swiss *nu/nu* athymic mice (female, 25 g) were purchased from the National Cancer Institute-Frederick Cancer Center (NCI), (Frederick, MD). The mice were housed under standard conditions in MIT approved facilities with 12 hour light/dark cycles and food and water *ad libitum*. All protocols were performed in compliance with the regulations of the Animal Care Committee at MIT.

Bio-Distribution. E2-7α (25 mg/kg) spiked with 5 μCi of ^{14}C-E2-7α were dissolved in 50 μL of DMSO and injected IV into 25 g male NIH Swiss Webster Mice or in 50 uL of a CR-EL based solution (43% CR-EL, 30% saline, 27% ethanol) and injected either IP or IV. Mice were sacrificed by carbon dioxide asphyxiation at 0.25, 1, 2, 4, 6, and 24 hours post injection. Blood was obtained by cardiac puncture. The following internal organs were removed surgically: lung, liver, spleen, kidney, GI, feces, and in some instances adipose, heart, and skeletal muscle. Approximately 100 mg of each tissue (10 μL of whole blood) were isolated for liquid scintillation counting. To each tissue sample was added 1mL of Solvable (Packard Biosciences, Meriden, CT) and heated to 65°C for 3 hours or until the tissue was completely dissolved. Two 100 μL aliquots of 30% hydrogen peroxide were added to the cooled off solution to decolorize. Approximately 15 mL of Hionic Flour scintillation fluid (Packard Biosciences, Meriden, CT), which is compatible with Solvable, was added and counted in a Beckman LS1801 Liquid Scintillation Counter. The data is calculated as % injected dose per gram of tissue (% ID/g).

Pharmacokinetic Analysis. Pharmacokinetic parameters after administration of E2-7α were calculated by standard noncompartmental methods with GraphPad Prism version 3.00 for Windows (GraphPad Software, San Diego California USA). The area under the blood concentration Vs time curve (AUC) was calculated by the linear trapezoidal rule. The systemic clearance (CL) was calculated by dividing the dose by the AUC. The volume of distribution (V_d) was calculated by dividing the dose by the extrapolated concentration of drug in the blood at time equals zero hour. Since the drug concentration (post-peak) declined nearly exponentially, the half-life ($t_{1/2}$) was determined by nonlinear regression analysis using a single phase exponential decay model. C_{max} and t_{max} were read directly from the data.

Plasma Analysis. Whole blood was collected by cardiac puncture from the mice after ^{14}C-E2-7α injection. The plasma was isolated by adding two volumes of acetonitrile to one volume of whole blood to precipitate the red blood cells and plasma proteins. The

colloidal suspension was centrifuged for 5 min at 13,000 × G and the supernatant was collected and dried using a speed-vac. The dried residue was reconstituted with 100 μL of acetonitrile and injected onto a Rainin HPLC with a Rainin UV-1 UV Detector monitored at 260 nm and an in-line Packard Flow Scintillation Analyzer Model 150TR. The analyses were performed using a Beckman ODS 4.6 x 250 mm Ultrasphere column eluted at 1 mL/min with a 20 min linear gradient of 50% 0.1 M ammonium acetate/10% acetonitrile, 50% methanol to 100% methanol. Only the radioactive ^{14}C-E2-7α parent peak was used to determine the concentration of the compound in plasma. A ^{14}C-E2-7α standard was counted on a Beckman LS1801 Liquid Scintillation Counter prior to injection onto the HPLC. It was determined that an area under the curve (AUC) of 432,000 corresponded to 13,300 CPM.

Acute Toxicity. Groups of 3-4 NIH Swiss *nu/nu* athymic mice from the NCI were injected IP with 25 – 200 mg/kg of E2-7α formulated in a CR-EL solution (43% CR-EL, 30% saline, 27% ethanol). Additionally, 4 mice were injected with the vehicle only and 4 others were left untreated as controls. The mice were sacrificed by carbon dioxide asphyxiation 24 hours after the injection. Blood was obtained by cardiac puncture and sent to IDEXX (formerly Tufts Veterinary Diagnostic Laboratory, North Grafton, MA) for hematology and blood chemistry analysis.

Isolation of E2-7α DNA Adducts *in Vivo*. E2-7α (25 mg/kg, not radiolabeled) was injected into NIH Swiss Webster mice by IP injection. The mice were sacrificed after 4 hours by carbon dioxide asphyxiation. The liver was removed surgically, snap frozen on dry ice, and stored at -80°C until it could be worked up. The liver sample was thawed and homogenized in a Dounce homogenizer on wet ice with 15 mL of cold (4°C) 0.01 M Tris (pH 6.9), 0.25M sucrose, 2 mM calcium chloride buffer. The homogenate was filtered through coarse and then a fine nylon mesh to remove all connective tissue. To this solution was added 25% Triton X-100 to make a final concentration of 5%. The solution was briefly vortexed and then centrifuged at 1000 × G in a Sorvall RC-2B Centrifuge with a GSA rotor at 4°C for 20 min The supernatant was removed by aspiration and the nuclear pellet was resuspended in 2.5 mL of buffer. To this solution

118

was added 5% sodium dodecyl sulfate (SDS) and 5 M sodium chloride (NaCl) to make a solution with a final concentration of 1% SDS and 1 M NaCl. An equal volume of chloroform:isoamyl alcohol (24:1) was then added and the biphasic mixture was shaken vigorously for 15 min The mixture was then centrifuged at 7000 × G for 15 min at 4°C. The aqueous phase was collected and re-extracted with another volume of chloroform:isoamyl alcohol, shaken, and centrifuged. The aqueous phase was then collected and the nucleic acids were precipitated with 3 volumes of ice cold ethanol and chilled at -20°C for 20-30 min and subsequently pelleted by centrifugation at 7000 × G for 15 min at 4°C. The nucleic acids were washed 2 times with cold ethanol and then dried *in vacuo*. The dried pellet was reconstituted with 2 mL of 0.05 M Tris (pH 7.5), 0.1 M NaCl on ice. In order to remove any contaminating RNA, 0.5 mg of RNAse A was added and incubated at 37°C for 10 min The reaction was stopped by cooling on ice, the NaCl concentration was adjusted to 0.9 M, and the DNA was extracted by subsequent additions of chloroform:isoamyl alcohol as indicated above. The aqueous phase from the second extraction was isolated and the DNA was precipitated with 3 volumes of ice cold ethanol, centrifuged, and washed 2 times as above. The DNA was finally hydrolyzed in 0.1 N HCl for 30 min at 70°C. The solution was then neutralized with 1N NaOH and adjusted to 20 mM Tris-HCl (pH 7.4), 10% methanol. The hydrolyzed DNA was loaded onto a C18 Sep-Pak ® (Waters Co. Milford, MA) column and eluted sequentially with 10 mL of 10% and 50% aqueous methanol solutions and finally with 100% methanol. The 100% methanol fraction was reduced *in vacuo* and analyzed by HPLC and mass spectrometry. HPLC analyses were performed using a Beckman ODS 4.6 x 250 mm Ultrasphere column eluted at 1 mL/min with a 20 min linear gradient of 50% 0.1 M ammonium acetate/10% acetonitrile, 50% methanol to 100% methanol. Aliquots of samples obtained from HPLC fractionation were analyzed by electrospray ionization mass spectrometry (ESI-MS) using flow injection (0.2 mL/min) in methanol:water:acetontrile (50:45:5) in positive ion mode.

Results

Bio-Distribution and Pharmacokinetics. E2-7α was injected into mice by different routes of administration and vehicles in an effort to obtain pharmacologically relevant

information about the compound. Initial studies incorporated DMSO as the delivery vehicle and the solution was administered IV. The results of the DMSO IV administration are summarized in Table 3.1 and are reported as percent injected dose per gram (% ID/g). The concentration of E2-7α in whole blood is illustrated in Figure 3.1 and has a peak concentration of 7.8 μM at 15 min. E2-7α accumulated predominantly in the lungs but also in the liver, kidneys, and spleen at the earliest time points. However, at the 2 and 4 hour time points the majority of the drug was found in the feces, indicating the liver as the primary metabolic route with excretion through the feces. The significantly higher accumulation of E2-7α in the lungs over all other tissues was a matter of concern especially considering the lungs were not the desired target organ. Therefore, a new vehicle was investigated.

The new vehicle was formulated with 43% Cremophor-EL (CR-EL), 30% saline, and 27% ethanol. Due to the high viscosity of the solution, a pilot experiment was conducted to compare and contrast an IP and an IV administration. Mice were injected by either route and sacrificed at 2 and 4 hours. The results of the pilot bio-distribution experiment are summarized in Figure 3.2 with the quantitative results shown in Table 3.2. The concentration of E2-7α in the lungs was significantly diminished in both the IP and IV routes of administration. At two hours the lungs accumulated 21% ID/g with the DMSO vehicle. In the CR-EL based vehicle, only 4% of the injected dose per gram of tissue distributed to the lungs for the IV administration and only 1% ID/g for the IP administration. E2-7α formulated in the CR-EL based vehicle, when injected IP or IV, distributed to the remaining organs to a similar extent as in the DMSO based vehicle.

There were, however, some noticeable differences between the IP and IV routes of administration with the CR-EL based vehicle. E2-7α seemed to be excreted more rapidly when administered IV as evident by the higher concentrations found in the feces at both the 2 and 4 hour time points. The feces contained ~ 15% of the ID/g tissue at both the 2 and 4 hour time point when administered IV; however, only 3% ID/g at 2 hours and 8% ID/g at 4 hours were in the feces when E2-7α was administered IP. Not surprisingly the GI tissue had a higher uptake with the IP administration. Interestingly, the concentration found in the blood by either route was essentially the same.

The similarity between the IP and IV routes did not provide an obvious optimal means of administration. However, the addition of CR-EL to the vehicle did cause the solution to be much more viscous; therefore, IP administration was deemed to be better as it could be more easily incorporated into future tumor therapy experiments when the compound would have to be administered daily. Additionally, when administered IV, E2-7α seemed to be excreted more rapidly through the feces than when injected IP. Since we want the drug to remain active in the body for long periods of time, the IP administration was again considered to be slightly more favorable. A full bio-distribution experiment was therefore performed in order to obtain more detailed pharmacological information.

E2-7α was formulated in the CR-EL based vehicle and administered IP. The results of this experiment are summarized in Table 3.3. The results follow a typical IP administration profile – the organs accumulate compound over time until it is eventually excreted. The organs with the most incorporation of E2-7α include: the liver, spleen, GI, and kidneys. Additionally E2-7α accumulates in the feces to reach a peak concentration of 10 - 11% between 4 and 6 hours. By 24 hours the majority of the compound has been excreted. The concentration of E2-7α in whole blood and in plasma are shown in Figure 3.3A and B, respectively. The peak concentration is 39 μM in whole blood and 36 μM in plasma, both at the 1 hour time point.

The concentration of E2-7α in whole blood was determined by liquid scintillation counting. However, the concentration of E2-7α in plasma was conducted by precipitating the red blood cells and proteins from the plasma and analyzing the serum only by HPLC. The concentration of E2-7α in plasma was derived from the integration of the AUC of the 24 min peak on the HPLC. The 15 min, 1 hour, and 2 hour time points are shown in Figure 3.4 A-C. In the 15 min and 1 hour time points the only radioactive peak that is present corresponds to intact E2-7α. However, the 2 hour time point has a second radioactive peak at 13 min which is likely a metabolic breakdown product. Only the AUC of the 24 min peak was used to calculate the plasma curve shown in Figure 3.3B. The discrepancy between the whole blood curve and the plasma curve is likely due to protein binding, incorporation of E2-7α into erythrocytes, and metabolic products containing the ^{14}C atom in the vasculature.

The pharmacological parameters of E2-7α by IV (DMSO) and by IP (CR-EL based vehicle) administration were also calculated. Table 3.4 compares the following pharmacological parameters by both routes of administration: AUC: area under the blood concentration-Vs-time curve; $t_{1/2}$: half-life; CL: clearance; V_d: volume of distribution; C_{max}: maximum concentration in blood; t_{max}: time at which C_{max} was achieved. As expected the two different routes of administration and vehicles yield very different results. Interestingly the C_{max} and AUC of the IP administration is greater than that of the IV administration.

Acute Toxicity. The acute toxicity of E2-7α was determined by injecting 3-4 NIH Swiss Nude mice with 0-200 mg/kg of E2-7α IP. The mice were sacrificed 24 hours post-injection and their blood was obtained for hematology and blood chemistry analysis. The results of these findings are summarized in Table 3.5 and Table 3.6, respectively. Values that are abnormally high or low are shown in bold and all values are expressed in terms of measurable units with the exception of neutrophils, lymphocytes, monocytes, and eosinophils, which are expressed in relative terms as percent of total white blood cells. The most notable observation is that at the 200 mg/kg dose liver toxicity is evident with elevated levels of aspartate aminotransferase (AST), alanine aminotransferase (ALT), amylase, and lipase. Additionally the ratio of neutrophils to lymphocytes is dramatically increased with the 200 mg/kg dose and is also somewhat evident in the 150 mg/kg dose. The dose at which 50% of the mice die (LD_{50}) was unfortunately not reached. Therefore the LD50 is estimated to be >> 200 mg/kg.

***E2-7α* Forms DNA Adducts with Guanine Residues *in Vivo*.** E2-7α (25 mg/kg) was injected IP into mice. The liver was harvested and homogenized in order to isolate E2-7α DNA adducts that had formed *in vivo*. The DNA was isolated, hydrolyzed, and injected onto an ESI-MS. Figure 3.5 shows the main molecular ion at 813.5 m/z. This is the same mass as the ion observed when E2-7α was reacted with DNA *in vitro* as discussed in Chapter 2. CID of the 813.5 m/z peak resulted in the same 662.4 m/z and 372.2 m/z fragmentation as observed previously (data not shown). This gave us confidence that the

813.5 m/z molecular ion was indeed an E2-7α-guanine adduct in which one arm had been hydrolyzed.

Discussion

E2-7α was dissolved in DMSO and injected IV in an initial attempt to gain insight into the pharmacological properties of the compound. The liver, kidney, and spleen accumulated a significant fraction of the compound at the earliest time points. E2-7α seemed to be excreted rapidly through the feces since the 2 and 4 hour time points had significant accumulation (27 and 16% ID/g, respectively). Surprisingly, the lungs also accumulated a significant fraction of the dose. In fact, 4-fold more E2-7α was found in the lungs at every time point than in any other tissue (the only exception is the feces from 2-6 hours as the compound was being excreted). The reason for the high lung uptake is was not established but warrants speculation. It is possible that the DMSO was taken up by the blood extremely rapidly, thus causing E2-7α to aggregate and form a micelle suspension. From the tail vein the blood is transported into the lungs for oxygenation, and therefore E2-7α aggregates could potentially get trapped in the blood vessels surrounding the alveoli. In general, all IV bloodborne particles >7-8 microns are preferentially trapped in the pulmonary capillary bed. (Illum and Davis 1982; Rapp and Bivins 1983) Another possibility is E2-7α may have partitioned into the surfactant material (composed of mostly dipalmitoyl phosphatidyl choline and a smaller amount of phosphatidyl glycerol and various proteins) that coats the lungs when administered in DMSO.

Based on the undesirable effect of high accumulation of E2-7α in lung tissue, we modified the vehicle to include 43% CR-EL, 30% saline, and 27 %ethanol. An initial pilot experiment was performed in which we compared the IP and IV routes of administration of E2-7α in the CR-EL formulation. Both routes of administration displayed adequate distribution into tissues. However, one concern with the IV administration is the rapid clearance into the feces. At the 2 and 4 hour time points, the concentration of E2-7α in the feces was 5-fold and 2-fold higher than when administered by the IV route. The high concentration of E2-7α in the feces and the need to move forward with tumor ablation studies suggested the IP route of administration as being

better. Most anticancer agents are administered IV; however, work from the Sparreboom laboratory in Rotterdam has shown that the anticancer agent paclitaxel, when formulated with CR-EL, has improved pharmacokinetics in patients when administered IP rather than IV (Gelderblom et al. 2002).

E2-7α was therefore formulated in the CR-EL based vehicle and injected into mice in order to observe a complete pharmacokinetic profile with this new vehicle. E2-7α was distributed throughout the major internal organs with the highest accumulations in the liver, intestines, and spleen. The accumulation in the lungs was significantly lower than when E2-7α was formulated in DMSO (10- to 50-fold reduction at the earliest time points). Additionally, the excretion from the feces was also reduced – from 26 to 3% ID/g at 2 hours and 16 to 10% ID/g at 4 hours. The longer E2-7α remains *in vivo,* the more likely the compound could deleteriously affect the health of a tumor.

The differences in the concentration of E2-7α in blood between the two vehicles are also dramatically different. E2-7α reached a peak concentration (C_{max}) of 8 μM at 15 min when dissolved in DMSO and injected IV. The C_{max} of E2-7α when administered IP in CR-EL was nearly 5-times greater (39 μM) than when it was injected IV in DMSO. Furthermore, the C_{max} achieved with the CR-EL based vehicle when injected IP is 4-times higher than the 10 μM dose necessary to kill the ER(+) MCF-7 cells *in vitro* (Mitra et al. 2002). The t_{max} was at the one hour time point, implying a slow release from the CR-EL solution. The release of E2-7α from the CR-EL solution was slow enough to produce a >10 μM concentration in plasma for 2 hours.

The total exposure of E2-7α, as assessed by the AUC, was 7.5-fold greater when administered using CR-EL IP. The large volume of distribution in both cases indicates that the hydrophobicity of E2-7α results in rapid penetration into extravascular compartments with favorable tissue kinetics. Additionally, the removal of E2-7α from the body was 2.5-fold slower, as measured by the CL, and the $t_{1/2}$ was nearly 2-times greater when the compound was administered using the CR-EL vehicle. The increased systemic E2-7α exposure and decreased clearance in the IP administration is likely a result of the inclusion of CR-EL in the vehicle formulation. Paclitaxel, when formulated with CR-EL, has a greater systemic exposure and reduced clearance when it is administered IP versus IV. Kinetic experiments revealed that this effect is primarily

caused by reduced cellular uptake of the drug from large spherical micellar-like structures with a highly hydrophobic interior, which act as the principal carrier of circulating drug (ten Tije et al. 2003). This may help explain the dramatic difference in systemic exposure and clearance between the CR-EL and DMSO vehicles. The pharmacokinetic parameters suggest that the CR-EL based vehicle would likely result in better tumor ablation because the systemic exposure is much greater than that of E2-7α formulated in DMSO and injected IV and the clearance is much less.

Additional evidence that the CR-EL formulation administered IP may be therapeutic for the treatment of tumors stems from work on chlorambucil. Pharmacokinetic data from Newell et al, show the $t_{1/2}$ of chlorambucil is 2.4 hours and the C_{max} is 40 μM when a therapeutic dose of 10 mg/kg was administered sub-cutaneously in rats. Both the $t_{1/2}$ and the C_{max} are very similar to what was observed with a 25 mg/kg dose of E2-7α (A 10 mg/kg dose of chlorambucil is 33 μmol/kg and a 25 mg/kg dose of E2-7α is 35 μmol/kg. Therefore, the dose to an animal on a mole basis is essentially equivalent and a comparison between the compounds is straightforward). Furthermore, the total exposure of drug is greater for E2-7α than for chlorambucil (302 Vs 22 μg x Hr/mL) (Newell, Shepherd, and Harrap 1981). The exposure necessary for E2-7α to be therapeutically active could be much less than what is needed for chlorambucil if the repair shielding and transcription factor hijacking hypothesis are valid. In either case, E2-7α would be selectively retained in tumor tissue, and therefore potentially fewer DNA adducts would be required for tumor lethality. Additionally, the validity of the repair shielding and transcription factor hijacking mechanisms would suggest a greater therapeutic index for E2-7α as compared to chlorambucil, thus resulting in a less arduous course of treatment for a patient.

Blood chemistry and hematological analyses were performed in order to assess the acute toxicity to mice injected with increasing doses of E2-7α. No toxicity was evident at doses below 150 mg/kg. At the 150 mg/kg dose, a slight alteration in the ratio of lymphocytes to neutrophils was observed, such that the ratio of neutrophils increased. Furthermore, at the 200 mg/kg dose a notable increase in the percentage of neutrophils compared to the percentage of lymphocytes was observed. At the 200 mg/kg dose 72% of the white blood cells were neutrophils while 25% were lymphocytes, whereas in the

control group 80% of the white blood cells were lymphocytes and only 18% were neutrophils. Higher neutrophil and lower lymphocyte levels indicate an active infection (or in this case possible sensitivity to E2-7α). Despite the alteration in the ratio of lymphocytes to neutrophils, the total number of leukocytes remained very much unaffected. This fact is fortunate but rather surprising as many anticancer agents, including chlorambucil, induce myelosuppression. The dose limiting toxicity of chlorambucil is, in fact, neutropenia, or a decrease in neutrophils (Blumenreich et al. 1988). E2-7α not only does not induce myelosuppression but either stimulates neutrophils or inhibits the proliferation of lymphocytes in order to alter their respective ratios.

Like the hematology report, the blood chemistry profile of an acute dose of E2-7α is largely unaffected. Again, only at the 200 mg/kg dose is any toxicity evident: ALT, AST, amylase, and lipase are all elevated. These enzymes are all involved in liver function and therefore an increase in the levels of these enzymes signifies hepatotoxicity. Furthermore, blood urea nitrogen, BUN, is decreased as compared to the control mice, again indicative of hepatotoxicity (or possibly renal toxicity). Amino acids are catabolized by the liver to produce ammonia. The ammonia is combined to form urea, which is transported to the kidneys for excretion. Therefore, a decreased BUN is indicative of renal toxicity as a result of decreased urea metabolism in the liver. Hepatotoxicity has also been documented in patients treated with chlorambucil (Blumenreich et al. 1988).

The LD_{50} of E2-7α could not be determined with this experiment. All mice survived when given an acute dose ranging from 25 to 200 mg/kg. Therefore the LD_{50} is estimated to be >> 200 mg/kg. Based on other evidence not yet discussed, I estimate the LD_{50} of E2-7α after an acute dose to be approximately 300 mg/kg. (NOTE: This evidence stems from the fact that 11β, our compound used to target prostate cancer, is approximately 2.5 times more toxic than E2-7α. The LD_{50} of 11β has been estimated to be between 100 and 150 mg/kg. These data will be forthcoming in the following chapters.)

In Chapter 2, the identification of E2-7α DNA adducts formed *in vitro* was discussed. Using ESI-MS techniques, we illustrated that E2-7α covalently modified

guanine, most likely at the N7 position. The identification of these adducts was remarkable considering the related nitrogen mustard, chlorambucil, has a relatively short half-life of only 18 minutes in a non-nucleophilic 0.2 M cacodylic acid solution (pH 6.8) at 37°C (Haapala et al. 2001). The rapid decomposition of chlorambucil is a result of an intramolecular, rate-determining attack of the unprotonated nitrogen atom to form an aziridinium ion intermediate followed by attack of an external nucleophile (such as water) (Chatterji, Yeager, and Gallelli 1982; Kundu, Schullek, and Wilson 1994; Owen and Stewart 1979). Hence, chlorambucil (and other nitrogen mustards) is a reactive compound that decomposes rapidly in aqueous solutions and forms covalent bonds with other nucleophiles.

In blood, where the chloride ion concentration approximates 100 mM, chlorambucil has a much longer half-life of 2.4 hours (Newell, Shepherd, and Harrap 1981). Since chlorambucil still had somewhat of a short half-life in blood, we chose the four hour time point to look for E2-7α DNA adducts to maximize the number of adducts that could form. We believed that 4 hours would be ample time for E2-7α to react with DNA and hopefully it would not be entirely metabolized. The pharmacokinetic analysis revealed that the highest amount of drug accumulated in the liver, approximately 5% ID/g between 2 and 6 hours. Therefore, liver tissue was analyzed for the presence of DNA adducts.

As in Chapter 2, a molecular ion with a mass of 813.5 m/z was found. This is consistent with one arm of the nitrogen mustard adducted to guanine whereas the second arm had been hydrolyzed. Unfortunately, there is no way of telling when the second, non-reacting arm of the nitrogen mustard warhead underwent hydrolysis. It is possible that the second arm remained chlorinated *in vivo* and only in the procedure used to isolate the DNA adducts did the chloroethyl arm convert to hydroxyethyl. However, this may be an unlikely scenario as the half-life of the related nitrogen mustards, chlorambucil and melphalan, were found to be 2.4 hours and 1.5 hours, respectively, in plasma (Honess et al. 1985; Newell, Shepherd, and Harrap 1981). Currently, we do not have any data on the hydrolysis rate of E2-7α.

The identification of E2-7α DNA adducts *in vivo* is extremely encouraging even though the adducts were found in non-target tissue. This data illustrates that E2-7α can

be injected into a mouse, distribute throughout the body, and form DNA adducts while remaining intact. The repair shielding and transcription factor hijacking hypotheses require E2-7α to form DNA adducts in target tissues and attract tumor specific proteins. In non-target tissues, we expect the adducts to be repaired since the tissue would lack the tumor specific protein for which the molecule was designed to attract. Therefore, the formation of DNA adducts in non-target tissues is expected and in this case it serves as an illustration of the robustness of the molecule: E2-7α was administered to mice, distributed throughout the body, remained intact, and covalently modified DNA.

Conclusion

E2-7α has previously been shown to contain properties favorable to our intended mechanisms of action: it has a high RBA (46) for the ER, it is capable of covalently modifying DNA, its log D (2.22) indicates it should have favorable pharmacokinetics, and it displays differential toxicity in favor of killing the ER(+) MCF-7 cell line over ER(-) MDA-MB231 line (Mitra et al. 2002; Sharma et al. 2004). These results have been described in Chapter 2. Based on its log D and other properties making it an attractive chemotherapeutic agent, we have continued to investigate the compound by monitoring its *in vivo* pharmacokinetics, acute toxicity, and ability to adduct DNA and remain intact.

E2-7α, when formulated with a CR-EL based vehicle and injected IP, illustrates good overall distribution into tissues. At 25 mg/kg, the peak plasma concentration was 39 μM (4-fold higher than what was necessary to kill ER(+) MCF-7 cells in culture) and remained greater than 10 μM for 2 hours. The AUC, C_{max}, CL, and $t_{1/2}$ with the CR-EL vehicle are more favorable as compared to the DMSO based vehicle injected IV. The DMSO vehicle suffered from drawbacks such as high lung uptake, quicker clearance and lower systemic exposure. Therefore, the CR-EL based vehicle was used for addressing the acute toxicity of E2-7α. Very little toxicity was evident until the dose reached 200 mg/kg. At this dose, moderate liver toxicity was evident as was an elevated level of neutrophils as compared to lymphocytes. The LD_{50} was not established as all mice survived the 24 hour period after the injection. Finally, E2-7α was shown to be capable of remaining intact and forming DNA adducts in liver tissue. The DNA adducts

identified were the same as those found *in vitro* and described in Chapter 2: a mono-guanine adduct with the other arm of the nitrogen mustard having undergone hydrolysis.

In summary, these results further support the notion of E2-7α as a potential drug candidate. Following the encouraging pharmacokinetic results, we have continued to use the CR-EL based vehicle for tumor ablation studies. Chapter 4 will describe the effectiveness of E2-7α as an anticancer agent using xenograft animal models. I shall also quantify the penetrance of E2-7α into xenograft tumor tissue and describe the toxicity to mice after a therapeutic dose of E2-7α.

Future Work

CR-EL has provided us with a means of administering E2-7α into mice. However, it is by no means an ideal delivery vehicle. The literature is inundated with reports on the toxic side effects of CR-EL. A number of studies have reported that CR-EL induced side effects such as hypersensitivity, neurotoxicity, nephrotoxicity, and the extraction of plasticizers from intravenous infusion lines (Cheon et al. 2003; Gregory and DeLisa 1993; Mazzo et al. 1997; Onetto et al. 1993). Nonetheless, the anticancer agent Taxol (paclitaxel) continues to use a vehicle containing CR-EL, although the side effects are now diminished with various pretreatments. Despite the continued use of Taxol with CR-EL in the treatment of patients with cancer, the scientific community realizes that a need exists to eliminate CR-EL from the current formulation. This is the subject of many articles and reviews (Gelderblom et al. 2002; Singla, Garg, and Aggarwal 2002; ten Tije et al. 2003).

We also acknowledge the limitations of CR-EL, especially with such a high concentration (43%) in our vehicle. In this effort we have begun a collaboration with the Sasisekharan Laboratory at MIT in an effort to formulate E2-7α using liposomes. We have conducted a pilot experiment in which we injected a liposomal solution of our other compound, 11β, into two mice. Blood was taken for several hours and worked up to show that the liposomes circulate in plasma for a considerable period of time. In fact, as much as 80% of the drug was still circulating in blood 24 hours later. Unfortunately, a full bio-distribution experiment was not able to confirm these results. The most likely reason was the lipids had oxidized and the liposomes were unstable at injection and

unable to transport our molecule effectively. However, this joint effort is ongoing and we anticipate promising results in the near future. If a suitable alternative delivery agent cannot be found, it is possible to continue the use with CR-EL since Taxol is formulated as a concentrated solution of 6 mg per mL of CR-EL:dehydrated ethanol (1:1 v/v) which must be further diluted 5 to 20-fold with saline prior to IV administration (Goldspiel 1994).

Any new delivery agent would have to undergo the same rigorous experiments, described in this chapter, as the current vehicle: bio-distribution, pharmacokinetic analysis, and acute toxicity. However, the work here sets a foundation for which alternative delivery agents can be judged.

Even though the LD_{50} of E2-7α using the CR-EL based vehicle was not reached, I believe it to be in the best interest of this researcher to delay repeating these experiments until such a time as a more clinically relevant vehicle can be used. For now, the best guess is that E2-7α will have an LD_{50} of approximately 300 mg/kg.

Finally, Charles Morton and I have begun work using human liver microsomes to address the metabolic fate of E2-7α. Initial experiments have not provided much useful information; however, a recent search of the literature indicates that we may have been using too much drug for the assay and thus saturated the system. We are confident that in the near future we will be able to identify the metabolites of E2-7α and also the P450s likely responsible for its breakdown.

Reference List

Barret, J.M. and Hill, B.T. DNA repair mechanisms associated with cellular resistance to antitumor drugs: potential novel targets. *Anticancer Drugs* **9**, 105-123 (1998)

Blumenreich, M.S., Woodcock, T.M., Sherrill, E.J. et al. A phase I trial of chlorambucil administered in short pulses in patients with advanced malignancies. *Cancer Invest* **6**, 371-375 (1988)

Chatterji, D.C., Yeager, R.L., and Gallelli, J.F. Kinetics of chlorambucil hydrolysis using high-pressure liquid chromatography. *J. Pharm. Sci.* **71**, 50-54 (1982)

Cheon, L.S., Kim, C., Chan, K., I et al. Polymeric micelles of poly(2-ethyl-2-oxazoline)-block-poly(epsilon-caprolactone) copolymer as a carrier for paclitaxel. *J. Control Release* **89**, 437-446 (2003)

Dolan, M.E. Inhibition of DNA repair as a means of increasing the antitumor activity of DNA reactive agents. *Adv. Drug Del. Rev.* **26**, 105-118 (1997)

Ferno, M., Borg, A., Johansson, U. et al. Estrogen and progesterone receptor analyses in more than 4,000 human breast cancer samples. A study with special reference to age at diagnosis and stability of analyses. Southern Swedish Breast Cancer Study Group. *Acta Oncol.* **29**, 129-135 (1990)

Frankfurt, O.S. Inhibition of DNA repair and the enhancement of cytotoxicity of alkylating agents. *Int. J. Cancer* **48**, 916-923 (1991)

Gelderblom, H., Verweij, J., van Zomeren, D.M. et al. Influence of Cremophor El on the bioavailability of intraperitoneal paclitaxel. *Clin. Cancer Res.* **8**, 1237-1241 (2002)

Goldspiel, B.R. Pharmaceutical issues: preparation, administration, stability, and compatibility with other medications. *Ann. Pharmacother.* **28**, S23-S26 (1994)

Gregory, R.E. and DeLisa, A.F. Paclitaxel: a new antineoplastic agent for refractory ovarian cancer. *Clin. Pharm.* **12**, 401-415 (1993)

Haapala, E., Hakala, K., Jokipelto, E. et al. Reactions of N,N-bis(2-chloroethyl)-p-aminophenylbutyric acid (chlorambucil) with 2'-deoxyguanosine. *Chem. Res. Toxicol.* **14**, 988-995 (2001)

Honess, D.J., Donaldson, J., Workman, P., and Bleehen, N.M. The effect of systemic hyperthermia on melphalan pharmacokinetics in mice. *Br. J. Cancer* **51**, 77-84 (1985)

Hurley, L.H. DNA and its associated processes as targets for cancer therapy. *Nature Rev. Cancer* **2**, 188-200 (2002)

Illum, L. and Davis, S.S. The targeting of drugs parenterally by use of microspheres. *J. Parenter. Sci. Technol.* **36**, 242-248 (1982)

Kundu, G.C., Schullek, J.R., and Wilson, I.B. The alkylating properties of chlorambucil. *Pharmacol. Biochem. Behav.* **49**, 621-624 (1994)

Mazzo, D.J., Nguyen-Huu, J.J., Pagniez, S., and Denis, P. Compatibility of docetaxel and paclitaxel in intravenous solutions with polyvinyl chloride infusion materials. *Am. J. Health Syst. Pharm.* **54**, 566-569 (1997)

Mitra, K., Marquis, J.C., Hillier, S.M. et al. A rationally designed genotoxin that selectively destroys estrogen receptor-positive breast cancer cells. *J. Amer. Chem. Soc.* **124**, 1862-1863 (2002)

Newell, D.R., Shepherd, C.R., and Harrap, K.R. The pharmacokinetics of prednimustine and chlorambucil in the rat. *Cancer Chemother. Pharmacol.* **6**, 85-91 (1981)

Onetto, N., Canetta, R., Winograd, B. et al. Overview of Taxol safety. *J. Natl. Cancer Inst. Monogr* 131-139 (1993)

Owen, W.R. and Stewart, P.J. Kinetics and mechanism of chlorambucil hydrolysis. *J. Pharm. Sci.* **68**, 992-996 (1979)

Rapp, R.P. and Bivins, B.A. Final in-line filtration: removal of contaminants from IV fluids and drugs. *Hosp. Formul.* **18**, 1124-1128 (1983)

Rink, S.M., Yarema, K.J., Solomon, M.S. et al. Synthesis and biological activity of DNA damaging agents that form decoy binding sites for the estrogen receptor. *Proc. Natl. Acad. Sci. U. S. A* **93**, 15063-15068 (1996)

Sharma, U., Marquis, J.C., Nicole, D.A. et al. Design, synthesis, and evaluation of estradiol-linked genotoxicants as anti-cancer agents. *Bioorg. Med. Chem. Lett.* **14**, 3829-3833 (2004)

Singla, A.K., Garg, A., and Aggarwal, D. Paclitaxel and its formulations. *Int. J. Pharm.* **235**, 179-192 (2002)

Teicher, B.A. Cancer Principles and Practice. <u>Antitumor alkylating agents</u> 5,405-417
(1997)

ten Tije, A.J., Verweij, J., Loos, W.J., and Sparreboom, A. Pharmacological effects of
formulation vehicles : implications for cancer chemotherapy. *Clin.*
Pharmacokinet. **42**, 665-685 (2003)

Distribution of E2-7α in Mouse Tissue with a DMSO Based Vehicle

Tissue	0.25 hr	1 hr	2 hr	4 hr	6 hr	24 hr
Blood	0.90 ± 0.22	0.83 ± 0	0.19 ± 0.12	0.46 ± 0.22	0.31 ± 0.26	0.15 ± 0.00
Lung	43.3 ± 13.2	53.8 ± 0	21.9 ± 15.9	14.26 ± 0.2	4.31 ± 0.99	0.41 ± 0.16
Liver	11.8 ± 1.3	14.3 ± 0	5.79 ± 2.1	4.24 ± 0.47	0.58 ± 0.08	2.63 ± 0.32
Spleen	2.71 ± 0.9	3.21 ± 0	1.41 ± 0.24	1.70 ± 0.20	0.20 ± 0.07	1.19 ± 0.02
Kidney	3.84 ± 1.06	5.4 ± 0	2.27 ± 0.78	2.06 ± 0.39	0.44 ± 0.16	0.75 ± 0.03
GI	0.82 ± 0.41	0.38 ± 0	0.58 ± 0.06	0.99 ± 0.13	0.17 ± 0.06	0.18 ± 0.04
Feces	0.69 ± 0.43	1.16 ± 0	26.5 ± 22.7	16.2 ± 0.9	2.68 ± 0.33	0.52 ± 0.14
Adipose	0.31 ± 0.09	0.18 ± 0	0.2 ± 0.11	0.19 ± 0.05	0.04 ± 0	0.10 ± 0.02

Table 3.1 Mice were injected IV with 5 μCi of ^{14}C-E2-7α dissolved in DMSO. They were sacrificed at 0.25, 1, 2, 4, 6, or 24 hours after the injection. The results are reported as the mean percent injected dose per gram (of each organ) ± standard deviation.

Pilot Bio-Distribution of E2-7α using a New Cremophor Based Vehicle

Tissue	2 Hr. IV	2 Hr. IP	4 Hr. IV	4 Hr. IP
Blood	0.6 ± 0.1	0.4 ± 0.18	0.34 ± 0.03	0.19 ± 0
Heart	1.29 ± 0.48	0.31 ± 0.07	0.42 ± 0.23	0.34 ± 0.12
Lung	4.17 ± 0.74	1.07 ± 0.32	2.59 ± 0.98	1.35 ± 0.46
Liver	5.51 ± 1.23	3.3 ± 0.11	2.45 ± 0.42	2.95 ± 0.97
Spleen	1.91 ± 0.22	2.84 ± 0.72	0.89 ± 0.27	2.46 ± 0.3
Kidney	3.78 ± 0.86	1.44 ± 0.25	1.92 ± 0.7	1.55 ± 0.43
GI	1.41 ± 0.62	4.25 ± 0.42	0.98 ± 0.39	4.23 ± 2.59
Feces	15.97 ± 6.22	2.7 ± 2.23	14.82 ± 8.68	8.02 ± 0.36
Muscle	0.58 ± 0.1	0.4 ± 0.19	0.44 ± 0.4	0.19 ± 1

Table 3.2 Mice were injected either IP or IV with 5 μCi of ^{14}C-E2-7α dissolved in 43% CR-EL, 30% saline, 27% ethanol. They were sacrificed at either 2 or 4 hours after the injection. The results are reported as the mean percent injected dose per gram (of each organ) ± standard deviation.

Bio-Distribution of E2-7α in Mouse Tissue using a Cremophor Based Vehicle

Tissue	0.25 hr	1 hr	2 hr	4 hr	6 hr	24 hr
Blood	0.6 ± 0	1.48 ± 0	0.82 ± 0	0.86 ± 0	0.89 ± 0	0.3 ± 0
Heart	0.11 ± 0	0.28 ± 0.08	0.68 ± 0.17	0.48 ± 0.09	0.51 ± 0.17	0.29 ± 0.21
Lung	0.36 ± 0	1.06 ± 0.24	1.79 ± 0.31	1.74 ± 0.55	1.99 ± 0.35	1.58 ± 0.39
Liver	2.4 ± 0	3.99 ± 0.39	5.84 ± 1.06	4.93 ± 0.9	4.03 ± 1.33	1.86 ± 0.13
Spleen	1.2 ± 0	3.91 ± 0.82	4.77 ± 1.11	4.42 ± 0.23	3.93 ± 0.29	2.16 ± 0.3
Kidney	0.48 ± 0	1.36 ± 0.09	2.01 ± 0.12	2.49 ± 0.19	2.39 ± 0.89	0.97 ± 0.17
GI	2.05 ± 0	2.44 ± 0.7	5.22 ± 1.31	4.06 ± 0.99	4.45 ± 1.51	2.03 ± 0.62
Feces	1.02 ± 0	0.79 ± 0.48	2.6 ± 0.64	9.87 ± 1.16	11.4 ± 3.28	1.75 ± 0.31
Muscle	0.22 ± 0	0.29 ± 0.14	0.25 ± 0.14	0.17 ± 0.05	0.16 ± 0.04	0.09 ± 0.01

Table 3.3 Mice were injected IP with 5 µCi of ^{14}C-E2-7α dissolved in 43 % CR-EL, 30 % saline, 27 % ethanol. They were sacrificed at 0.25, 1, 2, 4, 6, or 24 hours after the injection. The results are reported as the mean percent injected dose per gram (of each organ) ± standard deviation.

E2-7α has Better Pharmacokinetics when Formulated with CR-EL

Parameter	DMSO IV	CR-EL IP
AUC^a (µg x hr/mL)	40	302
$t_{1/2}{}^b$ (hr)	2.4	4.4
CL^c (mL/hr)	15.6	6.2
$V_d{}^d$ (L/kg)	4.4	2.7
$C_{max}{}^e$ (µM)	7.9	38.7
$t_{max}{}^f$ (hr)	0.25	1

Table 3.4 Pharmacokinetic parameters following the administration of E2-7α by two different routes of administration: IV with DMSO as the vehicle or IP with a CR-EL based vehicle. [a] area under the blood concentration-Vs-time curve, [b] half-life, [c] clearance, [d] volume of distribution, [e] maximum concentration in blood, [f] time at which C_{max} was achieved.

Acute Toxicity of E2-7α:
Hematology

Test	Control N = 4	Vehicle N = 3	25 mg/kg N = 3	50 mg/kg N = 4	75 mg/kg N = 4	100 mg/kg N = 4	150 mg/kg N = 4	200 mg/kg N = 4	Taconic Nude
WBC (x mm³)	7.3	6.1	9.5	4.8	5.3	5.2	5.9	6.6	4.3-13.5
RBC (x 10⁶ mm³)	10.1	10.2	9.8	9.2	9.6	9.9	10.1	8.5	6.9-8.52
Hgb (g/dL)	15.2	15.4	15.1	14.2	14.5	14.5	14.6	12.9	7.5-15.2
HCT (%)	55.1	56.0	52.1	49.4	51.4	53.8	53.8	48.1	39.4-43.5
Neutrophils (%)	17.5	27.3	17.7	32.5	25.3	26.3	46.8	*71.5*	7.0-39
Lymphs (%)	80.0	70.3	78.7	64.8	71.0	71.3	51.5	*25.0*	56-92
Monos (%)	1.0	2.3	3.0	1.3	1.3	1.7	2.0	2.0	0-7
Eos (%)	1.0		0.7	1.5	1.0	1.0	1.0	1.0	0-4
Platelets (10³/µL)	1138.3	1257.3	977.3	963.3	1037.8	1126.7	875.0	948.8	790-1014
MCV (fL)	54.8	55.0	53.1	53.5	46.8	54.6	53.1	56.4	51.1-53.4
MCH (pg)	15.1	15.1	15.5	15.4	15.2	14.8	14.5	15.2	17.6-19.1
MCHC (g/dL)	27.7	27.4	29.0	28.9	28.4	27.1	27.2	27.2	34.3-36.1

Table 3.5 Hematology report for mice injected with E2-7α. Values in bold represent abnormally elevated or suppressed levels. Only the ratio of neutrophils to lymphocytes is altered at the highest dose of 200 mg/kg.

(Note: Since the test groups contained relatively few mice, the abnormal levels are deviations from the normal range and do not necessarily reflect statistical significance.)

Acute Toxicity of E2-7α: Blood Chemistry

Test	Control N = 4	Vehicle N = 3	25 mg/kg N = 3	50 mg/kg N = 4	75 mg/kg N = 4	100 mg/kg N = 4	150 mg/kg N = 4	200 mg/kg N = 4	Taconic Nude
Alk. Phosphatase (IU/L)	136	137	140	134	122	113	102	97	96-117
ALT (SGPT) (IU/L)	45	57	65	34	35	54	52	*1011*	
AST (SGOT) (IU/L)	186	136	126	96	117	110	167	*1337*	61-119
CK (IU/L)	814	527	412	323	493	279	681	313	
GGT (IU/L)	0.3	0.0	0.0	0.0	0.8	0.5	0.0	0.0	
Albumin (g/dL)	3.4	3.6	3.5	3.4	3.3	3.4	3.4	3.1	3.4-4.1
Total Protein (g/dL)	5.3	5.5	5.6	5.5	5.4	5.5	5.6	4.9	4.8-5.6
Globulin (g/dL)	1.9	1.9	2.1	2.1	2.1	2.1	2.3	1.8	1.1-1.6
Total Bilirubin (mg/dL)	0.1	0.1	0.1	0.2	0.1	0.1	0.1	0.2	0.3-0.8
Direct Bilirubin (mg/dL)	0.1	0.1	0.0	0.0	0.0	0.1	0.1	0.1	
BUN (mg/dL)	23.5	26.7	26.7	25.3	25.5	22.0	23.8	*14.0*	30-37
Creatinine (mg/dL)	0.2	0.3	0.3	0.4	0.3	0.3	0.3	0.2	0.5-0.7
Cholesterol (mg/dL)	143	141	133	121	125	132	127	127.0	116-155
Glucose (mg/dL)	237	314	278	267	187	212	197	167.7	173-288
Calcium (mg/dL)	10.6	11.7	11.5	11.3	10.7	10.9	11.2	11.1	10.0-12.0
Phosphorous (mg/dL)	10.4	11.9	11.4	10.6	9.4	11.2	10.7	11.6	12.3-16.1
Bicarbonate (mEq/L)	28.8	24.7	26.7	28.3	29.3	30.5	28.3	40.0	
Chloride (mEq/L)	106	103	106	106	109	108	107	100.3	118-124
Potassium (mEq/L)	9.7	11.7	10.7	10.3	8.3	10.1	9.9	7.8	13.8-16.7
Sodium (mEq/L)	153	154	153	152	155	152	153	154.7	157-163
A/G Ratio	1.8	1.9	1.6	1.7	1.6	1.6	1.5	1.8	
B/C Ratio	103.4			68.3	87.8	72.2	80.0	80.0	
Indirect Bilirubin (mg/dL)	0.0	0.0	0.1	0.2	0.1	0.1	0.1	0.1	
Na/K Ratio	16.3	13.0	15.0	15.0	18.5	15.0	16.3	19.7	
Anion Gap (mEq/L)	27.8	33.5	31.3	28.0	24.8	23.8	28.3	22.0	
Amylase (IU/L)	1283	1518	1303	1357	1203	1287	1682	*7275*	
Lipase (IU/L)	79	80	106	140	107	191	490	*2977*	

Table 3.6 Blood Chemistry report for mice injected with E2-7α. Values in bold represent abnormally elevated or suppressed levels. Slight evidence of liver toxicity is observed with elevated levels of liver enzymes, including: ALT, AST, amylase, and lipase.

(Note: Since the test groups contained relatively few mice, the abnormal levels are deviations from the normal range and do not necessarily reflect statistical significance.)

Clearance of E2-7α from Blood after Administration with a DMSO Based Vehicle
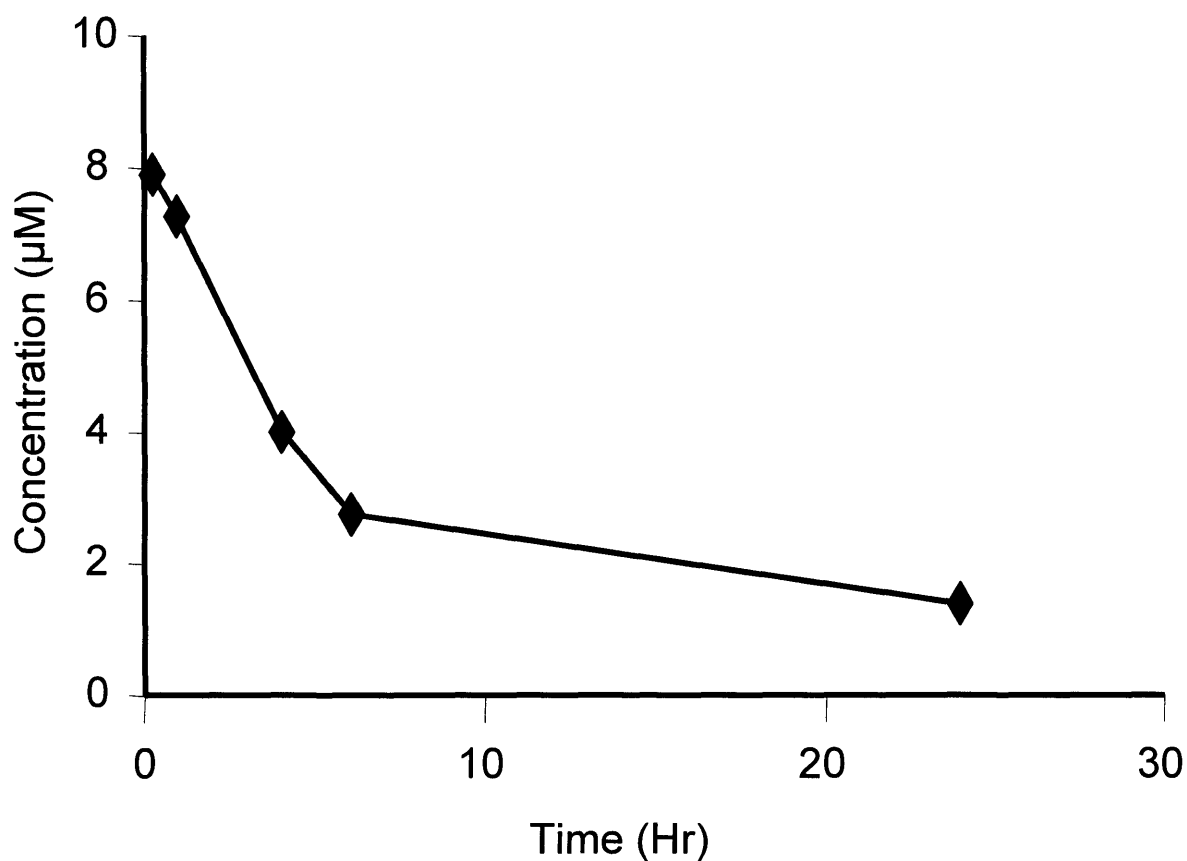
Fig 3.1 Concentration of E2-7α in whole blood after an IV administration of the compound dissolved in DMSO. The peak concentration is 7.8 μM.

Pilot Bio-Distribution of E2-7α using a New Cremophor Based Vehicle
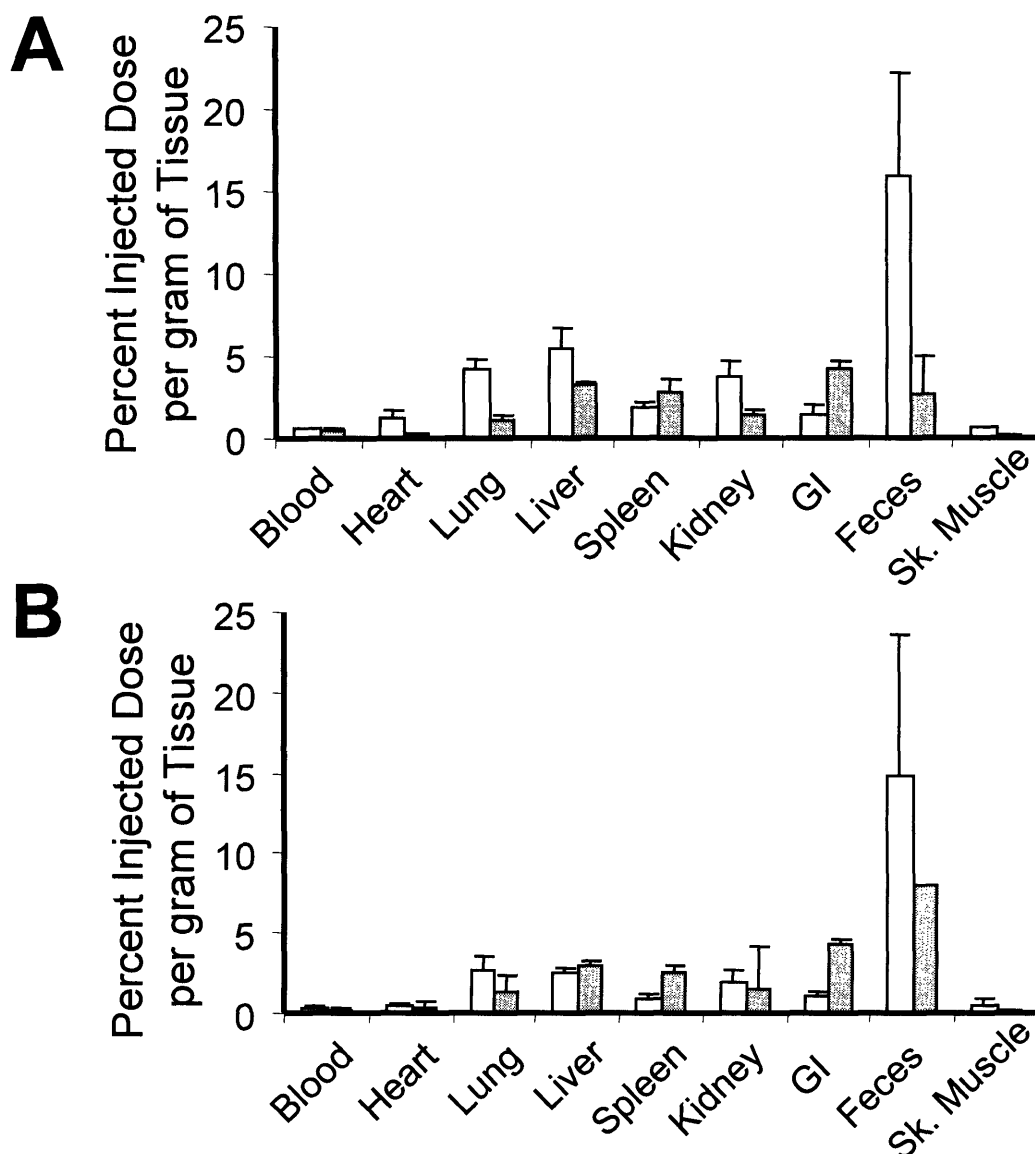
Fig 3.2 Mice were injected either IV (□) or IV (▦) with 5 μCi of ^{14}C-E2-7α dissolved in 43% CR-EL, 30% saline, 27% ethanol. They were sacrificed at either 2 **(A)** or 4 hours **(B)** after the injection. The results are reported as the mean percent injected dose per gram (of each organ) ± standard deviation.

Clearance of E2-7α from Blood and Plasma after Administration with a Cremophor-EL Based Vehicle

A

B
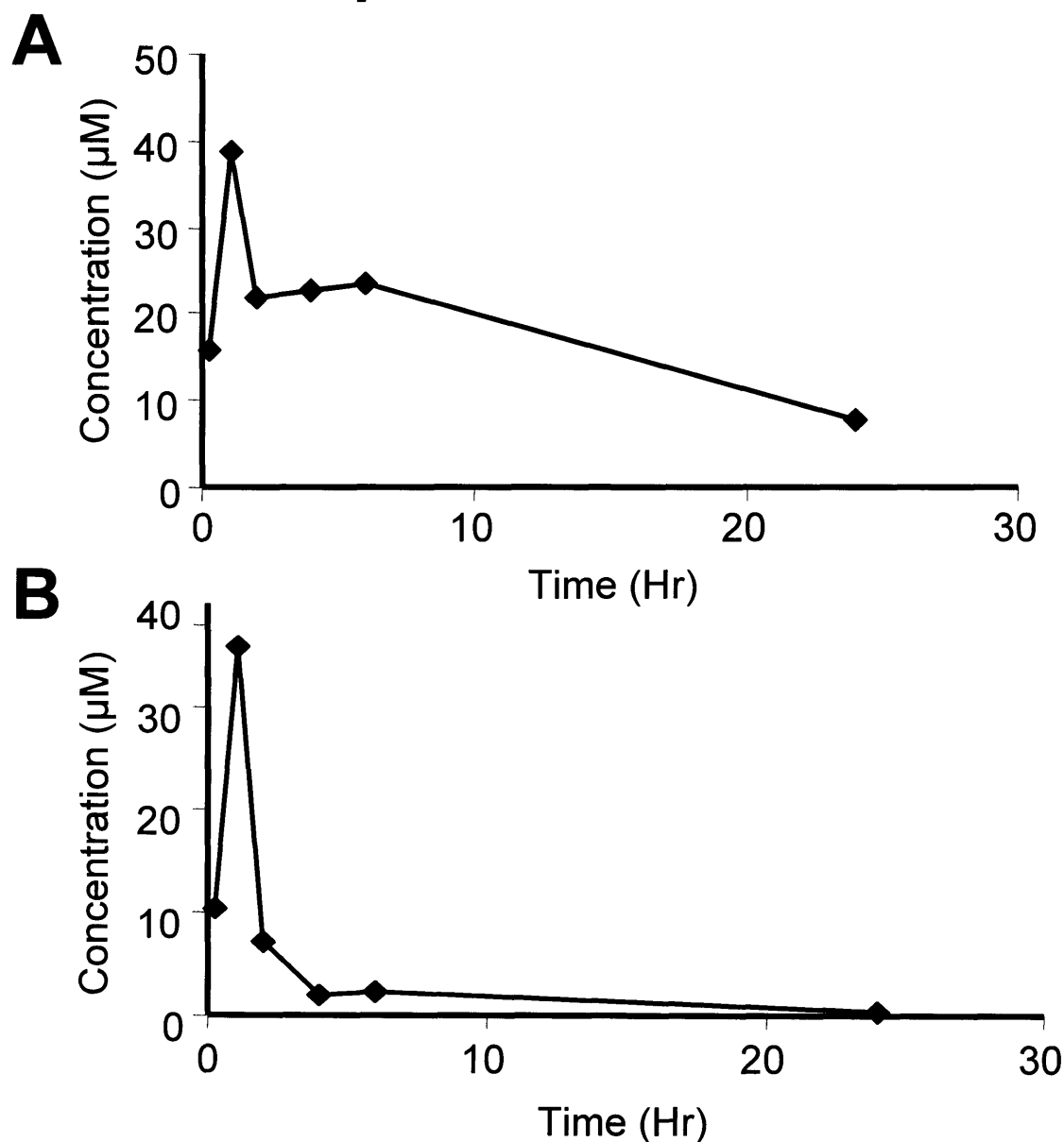
Fig 3.3 Clearance of E2-7α from Blood **(A)** and Plasma **(B)**. E2-7α was administered to mice and the concentration in whole blood and plasma was determined. The peak concentration is 39 μM in whole blood and 36 μM in plasma, both at one hour.

Intact E2-7α is the Major Radioactive Product in Mouse Plasma

A

B

C

Time (min)
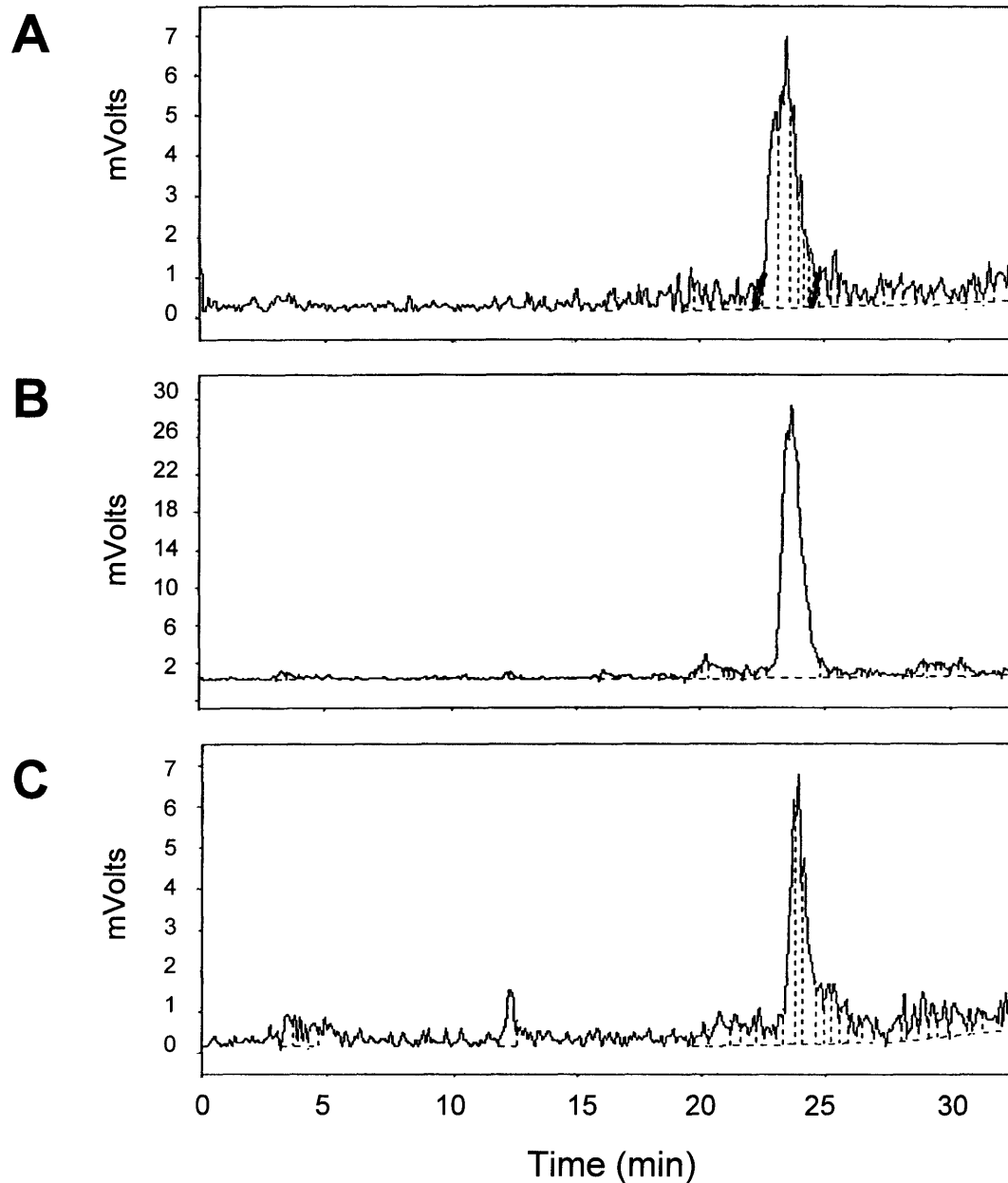
Fig 3.4 HPLC traces of intact E2-7α in plasma **A.** 15 min **B.** 1 hour **C.** 2 hour. Plasma was isolated from whole blood, precipitated with acetonitrile and injected onto HPLC. The peak at 24 min is intact E2-7α. The peak at 13 min in **3C** is probably a metabolic breakdown product.

E2-7α Forms DNA Adducts in Mouse Liver Tissue
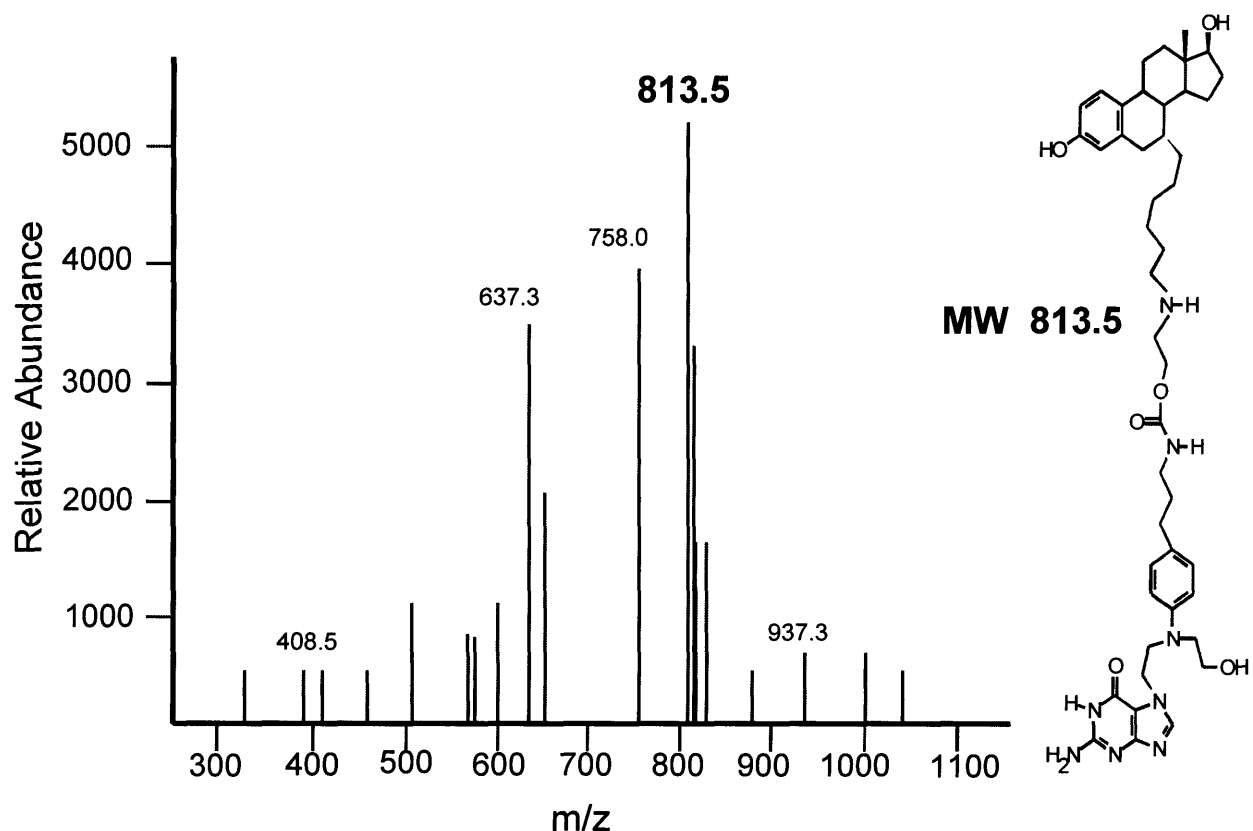
Fig 3.5 E2-7α DNA adduct isolated from the liver of a mouse. The same 813.5 m/z molecular ion is evident as was seen in the *in vitro* adduction experiments discussed in Chapter 2.

Chapter 4

Probing the Biochemical Mechanisms of
E2-7α *in Vivo:*

Efficacy against ER(+) Tumors, DNA Adduct Levels
and Chronic Toxicity

Introduction

Breast cancer is the most frequently diagnosed malignancy among women in the US, accounting for 30% of all cancers diagnosed, (Greenlee et al. 2000) with an incidence of 135 cases per 100,000 women and a death rate of 27.7 per 100,000 women (Weir et al. 2003). Despite increased mammography screening and new genomics-based drugs, such as Herceptin, an estimated 40,000 women will have died from breast cancer in 2004 (according to the American Cancer Society's statistics for 2003-2004). Most women are treated with a combination of surgery and an adjuvant therapy such as radiation, hormone therapy, or chemotherapy. The decision to use chemotherapy or hormone therapy depends on the presence or absence of the estrogen receptor (ER) in the primary tumor. Approximately half of breast cancers overexpress the ER (Ferno et al. 1990). The anti-estrogens, tamoxifen and raloxifene, reduce the incidence of cancer relapse in ER expressing tumors and can even delay or prevent the development of breast cancer in women at high risk (Peto and Mack 2000). These compounds antagonize the effects of estrogen and therefore put tumor cells into a state of stasis, which can eventually lead to apoptosis (Lerner and Jordan 1990; Obrero, Yu, and Shapiro 2002). Hormonal therapy can be extended over long periods in which the ER(+) tumors are often held in check. However, the long term effectiveness of such therapies is complicated by the development of hormone resistant breast cancer (HRBC) (Katzenellenbogen 1991) and possible secondary carcinogenesis (Jordan 1995; Osborne et al. 1996). Additionally, ovarian tumors that express the ER do not respond well to endocrine therapy. Therefore, a need exists for more effective agents to target ovarian tumors and HRBC.

Clinicians have used a combination of agents that act by different biological mechanisms in order to overcome the resistance to front-line agents used to treat breast cancer. Hundreds of clinical trials have illustrated the additional therapeutic benefit of treating patients with combinations of drugs, instead of a single agent, for breast cancer treatment (Hortobagyi 1998). Another strategy is the design of a chemotherapeutic with additional built-in mechanisms to disrupt cellular signaling and transcriptional events necessary for growth and proliferation. We have reported on the design, synthesis, and biological properties of novel molecules that are capable of attacking a cancer cell by several mechanisms. These molecules consist of a DNA damaging warhead that can

covalently adduct DNA, as many conventional alkylating chemotherapeutics, and a ligand binding domain that can attract proteins found predominantly in a cancer cell. We have utilized the overexpression of the ER in many breast cancers (and in HRBC), by designing an agent that links a DNA damaging agent to an estradiol moiety capable of attracting the ER to the site of DNA damage. A DNA-adduct-ER complex could potentially inhibit repair enzymes from accessing the lesion, resulting in persistence of the adduct and eventually cell death. Furthermore, the ER is a transcription factor and a high binding affinity to the DNA-adduct could titrate the ER from necessary cellular transcriptional events, again resulting in cell death. These two mechanisms, DNA repair shielding and transcription factor hijacking, would produce lethal results for a cancer cell.

In Chapter 2, I described the biological properties of our current lead compound, E2-7α. E2-7α has a high RBA for the ER (46), is capable of forming DNA adducts with a high affinity for the ER, has a low log D (2.22), and displays differential toxicity in favor of killing the ER(+) MCF-7 cell line over the ER (-) MDA-MB231 line (Mitra et al. 2002; Sharma et al. 2004). In Chapter 3, I described the pharmacokinetics of E2-7α in two different vehicles, one of which was shown to be superior. Furthermore, the acute toxicity of E2-7α in the cremophor-EL (CR-EL) based vehicle was shown to be very moderate, and the identification of E2-7α DNA adducts isolated from liver tissue indicated that the compound could remain intact and alkylate DNA.

The results from these experiments have given us confidence in our compound and the methodology used to administer the compound to mice. This chapter will therefore describe the efficacy of E2-7α as a treatment for ER(+) HeLa xenografts implanted into mice. Furthermore, the toxicity to mice following the tumor therapy study will also be discussed. Finally, the results of studies focusing on quantifying the number of DNA adducts formed after a therapeutic dose of E2-7α in tumor tissue will also be discussed.

Through a collaboration with the Tannenbaum laboratory at MIT, I have employed the use of accelerator mass spectrometry (AMS) to quantify the number of DNA adducts found in tissue samples following administration of E2-7α into mice. Since this methodology is relatively new and only 200 articles were found on the topic in a recent PubMed search (half of which pertained to biological applications), I believe this

methodology requires a brief introduction. AMS has been used for the last 30 years but predominantly for radiocarbon dating of archaeological samples based on their $^{14}C:^{12}C$ or $^{14}C:^{13}C$ ratios. However, more recently its use has been expanded to the biomedical arena where it can detect many isotopes at the attomole level (Vogel et al. 1995; Vogel et al. 2001; Williams et al. 2002). This level of sensitivity can be achieved by measuring long-lived, rare isotopes of low natural abundance: ^3H, ^{10}Be, ^{14}C, ^{26}Al, ^{36}Cl, ^{41}Ca, and ^{129}I (Turteltaub and Vogel 2000).

For biological applications, the most commonly used isotope is ^{14}C since drugs are often radiolabeled for metabolic and disposition analysis. The main advantage of AMS over scintillation counting is the extremely high sensitivity – radioactivity as low as 0.0001 dpm (decays per minute) have been reported (Garner 2000) (this contrasts to 100 decays per minute by traditional scintillation counting). This sensitivity is achieved through the use of mass spectrometers rather than the detection of individual radioactive decay events as current scintillation counting technology utilizes. Quantification of ^{14}C in a sample generally involves the conversion of the sample to graphite prior to the introduction into the ion source. However, the AMS in the Tannenbaum lab uses a slightly different technology in which the sample is combusted using a laser as a heat source and copper oxide as an accelerant. See Figure 4.1. One of the advantages of this approach is that the step of converting the sample to graphite in a slow and time consuming manner is eliminated. Furthermore, this approach theoretically can be linked to an HPLC for in-line analysis of metabolites in blood samples and, since the sample loading only requires the pipetting of the sample onto a disc, this process could be easily automated (Liberman et al. 2004).

The sample is volatilized by the laser and converted to atomic species that are then introduced into a negative ion mass analyzer. See Figure 4.2. The negative ion source removes ^{14}N as a contaminant. A low energy mass analyzer isolates masses of 14 amu, and a Van de Graf accelerator with a foil stripper converts the negatively charged ions to positively charged species. A second mass analyzer then isolates molecular ions with a mass of 14 amu and a charge of +2, i.e. $^{14}C^{2+}$.

Figure 4.3 depicts a representative data trace of a sample subject to AMS analysis. In this case ^{14}C-E2-7α was administered to a mouse and its liver was isolated,

homogenized, and then analyzed by AMS. The homogenate was diluted 500-, 2,000-, or 10,000-fold in an effort to determine the lower detection limit. ^{14}C-BSA of a known specific activity was used as a standard. The samples were loaded onto a disc that rotates clockwise in the sample chamber, and each sample is spotted in duplicate or triplicate with approximately 5° of rotational separation between each sample; therefore, a peak is observed every time ^{14}C from the sample is detected. The area under each peak correlates to the amount of ^{14}C in each sample. The results illustrate that the AMS is capable of detecting the 60 counts per minute (CPM) in the homogenate even when the sample is diluted 10,000-fold. By contrast, a traditional liquid scintillation counter has a limit of detection near 60 CPM. The AMS is, therefore, at least 10,000 times more sensitive than traditional liquid scintillation counting. A high concentration of ^{12}C content in a sample interferes with the detection of ^{14}C and consequently the sensitivity of AMS can be much greater than what was seen here with a crude liver homogenate sample.

The power of AMS is only now being recognized and the technique is finding its way into a diverse array of biological applications. Studies have been published using the technology for the quantification of drug in blood samples using levels of radioactivity that are lower than what is mandated by law to report. AMS technology has also been used in the detection of covalently modified protein or DNA samples by drugs or their reactive metabolites (Turteltaub and Dingley 1998). Furthermore, AMS technology can be used to image ligand binding in tissue samples and isotopes other than ^{14}C, such as ^{41}Ca and ^{26}Al, can be used in biological tracing studies. Further information on the applications of AMS to biochemistry, pharmacology, toxicology, and nutritional sciences can be found in several reviews (Garner 2000; Ross et al. 2004; Turteltaub and Vogel 2000; White and Brown 2004).

Materials and Methods

Animals. Four to six week old NIH Swiss *nu/nu* athymic mice (25g) were purchased from the National Cancer Institute-Frederick Cancer Center (NCI), (Frederick, MD). The mice were housed under standard conditions in MIT approved facilities with 12 hour

light/dark cycles and food and water *ad libitum*. All protocols were performed in compliance with the regulations of the Animal Care Committee at MIT.

Cell Culture. The human cervical cancer cell line, HeLa, was obtained from the American Type Culture Collection (Rockville, MD). The cell line was maintained in DMEM with glutamax (Gibco) supplemented with 10% fetal bovine serum in a humidified CO_2/air atmosphere at 37°C. HeLa cells were stably transfected with the human ER-ligand binding domain (ER-LBD) by John Marquis and Peter Rye using the Becton Dickinson Biosciences (Clontech) Tet-Off gene expression system. When the cells were used for injection into mice, the cells were grown in a P-150 plate to 50-70% confluence. The cells were trypsinized, washed, and pelleted.

Tumor Therapy. ER-LBD (+) HeLa cells were collected and suspended in 50% saline, 50% Matrigel (Becton Dickinson, Franklin Lakes, NJ) and diluted to a concentration of 10×10^6 cells/mL. A 0.25 mL aliquot of the cell suspension was injected into the right hind flank of each mouse. Therapy commenced when a palpable tumor of approximately 5 x 5 mm formed (5-7 days for HeLa cells). E2-7α was formulated in 43% CR-EL, 30% saline, and 27% ethanol and administered either IP at a dose of 75 mg/kg or sub-cutaneously (Sub-Q) at a dose of 25 mg/kg. Sub-Q doses were injected adjacent to the tumor and not directly into the tissue. Chlorambucil was also formulated in 43% CR-EL, 30% saline, and 27% ethanol but injected at a dose of 15 mg/kg. The vehicle controls consisted of only 43% CR-EL, 30% saline, and 27% ethanol Tumor dimensions were measured five times per week with vernier calipers. Tumor volumes were calculated using the formula of an ellipse: $\pi/6$ x (smaller diameter)^2 x larger diameter. Statistical analyses were performed using a paired t-test. The mice were treated with 3 cycles of 5 days on and 2 days off.

Assessment of Chronic Exposure of E2-7α. At the end of the HeLa tumor therapy study, mice were euthanized by CO_2 asphyxiation. Blood was obtained by cardiac puncture and sent to IDEXX (formerly Tufts Veterinary Diagnostic Laboratory, North

Grafton, MA) for hematology and blood chemistry analysis in order to assess the chronic toxicity to the mice.

Quantification of DNA Adducts in Tissue. Approximately 400,000 counts per minute (CPM) of ^{14}C-E2-7α were injected into NIH Swiss *nu/nu* mice with HeLa xenografts by either IP or Sub-Q injection. The mice injected IP were given a dose of 75 mg/kg and the Sub-Q group was injected with a 25 mg/kg dose (these doses are the same as what was used for the tumor therapy study). The mice were sacrificed after 4 hours by carbon dioxide asphyxiation. The liver was surgically removed, snap frozen on dry ice, and stored at -80°C until it could be processed further. The liver and tumor samples were thawed and homogenized in a Dounce homogenizer on wet ice with 15 mL of cold (4°C) 0.01M Tris (pH 6.9), 0.25M sucrose, 2 mM calcium chloride buffer. The homogenate was filtered through coarse and then a fine nylon mesh to remove all connective tissue. 25% Triton X-100 was added to make a final concentration of 5%. The solution was briefly vortexed and then centrifuged at 1000G in a Sorvall RC-2B Centrifuge with a GSA rotor at 4°C for 20 min. The supernatant was removed by aspiration and the nuclear pellet was resuspended in 2.5 mL of buffer. To this solution was added 5% sodium dodecyl sulfate (SDS) and 5 M sodium chloride (NaCl) to make a solution with a final concentration of 1% SDS and 1 M NaCl. An equal volume of chloroform:isoamyl alcohol (24:1) was then added and the biphasic mixture was shaken vigorously for 15 min. The mixture was centrifuged at 7000G for 15 min at 4°C, and the aqueous phase was collected, re-extracted with another volume of chloroform:isoamyl alcohol, shaken, and centrifuged. The aqueous phase was then collected and the nucleic acids were precipitated with 3 volumes of ice cold ethanol and chilled at -20°C for 20-30 min and subsequently pelleted by centrifugation at 7000G for 15 min at 4°C. The nucleic acids were washed 2 times with cold ethanol and then dried *in vacuo*. The dried pellet was reconstituted with 2 mL of 0.05 M Tris (pH 7.5), 0.1 M NaCl on ice. In order to remove any contaminating RNA, 0.5 mg of RNAse A was added and incubated at 37°C for 10 min. The reaction was stopped by cooling on ice, the NaCl concentration was adjusted to 0.9 M, and the DNA was extracted by subsequent additions of chloroform:isoamyl alcohol as indicated above. The aqueous phase from the second extraction was isolated

and the DNA was precipitated with 3 volumes of ice cold ethanol, centrifuged, and washed 2 times as above. The DNA was then given to Paul Skipper and Rosa Liberman, both in the Tannenbaum laboratory at MIT, for analysis by AMS as described in Liberman, et al. (Liberman et al. 2004).

Results

E2-7α Inhibits the Growth of HeLa Xenografts. E2-7α was administered to mice containing HeLa xenografts to assess its potential as a chemotherapeutic agent. Figure 4.4 shows the results of the treatment of the mice after 3 weekly, 5 day cycles of 75 mg/kg administered IP and Figure 4.5 shows representative mice from each group. Figure 4.6 shows the results of mice treated with 25 mg/kg administered Sub-Q. As evident in the graph, E2-7α had a significant effect on the xenografts (P=0.0003 and 0.0030, respectively) as it inhibited their growth by 70% as assessed on the final day of the study (mean tumor volume of treated versus mean tumor volume of the control on day 18). The dose was well tolerated as evident by the modest weight loss of 10% in the IP treated group (Fig 4.7) and 0% in the Sub-Q group. These data indicate that E2-7α inhibits the growth of the HeLa xenografts and this therapeutic dose is well tolerated by the mice.

Chlorambucil was administered to mice in order to gauge the efficacy of E2-7α against a proven chemotherapeutic. As in the previous results, E2-7α inhibited the growth of the HeLa xenografts but to a slightly lesser extent, 40% as assessed on the last day of therapy. Chlorambucil, however, actually induced a reduction in the size of the tumor by approximately 50% (inhibited the growth of the tumor by 83 %). See Figure 4.8. Despite the therapeutic benefit in the shrinking of the HeLa xenograft, chlorambucil was almost two-fold more toxic to the mice than E2-7α as indicated by the nearly 20% reduction in body weight. Mice treated with E2-7α lost only 10% of their body weight. See Figure 4.9.

Chronic Doses of E2-7α are Well Tolerated by Mice. Following the administration of 3 cycles of E2-7α, mice were sacrificed in order to assess the toxicity after chronic exposure to the compound. Weight loss was limited to 10% in IP treated animals and 0%

in the Sub-Q treated mice. Mice treated with the lower Sub-Q dose of E2-7α showed no differential toxicity as compared to the Sub-Q vehicle group and therefore will not be discussed further. The results from the hematology and blood chemistry reports for the mice injected with 75 mg/kg of E2-7α or vehicle alone via IP injection are shown in Tables 4.1 and 4.2, respectively. Slight leukopenia was evident in mice treated with 75 mg/kg E2-7α IP – a reduction in white blood cells from 6.9 to 3.9 (x mm^3) as compared to the tumor bearing mice. The IP vehicle group also saw a moderate reduction in white blood cells to an average of 5.4 (x mm^3). Additionally, an alteration in the ratio of neutrophils to lymphocytes was observed in the E2-7α treated group such that the percentage of neutrophils increased as compared to the percentage of lymphocytes. Creatinine kinase (CK), an indicator of muscle and cardiac toxicity, was elevated slightly in all mice bearing a tumor and is therefore unlikely to be related to E2-7α toxicity. Finally, aspartate aminotransferase (AST) and alkaline phosphatase were slightly elevated in the treated and vehicle control groups and is unlikely to be related to E2-7α toxicity. Overall, the toxic profile of a 75 mg/kg dose of E2-7α administered IP was extremely moderate.

E2-7α Forms DNA Adducts in Tumor and Liver Tissue. HeLa xenograft mice were injected with ^{14}C-E2-7α either Sub-Q with a 25 mg/kg dose or IP with a 75 mg/kg dose. The mice were sacrificed four hours following administration of the compound, the liver and tumor tissue was surgically removed, and the DNA was isolated in order to quantify the number of DNA adducts per cell. Figure 4.10 illustrates the number of DNA adducts formed per tumor or liver cell by either route of administration. Even though the Sub-Q dose was 3-fold lower than the IP dose, twice as many adducts formed in tumor cells when E2-7α was administered Sub-Q (16,000 Vs 7,500 adducts per cell). Not surprisingly, the number of DNA adducts formed in liver tissue was greater when the compound was administered IP than when injected Sub-Q (13,000 Vs 3,000 adducts per cell).

Discussion

In the previous two chapters, I described several experiments indicating the potential of E2-7α to be an effective anticancer agent in the treatment of ER(+) cancers. E2-7α has a low log D, differential toxicity in favor of an ER(+) MCF-7 cell line over an ER(-) MDA-MB231 cell line, favorable pharmacokinetics and a low toxicity profile at doses as high as 200 mg/kg. Furthermore, DNA adducts were isolated from liver tissue, indicating that the compound remains intact and is not rapidly degraded by metabolic processes prior to reaching its intended target. These results prompted further research in assessing the chemotherapeutic value of E2-7α.

Although we had previously used the ER(+) MCF-7 cell line in culture and showed excellent ER-selective cytotoxicity, we decided not to use these cells because they require an estradiol pellet in order for the cells to grow into tumors. Based on our hypothesized mechanisms, we reasoned that high levels of estrogen could titrate away the activity of E2-7α. Therefore, we decided to proceed with an ER-LBD-expressing HeLa cell line that was designed in our laboratory. These cells are not dependent on estradiol for growth.

The ability of E2-7α to inhibit the growth of ER-LBD (+) HeLa xenografts in nude mice was therefore addressed. Mice were treated with E2-7α at a dose of 75 mg/kg injected IP or 25 mg/kg injected Sub-Q for 3 cycles of 5 days on and 2 days off. HeLa cells are a rapidly growing cell line and xenograft tumors are apparent as early as 5 days after inoculation of 3×10^6 cells. The Sub-Q dose of 25 mg/kg inhibited the growth of ER(+) HeLa xenografts by 81% whereas the IP dose of 75 mg/kg inhibited the growth by 72%, as compared to the control groups on the 18th day of therapy. This result illustrates that much of the dose when administered IP does not distribute to the tumor. The rationale in the design of our molecules, however, is such that we expect the compound to distribute throughout the body, but selective retention could occur in the tumor because of the presence of the ER and its high affinity for E2-7α. Therefore, we do not necessarily require a large fraction of the dose to reach the tumor. Nevertheless, we would want to use as low of a dose as possible when treating patients to minimize toxic side effects to the patient and to minimize the costs associated with the therapy both to the patient and to the manufacturer.

The poor distribution of E2-7α to tumor tissue could also be a reason why the growth inhibition of ER-LBD HeLa xenografts by chlorambucil was so much more effective than E2-7α. Chlorambucil shrank the tumors after only 11 days of therapy while E2-7α inhibited their growth but did not actually shrink them. In Chapter 2, I reported the log P of chlorambucil (1.44 by HPLC but -0.66 in other literature reports) (Greig et al. 1990) and E2-7α (5.32). Even though E2-7α would likely be ionized under physiological conditions, the log P clearly illustrates that chlorambucil is much more water soluble than E2-7α. Therefore, one of the possible reasons why chlorambucil was more effective in shrinking the growth of the ER-LBD (+) HeLa xenografts was increased distribution to the tumor as a result of its increased water solubility.

Despite the increased efficacy of chlorambucil in treating the xenografts, toxicity to the mice was much greater than when E2-7α was administered. In fact, chlorambucil was 2-fold more toxic than E2-7α as assessed by the percent of weight loss during the therapy. Overall, E2-7α is well tolerated by mice injected with a 75 mg/kg therapeutic dose administered IP. Weight loss was limited to less than 10% in all mice treated with 2 or 3 cycles of E2-7α. The dose limiting toxicity for tumor ablation therapy could be leukopenia since the white blood cell level dropped from 6.9 (x mm^3) to 3.9 (x mm^3), although the normal mouse range provided by Taconic is as low as 4.3 (x mm^3). This fact is not surprising as many anticancer agents, including chlorambucil, induce myelosuppression. The dose limiting toxicity of chlorambucil is, in fact, neutropenia, or a decrease in neutrophils (Blumenreich et al. 1988). As in the acute dose of E2-7α, the ratio of neutrophils to lymphocytes is altered such that the percent of neutrophils increases as compared to the percent lymphocytes. The alteration seen here, however, is to a much greater extent. The elevation of neutrophils and suppression of lymphocytes is commonly the result of an active infection.

Alternatively, the elevation of neutrophils and suppression of lymphocytes may indicate that E2-7α is interacting with the glucocorticoid receptor (GR). The GR is a member of the same class of nuclear hormone receptors as the ER and AR. Corticosteroids, the natural ligands for the GR, have profound effects on lymphocytes and neutrophils. Corticosteroids actually induce the apoptosis of lymphocytes, (Di et al. 2000; Negoescu et al. 1998) whereas they inhibit the death of neutrophils *in vitro* (Cox

154

and Austin 1997; Liles et al. 1996). The mechanisms by which human lymphocyte and neutrophil apoptotic responses to glucocorticoids differ are unknown. However, glucocorticoid action is mediated through the GR and therefore these apoptotic differences may arise from downstream targets of the GR (O'Malley 1971; Strickland et al. 2001; Wenzel et al. 1997). An off-target interaction of E2-7α with the GR may mediate the alteration of the neutrophil to lymphocyte ratio.

The blood chemistry profile after chronic administration of E2-7α is also extremely mild. CK is elevated in all tumor bearing mice and therefore the increased levels are unlikely related to the compound or the vehicle. AST and alkaline phosphatase were both slightly elevated in the treated and vehicle control groups. These enzymes are typically elevated in cases of hepatotoxicity. However, the levels are only slightly elevated, and the fact that these enzymes are elevated in both the treated and control groups eliminates the possibility of E2-7α induced toxicity.

The toxicity in the mice is likely a result of the formation of DNA adducts in non-target tissues (Bank 1992; Fox and Scott 1980; van Zeeland 1996). Nitrogen mustards elicit their mechanism of action by the alkylation of DNA. They are capable of producing a number of different DNA adducts, the majority of which are monoadducts as a result of a single alkylation event. A small proportion of monoadducts then go on to form crosslinks as a result of a second alkylation (Kundu, Schullek, and Wilson 1994; Povirk and Shuker 1994; Sunters et al. 1992). The formation of crosslinks between the 2 strands of DNA, interstrand crosslinking, is considered to be a critical event, and there is clear evidence that their formation and subsequent persistence correlates with in vitro cytotoxicity (O'Connor and Kohn 1990; Sunters et al. 1992). The two main reasons for the low abundance of the toxic cross-link adducts are a slower rate of alkylation for the second arm of a nitrogen mustard (Gould, Nixon, and Tilby 2004; Ross, Ewig, and Kohn 1978) and a comparatively quick rate of repair of a monoadduct. Compounds such as chlorambucil and melphalan form a critical number of adducts so as to saturate the repair capacity of a cell and thus result in lethal effects to a tumor cell. A potential advantage of E2-7α is its ability to attract the ER. An association between the ER and an E2-7α monoadduct could provide more time for the formation of a cross-link and thus render an E2-7α monoadduct more toxic than a monoadduct from other nitrogen mustards.

We incorporated AMS in an effort to quantify DNA adducts after therapeutic doses of E2-7α. We determined the number of adducts formed after a 75 mg/kg IP dose was approximately half of a 25 mg/kg Sub-Q dose (7,500 and 16,000 adducts per cell, respectively). The level of adduction seen here with E2-7α is much less than what has been reported previously for a patient with plasma cell leukemia treated with high doses of melphalan. In the tumor cells of this patient, 160,000 melphalan-DNA adducts formed after a therapeutic dose (Tilby et al. 1993). This number is at least 10-fold higher than what was observed in HeLa xenografts treated with E2-7α, also at a therapeutically beneficial level. Although it is somewhat difficult to compare directly two different compounds (with different pharmacokinetics and aqueous solubility) in two different cell types, such a drastic difference in DNA adduct burden may imply mechanism(s) other than saturation of the DNA repair machinery may play a role in the cytotoxicity of E2-7α. Until such a time as a direct comparison of DNA adduct levels achieved by doses of melphalan and E2-7α in the same cell type can be made, speculation on additional mechanisms, related or unrelated to DNA alkylation, is futile at best. One possibility, however, is the repair shielding hypothesis by which we designed E2-7α. Since the HeLa cells only contain the ER-LBD, the transcription factor hijacking hypothesis cannot be valid in this cell line as the LBD alone can not induce transcription.

Conclusion

In previous chapters, I have discussed many of the properties suggesting that E2-7α could act as a chemotherapeutic agent – high affinity for the ER, differential toxicity in favor of killing ER expressing cell lines, and favorable pharmacokinetics. Here I have described experiments indicating that E2-7α can inhibit the growth of ER(+) HeLa xenografts in mice by as much as 82%. Furthermore, following the administration of an IP dose of 75 mg/kg, the mice lost only 10% of their body weight and showed essentially no signs of organ specific toxicity. This illustrates that the dose is very well tolerated and possibly even higher doses could be administered in order to achieve better tumor inhibition. Finally, the results of the AMS experiment illustrated that 10-15,000 DNA adducts formed in the HeLa xenografts 4 hours after the administration of ^{14}C-E2-7α.

These adduct levels are substantially lower than what has been previously reported with other compounds and may implicate the repair shielding hypothesis.

Future Work

As discussed in the future directions section of Chapter 3, there is an acute need for a new delivery vehicle. The results here illustrate a dose much lower than 75 mg/kg can be effective provided that more of the dose accesses the tumor – a 3-fold lower dose of E2-7α was actually more effective in inhibiting the growth of the ER(+) HeLa xenografts as a result of administering the compound by a different route of injection (Sub-Q). The results from this chapter further illustrate the necessity in exploring new formulation options. Upon obtaining a new vehicle, tumor therapy and chronic toxicity experiments would need to be completed. However, the work here is a foundation for which subsequent vehicles can be judged.

The results obtained with both the acute (Chapter 3) and chronic toxicity experiments reveal an interesting phenomenon with respect to the ratio of neutrophils to lymphocytes. In both toxicity experiments, the percent of white blood cells that were neutrophils increased as compared to the percent that were lymphocytes. One possible explanation involves the glucocorticoid receptor. If the GR has an affinity for the estradiol moiety of E2-7α, it may be possible that the compound is acting as a corticosteroid resulting in the induction of apoptosis in lymphocyte cells and the stimulation of neutrophil proliferation. One way to address this issue is to obtain an RBA for the GR. Additionally, lymphocytes and neutrophils in culture could be exposed to E2-7α in order to monitor an induction of apoptosis and increased proliferation. Since E2-7α is a reactive nitrogen mustard and may actually be toxic to both cell lines because of its DNA damaging properties, a "defanged" version could be made by replacing the chloride atoms with hydroxyl or methoxy substituents. These unreactive molecules would not be able to damage DNA and therefore may be capable of stimulating neutrophil proliferation.

John Marquis and Peter Rye have constructed an ER-LBD-expressing HeLa cell line using the tet-off expression system. These cells were designed with the hope that E2-7α would be more toxic to the ER-LBD-expressing HeLa cells than to the ones

containing an empty vector. Unfortunately, E2-7α is equitoxic to both cell lines in culture and when implanted as xenografts (data not shown). Western blot analysis has illustrated that the ER-LBD is indeed present and ligand binding experiments using whole cell extracts from the ER-LBD-expressing HeLa cells indicate the protein is capable of binding estradiol at levels similar to what has been seen with the full length protein. Despite this evidence, the repair shielding hypothesis is not necessarily ruled out as a potential contributing mechanism for E2-7α induced cytotoxicity. Under normal circumstances, ligand binding would induce conformational changes that would allow the ER to dimerize and attract coactivators (Klinge et al. 1997; Ylikomi et al. 1998). The truncated version of the protein in HeLa cells may not be of sufficient size to shield DNA adducts from repair enzymes. Furthermore, the ER-LBD does not contain the DNA binding domain or the transcriptional activation region which are necessary for the initiation of transcription. Therefore, any cytotoxic contribution from transcription factor hijacking would be absent in the ER-LBD HeLa cells.

Ideally an isogenic cell line containing the full length ER would be used in order to assess any differential toxicity in response to E2-7α. One such cell line has been described by Jiang and Jordan. Using MDA-MB231 cells, these researchers have derived isogenic clones with the ER (MDA-S30) and without the ER (MDA-10A). The growth of the S30 cells were found to be inhibited by estradiol at concentrations as low as 10^{-10} M and prolonged the doubling time of the culture by 2.5 fold at this concentration. Estradiol had no effect on the MDA-10A clone, however (Jiang and Jordan 1992). Since E2-7α contains an estradiol moiety and the concentrations currently used to treat cells in culture are 10^5 fold higher, it likely would inhibit the growth of the S30 line as a result of the same surprising antagonistic properties as was seen with estradiol. Therefore, it would be impossible to parse out repair shielding and transcription factor hijacking effects with these cells. Other cell lines have also been transfected with the ER – Chinese hamster ovary (Kushner et al. 1990), HeLa (Maminta, Molteni, and Rosen 1991; Touitou, Mathieu, and Rochefort 1990), and osteosarcoma (Watts, Parker, and King 1989) – but in all cases estradiol has an inhibitory effect on cell growth.

In lieu of this research, we have decided the best option is to test the efficacy of E2-7α in other ER expressing cell lines. Towards this end we have initiated a

collaboration with the Tyler Jacks Laboratory at MIT. Daniela Dinelescu, et al. recently described their work in the cover article of Nature Medicine. They have designed an (ER expressing) endometrioid ovarian adenocarcinoma mouse model based on the activation of a K-ras oncogenic allele. This model induces invasive and widely metastatic endometrioid ovarian adenocarcinomas with complete penetrance and a disease latency of only 7 weeks. This ovarian cancer model recapitulates the specific tumor histomorphology and metastatic potential of the human disease (Dinulescu et al. 2005). We will be working closely with Dinelescu in testing our compounds in her model.

Reference List

Bank, B.B. Studies of chlorambucil-DNA adducts. *Biochem. Pharmacol.* **44**, 571-575 (1992)

Blumenreich, M.S., Woodcock, T.M., Sherrill, E.J. et al. A phase I trial of chlorambucil administered in short pulses in patients with advanced malignancies. *Cancer Invest* **6**, 371-375 (1988)

Cox, G. and Austin, R.C. Dexamethasone-induced suppression of apoptosis in human neutrophils requires continuous stimulation of new protein synthesis. *J. Leukoc. Biol.* **61**, 224-230 (1997)

Di, B.A., Secchiero, P., Grilli, A. et al. Morphological features of apoptosis in hematopoietic cells belonging to the T-lymphoid and myeloid lineages. *Cell Mol. Biol. (Noisy. -le-grand)* **46**, 153-161 (2000)

Dinulescu, D.M., Ince, T.A., Quade, B.J. et al. Role of K-ras and Pten in the development of mouse models of endometriosis and endometrioid ovarian cancer. *Nat. Med.* **11**, 63-70 (2005)

Ferno, M., Borg, A., Johansson, U. et al. Estrogen and progesterone receptor analyses in more than 4,000 human breast cancer samples. A study with special reference to age at diagnosis and stability of analyses. Southern Swedish Breast Cancer Study Group. *Acta Oncol.* **29**, 129-135 (1990)

Fox, M. and Scott, D. The genetic toxicology of nitrogen and sulphur mustard. *Mutat. Res.* **75**, 131-168 (1980)

Garner, R.C. Accelerator mass spectrometry in pharmaceutical research and development--a new ultrasensitive analytical method for isotope measurement. *Curr. Drug Metab* **1**, 205-213 (2000)

Gould, K.A., Nixon, C., and Tilby, M.J. p53 elevation in relation to levels and cytotoxicity of mono- and bifunctional melphalan-DNA adducts. *Mol. Pharmacol.* **66**, 1301-1309 (2004)

Greenlee, R.T., Murray, T., Bolden, S., and Wingo, P.A. Cancer statistics, 2000. *CA Cancer J. Clin.* **50**, 7-33 (2000)

Greig, N.H., Genka, S., Daly, E.M. et al. Physicochemical and pharmacokinetic parameters of seven lipophilic chlorambucil esters designed for brain penetration. *Cancer Chemother. Pharmacol.* **25**, 311-319 (1990)

Hortobagyi, G.N. Treatment of breast cancer. *N. Engl. J. Med.* **339**, 974-984 (1998)

Jiang, S.Y. and Jordan, V.C. Growth regulation of estrogen receptor-negative breast cancer cells transfected with complementary DNAs for estrogen receptor. *J. Natl. Cancer Inst.* **84**, 580-591 (1992)

Jordan, V.C. Tamoxifen and tumorigenicity: a predictable concern. *J. Natl. Cancer Inst.* **87**, 623-626 (1995)

Katzenellenbogen, B.S. Antiestrogen resistance: mechanisms by which breast cancer cells undermine the effectiveness of endocrine therapy. *J. Natl. Cancer Inst.* **83**, 1434-1435 (1991)

Klinge, C.M., Brolly, C.L., Bambara, R.A., and Hilf, R. hsp70 is not required for high affinity binding of purified calf uterine estrogen receptor to estrogen response element DNA in vitro. *J. Steroid Biochem. Mol. Biol.* **63**, 283-301 (1997)

Kundu, G.C., Schullek, J.R., and Wilson, I.B. The alkylating properties of chlorambucil. *Pharmacol. Biochem. Behav.* **49**, 621-624 (1994)

Kushner, P.J., Hort, E., Shine, J. et al. Construction of cell lines that express high levels of the human estrogen receptor and are killed by estrogens. *Mol. Endocrinol.* **4**, 1465-1473 (1990)

Lerner, L.J. and Jordan, V.C. Development of antiestrogens and their use in breast cancer: eighth Cain memorial award lecture. *Cancer Res.* **50**, 4177-4189 (1990)

Liberman, R.G., Tannenbaum, S.R., Hughey, B.J. et al. An interface for direct analysis of (14)c in nonvolatile samples by accelerator mass spectrometry. *Anal. Chem.* **76**, 328-334 (2004)

Liles, W.C., Kiener, P.A., Ledbetter, J.A. et al. Differential expression of Fas (CD95) and Fas ligand on normal human phagocytes: implications for the regulation of apoptosis in neutrophils. *J. Exp. Med.* **184**, 429-440 (1996)

Maminta, M.L., Molteni, A., and Rosen, S.T. Stable expression of the human estrogen receptor in HeLa cells by infection: effect of estrogen on cell proliferation and c-myc expression. *Mol. Cell Endocrinol.* **78**, 61-69 (1991)

Mitra, K., Marquis, J.C., Hillier, S.M. et al. A rationally designed genotoxin that
selectively destroys estrogen receptor-positive breast cancer cells. *J. Amer. Chem.
Soc.* **124**, 1862-1863 (2002)

Negoescu, A., Guillermet, C., Lorimier, P. et al. Importance of DNA fragmentation in
apoptosis with regard to TUNEL specificity. *Biomed. Pharmacother.* **52**, 252-258
(1998)

O'Connor, P.M. and Kohn, K.W. Comparative pharmacokinetics of DNA lesion
formation and removal following treatment of L1210 cells with nitrogen
mustards. *Cancer Commun.* **2**, 387-394 (1990)

O'Malley, B.W. Mechanisms of action of steroid hormones. *N. Engl. J. Med.* **284**, 370-
377 (1971)

Obrero, M., Yu, D.V., and Shapiro, D.J. Estrogen receptor-dependent and estrogen
receptor-independent pathways for tamoxifen and 4-hydroxytamoxifen-induced
programmed cell death. *J. Biol. Chem.* **277**, 45695-45703 (2002)

Osborne, M.R., Hewer, A., Hardcastle, I.R. et al. Identification of the major tamoxifen-
deoxyguanosine adduct formed in the liver DNA of rats treated with tamoxifen.
Cancer Res. **56**, 66-71 (1996)

Peto, J. and Mack, T.M. High constant incidence in twins and other relatives of women
with breast cancer. *Nat. Genet.* **26**, 411-414 (2000)

Povirk, L.F. and Shuker, D.E. DNA damage and mutagenesis induced by nitrogen
mustards. *Mutat. Res.* **318**, 205-226 (1994)

Ross, S.A., Srinivas, P.R., Clifford, A.J. et al. New technologies for nutrition research. *J.
Nutr.* **134**, 681-685 (2004)

Ross, W.E., Ewig, R.A., and Kohn, K.W. Differences between melphalan and nitrogen
mustard in the formation and removal of DNA cross-links. *Cancer Res.* **38**, 1502-
1506 (1978)

Sharma, U., Marquis, J.C., Nicole, D.A. et al. Design, synthesis, and evaluation of
estradiol-linked genotoxicants as anti-cancer agents. *Bioorg. Med. Chem. Lett.* **14**,
3829-3833 (2004)

Strickland, I., Kisich, K., Hauk, P.J. et al. High constitutive glucocorticoid receptor beta in human neutrophils enables them to reduce their spontaneous rate of cell death in response to corticosteroids. *J. Exp. Med.* **193**, 585-593 (2001)

Sunters, A., Springer, C.J., Bagshawe, K.D. et al. The cytotoxicity, DNA crosslinking ability and DNA sequence selectivity of the aniline mustards melphalan, chlorambucil and 4-[bis(2-chloroethyl)amino] benzoic acid. *Biochem. Pharmacol.* **44**, 59-64 (1992)

Tilby, M.J., Newell, D.R., Viner, C. et al. Application of a sensitive immunoassay to the study of DNA adducts formed in peripheral blood mononuclear cells of patients undergoing high-dose melphalan therapy. *Eur. J. Cancer* **29A**, 681-686 (1993)

Touitou, I., Mathieu, M., and Rochefort, H. Stable transfection of the estrogen receptor cDNA into Hela cells induces estrogen responsiveness of endogenous cathepsin D gene but not of cell growth. *Biochem. Biophys. Res. Commun.* **169**, 109-115 (1990)

Turteltaub, K.W. and Dingley, K.H. Application of accelerated mass spectrometry (AMS) in DNA adduct quantification and identification. *Toxicol. Lett.* **102-103:435-9.**, 435-439 (1998)

Turteltaub, K.W. and Vogel, J.S. Bioanalytical applications of accelerator mass spectrometry for pharmaceutical research. *Curr. Pharm. Des* **6**, 991-1007 (2000)

van Zeeland, A.A. Molecular dosimetry of chemical mutagens. Relationship between DNA adduct formation and genetic changes analyzed at the molecular level. *Mutat. Res.* **353**, 123-150 (1996)

Vogel, J.S., Grant, P.G., Buchholz, B.A. et al. Attomole quantitation of protein separations with accelerator mass spectrometry. *Electrophoresis* **22**, 2037-2045 (2001)

Vogel, J.S., Turteltaub, K.W., Finkel, R., and Nelson, D.E. Accelerator mass spectrometry. *Anal. Chem.* **67**, 353A-359A (1995)

Watts, C.K., Parker, M.G., and King, R.J. Stable transfection of the oestrogen receptor gene into a human osteosarcoma cell line. *J. Steroid Biochem.* **34**, 483-490 (1989)

Weir, H.K., Thun, M.J., Hankey, B.F. et al. Annual report to the nation on the status of cancer, 1975-2000, featuring the uses of surveillance data for cancer prevention and control. *J. Natl. Cancer Inst.* **95**, 1276-1299 (2003)

Wenzel, S.E., Szefler, S.J., Leung, D.Y. et al. Bronchoscopic evaluation of severe asthma. Persistent inflammation associated with high dose glucocorticoids. *Am. J. Respir. Crit Care Med.* **156**, 737-743 (1997)

White, I.N. and Brown, K. Techniques: the application of accelerator mass spectrometry to pharmacology and toxicology. *Trends Pharmacol. Sci.* **25**, 442-447 (2004)

Williams, K.E., Carver, T.A., Miranda, J.J. et al. Attomole detection of in vivo protein targets of benzene in mice: evidence for a highly reactive metabolite. *Mol. Cell Proteomics.* **1**, 885-895 (2002)

Ylikomi, T., Wurtz, J.M., Syvala, H. et al. Reappraisal of the role of heat shock proteins as regulators of steroid receptor activity. *Crit Rev. Biochem. Mol. Biol.* **33**, 437-466 (1998)

E2-7α Shows Minimal Toxic Side Effects as Assessed by Hematology Profile after Tumor Ablation Therapy

Test	IP N = 3	IP Vehicle N = 3	Tumor Ave N = 4	Norm. Ave N = 4	Taconic Nude
WBC (x mm³)	*3.9 ± 0.9*	5.4 ± 2.1	6.9 ± 1.6	5.4 ± 0.4	4.3-13.5
RBC (x 10⁶ mm³)	8 ± 0.6	9.6 ± 0.3	8.3 ± 2.1	9.3 ± 0.8	6.9-8.52
Hgb (g/dL)	12.3 ± 0.6	14.3 ± 0.8	9.3 ± 2.4	11.3 ± 0.3	7.5-15.2
HCT (%)	44.4 ± 0.5	51.7 ± 2.7	45.1 ± 10.3	50.6 ± 3.3	39.4-43.5
Neutrophils (%)	*90.5 ± 0.7*	46 ± 5.2	41.5 ± 11.8	42 ± 8.3	
Lymphs (%)	*9 ± 1.4*	52 ± 3.5	58 ± 12.1	57.8 ± 7.8	
Monos (%)	1 ± 0	3 ± 0			0.04-0.68
Eos (%)					0-0.19
Platelets (10³/µL)	871 ± 106	1142 ± 92	934 ± 542	1101 ± 372	790-1014
MCV (fL)	55.8 ± 3.4	45.1 ± 16.9	54.4 ± 3.6	54.3 ± 1.3	51.1-53.4
MCH (pg)	15.5 ± 0.4	15 ± 0.4	11.2 ± 2	12.2 ± 0.9	17.6-19.1
MCHC (g/dL)	27.7 ± 1	27.7 ± 0.1	20.6 ± 2.5	22.4 ± 1.1	34.3-36.1

Table 4.1 Hematology report for mice injected with E2-7α . Values in bold represent abnormally elevated or suppressed levels. The most notable toxicity is leukopenia. Additionally the ratio of neutrophils to lymphocytes is altered in the IP treated group.

(Note: Since the test groups contained relatively few mice, the abnormal levels are deviations from the normal range and do not necessarily reflect statistical significance.)

E2-7α Shows Minimal Toxic Side Effects as Assessed by Blood Chemistry Profile after Tumor Ablation Therapy

Test	IP N = 3	IP Vehicle N = 3	Tumor Ave N = 4	Norm. Ave N = 4	Taconic Nude
Alk. Phosphatase (IU/L)	95 ± 17	*389 ± 72*	58 ± 18	65 ± 8	96-117
ALT (SGPT) (IU/L)	29 ± 8	55 ± 11	36 ± 10	26 ± 7	
AST (SGOT) (IU/L)	*171 ± 79*	*150 ± 118*	112 ± 46	64 ± 22	61-119
CK (IU/L)	*462 ± 334*	*606 ± 505*	*722 ± 411*	184 ± 146	
GGT (IU/L)	1.0 ± 1.0	1.3 ± 1.2	1.8 ± 0.5	2 ± 0	
Albumin (g/dL)	2.7 ± 0.2	3.2 ± 0.2	2.8 ± 0.7	2.9 ± 0.1	3.4-4.1
Total Protein (g/dL)	4.7 ± 0.3	5.5 ± 0.5	5 ± 0.6	5.4 ± 0.3	4.8-5.6
Globulin (g/dL)	2 ± 0.1	2.3 ± 0.3	2.3 ± 0.1	2.6 ± 0.2	1.1-1.6
Total Bilirubin (mg/dL)	0.1 ± 0	0.1 ± 0	0.2 ± 0	0.1 ± 0.1	0.3-0.8
Direct Bilirubin (mg/dL)	0 ± 0.1	0 ± 0	0.1 ± 0.1	0 ± 0.1	
BUN (mg/dL)	24.3 ± 0.6	19.3 ± 4.2	20 ± 34.7	18.8 ± 2.2	30-37
Creatinine (mg/dL)	0.2 ± 0	0.2 ± 0.1	0.3 ± 0.1	0.3 ± 0.1	0.5-0.7
Cholesterol (mg/dL)	90 ± 9	99 ± 11	215 ± 187	133 ± 11	116-155
Glucose (mg/dL)	195 ± 32	234 ± 10	238 ± 31	253 ± 13	173-288
Calcium (mg/dL)	10.1 ± 0.3	10 ± 1.7	10.5 ± 0.4	10.5 ± 0.5	10.0-12.0
Phosphorous (mg/dL)	8.6 ± 1.7	9.3 ± 1.8	6.4 ± 0.9	9.5 ± 1.8	12.3-16.1
Bicarbonate (mEq/L)	26 ± 4.4	26.7 ± 4.5	28 ± 2.4	28.3 ± 2.2	
Chloride (mEq/L)	113 ± 2	92 ± 22	108 ± 2	108 ± 1	118-124
Potassium (mEq/L)	11.8 ± 4.3	8.1 ± 2.8	6.7 ± 1	7 ± 0.7	13.8-16.7
Sodium (mEq/L)	155 ± 6	132 ± 29	152 ± 3	153 ± 2	157-163
A/G Ratio	1.4 ± 0.1	1.4 ± 0.1	1.3 ± 0.3	1.1 ± 0.1	
B/C Ratio	122 ± 3	87 ± 31	79.2 ± 22.4	69.6 ± 12	
Indirect Bilirubin (mg/dL)	0.1 ± 0.1	0.1 ± 0	0 ± 0	0 ± 0	
Na/K Ratio	14.3 ± 4.7	16.7 ± 3.1	23.8 ± 4.3	22.3 ± 2.1	
Anion Gap (mEq/L)	27.7 ± 4.7	21 ± 13.1	21.3 ± 0.5	24 ± 4.2	
Amylase (IU/L)	1458 ± 362	1155 ± 372		1283 ± 180	
Lipase (IU/L)	129 ± 122	73 ± 5		79 ± 19	

Table 4.2 Blood Chemistry report for mice injected with E2-7α. Values in bold represent abnormally elevated or suppressed levels. E2-7α is very well tolerated by the mice.

(Note: Since the test groups contained relatively few mice, the abnormal levels are deviations from the normal range and do not necessarily reflect statistical significance.)

Accelerator Mass Spectrometry: Sample Loading

1 µL sample

CuO

Laser

He (in)

He and Sample

To the Sample Chamber
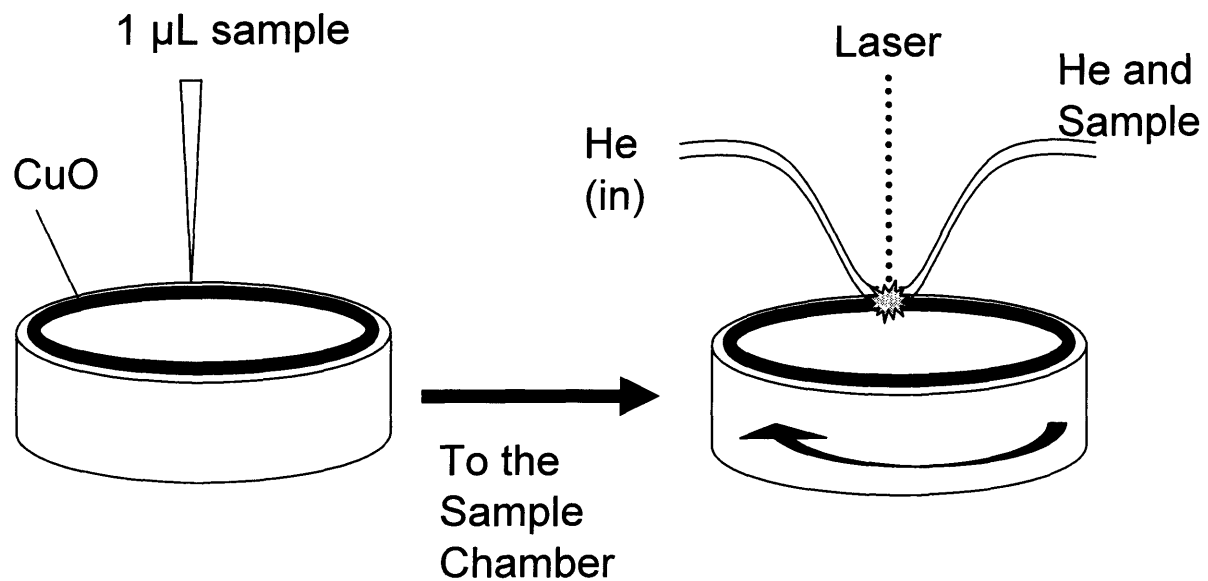
Fig 4.1 AMS sample loading and conversion to molecular ions. Sample is pipetted onto a ceramic disc containing copper oxide (CuO). A high powered laser combusts the sample, using CuO as an accelerant, converting the sample into molecular ions. These ions are then passed into the negative ion source seen in Fig 4.2.

Accelerator Mass Spectrometry: Sample Combustion to $^{14}C^{2+}$ Detection

Tandem Accelerator

low energy mass analyzer

negative ion beam

positive ion beam

high energy mass and energy analyzer

$^{14}C^-$ $^{12}CH_2^-$

^{14}C (1+, 2+, ...)

$^{13}CH^-$

$^{12}CH_2^{2+}$ (residual)

$^{12}C^-$
$^{13}C^-$
$^{14}C^-$

$^{12}CH_2^-$
$^{13}CH_2^-$
$^{16}CH^-$
$^{16}O^-$

$^{14}N^-$

1 MV high voltage terminal

foil stripper

$^{14}C^{2+}$

He and Sample inlet

negative ion source

ion detector

counts
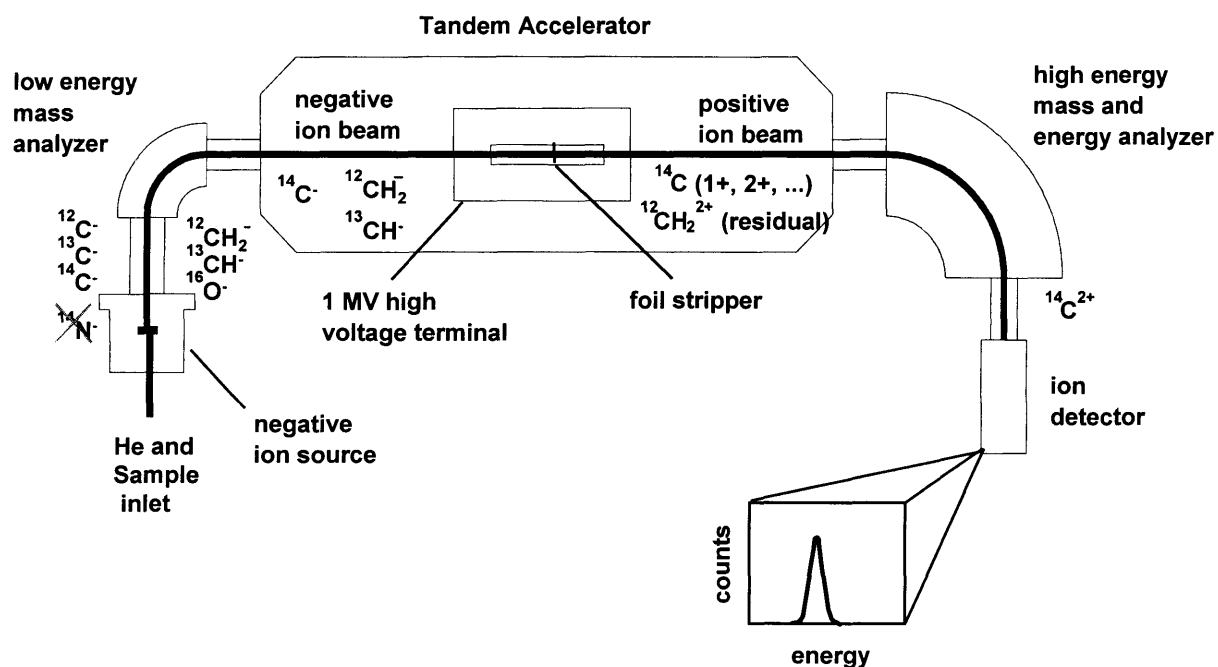
energy

Fig 4.2 Schematic of an Accelerator Mass Spectrometer. The sample is introduced into the negative ion source through the He line following combustion, eliminating ^{14}N as a contaminant in ^{14}C analysis. A low energy mass analyzer isolates molecular ions of 14 m/z. These negatively charged carbon ions are accelerated by a tandem Van De Graff accelerator and the valence electrons are stripped resulting in positively charged carbon ions. A second high energy mass spectrometer isolates ions with the correct charge and energy, in this case $^{14}C^{2+}$.

AMS is >10,000-Fold More Sensitive than Traditional Scintillation Counting
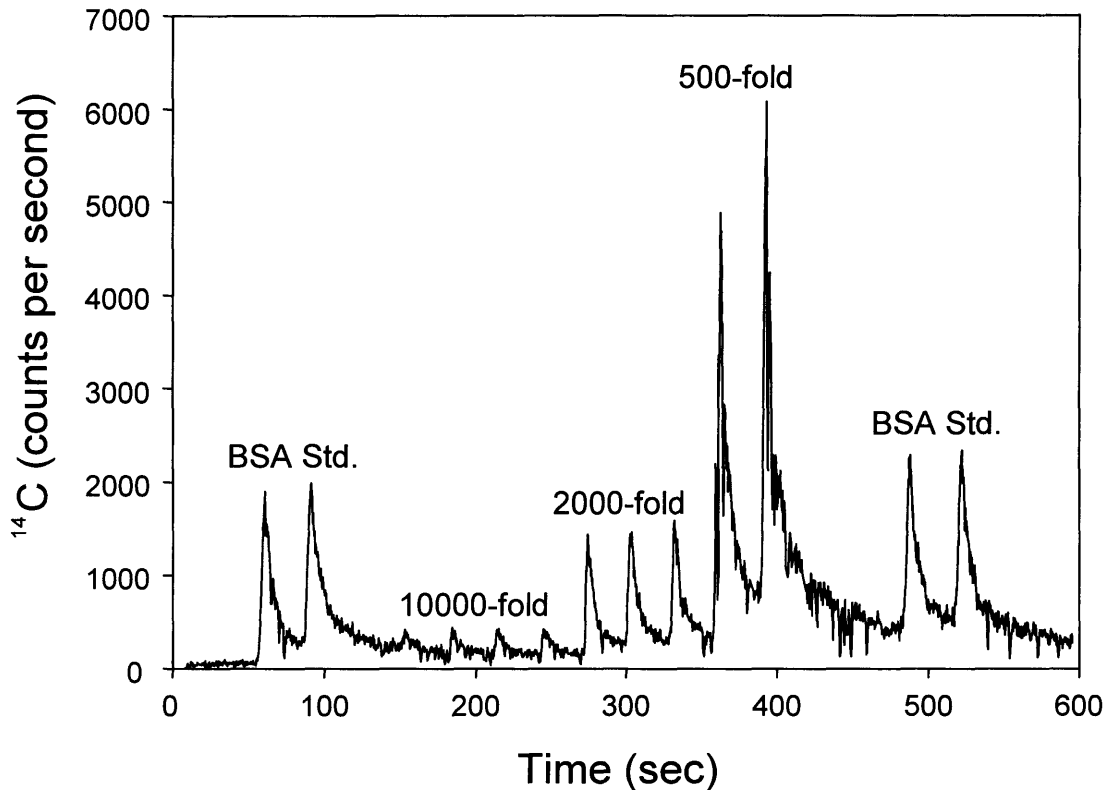
Dilution	Disc 1	Disc 2	Average
10000	52.4 ± 1.6	59.5 ± 8.3	56.5 ± 7.0
2000	64.5 ± 7.3	69.9 ± 2.5	67.2 ± 5.7
500	67.8 ± 1.8	65.5 ± 7.7	66.9 ± 5.7

Fig 4.3 Liver homogenate for a ^{14}C E2-7α treated mouse. The cellular homogenate was loaded onto a disc after several dilutions (500-10,000-fold). BSA was used as a standard. The peak area is related to the concentration of ^{14}C. Normalized CPM (to take into account the dilution factors) are in the table. Sixty CPM is near background for our scintillation counter. AMS is therefore at least ~10,000 times more sensitive than traditional scintillation counting.

E2-7α Inhibits the Growth of HeLa Xenografts when Administered Intraperitoneally

Fig 4.4 E2-7α therapy of HeLa xenografts in mice. Groups of 5 mice were injected IP with 75 mg/kg of E2-7α (●) or vehicle only (o). The vehicle was 43% Cremophor-EL, 30% saline, 27% ethanol. Error bars are the standard deviation of the mean and a paired t-test provided a P= 0.0003. The gray bars indicate days of treatment.

HeLa Xenograft Bearing Mice Treated with E2-7α have Smaller Tumors than Mice Treated with Vehicle Alone
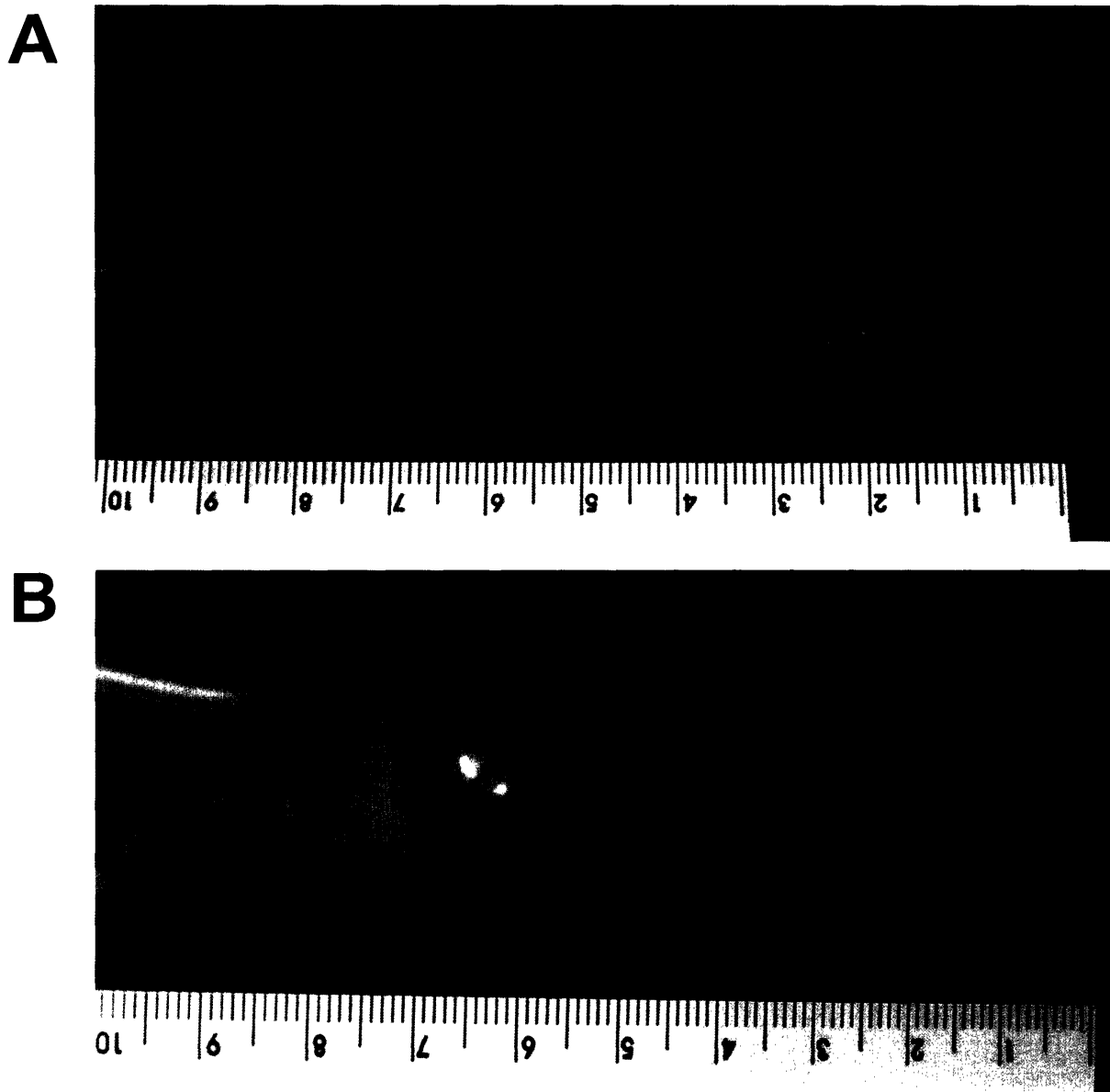
Fig 4.5 Pictures of HeLa xenograft bearing NIH Swiss Nude mice. **A.** A mouse treated IP with 3 cycles of 75 mg/kg E2-7α. **B.** A mouse treated with vehicle alone.

E2-7α Inhibits the Growth of HeLa Xenografts when Administered Sub-Cutaneously
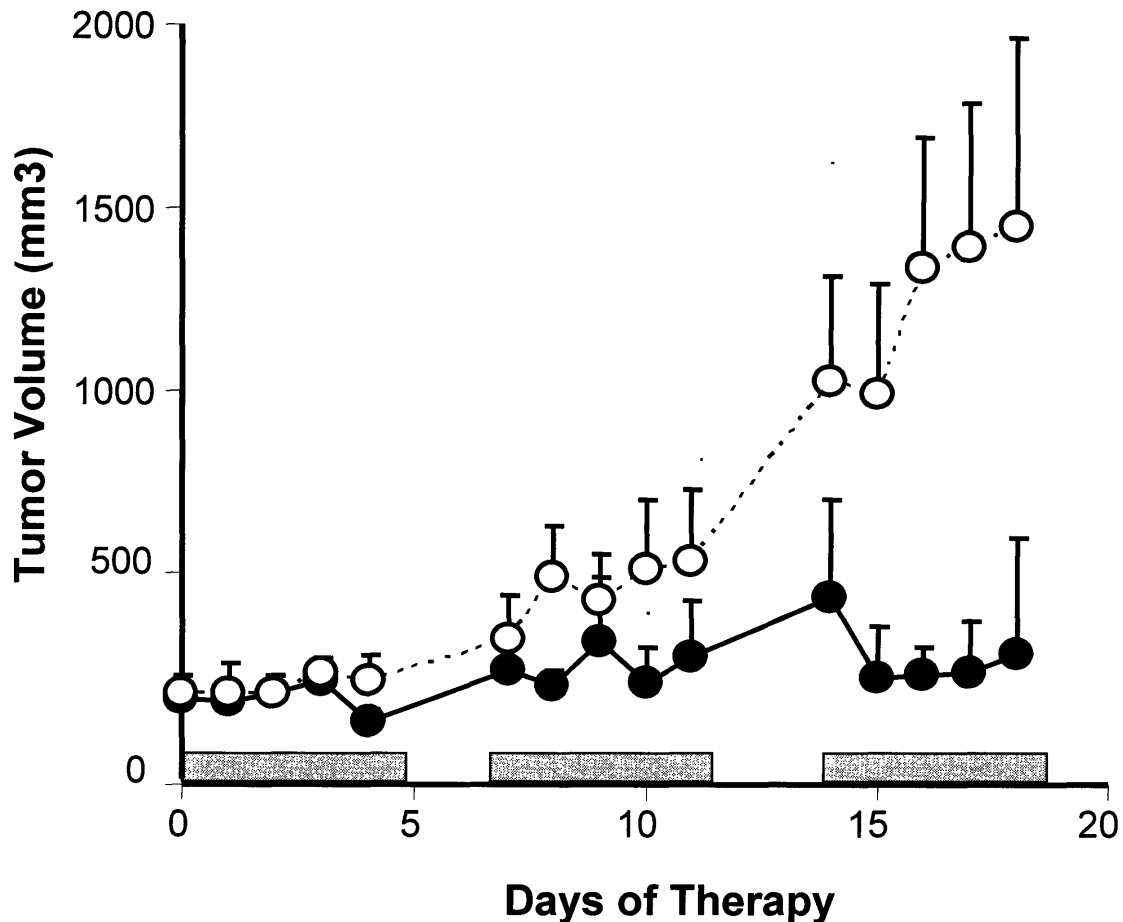
Fig 4.6 E2-7α therapy of HeLa xenografts in mice. Groups of 5 mice were injected Sub-Q with 25 mg/kg of E2-7α (●) or vehicle only (○). The vehicle was 43% Cremophor-EL, 30% saline, 27% ethanol. The injection was proximal to, but not directly into, the tumor. Error bars are the standard deviation of the mean and a paired t-test provided a P= 0.0030. The gray bars indicate days of treatment.

E2-7α is Well Tolerated by Mice Treated with 75 mg/kg Intraperitoneally
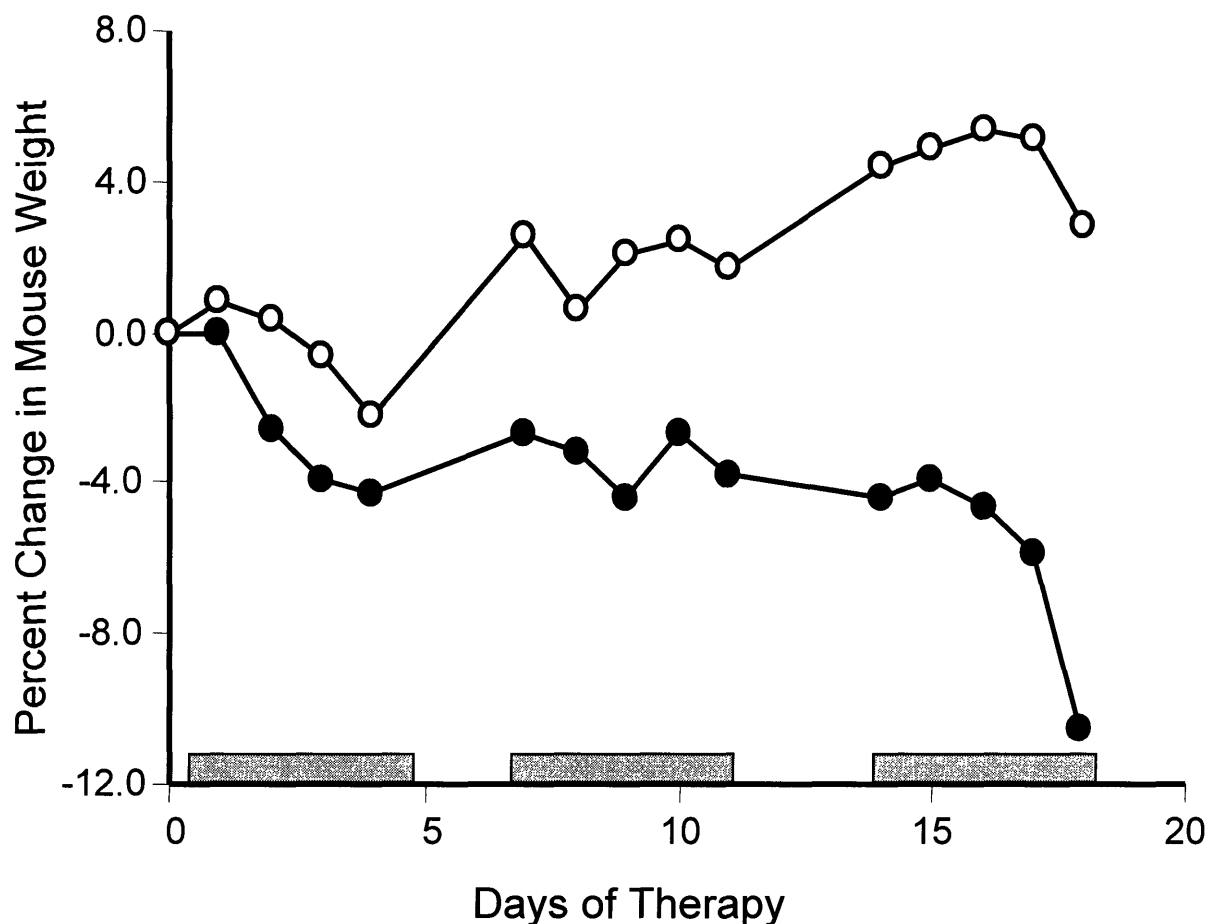
Fig 4.7 Percent change in mouse body weight after E2-7α therapy of HeLa xenografts in mice. Groups of 5 mice were injected IP with 75 mg/kg of E2-7α (●) or vehicle only (o). The vehicle was 43% Cremophor-EL, 30% saline, 27% ethanol. The treated mice lost approximately 10% of their body weight after three cycles of therapy.

Comparison of Chlorambucil and E2-7α
Against HeLa Xenografts
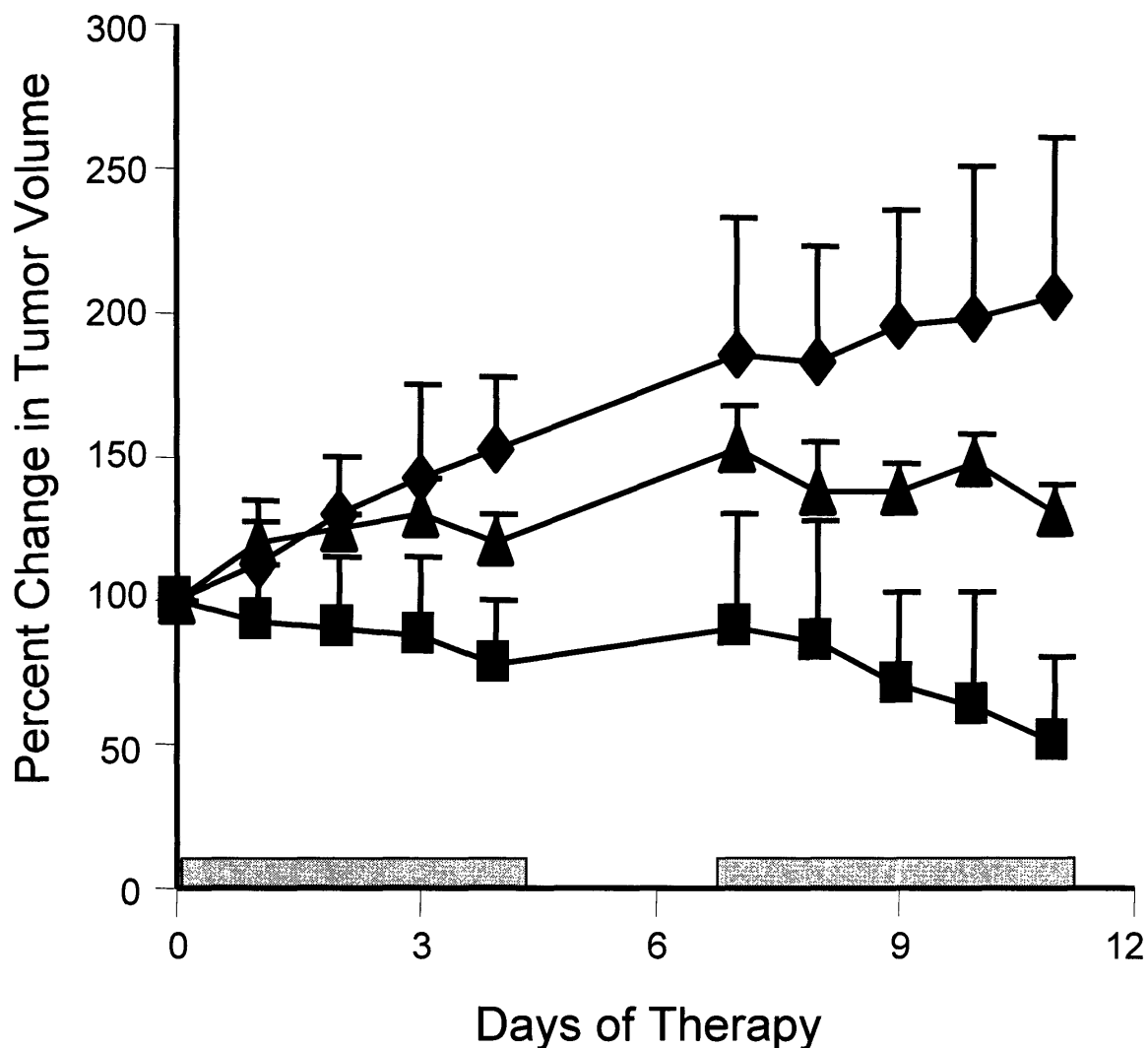
Fig 4.8 Percent change in tumor volume after IP injections of E2-7a (▲), chlorambucil (■), or vehicle alone (◆). Error bars are the standard deviation of the mean and a paired t-test provided a P< 0.006 for both chlorambucil and E2-7α as compared to the vehicle group. The gray bars indicate days of treatment.

Chlorambucil is Two-Fold More Toxic than E2-7α as Assessed by Weight Loss in Mice
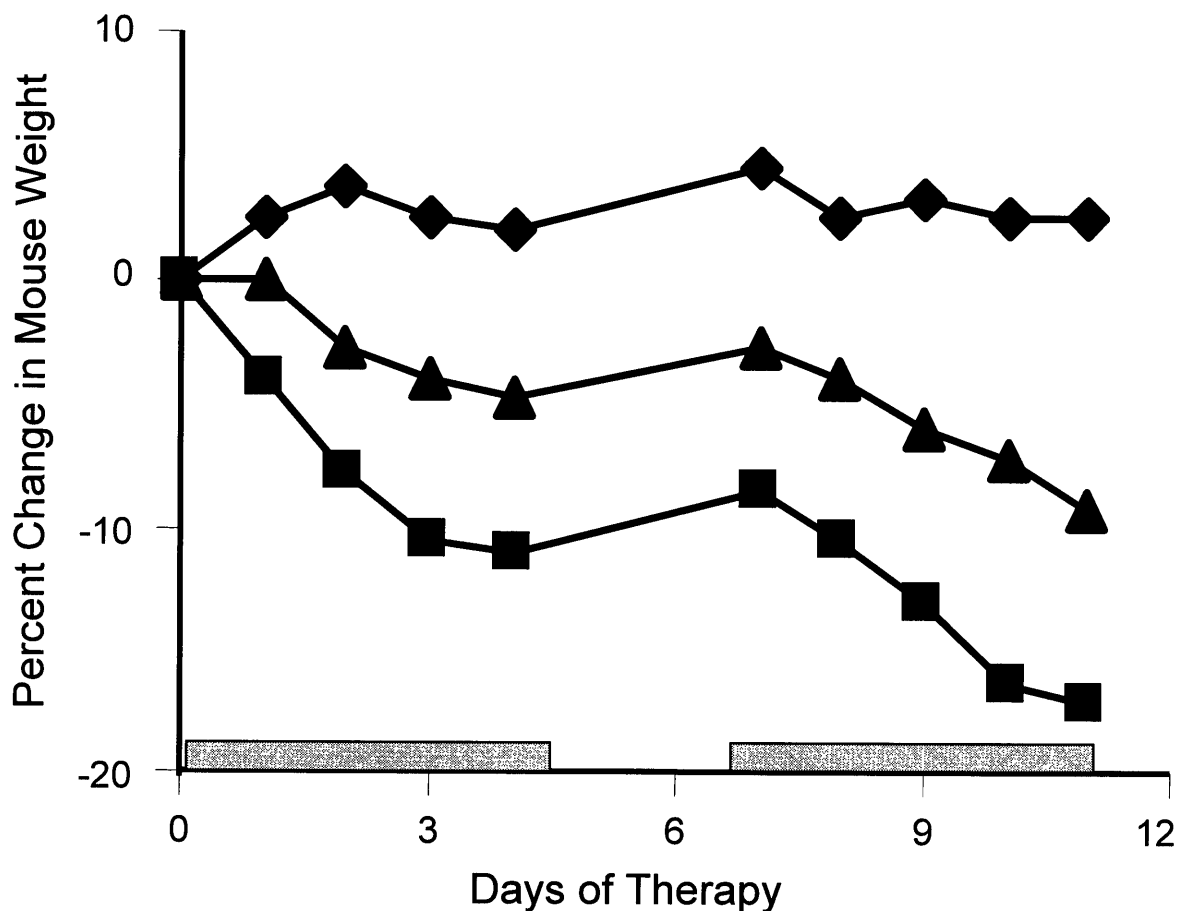
Fig 4.9 Percent change in mouse body weight after IP injections of E2-7a (▲), chlorambucil (■), or vehicle alone (◆). The treated mice lost approximately 10% of their body weight after two cycles of therapy.

E2-7α Readily Forms Adducts with DNA in Mouse Liver and Tumor Tissue
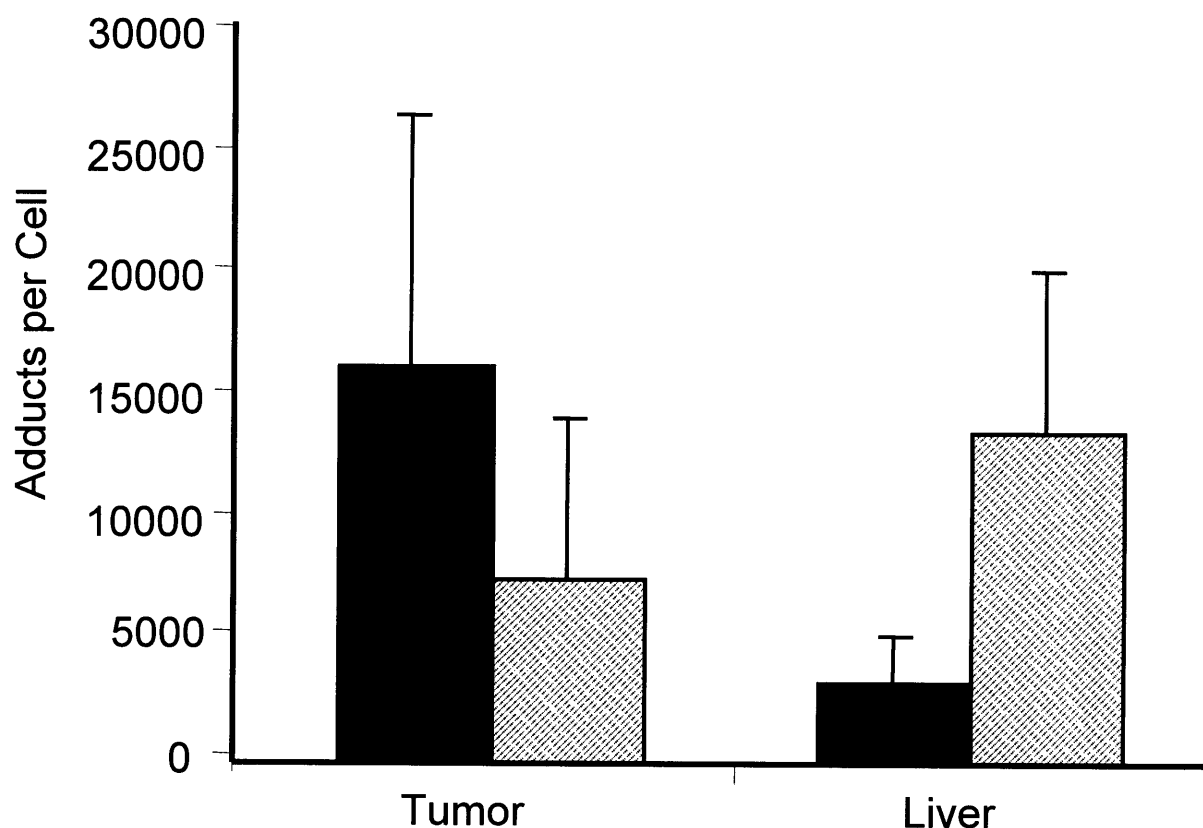
Fig 4.10 Number of DNA adducts per cell in tumor and liver tissue by AMS analysis. Mice were injected with 25 mg/kg ^{14}C-E2-7α Sub-Q (▆) or 75 mg/kg IP (▨). They were sacrificed 4 hours after administration of the compound. More adducts formed in tumor tissue with the Sub-Q route of administration despite the fact that it was a 3-fold lower dose. Errors bars are the standard deviation of the mean.

Chapter 5

The Repair of E2-7α DNA Adducts and Implications into Mechanism

Introduction

DNA alkylating agents represent one class of anticancer agents, but nitrogen mustard compounds, such as chlorambucil and melphalan, have only modest success in the clinic and their uses have been mainly limited to therapies of hematological cancers. These agents achieve their cytotoxicity by forming covalent adducts with DNA (Hurley 2002; Teicher 1997). Unfortunately, patients on these chemotherapies often suffer from serious side effects, with neutropenia being dose limiting, as a result of the formation of DNA adducts in non-target tissues (Blumenreich et al. 1988; Inoue et al. 1987). By inhibiting the DNA repair machinery selectively in cancer cells, a clinician could increase the therapeutic index of the alkylating agents and provide a better outcome for the patient with fewer toxic side effects (Barret and Hill 1998; Dolan 1997; Frankfurt 1991).

An additional way to improve the therapeutic outcome for a patient is by using an alkylating agent in combination with other agents that act by different mechanisms. Many clinical trials have illustrated the additional therapeutic benefit of combination drug therapies over the use of single agents for breast cancer treatment (Hortobagyi 1998). Rather than using several drugs in combination, we have set out to design a single agent that can simultaneously function by several different mechanisms. Our compounds are designed to disrupt DNA repair processes and cellular signaling and transcriptional events that are necessary for cell growth and proliferation.

The molecules that we have designed consist of a DNA damaging warhead that can form covalent adducts with DNA, like many conventional alkylating chemotherapeutics. They additionally have a ligand binding domain that can attract proteins found predominantly in a cancer cell. We have utilized the fact that the estrogen receptor (ER) is over expressed in many breast cancers (Ferno et al. 1990) by designing an agent that links a DNA damaging agent to an estradiol moiety capable of attracting the ER to the site of DNA damage. A DNA-adduct-ER complex could potentially inhibit repair enzymes from accessing the lesion, resulting in persistence of the adduct and eventual cell death. This mechanism would be selective to ER-expressing breast cancer cells because other cells of the body would not contain high levels of the ER. Furthermore, the ER is a transcription factor, so a high binding affinity to the DNA-adduct could titrate the ER from necessary cellular transcriptional events, again resulting

in cell death. These two mechanisms, DNA repair shielding and transcription factor hijacking, could produce lethal results for a cancer cell. Rink, et al. rationally designed a molecule that could exert its cytotoxic potential by the combination of these mechanisms (Rink et al. 1996).

A second derivative, E2-7α, was later synthesized and shown to have better affinity for the ER, as well as increased toxicity to ER(+) cells, than the molecules designed by Rink (Mitra et al. 2002). In the previous chapters, I have described many experiments by which E2-7α and a series of derivatives function (Mitra et al. 2002; Sharma et al. 2004). The evidence presented illustrates that the compound binds the ER with good affinity, adducts DNA, is selectively more toxic to cells expressing the ER, and is therapeutically effective in an ER(+) xenograft mouse model. Many of these experiments suggest the possibility that the repair shielding and, possibly, the transcription factor hijacking mechanisms play a role in the cytotoxicity of the compound. Here, however, I shall present more direct evidence in support of the repair shielding phenomenon using the AMS technology I described in the previous chapter. Furthermore, I have used a biochemical whole cell extract assay to characterize the repair pathway by which E2-7α-DNA adducts are likely repaired.

Materials and Methods

Preparation of Plasmid DNA Substrates Containing Damage. pGEM plasmid DNA was randomly modified by UV or E2-7α. UV damaged pGEM DNA was prepared by irradiating DNA at a concentration of 50 μg/mL in 20 μL droplets with 450 J/m^2 of UV light (254 nm). The irradiated DNA was treated with the *E. coli* Nth protein (endonuclease III) (New England Biolabs, Beverly, MA) to remove pyrimidine hydrates (which produce background nicking and are a substrate for base excision repair) at 37°C for 30 min, heated at 65°C for 2 min, and then subjected to sucrose banding for the isolation of super coiled plasmid (see below). The pGEM plasmid DNA was also allowed to react with 100 μM E2-7α in TE (10 mM Tris-Cl, 1 mM EDTA) buffer (pH 7.5), at 37°C for 1 hour. After drug modification, unreacted drug molecules were removed by phenol/chloroform extraction followed by ethanol precipitation. The DNA pellet was dissolved in TE at a concentration of 500 μg/mL and then layered on top of a

12 mL sucrose gradient containing 5-20% sucrose in 1.0 M NaCl, 5 mM EDTA, 25 mM Tris-HCl (pH 7.5). The gradient was centrifuged at 4°C for 21 hours at 31,000 rpm in a Beckman SW41Ti rotor. After centrifugation, fractions of 0.5 mL were collected by pumping out from the bottom of the tube. The fractions (10 µL each) were run on a 0.8% agarose gel containing 0.5 µg/mL ethidium bromide. The fractions of supercoiled DNA were pooled, concentrated using a Centricon (YM-50) filtration system, and stored in TE buffer (pH 8.0).

Repair Synthesis Assay. The repair reaction mixture (50 µL) contained 200 ng pBR322 (undamaged internal control) plasmid, 200 ng damaged pGEM, 40 mM Hepes-KOH (pH 7.8), 70 mM KCl, 5 mM MgCl$_2$, 0.5 mM dithiothreitol, 2 mM ATP, 20 µM of dGTP, 20 µM of dCTP, 20 µM of TTP, 8 µM dATP, 23 mM phosphocreatine, 2.5 µg creatinine phosphokinase, 18 µg bovine serum albumin, 2 µCi [α-^{32}P]-dATP, and HeLa whole cell extract, as described (Wood, Biggerstaff, and Shivji 1995). For the reaction containing the ER-LBD (ligand binding domain), the plasmid substrates in 10 µL of TE were incubated with 10 µL of ER-LBD in whole cell extract buffer at room temperature for 20 min, and then combined with the repair reaction mixture. For the reaction containing XPA-antibody and/or XPA protein, the plasmid substrates in 10 µL of TE were incubated with a 20 µL mixture including whole cell extracts, XPA-antibody, XPA protein, and whole cell extract buffer at 30°C for 30 min, and then combined with the repair reaction mixture. The repair reaction was conducted at 30°C for 1 hour. After incubation, EDTA (20 mM final concentration) and RNAse A were added to the reaction, thoroughly mixed and incubated at 37°C for 10 min. SDS (0.5% final concentration) and proteinase K (190 µg/mL final concentration) were added, thoroughly mixed, and incubated at 37°C for 30 min. The DNA was then extracted with phenol/chloroform, precipitated with ammonium acetate, and washed with 70% ethanol. The DNA pellet was dried, resuspended in *Hind III* buffer (New England Biolabs, Beverly, MA), digested with *Hind III*, and separated on 0.8% agarose gel containing 0.5 µg/mL ethidium bromide. The gel was photographed under UV transillumination and subsequently dried on gel blot paper. The dried gel was exposed to a phosphor screen, scanned by PhosphorImager (Storm 840, Molecular

Dynamics), and analyzed using ImageQuaNT software to quantify the radioactivity incorporated into DNA.

Cell Culture. The human cervical breast cancer cell lines, MCF-7 and MDA-MB231, were obtained from the American Type Culture Collection (Rockville, MD). Both cell lines were maintained in Minimal Essential Media (MEM) (Gibco) supplemented with 10% fetal bovine serum, 2 mM glutamine, and 1 mM sodium pyruvate in a humidified CO_2/air atmosphere at 37°C. GM02345 cells were purchased from the Coriell Institute for Medical Research (Camden, NJ) and cultured in Roswell Park Memorial Institute (RPMI) medium with 10% fetal bovine serum, and 2 mM glutamine in a humidified CO_2/air atmosphere at 37°C.

Repair of E2-7α DNA adducts in MCF-7 and MDA-MB231 cells. MCF-7 cells were exposed to a 0.75 μM dose of ^{14}C-E2-7α (specific activity 50 μCi/μmol) or 0.15 μM melphalan (specific activity 50 μCi/μmol) for 2 hours. MDA-MB231 cells were exposed to a 0.25 μM dose of ^{14}C-E2-7α (specific activity 50 μCi/μmol) or 0.25 μM melphalan (specific activity 50 μCi/μmol) for 2 hours. At the end of the treatment, the media was removed, the cells were washed 3 times with PBS and fresh media was added. Repair of the DNA adducts was monitored by harvesting cells 0, 1, 3, 6, 9, 15, and 24 hours after the removal of ^{14}C-E2-7α. The DNA was then isolated as indicated below.

Quantification of DNA Adducts in cells. MCF-7 and MDA-MB231 cells were exposed to various doses of ^{14}C-E2-7α dissolved in DMSO. At the end of the incubation the cells were scraped, pelleted, and washed with phosphate buffered saline (PBS). The cells were resuspended in 2 mL of cold (4°C) 10 mM Tris (pH 6.9), 250 mM sucrose, 2 mM calcium chloride buffer. Triton X-100 (25% in water) was added to make a final concentration of 5%. The solution was briefly vortexed and then centrifuged at 1000G in a Sorvall RC-2B Centrifuge with a GSA rotor at 4°C for 20 min. The supernatant was removed by aspiration and the nuclear pellet was resuspended in 1 mL of buffer. To this solution was added 5% sodium dodecyl sulfate (SDS) and 5 M sodium chloride (NaCl) to make a solution with a final concentration of 1% SDS and 1 M NaCl. An equal volume

of chloroform:isoamyl alcohol (24:1) was then added and the biphasic mixture was shaken vigorously for 15 min. The mixture was then centrifuged at 7000G for 15 min at 4°C. The aqueous phase was collected and re-extracted with another volume of chloroform:isoamyl alcohol, shaken, and centrifuged. The aqueous phase was then collected, and the nucleic acids were precipitated with 3 volumes of ice cold ethanol, chilled at -20°C for 20-30 min, and subsequently pelleted by centrifugation at 7000G for 15 min at 4°C. The nucleic acids were washed 2 times with cold ethanol and then dried *in vacuo*. The dried pellet was reconstituted with 0.5 mL of 0.05 M Tris (pH 7.5), 0.1 M NaCl on ice. In order to remove any contaminating RNA, 0.2 mg of RNAse A was added and incubated at 37°C for 10 min. The reaction was stopped by cooling on ice, the NaCl concentration was adjusted to 0.9 M, and the DNA was extracted by subsequent additions of chloroform:isoamyl alcohol as indicated above. The aqueous phase from the second extraction was isolated and the DNA was precipitated with 3 volumes of ice cold ethanol, centrifuged, and washed 2 times as above. The concentration of the DNA was obtained by monitoring the absorbance at 260 nm. The DNA was dissolved in 0.1-0.5 mL of water, depending on the DNA concentration, and then given to Paul Skipper and Rosa Liberman, both in the Tannenbaum laboratory at MIT, for analysis by Accelerator Mass Spectrometry (AMS) as described in Liberman, et al. (Liberman et al. 2004)

Results

Repair of E2-7α DNA Adducts *in vitro* and the Role of NER. Nucleotide excision repair (NER) is one of the many repair pathways a cell uses to defend itself from exogenous and endogenous DNA damage (Friedberg, Walker, and Siede 1995). NER is most closely associated with the removal of cyclobutane pyrimidine dimers and (6-4) photoproducts as a result of exposure to UV-C light (Beukers and Berends 1960; Boyce and Howard-Flanders 1964; Setlow and Carrier 1964). However, NER has also been shown to be involved in the removal of bulky alkylating agents such as cisplatin and melphalan (Grant, Bessho, and Reardon 1998; Kartalou and Essigmann 2001b; Reardon et al. 1999). Research from Rick Wood's laboratory has provided an *in vitro* means of monitoring NER using whole cell extracts, appropriate buffers, ^{32}P-dATP, and plasmid substrates (Wood, Biggerstaff, and Shivji 1995). The design of this system is illustrated

in Figure 5.1. Briefly, a plasmid is exposed to a damaging agent (in our case either UV light or E2-7α) and globally modified. The adducted plasmid is then incubated with cellular extracts which contain the proteins necessary for repair. Since NER typically removes a patch of bases 26-29 nucleotides in length (de Laat, Jaspers, and Hoeijmakers 1999; de and Hoeijmakers 2000; Petit and Sancar 1999; Prakash and Prakash 2000), rather than a single base as is the case for base excision repair (BER), radiolabeled ^{32}P-dATP will be incorporated into essentially all repair patches. The amount of radioactive incorporation is thus related to the amount of DNA repair.

The amount of repair is dependent on the incubation time of the damaged plasmid substrates with the HeLa whole cell extracts (data not shown) and on the protein concentration in the incubation reaction. Figure 5.2 shows the results of E2-7α damaged pGEM plasmid incubated with increasing amounts of cell extracts (70-280 µg/reaction). The agarose gel in Figure 5.2A depicts increased repair in the E2-7α damaged pGEM plasmid with increasing whole cell extract concentration. The amount of repair in the undamaged pBR plasmid is independent of cell extract concentration as evident by the same low level of background repair in all three lanes. As indicated by Wood, et al. the results after exposure to a phosphor screen can be quantified by determining the ratio of repair in the damaged plasmid (pGEM) to that of the internal control (pBR) (Wood, Biggerstaff, and Shivji 1995). These values are then normalized for any differences in DNA recovery between the tracks by densitometric scan of the ethidium-bromide stained gel. Figure 5.2B shows the results of this quantification. As expected, E2-7α damaged pGEM plasmids are repaired the most in the lane with the greatest amount of whole cell extracts (280 µg in lane 3). This indicates that E2-7α DNA adducts can be repaired by this system, and that this system can be used further in monitoring the repair of these adducts.

Since NER has been shown to be involved in the removal of bulky adducts and alkylating agents (Grant, Bessho, and Reardon 1998; Kartalou and Essigmann 2001b; Reardon et al. 1999), we wanted to assess the contribution of NER in the repair of E2-7α DNA adducts. The NER pathway has been characterized and consists of more than two dozen proteins (Fig 5.3). In human cells, NER involves the recognition of DNA damage, incision of the DNA strand containing the lesion, and synthesis and ligation in the region

of the excised oligonucleotide (Costa et al. 2003; de Laat, Jaspers, and Hoeijmakers 1999; Lindahl and Wood 1999; Wood 1997). The dual incision factors are the XPA protein, the single-strand DNA binding heterotrimer RPA, the XPC-hHR23B complex, the 6-9 subunit TFIIH complex, and two nucleases, XPG and ERCC1-XPF. A key intermediate is an open unwound structure formed around the lesion in a reaction that uses ATP-dependent helicase activities of XPB and XPD, two of the TFIIH subunits. This intermediate creates sites for cutting by the XPG and ERCC1-XPF enzymes, which recognize junctions between single-strand and duplex DNA and cut with specific polarities. A 24- to 32- residue oligonucleotide is released, and the gap is filled in by POL δ or ε holoenzyme (Budd and Campbell 1997; Wood and Shivji 1997) and sealed by DNA ligase I (Nocentini 1999; Tomkinson and Levin 1997).

The XPA protein is involved in the initial DNA adduct recognition event and is therefore an ideal protein to inhibit in order to suppress the activity of NER (Asahina et al. 1994; Jones and Wood 1993; Robins et al. 1991). Kuraoka, et al. have indeed inhibited NER by targeting antibodies specific for XPA (Kuraoka et al. 2000). He and Rick Wood have kindly supplied us with both the XPA antibody and XPA protein. Upon addition of XPA antibody to HeLa whole cell extracts, the repair of both UV damaged and E2-7α damaged pGEM plasmids is diminished. Figure 5.4A depicts the agarose gel after exposure to a phosphor screen and Figure 5.4B quantifies the differences in each lane. The pBR plasmid is an internal control that serves as a measure of background DNA damage. The ratio of the damaged (pGEM) to undamaged (pBR) plasmids in the positive control is set as 100 % repair. As compared to the positive control in which no XPA antibody was added, the repair of UV damaged plasmid decreased by 75%, whereas the repair of E2-7α damaged plasmid decreased by 60%. Furthermore, the decrease in repair of the damaged plasmids is specific to NER as the addition of XPA protein to cellular extracts containing the XPA antibody restores the activity. Figure 5.5A depicts the agarose gel after exposure to a phosphor screen and Figure 5.5B depicts the data graphically. As seen in Figure 5.4, the addition of XPA antibody decreases the amount of repair of E2-7α damaged pGEM plasmids by approximately 50% as compared to the positive control. However, upon addition of XPA protein, the repair capacity of the extracts is restored.

It is of interest to note that the magnitude in the inhibition of NER by the XPA antibody was considerably less for E2-7α damaged DNA than for UV damaged DNA (i.e., cyclobutane pyrimidine dimers and (6-4) photoproducts). In fact, XPA antibody inhibited the repair of UV induced lesions by 75% *versus* only a 50% inhibition in the repair of E2-7α induced DNA damage. One possible reason for this difference is that other DNA repair mechanisms may be involved in the repair of E2-7α induced DNA damage. In order to address this possibility, an XPA$^{-/-}$ cell line, GM02345, was cultured in order to obtain cellular extracts that were completely deficient in NER (Jones and Wood 1993; Robins et al. 1991). As expected, UV damaged plasmids incubated in GM02345 cellular extracts were not repaired (Fig 5.6). Surprisingly, E2-7α DNA adducts were still repaired, although to a lesser degree than when the E2-7α DNA damaged plasmids were incubated with NER proficient HeLa cell extracts (Fig 5.6). This result may indicate that other modes of DNA repair are involved in the removal of E2-7α adducts.

E2-7α DNA Adducts Persist Longer in ER Expressing Cells. In Chapter 2, I described the results of an experiment conducted by John Marquis that illustrate the differential toxicity of E2-7α towards ER(+) cells. The ER(+) MCF-7 cell line is approximately two fold more sensitive to E2-7α than is the ER(-) MDA-MB231 cell line. The differential toxicity is likely not the result of increased accumulation of E2-7α in the MCF-7 cell line since a 10 µM dose produced roughly the same number of DNA adducts in both cell lines over a 24 hour period. (Note: The data are not shown here because for an unknown reason replicate experiments produced a 3-4 fold difference in DNA adduct levels. However, the results from each individual experiment were analyzed by AMS several times and in both cases the initial values were reproduced. This suggests that the differences between the two experiments are unrelated to the analyzing methodology of AMS.)

An alternative possibility for the observed differential toxicity between the two cell lines is the desired repair shielding and/or transcription factor hijacking mechanisms by which we designed E2-7α. If the repair shielding phenomenon is a valid mechanism for the increased toxicity of E2-7α towards MCF-7 cells, then the rate of repair in these

cells should be less than that of the MDA-MB231 cells. In order to address this question we treated both cell lines for a brief two hour period with [^{14}C]E2-7α, replaced the drug containing media with fresh drug-free media, isolated the DNA at various time points, and analyzed the number of DNA adducts over time by AMS. Figure 5.7A illustrates the removal of E2-7α DNA adducts is indeed slower in the ER(+) MCF-7 cell line than in the ER(-) MDA-MB231 cell line. To ensure the differences in removal of E2-7α was not related to differential repair capacity between the two cell lines, we also treated both lines with [^{14}C]-melphalan. Figure 5.7B illustrates that the repair capacity of both cell lines is essentially the same in the removal of melphalan DNA adducts. These results suggest that the repair shielding mechanism may indeed be a valid reason for the differential toxicity between the two cell lines.

Discussion

The covalent modification of DNA in malignant cells is one approach that has been used clinically to rid a patient from potentially fatal tumors (Hurley 2002; Teicher 1997). One means of improving the therapeutic index of alkylating agents is by inhibiting the DNA repair machinery selectively in cancer cells (Barret and Hill 1998; Dolan 1997; Frankfurt 1991). Towards this end, we have rationally designed an agent, E2-7α, capable of forming DNA adducts and attracting tumor specific proteins (Mitra et al. 2002; Sharma et al. 2004). E2-7α was designed to attract the ER, which is aberrantly expressed in approximately 50% of all breast cancers (Ferno et al. 1990). The attraction of the ER to the site of an E2-7α lesion could inhibit repair enzymes from accessing the lesion and disrupt signaling events in a cancer cell since the ER is also a transcription factor. Furthermore, these adducts would be readily repaired in non-cancerous cells where the ER is not abundant and the overall toxicity to a patient could be significantly reduced.

In order to address these possible mechanisms, I first monitored the repair of E2-7α using an *in vitro* whole cell extract assay developed by the Wood laboratory (Wood, Biggerstaff, and Shivji 1995). E2-7α DNA adducts were found to be repaired by the NER pathway since an antibody against XPA, a protein involved in the initial recognition event of NER, diminished the amount of repair of E2-7α damaged plasmids.

Furthermore, the addition of XPA protein to cellular extracts containing XPA antibody restored the repair capacity of the extracts. Interestingly, however, the suppression of repair of E2-7α DNA adducts occurred to a lesser degree than the suppression of repair of UV damaged plasmids. Approximately 80% fewer UV induced DNA adducts were repaired upon the addition of XPA antibody, whereas only 50% of DNA adducts were removed in plasmids damaged with E2-7α. This observation prompted me to use a cell line completely deficient in NER activity, the XPA$^{-/-}$ GM02345 (Jones and Wood 1993; Robins et al. 1991). UV induced DNA lesions were completely unrepaired using cellular extracts derived from these cells. However, E2-7α damaged plasmids were still repaired, although only 25% as efficiently as HeLa cell extracts that are proficient in NER activity.

One explanation for this result could be E2-7α DNA adducts depurinate readily and at a much faster rate than the depyrimidination of cyclobutane pyrimidine dimers or (6-4) photoproducts (the major UV induced adducts monitored in this assay). Pyrimidine nucleosides are considerably more stable than purine nucleosides with respect to the glycosidic linkage of the base to deoxyribose. The mechanism of depyrimidination is the same as for depurination, but the loss of cytosine and thymine occur at rates of only 1/20 of that for adenine and guanine (Lindahl and Karlstrom 1973). Furthermore, the observed rate of decomposition of an N7-deoxyguanosine chlorambucil adduct in a 0.2 M cacodylic acid buffer (pH 6.8) at 37°C was 0.73 x 10^{-2} min^{-1} with the only reported stable product resulting from the cleavage of the glycosidic bond to produce *N*-(7-guanyl)ethyl-*N*-hydroxyethyl-*p*-aminophenylbutyric acid (Haapala et al. 2001). These two lines of evidence suggest that the depurination of E2-7α DNA adducts may help explain the somewhat surprising results that NER is not solely responsible for the repair of the lesions.

Other modes of DNA repair are likely involved in the repair of E2-7α DNA adducts directly or through the possible depurination events. Depurination (and depyrimidination) produce apurinic (and apyrimidinic) sites (AP sites). These AP sites are substrates for AP endonucleases that catalyze the incision of DNA exclusively at AP sites, thereby preparing the DNA for subsequent excision, repair synthesis, and DNA ligation (Friedberg et al. 1981; Lindahl 1979; Lindahl 1982). Although we currently have no evidence that E2-7α forms adducts with adenine, any adducts that are formed and

depurinate would form an AP site. An AP endonuclease would then repair the lesion and incorporate [α-^{32}P]dATP from our reaction mixture. As a note, 20% of melphalan adducts are at the N3 position of adenine (Osborne and Lawley 1993).

In addition to the incorporation of radiolabeled ATP by AP endonucleases, glycosylases involved in the BER pathway may also play a role in the repair of E2-7α DNA adducts. Even though NER is generally considered to be involved in the repair of bulky alkylating agents such as chlorambucil, cisplatin, and melphalan (Grant, Bessho, and Reardon 1998; Kartalou and Essigmann 2001b; Reardon et al. 1999), there is evidence that BER plays a role in the repair of these lesions as well. For example, both the bacterial and human 3-methyladenine-DNA glycosylase (MPG) can remove chlorambucil adducts from oligonucleotides (Lindahl 1993). Additionally, reviews by Kartalou and Essigmann indicate the possible involvement of mismatch repair, BER, recombination and other repair pathways in the removal of cisplatin DNA adducts (Kartalou and Essigmann 2001a; Kartalou and Essigmann 2001b). These additional repair pathways may also play a role in the removal of E2-7α adducts. The results here are consistent with the fact that bulky alkylating agents are generally substrates for NER, but our results also imply other repair pathways may be playing a role in the removal of E2-7α DNA adducts.

E2-7α was designed to disrupt the repair pathways discussed above by attracting the ER to the site of DNA adducts. Using the same DNA repair assay that I used to illustrate the role of NER on the repair of E2-7α damaged plasmids, Hyun-Ju Park, a former post-doctoral fellow in the Essigmann laboratory, tested the repair shielding hypothesis by co-incubating the ER-LBD with cell extracts. Figure 5.8 illustrates the results of her experiments. The ER-LBD inhibited the repair of E2-7α damaged plasmids but not UV damaged plasmids. This finding provided the first line of evidence that the repair shielding hypothesis may indeed be valid.

A second line of evidence was described in Chapter 2 in that E2-7α is selectively more toxic towards the ER(+) MCF-7 cell line over the ER(-) MDA-MB231 line. The results by Park indicate that the repair shielding phenomenon may be a contributing factor in the differential toxicity. I have provided additional evidence in support of the repair shielding mechanism by treating the ER(+) MCF-7 and ER(-) MDA-MB231 cell

lines with E2-7α and monitoring the repair of the DNA adducts in the two lines. In the MCF-7 cells, the DNA adducts seemed to take slightly longer to reach peak adduction level (as evident by the 3 hour time point in Figure 5.7A), and the adducts persisted longer than they did in the MDA-MB231 cells. In fact only 20% of E2-7α DNA adducts were removed after 15 hours in the MCF-7 cells while 70% were removed in MDA-MB231 cells at the same time point (as compared to the peak adduction level). Furthermore, the evidence from both cell lines treated with melphalan indicated that there is likely no differential repair capacity between the two cell lines. Reduction in adduct levels with time did not result from dilution through DNA synthesis or from selective loss of highly damaged cells, because during the 24 h after exposure to E2-7α or melphalan, there were no significant increases in intact or apoptotic cells and the doubling time of both cell lines is approximately the same. These results suggest that repair shielding of E2-7α DNA adducts may be a cause of the differential toxicity towards the MCF-7 cells.

The design of the experiment was such that the initial number of DNA adducts formed in either cell line by either drug would be essentially the same. As shown in Figure 5.7 all combinations produced roughly 2,000 DNA adducts per cell. This low level of initial adducts was chosen because we did not want to saturate the repair capacity of the cell or cause the cells to undergo apoptosis. Therefore sub-lethal doses of both drugs were given to cells. Surprisingly, however, the increase in DNA adduct formation after removal of the drugs was drastically different. In the case of E2-7α, the peak level in both cell lines was 10,000 adducts per cell 3 hours after the withdrawal of drug. However, cells treated with melphalan reached a peak adduct level of only ~3,000 adducts per cell, also 3 hours after the removal of drug from the media. These differences may be the result of how these two compounds differ in their entry into cells. Melphalan is taken up by amino acid transporter systems that discriminate between melphalan and hydrolyzed melphalan (Begleiter et al. 1979), whereas it is likely that E2-7α enters through passive diffusion.

In order to show that the two cell lines do not differ in their repair capacity, it would be ideal to see a greater degree of repair from peak adduction levels when cells are treated with melphalan. Unfortunately, this may not be possible. In a recent publication by Gould, et al. the rate of repair of melphalan DNA adducts was addressed. Gould

treated myeloblastic leukemia, ML1, cells with 33 μM or 66 μM doses of melphalan for 1 hour, exchanged the drug-containing media for drug-free media, and monitored the level of DNA adduction. At both doses approximately 50% of the adducts were removed by 24 hours (as compared to the peak adduction level at 4 hours) (Gould, Nixon, and Tilby 2004). Likewise, approximately 50% of the melphalan DNA adducts were removed from both the MCF-7 and MDA-MB231 cells by 24 hours (also, as compared to the peak adduction level at 3 hours). Gould also found that the peak adduction level is 50% greater than the initial adduction level, as we did. Finally, it is interesting to note that the number of DNA adducts formed in Gould's work is approximately 100-fold higher than what we observed with an approximately 100-fold lower dose. These results suggest that the formation of DNA adducts is dose dependent but the rate of repair of these adducts is not.

Conclusion

The design of novel genotoxins that can selectively destroy cancer cells while sparing normal, healthy ones is a formidable challenge. Cancer cells have developed many mechanisms that allow for resistance to current therapies. We have rationally designed a multifunctional agent that has the ability to combat these mechanisms of resistance. We have combined the ability to adduct DNA and to disrupt cellular signaling into a single agent. The work from previous chapters has illustrated the ability of our lead compound, E2-7α, to form DNA adducts, attract tumor specific proteins (i.e., the ER), and selectively kill malignant cells that contain the ER.

Here I present the first line of evidence in support of our desired mechanisms of action. E2-7α DNA adducts persist longer in ER(+) MCF-7 cells than in ER(-) MDA-MB231 cells. Differences in repair capacity between the two cell lines is likely not a factor as both cell lines remove the same number of melphalan DNA adducts over a 24 hour period. Furthermore, evidence gathered by Hyun-Ju Park is in agreement with this result, as she illustrated that the addition of the ER to HeLa cell extracts diminished the amount of repair of E2-7α DNA adducts *in vitro*, whereas there was no difference in the removal of UV induced DNA adducts in the presence or absence of the ER. Finally, I have provided evidence that the repair of E2-7α DNA adducts is in part due to NER;

however, other repair pathways are also likely to be involved in a portion of these adducts.

The results presented here and in previous chapters provide strong evidence in support of the repair shielding and transcription factor hijacking mechanisms. Although no direct evidence in support of transcription factor hijacking was provided an interaction with the ER *in vivo* would likely disrupt cellular signaling events. The ER has a good affinity for E2-7α DNA adducts and its association with these adducts has proven to inhibit their repair in two independent experiments. We are optimistic about the fate of E2-7α in a clinical setting and hope to some day have the resources available to begin such an investigation.

Future Directions

I have illustrated that NER plays a role in the removal of E2-7α DNA adducts, however our evidence also illustrates other repair pathways are likely involved in the removal of the lesions. Using a similar methodology as what was employed here will help us understand what other repair pathways may be involved. The glycosylase, MPG, has previously been shown to repair chlorambucil DNA adducts (Lindahl 1993) and would therefore represent an initial target. Either cell extracts that are deficient in MPG or an antibody against the protein could be used to assess the role of this glycosylase in the repair of E2-7α DNA adducts. The repair of E2-7α by MPG could be of clinical value as it was recently shown to interact with the ER, and this interaction increased the catalytic rate of the enzyme (Likhite et al. 2004). If the ER is attracted to the site of E2-7α adduction, the interaction between the ER and MPG could result in increased repair of the adduct and as a result could be deleterious in the development of E2-7α as a clinical candidate. (Note: HeLa cells used to make the cellular extracts for the repair assay do not express the ER). If it is shown that MPG is not involved in the repair of E2-7α DNA adducts, we will continue our investigations into other glycosylases and other repair pathways.

I have had the privilege of being taught by some of the world's most renowned biochemists while a graduate student at MIT. One such individual, JoAnne Stubbe, taught me that you can never prove a mechanism, but rather you can only disprove other

alternatives. The evidence that I have presented in this chapter strongly suggests that the repair shielding mechanism is likely to play a role in the cytotoxicity of E2-7α. However, these experiments, while sound in design and execution, still contain gaps that need to be addressed. One possibility is that the differences seen in the rates of repair of E2-7α DNA adducts between the MCF-7 and MDA-MB231 cells may be due to differences in cell proliferation. If for example the MDA-MB231 cells grow at a quicker rate than MCF-7 cells, then this observation could explain some of the differences in the repair of the two cell lines. I do believe this is unlikely however, as the doubling time of MCF-7 and MDA-MB231 cells is very similar and after the treatment of these cells in our hands, there were no obvious differences in total cell number. To err on the side of caution, we plan on determining the concentration of DNA in the two cell lines over time using a protocol described in Smith and Engelward (Smith and Engelward 2000).

Furthermore, we would like to repeat the experiment in order to see if a higher dose of melphalan would result in a more dramatic repair profile. However, based on the work by Gould, et al., this is unlikely to be the case. Therefore, in order to show that differences in repair capacity of the MCF-7 and MDA-MB231 cell lines are not responsible for the differences observed for the removal of E2-7α DNA adducts, we may have to use another alkylating agent. Ideally, chlorambucil would be used since it is also a nitrogen mustard similar in structure to both melphalan and our E2-7α. However, [^{14}C]-chlorambucil is extremely expensive and may be cost prohibitive for our purposes. We currently possess a [^{14}C]-nitrogen mustard reaction intermediate that could be used instead and are in the process of exploring these options.

These experiments will make the results described in this chapter more concrete. In Chapter 8, I will describe the results of some experiments with our lead compound used to target prostate cancer, 11β. These results will illustrate that the treatment of androgen receptor-expressing LNCaP cells with this compound results in altered expression levels of several signaling proteins. These alterations may be consistent with the transcription factor hijacking mechanism but also may be entirely unrelated to DNA adduction. No such studies have been attempted with E2-7α (further work is still necessary to identify the mechanisms responsible for the cytotoxicity of 11β and these will be discussed in the Future Directions section of Chapter 8). Therefore, we must

begin to investigate cellular signaling events that could imply transcription factor hijacking or other mechanisms unrelated to DNA damage.

Reference List

Asahina, H., Kuraoka, I., Shirakawa, M. et al. The XPA protein is a zinc metalloprotein with an ability to recognize various kinds of DNA damage. *Mutat. Res.* **315**, 229-237 (1994)

Barret, J.M. and Hill, B.T. DNA repair mechanisms associated with cellular resistance to antitumor drugs: potential novel targets. *Anticancer Drugs* **9**, 105-123 (1998)

Begleiter, A., Lam, H.Y., Grover, J. et al. Evidence for active transport of melphalan by two amino acid carriers in L5178Y lymphoblasts in vitro. *Cancer Res.* **39**, 353-359 (1979)

Beukers, R. and Berends, F. Isolation and identification of the irradiation product of thymine. *Biochim. Biophys. Acta* **41**, 550-551 (1960)

Blumenreich, M.S., Woodcock, T.M., Sherrill, E.J. et al. A phase I trial of chlorambucil administered in short pulses in patients with advanced malignancies. *Cancer Invest* **6**, 371-375 (1988)

Boyce, R. and Howard-Flanders, P. Release of ultraviolet light-induced thymine dimers from DNA in *E.Coli* K-12. *Proc. Natl. Acad. Sci. U. S. A* **51**, 293-300 (1964)

Budd, M.E. and Campbell, J.L. The roles of the eukaryotic DNA polymerases in DNA repair synthesis. *Mutat. Res.* **384**, 157-167 (1997)

Costa, R.M., Chigancas, V., Galhardo, R.S. et al. The eukaryotic nucleotide excision repair pathway. *Biochimie* **85**, 1083-1099 (2003)

de Laat, W.L., Jaspers, N.G., and Hoeijmakers, J.H. Molecular mechanism of nucleotide excision repair. *Genes Dev.* **13**, 768-785 (1999)

de, B.J. and Hoeijmakers, J.H. Nucleotide excision repair and human syndromes. *Carcinogenesis* **21**, 453-460 (2000)

Dolan, M.E. Inhibition of DNA repair as a means of increasing the antitumor activity of DNA reactive agents. *Adv. Drug Del. Rev.* **26**, 105-118 (1997)

Ferno, M., Borg, A., Johansson, U. et al. Estrogen and progesterone receptor analyses in more than 4,000 human breast cancer samples. A study with special reference to age at diagnosis and stability of analyses. Southern Swedish Breast Cancer Study Group. *Acta Oncol.* **29**, 129-135 (1990)

Frankfurt, O.S. Inhibition of DNA repair and the enhancement of cytotoxicity of alkylating agents. *Int. J. Cancer* **48**, 916-923 (1991)

Friedberg, E.C., Bonura, T., Love, J.D. et al. The repair of DNA damage: recent developments and new insights. *J. Supramol. Struct. Cell Biochem.* **16**, 91-103 (1981)

Friedberg, E.C., Walker, G.C., and Siede, W. DNA Repair and Mutagenesis. ASM Press Washington, D.C. (1995)

Gould, K.A., Nixon, C., and Tilby, M.J. p53 elevation in relation to levels and cytotoxicity of mono- and bifunctional melphalan-DNA adducts. *Mol. Pharmacol.* **66**, 1301-1309 (2004)

Grant, D.F., Bessho, T., and Reardon, J.T. Nucleotide excision repair of melphalan monoadducts. *Cancer Res.* **58**, 5196-5200 (1998)

Haapala, E., Hakala, K., Jokipelto, E. et al. Reactions of N,N-bis(2-chloroethyl)-p-aminophenylbutyric acid (chlorambucil) with 2'-deoxyguanosine. *Chem. Res. Toxicol.* **14**, 988-995 (2001)

Hortobagyi, G.N. Treatment of breast cancer. *N. Engl. J. Med.* **339**, 974-984 (1998)

Hurley, L.H. DNA and its associated processes as targets for cancer therapy. *Nature Rev. Cancer* **2**, 188-200 (2002)

Inoue, K., Ogawa, M., Horikoshi, N. et al. [Phase II study of chlorambucil in patients with hematological malignancies]. *Gan To Kagaku Ryoho* **14**, 2672-2675 (1987)

Jones, C.J. and Wood, R.D. Preferential binding of the xeroderma pigmentosum group A complementing protein to damaged DNA. *Biochemistry* **32**, 12096-12104 (1993)

Kartalou, M. and Essigmann, J.M. Recognition of cisplatin adducts by cellular proteins. *Mutat. Res.* **478**, 1-21 (2001a)

Kartalou, M. and Essigmann, J.M. Mechanisms of resistance to cisplatin. *Mutat. Res.* **478**, 23-43 (2001b)

Kuraoka, I., Bender, C., Romieu, A. et al. Removal of oxygen free-radical-induced 5',8-purine cyclodeoxynucleosides from DNA by the nucleotide excision-repair pathway in human cells. *Proc. Natl. Acad. Sci. U. S. A* **97**, 3832-3837 (2000)

Liberman, R.G., Tannenbaum, S.R., Hughey, B.J. et al. An interface for direct analysis of (14)c in nonvolatile samples by accelerator mass spectrometry. *Anal. Chem.* **76**, 328-334 (2004)

Likhite, V.S., Cass, E.I., Anderson, S.D. et al. Interaction of estrogen receptor alpha with 3-methyladenine DNA glycosylase modulates transcription and DNA repair. *J. Biol. Chem.* **279**, 16875-16882 (2004)

Lindahl, T. DNA glycosylases, endonucleases for apurinic/apyrimidinic sites, and base excision-repair. *Prog. Nucleic Acid Res. Mol. Biol.* **22**, 135-192 (1979)

Lindahl, T. DNA repair enzymes. *Annu. Rev. Biochem.* **51**, 61-87 (1982)

Lindahl, T. Instability and decay of the primary structure of DNA. *Nature* **362**, 709-715 (1993)

Lindahl, T. and Karlstrom, O. Heat-induced depyrimidination of deoxyribonucleic acid in neutral solution. *Biochemistry* **12**, 5151-5154 (1973)

Lindahl, T. and Wood, R.D. Quality control by DNA repair. *Science* **286**, 1897-1905 (1999)

Mitra, K., Marquis, J.C., Hillier, S.M. et al. A rationally designed genotoxin that selectively destroys estrogen receptor-positive breast cancer cells. *J. Amer. Chem. Soc.* **124**, 1862-1863 (2002)

Nocentini, S. Rejoining kinetics of DNA single- and double-strand breaks in normal and DNA ligase-deficient cells after exposure to ultraviolet C and gamma radiation: an evaluation of ligating activities involved in different DNA repair processes. *Radiat. Res.* **151**, 423-432 (1999)

Osborne, M.R. and Lawley, P.D. Alkylation of DNA by melphalan with special reference to adenine derivatives and adenine-guanine cross-linking. *Chem. Biol. Interact.* **89**, 49-60 (1993)

Petit, C. and Sancar, A. Nucleotide excision repair: from E. coli to man. *Biochimie* **81**, 15-25 (1999)

Prakash, S. and Prakash, L. Nucleotide excision repair in yeast. *Mutat. Res.* **451**, 13-24 (2000)

Reardon, J.T., Vaisman, A., Chaney, S.G., and Sancar, A. Efficient nucleotide excision repair of cisplatin, oxaliplatin, and Bis-aceto-ammine-dichloro-cyclohexylamine-

platinum(IV) (JM216) platinum intrastrand DNA diadducts. *Cancer Res.* **59**, 3968-3971 (1999)

Rink, S.M., Yarema, K.J., Solomon, M.S. et al. Synthesis and biological activity of DNA damaging agents that form decoy binding sites for the estrogen receptor. *Proc. Natl. Acad. Sci. U. S. A* **93**, 15063-15068 (1996)

Robins, P., Jones, C.J., Biggerstaff, M. et al. Complementation of DNA repair in xeroderma pigmentosum group A cell extracts by a protein with affinity for damaged DNA. *EMBO J.* **10**, 3913-3921 (1991)

Setlow, R. and Carrier, W. The disappearance of thymine dimers from DNA: an error-correcting mechanism. *Proc. Natl. Acad. Sci. U. S. A* **51**, 226-231 (1964)

Sharma, U., Marquis, J.C., Nicole, D.A. et al. Design, synthesis, and evaluation of estradiol-linked genotoxicants as anti-cancer agents. *Bioorg. Med. Chem. Lett.* **14**, 3829-3833 (2004)

Smith, S.A. and Engelward, B.P. In vivo repair of methylation damage in Aag 3-methyladenine DNA glycosylase null mouse cells. *Nucleic Acids Res.* **28**, 3294-3300 (2000)

Teicher, B.A. Cancer Principles and Practice. <u>Antitumor alkylating agents</u> 5, 405-417 (1997)

Tomkinson, A.E. and Levin, D.S. Mammalian DNA ligases. *Bioessays* **19**, 893-901 (1997)

Wood, R.D. Nucleotide excision repair in mammalian cells. *J. Biol. Chem.* **272**, 23465-23468 (1997)

Wood, R.D., Biggerstaff, M., and Shivji, M.K. Detection and measurement of nucleotide excision repair synthesis by mammalian cell extracts in vitro. *Methods: Comp. Meth. Enz* **7**, 163-175 (1995)

Wood, R.D. and Shivji, M.K. Which DNA polymerases are used for DNA-repair in eukaryotes? *Carcinogenesis* **18**, 605-610 (1997)

An Assay for Monitoring Nucleotide Excision Repair
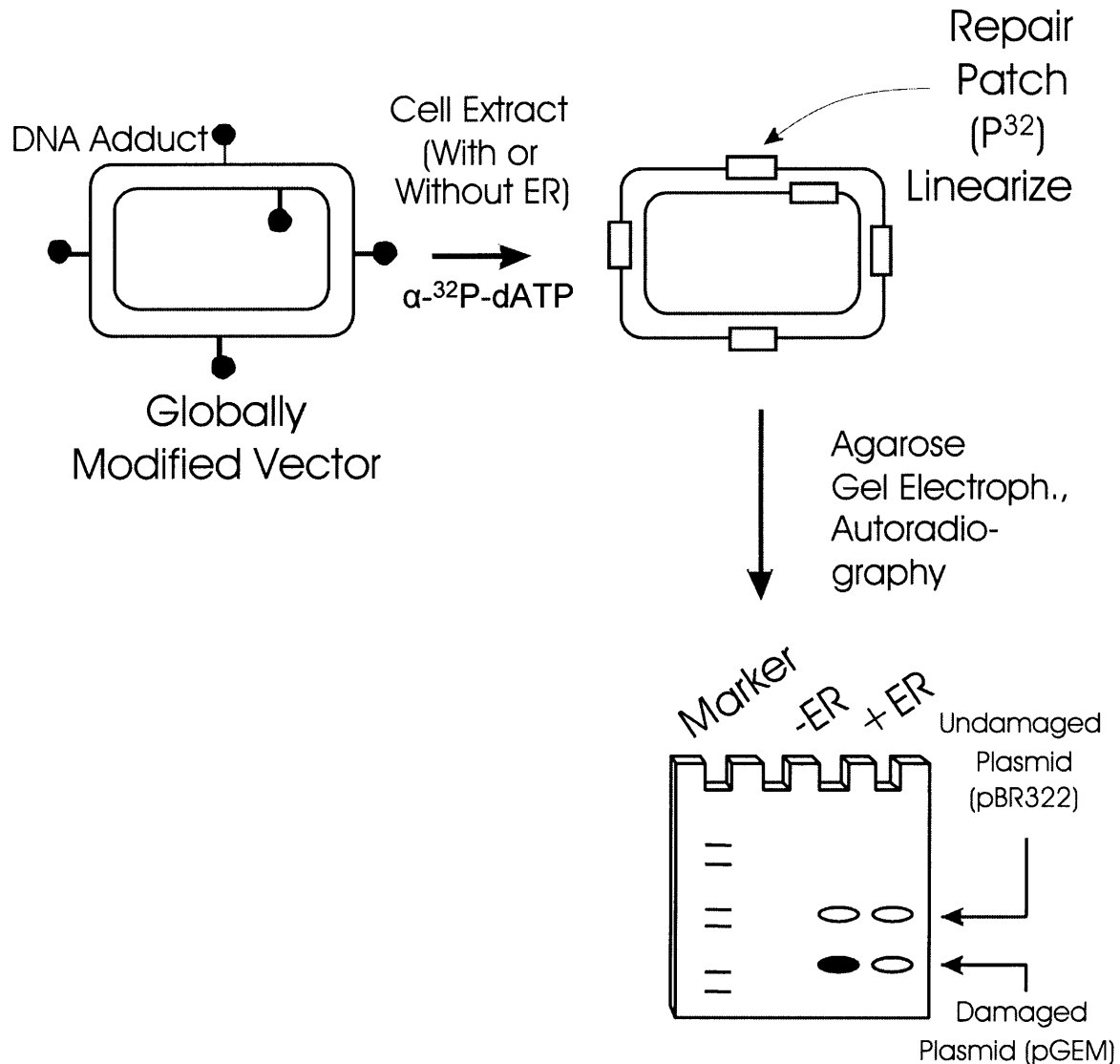
Fig 5.1 An *in vitro* system used to monitor DNA repair. Plasmid DNA is globally modified and incubated with cellular extracts and ^{32}P-dATP. The radiolabeled dATP is subsequently incorporated into the plasmid where the adduct was removed. The plasmid is then linearized and run on an agarose gel. The relative radioactive incorporation between lanes can be compared.

The Repair of E2-7α Damaged Plasmids is Dependent upon the Concentration of Cell Extracts

A

B
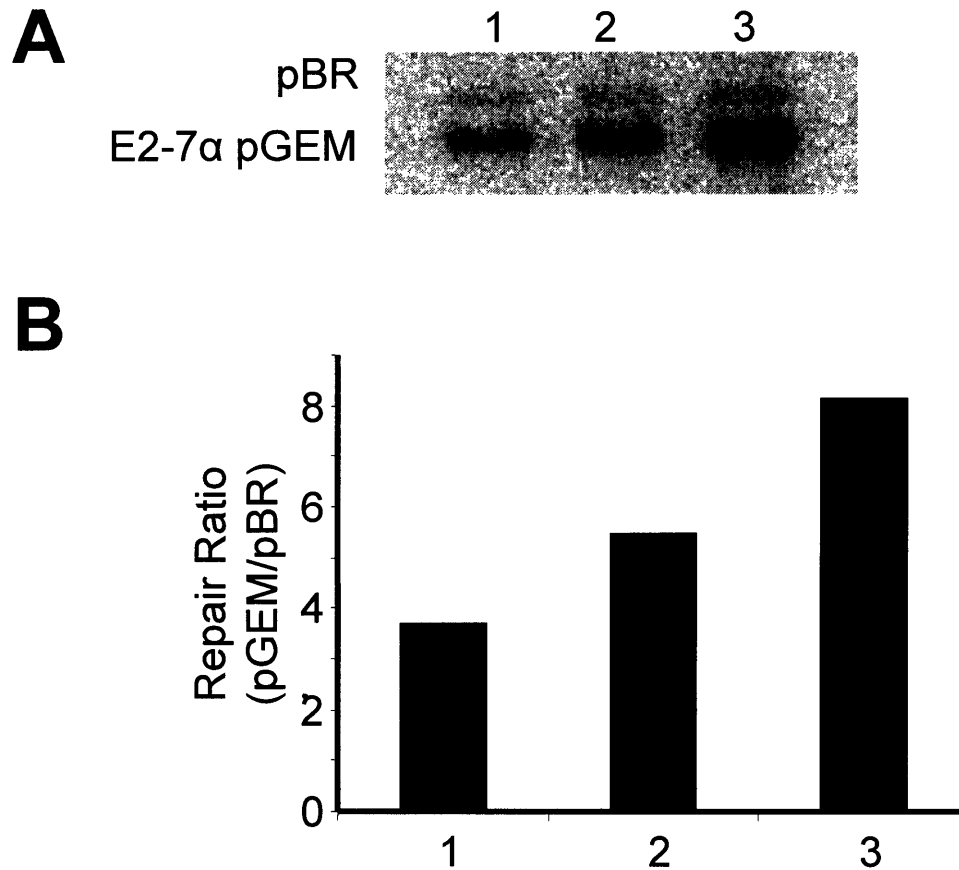
Fig 5.2 Assessing the repair of E2-7α damaged pGEM plasmids. **A.** Lane 1: 70 µg of HeLa whole cell extract, Lane 2: 140 µg of extract, Lane 3: 280 µg of extract. **B.** Quantification of the results expressed as ratio of repair in the damaged pGEM plasmid to that of the control pBR plasmid. E2-7α damaged pGEM plasmids are substrates for the repair assay and increasing concentration of cellular extracts increases the amount repair in the damaged (pGEM), but not in the undamaged (pBR) plasmids.

Nucleotide Excision Repair Pathway
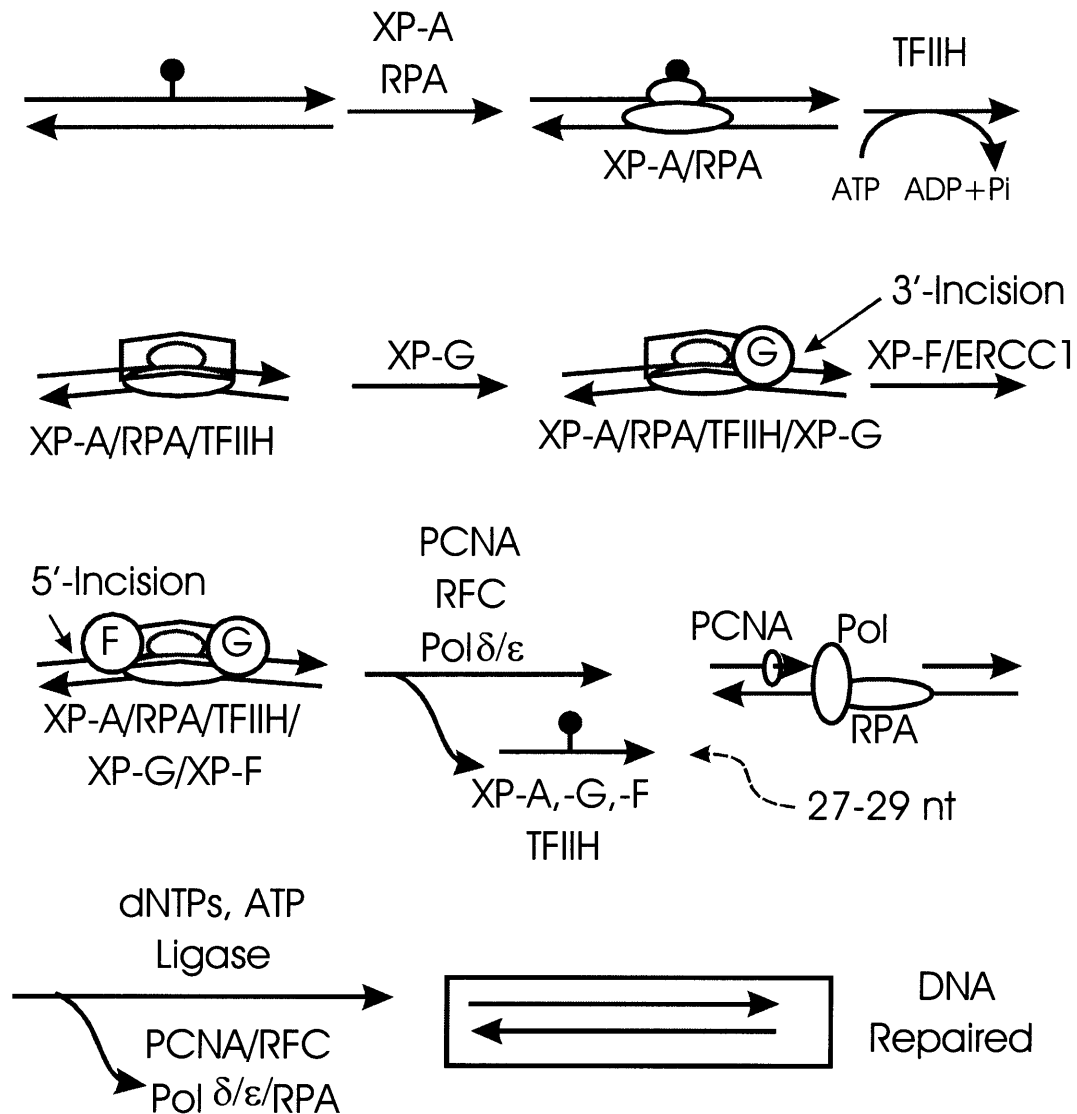
Fig 5.3 The Nucleotide excision repair pathway in mammalian cells. This pathway consists of DNA damage recognition (top row), dual incisions 5' and 3' to the damage (middle rows), and excision of the oligonucleotide, DNA synthesis, and ligation of the newly incorporated DNA (bottom rows).

Involvement of NER in the Repair of UV and E2-7α Damaged pGEM Plasmid

A

pBR

pGEM

1   2   3

B

Percent of Control

100
80
60
40
20
0

1   2   3
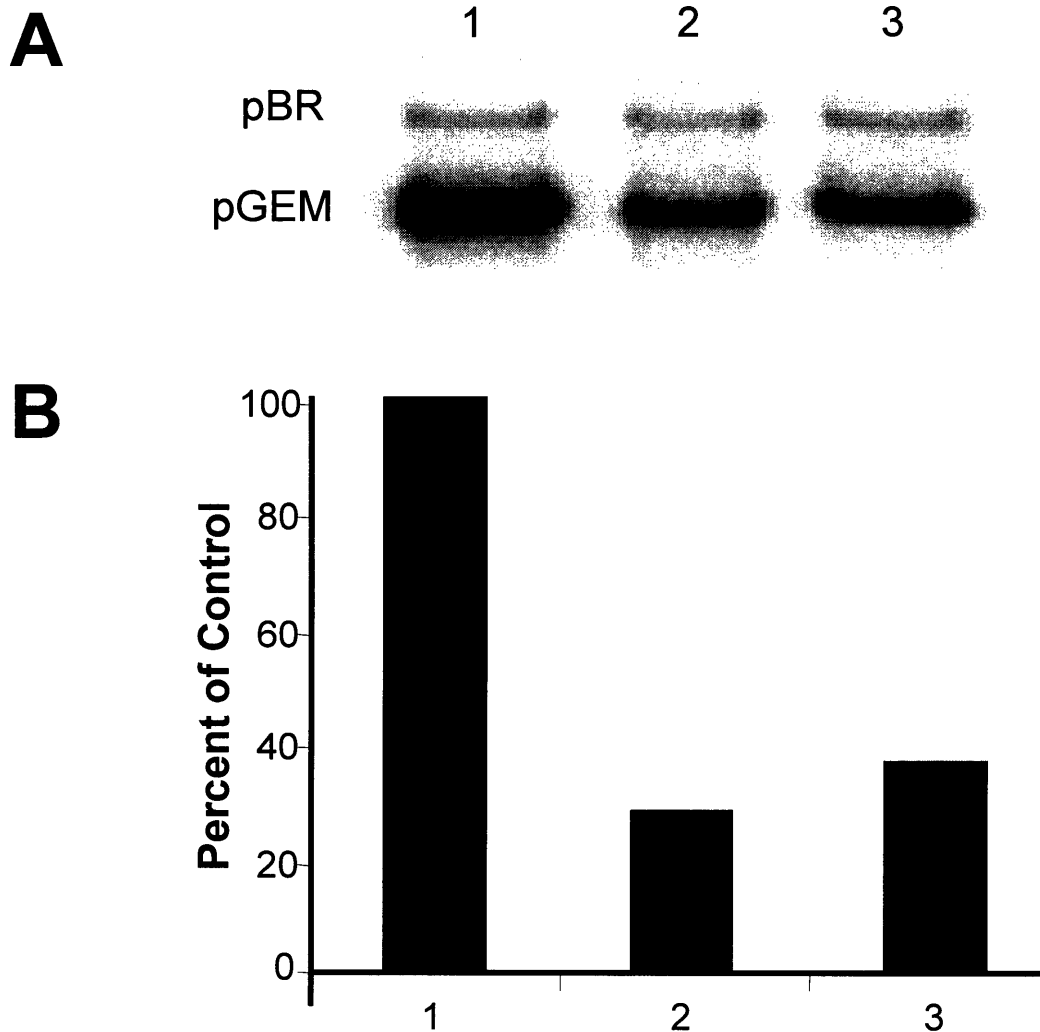
Fig 5.4 Inhibition of NER by XPA-antibody. **A.** Lane 1: positive control, Lane 2: UV damaged pGEM plasmid co-incubated with XPA-antibody, Lane 3: E2-7α damaged pGEM plasmid co-incubated with XPA-antibody. **B.** Quantification of the results expressed as percent of repair in the positive control. XPA-antibody suppressed the repair of both UV and E2-7α damaged plasmids as compared to a positive control where no XPA-antibody was present.

NER is Involved in the Repair of E2-7α DNA Adducts
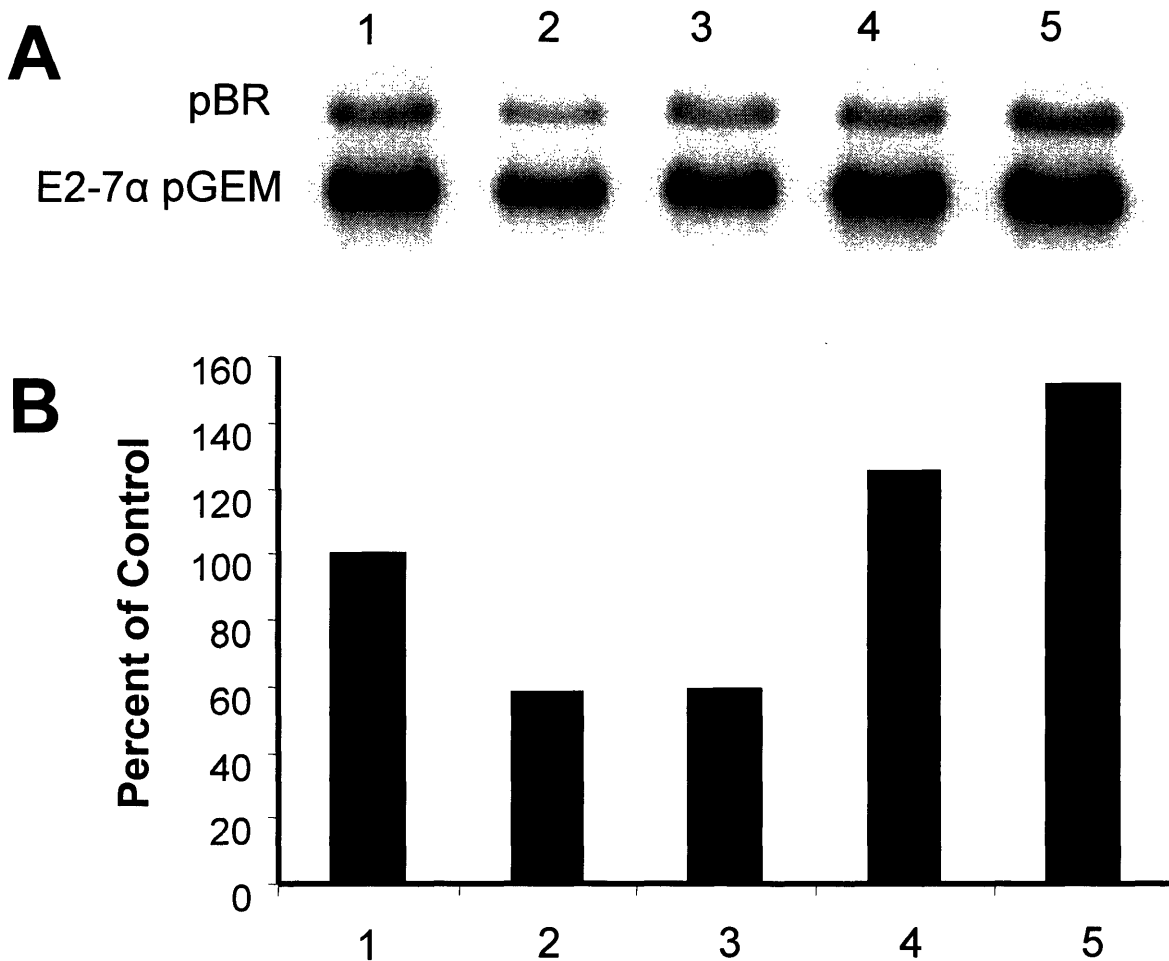
Fig 5.5 Inhibition of NER by XPA-antibody. The relative contribution of NER in the repair of E2-7α damaged pGEM plasmid was assessed. **A.** Lane 1: positive control, Lane 2: 1 μL XPA-antibody, Lane 3: 2 μL XPA-Antibody, Lane 4: 3 + 450 ng XPA, Lane 5: 3 + 900 ng XPA. **B.** Quantification of the results expressed as percent of repair in the positive control. Addition of XPA-antibody inhibits the repair of E2-7α adducts by 40%. Upon addition of XPA protein, the repair is restored, indicating that NER is involved in the repair of E2-7α DNA adducts.

E2-7α Damaged pGEM Plasmids are Still Repaired in Cell Extracts Deficient in NER

A

1   2   3   4   5

pBR

pGEM

B

Repair Ratio (pGEM/pBR)

14
12
10
8
6
4
2
0

1   2   3   4   5
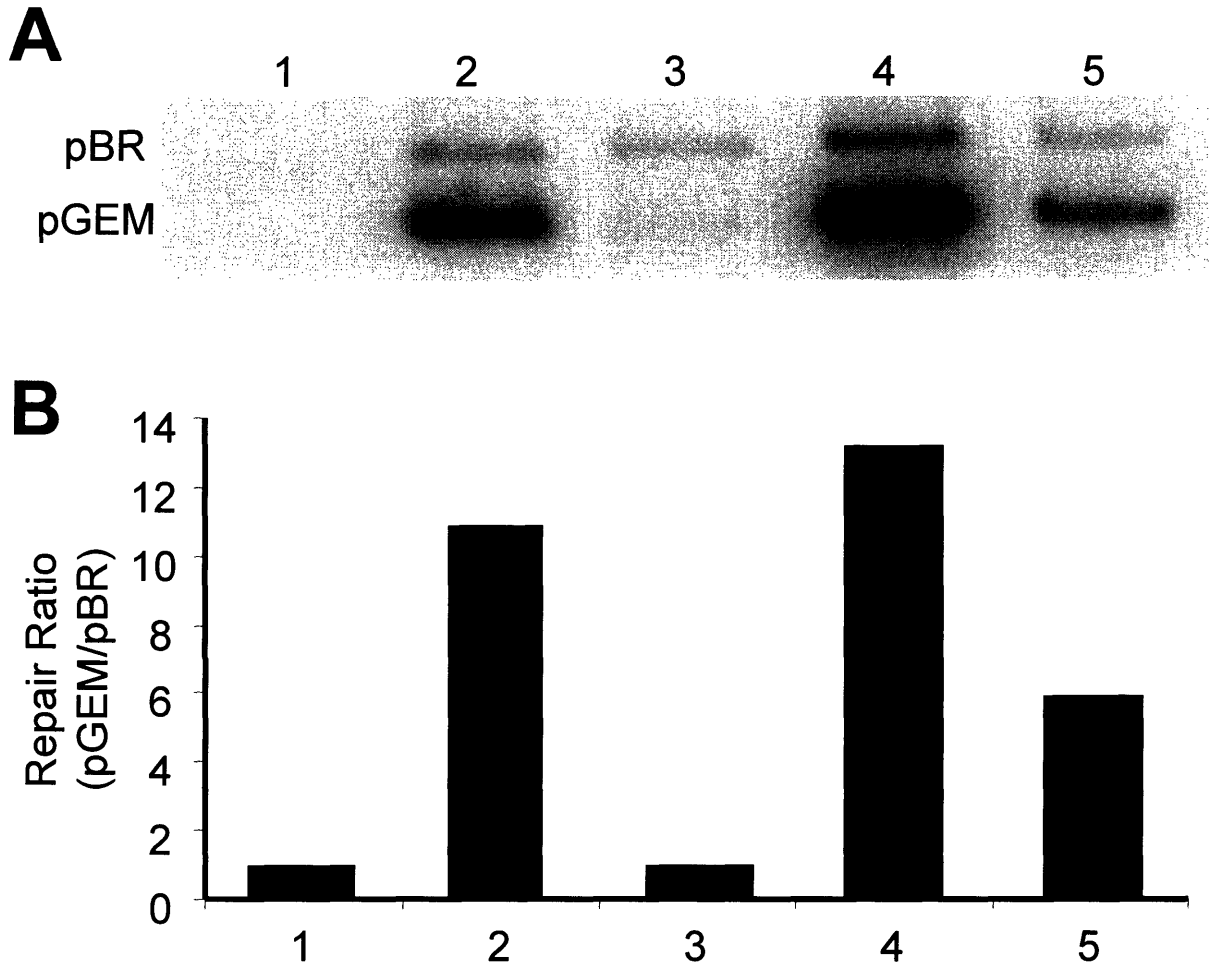
Fig 5.6 Repair of damaged plasmids in cell extracts that are proficient or deficient (XPA-/-) in NER. **A.** XPA proficient extracts: Lane 2 and 4. XPA-/- deficient extracts: Lane 3 and 5. No cell extracts (negative control): Lane 1. UV damaged pGEM: Lane 2 and 3. E2-7α damaged pGEM: Lane 4 and 5. **B.** Quantification of the results expressed as ratio of repair in the damaged pGEM plasmid to that of the control pBR plasmid. A ratio of 1 indicates no repair. UV damaged plasmids are not repaired in XPA-/- extracts. However, XPA-/- are still capable of repairing E2-7α damaged pGEM plasmids, possibly indicating pathways other than NER are involved in the repair of these lesions.

E2-7α DNA Adducts, but not Melphalan DNA Adducts, Persist Longer in ER (+) Cells
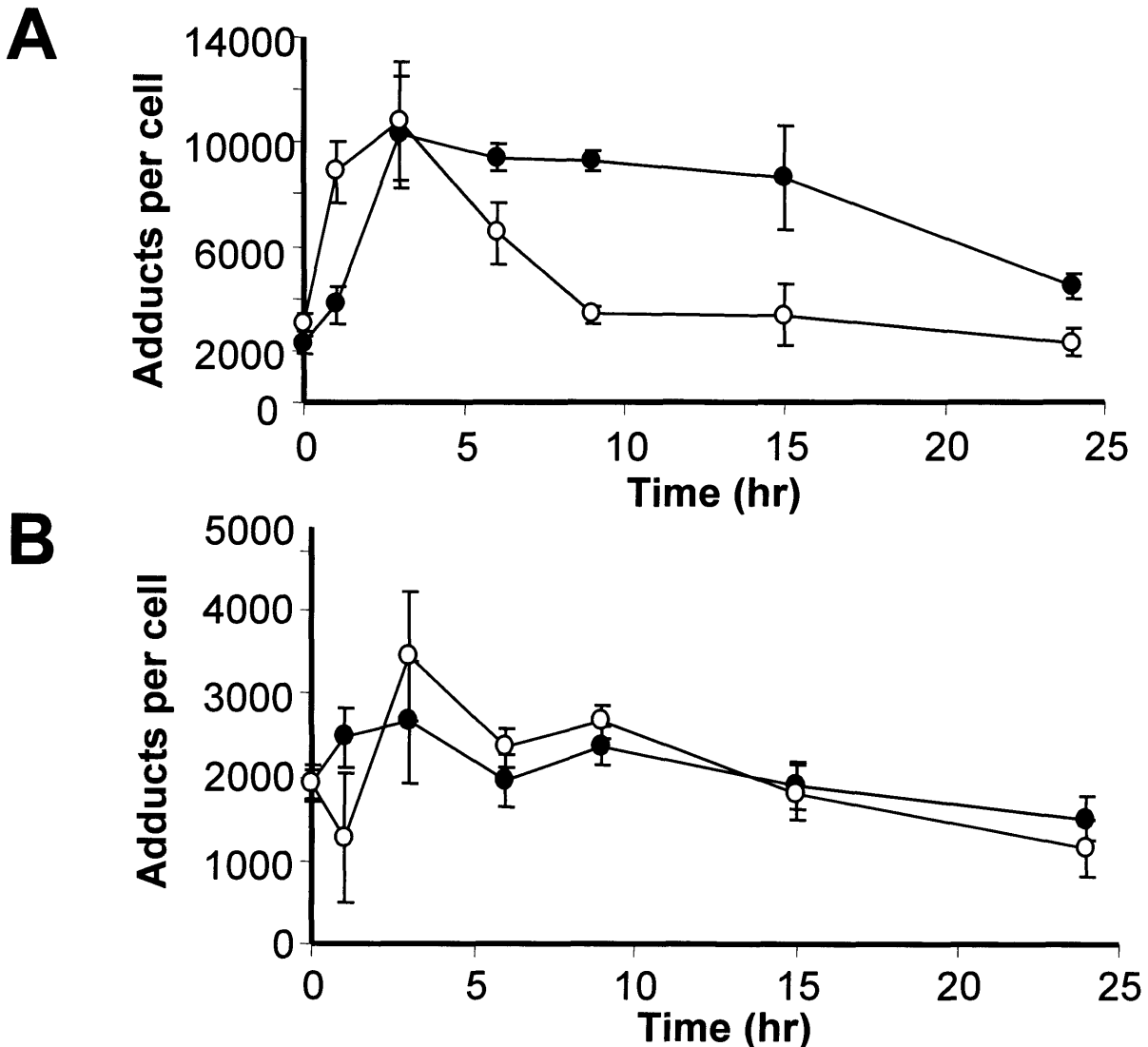
Fig 5.7 Repair of E2-7α **(A)** and Melphalan **(B)** in ER (+) MCF-7 cells (─●─) and ER (-) MDA-MB23 cells (─○─). E2-7α adducts persist longer in cells expressing the ER while melphalan adducts are repaired with similar kinetics independent of ER expression. These results suggest that E2-7α adducts are shielded from repair by the ER. Error bars are standard error of the mean of replicate AMS analyses, not replicate dosings.

The ER-LBD Inhibits the Repair of E2-7α DNA Adducts
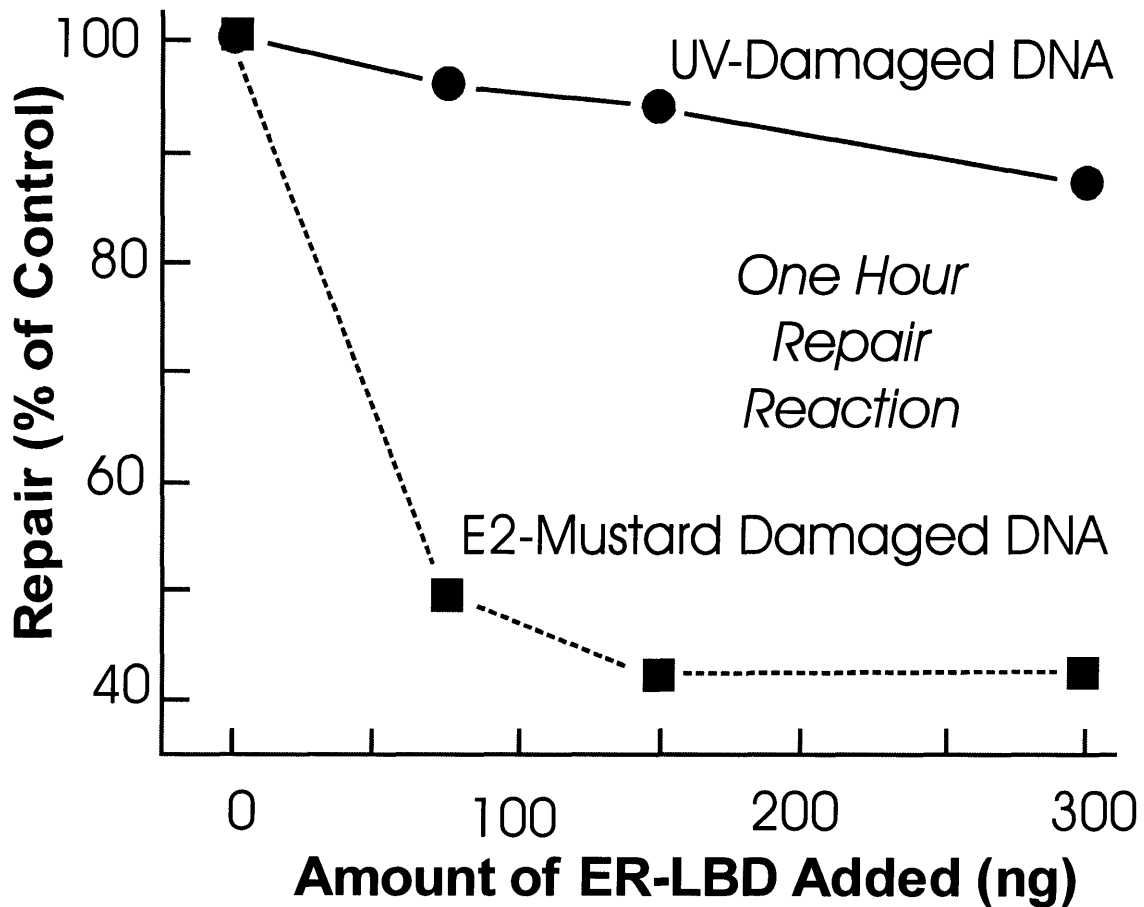
Fig 5.8 The ER-LBD blocks the repair of E2-7α DNA adducts. Increasing amounts of the ER-LBD inhibits the repair of E2-7α DNA adducts, but not DNA adducts induced by UV damage.

The work from the previous four chapters describes my results with our chemotherapeutic agent that targets ER(+) breast cancers. We have similarly designed an agent, 11β, that targets AR(+) prostate cancers. The work presented in the subsequent chapters will follow the same basic sequence as what was presented for E2-7α: *in vitro* experiments, pharmacokinetics, and finally therapeutic potential. In all chapters, I shall discuss how the results support our intended mechanism(s) of action.

Chapter 6

The Rational Design and Biophysical Properties of an Anti-cancer Agent that Targets Androgen Receptor Expressing Prostate Cancers

Introduction

DNA damaging agents were among the first chemotherapeutics used in the clinic and continue to remain an important component in combination chemotherapy regimens (Hurley 2002; Teicher 1997). DNA damaging agents, in combination with other drugs that act by different mechanisms, can place the tumor into a state of stasis and in some cases even cure the patient of their cancer. Such is the case in patients with testicular cancer treated with the DNA damaging agent cisplatin, in combination with etoposide and bleomycin. This therapy results in a cure rate of 93% in men with the disease (Masters and Koberle 2003) and is also effective in treating patients with cancers of the ovary, head, neck, and lung.

Until recently, the therapeutic landscape for men with advanced prostate cancer did not include traditional cytotoxic chemotherapeutic agents (Kish, Bukkapatnam, and Palazzo 2001; Morris and Scher 2000). The demonstration of the palliative effects of mitoxantrone combined with prednisone in patients with advanced prostate cancer has sparked interest in the development of new agents and regimens utilizing cytotoxic agents to improve patient outcomes (Martel et al. 2003; Morris and Scher 2003). The combination of the taxane, docetaxel, with prednisone has proven to be the most effective regimen to date with a mean increased survival time of 3 months in patients with advanced prostate cancer (Walsh 2005).

The paltry improvement in patient survival is due to the resistance of prostate cancers to cytotoxic drugs. Prostate cancers often overexpress anti-apoptotic proteins, such as Bcl-2, allowing for the tumors to survive the cytotoxic therapy regimens used to treat advanced stages of the disease (Lebedeva et al. 2000; Raffo et al. 1995; Vlietstra et al. 1998). Furthermore the utility of androgen ablation therapy is no longer beneficial in late stage disease as a result of a cellular transition from androgen-dependence to androgen-independence. Despite the increased expression of anti-apoptotic proteins in advanced prostate cancer, several studies have indicated that these cells are still capable of undergoing apoptosis (Denmeade et al. 1999; Marcelli et al. 2000; Wang et al. 1999). The ability to target resistance mechanisms and induce apoptosis in advanced stages of the disease is central to the development of more effective drugs and treatment regimens.

The strategy of combining several agents that can increase the effectiveness of alkylating agents is one approach to overcoming resistance. However, occasionally drug-drug interactions or overlapping side effects preclude certain multi-drug regimens from being used in the clinic. We have therefore employed a novel approach in which we have designed a single agent capable of alkylating DNA and simultaneously disrupting multiple cellular signaling pathways responsible for tumor growth and survival. In androgen –dependent and –independent prostate cancer, the AR is frequently over-expressed at both the mRNA and protein level (Gioeli 2004; Morris and Scher 2003; Wang, Ossowski, and Ferrari 2004). We have therefore taken advantage of this fact by designing molecules capable of covalently modifying DNA and attracting the AR to the site of the damage. Protein-adduct complexes formed in prostate cancer cells would likely camouflage the lesion from repair enzymes resulting in cellular toxicity. Furthermore, the attraction of the AR to DNA adducts would likely titrate away its normal transcriptional activities responsible for cell growth and survival. This two-pronged attack of DNA damage combined with the disruption of necessary cellular signaling events could produce a single molecule capable of inducing apoptosis in advanced prostatic cancers.

Based on the structural similarity of the AR with other steroid receptor proteins (Sack et al. 2001), we have incorporated the molecular features of molecules we have designed to target estrogen receptor (ER) expressing breast cancers (described in the previous 4 chapters). We linked an aniline nitrogen mustard to a testosterone-like ligand that has a high affinity for the AR. Previous work by Rink, et al. has illustrated the importance of a hexanyl chain linked to the steroid ligand in order for the remainder of our molecule to exit the steroid binding pocket (Rink et al. 1996). We decided on the attachment of the 6-carbon linker at the 11β position on the basis that the antiprogestin drug RU486 and several derivatives with long alkyl chains at this position retain a high affinity for the AR (Berrevoets, Umar, and Brinkmann 2002; Muddana et al. 2004).

There are a few examples in the literature of compounds that incorporate steroid receptor ligands combined with chemically reactive genotoxins (Brix et al. 1990; Eisenbrand et al. 1989; Knebel and von 1988). However, in most cases these agents are designed as a means of selectively delivering the genotoxin to the malignant cell. The

linkers in these molecules are designed to be hydrolyzed so as to release the active toxin within its target cell. Our molecules are designed for chemical stability as well as to resist hydrolysis and degradation by proteases and esterases. We intend for our molecules to form DNA adducts in many different tissue types. In non-target tissue we expect the adducts to be quickly repaired. However, in malignant tissue, we hope the expression of a tumor specific protein which our molecule was designed to attract (for example, the AR in prostate cancer) would cause a persistence of the adduct and thus result in cell lethality. Furthermore if the protein is a transcription factor (as is the AR), the DNA adducts could titrate away necessary cellular signaling events and therefore result in further toxicity to the cell.

We have designed and characterized a molecule, 11β (Fig 6.1A), which we believe can function by the intended mechanisms of action. In this chapter, I shall discuss the work which illustrates the ability of 11β to form DNA adducts and that the compound, both alone and when adducted to DNA, has a good affinity for the AR. I shall discuss my work on identifying DNA adducts formed after the treatment of 11β with salmon testes DNA. I shall also describe the solubility of our lead compound as assessed by measuring its log D using an HPLC methodology.

Furthermore, I shall briefly describe some experiments that others in the Essigmann laboratory have completed. Specifically, I shall discuss the RBA, the amount of DNA adduction as assessed by piperidine cleavage, the ability of DNA adducts to interact with the AR, the selective toxicity towards AR(+) LNCaP cells, and the molecular changes brought about by a 10 μM treatment of the LNCaP cells. In order to address the mechanistic features unrelated to DNA damage, i.e. repair shielding and transcription factor hijacking, we have synthesized an unreactive 11β derivative, 11β-dimethoxy. See Figure 6.1B. The results with the 11β-dimethoxy compound will also be discussed. Although I did not conduct some of these experiments, I believe it is very important to discuss them in brief as these results provide insight into mechanism and also have established a basis for my subsequent work.

Materials and Methods

Synthesis. The complete chemical synthesis of all 11β-substituted 17β-hydoxy-estra-Δ4(5),9(11)-3-one-linked genotoxicants have been conducted by various members of the Essigmann laboratory. The work is described in Marquis, et al (Marquis et al. 2005).

Mass Spectrometric Analysis of 11β DNA Adducts. Reaction of DNA with 11β was performed on a large scale to obtain sufficient material for structural analysis of covalent products. Salmon testes DNA (20 mg, Sigma-Aldrich) was dissolved in 20 mL of 5 mM sodium cacodylate, 25% *N,N*-dimethylformamide. To the DNA solution was added 100 μL of 10 mM E2-7α in DMSO, final concentration of 11β was 50 μM. After incubation for 16 hours at 37°C, unbound 11β was removed by extraction with phenol:chloroform:isoamyl alcohol (25:24:1) and subsequent ethanol precipitation. The DNA was then reconstituted in water and subsequently hydrolyzed in 0.1 N HCl for 30 min at 70°C. The solution was then neutralized with 1N NaOH and adjusted to 20 mM Tris-HCl (pH 7.4), 10% methanol. The hydrolyzed DNA was loaded onto a C18 Sep-Pak® (Waters Co.) column and eluted sequentially with 10 mL of 10% and 50% aqueous methanol solutions and finally with 100% methanol. The 100% methanol fraction was reduced *in vacuo* and analyzed by HPLC and mass spectrometry. HPLC analyses were performed using a Beckman ODS 4.6 x 250 mm Ultrasphere column eluted at 1 mL/min. with a 20 min. linear gradient of 50% 0.1 M ammonium acetate/10% acetonitrile, 50% methanol to 100% methanol. Aliquots of samples obtained from HPLC fractionation were analyzed by electrospray ionization mass spectrometry (ESI-MS) using flow injection (0.2 mL/min.) in methanol:water:acetontrile (50:45:5) in positive ion mode. The mass spectrometric analysis was conducted with the help of Dr. John Wishnok and Dr. Beatrice Zayas.

Cell Culture. The human prostate cell line, LNCaP was obtained from the American Type Culture Collection (Rockville, MD). The LNCaP cell line was maintained in RPMI 1640 supplemented with 2.5 mg/ml glucose, 10% fetal bovine serum (FBS; Hyclone, Salt Lake City, UT), 2 mM glutamax, 1 mM sodium pyruvate and 100 mM HEPES. Cells were grown in a humidified 5% CO_2/air atmosphere at 37°C.

Identification of DNA Adducts in cells. LNCaP cells were exposed for 6 hours to a 10µM dose of 11β dissolved in DMSO. At the end of the incubation the cells were scraped, pelleted, and washed with phosphate buffered saline (PBS). The cells were resuspended in 2 mL of cold (4°C) 0.01M Tris (pH 6.9), 0.25M sucrose, 2 mM calcium chloride buffer. Triton X-100 (25% solution) was added to make a final concentration of 5%. The solution was briefly vortexed and then centrifuged at 1000G in a Sorvall RC-2B Centrifuge with a GSA rotor at 4°C for 20 min. The supernatant was removed by aspiration and the nuclear pellet was resuspended in 1 mL of buffer. Sodium dodecyl sulfate (SDS) (5%) and sodium chloride (NaCl) (5 M) was added to make a solution with a final concentration of 1% SDS and 1 M NaCl. An equal volume of chloroform:isoamyl alcohol (24:1) was then added and the biphasic mixture was shaken vigorously for 15 min. The mixture was then centrifuged at 7000G for 15 min at 4°C. The aqueous phase was collected and re-extracted with another volume of chloroform:isoamyl alcohol, shaken and centrifuged. The aqueous phase was then collected and the nucleic acids were precipitated with 3 volumes of ice cold ethanol, chilled at -20°C for 20-30 min, and subsequently pelleted by centrifugation at 7000G for 15 min at 4°C. The nucleic acids were washed 2 times with cold ethanol and then dried in vacuo. The dried pellet was reconstituted with 0.5 mL of 0.05 M Tris (pH 7.5), 0.1 M NaCl on ice. In order to remove any contaminating RNA, 0.2 mg of RNAse A was added and incubated at 37°C for 10 min. The reaction was stopped by cooling on ice, the NaCl concentration was adjusted to 0.9 M, and the DNA was extracted by subsequent additions of chloroform:isoamyl alcohol as indicated above. The aqueous phase from the second extraction was isolated and the DNA was precipitated with 3 volumes of ice cold ethanol, centrifuged, and washed 2 times as above. The DNA was then hydrolyzed as described above and analyzed by ESI-MS for the characterization of DNA adducts.

Determination of the Partition Coefficient (log P):

Computer Simulation: In order to determine a feasible methodology for the determination of the log P (and log D) values of 11β (and E2-7α), the structure of various reference compounds, 11β, E2-7α, and the E2-7α derivatives were entered into the

following web sites: 1. http://www.logp.com and 2. http://www.molinspiration.com. The log P of the reference compounds determined by the computer simulations were compared to experimentally derived log P values found in the literature to test the accuracy of these simulations. This has been previously reported in Chapter 2 and will not be discussed further here. Based on the results described in Chapter 2, an HPLC methodology was employed.

HPLC: The log P of all compounds was determined by the HPLC method of Donovan and Pescatore. (Donovan and Pescatore 2002) Briefly, 1 mg of the test compound was dissolved in 1 mL internal standard solution: 2 mL toluene and 20 mg triphenylene dissolved in 200 mL of methanol. The compound/internal standard solution (2 µL) was injected into a Rainin HPLC with an octadecyl poly(vinyl alcohol) (ODP-50) 20x4 mm, 5 µm, 250 Å pore size column (Supelco), 10-100% 0.01 M sodium phosphate(pH adjusted)/methanol gradient over 9.4 min, and a flow rate of 1.5 mL. The pH of the aqueous buffer was incrementally adjusted by 1 pH unit (from pH 7 – 12) to find the pH that produced the longest retention time. At this pH, the compound was injected in triplicate. The compounds were detected at 260 nm by a Dynamax UV-1 detector. The log P of the test compound is calculated by Equation 6.1. The log D at physiological pH was calculated based on the equation derived by Horvath, Equation 6.2 (Horváth, Melánder, and Molnár 1977).

Results

11β Forms DNA Adducts with Guanine Residues *in vitro*. 11β contains a reactive aniline mustard capable of adducting DNA. The formation and identification of these adducts was determined using a combination of HPLC and ESI-MS. Figure 6.2 illustrates an HPLC trace after 11β was allowed to react with salmon testes DNA *in vitro*. The broad peak at 2-3 min corresponds to unreacted free bases while the peak at 16 min revealed a prominent signal at 813.5 m/z by ESI-MS (Fig 6.3A). Collision induced decay (CID) on the 813.5 molecular ion yielded prominent fragment ions at m/z 662.3 and 372.1. See Figure 6.3B. The 813.5 mass and the resulting CID are consistent with a chemical structure in which one ethylene arm of the mustard of 11β is attached to

guanine and the other has a substituted --hydroxyl group for the chlorine atom. See Figure 6.4 left panel. As shown in Figure 6.4 (left), these ions are consistent with the loss of the guanine fragment from the adduct (m/z 662.3) and from the fragmentation of the proposed structure at the secondary amino group in the linker (m/z 372.1). Confirmation of these structures and of the 813.5 molecular ion resulting from an 11β-Guanine adduct was provided by analysis of covalent products from E2-7α and a tetradeuterated analog of E2-7α (d_4-E2-7α) (Fig 6.4 right panel) as described in Chapter 2. Unfortunately, a tetradeuterated analog of 11β has yet to be synthesized and therefore the only comparison to be made is with the E2-7α analogs that have the same structure, with the exception of the steroid moiety, and same molecular weight. HPLC and ESI-MS analysis of the hydrolysis products of d_4-E2-7α under identical conditions identified a compound that formed a molecular ion of 817.5 with a similar HPLC retention time as the 11β compound that produced the m/z 813.5 ion. This result is consistent with a d_4-E2-7α-Guanine adduct. See Figure 6.4 right panel. CID on the 817.5 molecular ion yielded fragment ions of m/z 666.5 and 372.1, indicating that the m/z 666.5 ion contained the deuterated portion of the molecule while the m/z 372.1 did not. (as described in Chapter 2) These results with the E2-7α compounds support the proposed structure for the 11β-Guanine adduct and the proposed fragmentation pattern.

11β-Guanine Adducts are also Identified in LNCaP cells. LNCaP cells were exposed to a 10 μM dose of 11β for 6 hours and the DNA from these cells was isolated, hydrolyzed, and analyzed by ESI-MS for the identification of 11β-DNA adducts. A prominent 813.5 m/z signal was observed indicating the formation of an 11β-guanine adduct. See Figure 6.5. This result provides the first evidence that 11β forms DNA adducts in cells and the formation of these adducts is likely involved in the cytotoxic properties of the molecule.

The Partition Coefficient (log P): The log P of a compound can be predictive of aqueous solubility, absorption, and permeability (Lipinski et al. 1997). The lipophilicity of 11β and its dimethoxy analog was assessed by the HPLC method of Donovan and Pescatore (Donovan and Pescatore 2002). Based on the results described in Chapter 2,

we employed this methodology as a result of the suspected high lipophilicity of our compounds. A representative HPLC chromatogram is shown in Figure 6.6. 11β (11.48 min.) is bracketed by toluene (8.65 min.) and triphenylene (12.89 min.). The log P of 11β and 11β-dimethoxy was found to be 5.05 and 4.07, respectively. The log D at pH 7.4 was estimated using an equation derived by Horvath et al (Horváth, Melánder, and Molnár 1977). See equation 6.2. The log D of 11β and 11β-dimethoxy was calculated to be 2.00 and 0.97, respectively. The log D values indicate that the aqueous solubility of the 11β-dimethoxy compound is approximately 10-fold greater than 11β under physiological conditions.

Discussion

Our studies on E2-7α demonstrated that a selective antitumor agent could be created by incorporating additional mechanisms of action into a traditional alkylating chemotherapeutic agent. E2-7α and its predecessor, 2-PI, are multifunctional agents which have the ability to modify DNA covalently and attract tumor specific proteins to the site of these lesions (Mitra et al. 2002; Rink et al. 1996; Sharma et al. 2004). The results describing the biological activity of E2-7α were described in Chapters 2-5. Here, I report the application of our strategy to improve conventional chemotherapeutics through the creation of a novel molecule, 11β, designed to target AR(+) prostate cancers, which have been problematic from the clinical management perspective.

Key to the biological activity of 11β is the ability to modify DNA covalently and interact with the AR. Kasuhik Mitra, of the Essigmann Laboratory, illustrated that approximately 75% of the self-complimentary deoxyoligonucleotide, 5'[^{32}P]-d(ATTATTGGCCAATAAT)-3', was found to be piperidine labile after a 4 hour incubation with 100 μM 11β, indicative of the formation of covalent DNA adducts. (data not shown) (Marquis et al. 2005). Nicole Dinaut, also of the Essigmann Laboratory, illustrated the ability of 11β to bind to the AR in a competitive binding experiment. 11β was found to have a relative binding affinity (RBA) of 11 for the AR in LNCaP whole cell extracts, when compared to the synthetic androgen [^{3}H]-R1881 (Marquis et al. 2005). See Figure 6.7. Since the affinity for R1881 is about twice that of the natural ligand

dihydrotestosterone, an RBA of 11 implies that the affinity of 11β is approximately 20% that of the natural ligand (Zhao et al. 1999). Furthermore, 11β-DNA adducts were found to have a weaker yet still finite affinity for the AR (RBA = 0.2). Of note for experiments to be discussed later in this section, the 11β-dimethoxy compound was not able to adduct DNA, but had an affinity for the AR similar to that of 11β. These two experiments provided crucial evidence that shows 11β is capable of forming DNA adducts and that these adducts are capable of attracting the AR to the site of the lesion.

Since we had shown that 11β was capable of adducting DNA, we investigated whether it would act analogously to chlorambucil and predominantly adduct the N7 position of guanine. The N7 position of guanine is the most nucleophilic site in DNA and is therefore the most typical site of aniline mustard adduct formation (Singer and Grunberger 1983; Sunters et al. 1992; van Zeeland 1996). 11β was incubated with DNA *in vitro* and the formation of DNA adducts was characterized by ESI-MS. A molecular ion of 813.5 m/z was obtained, which is consistent with the substitution of the two chloro- groups by a guanine on one ethylene arm of the nitrogen mustard and a hydroxyl group on the other arm. Unfortunately, a tetradeuterated version of 11β has yet to be synthesized and therefore the only structural comparison which can be made is between the fragmentation pattern observed when E2-7α and a tetradeuterated version, d_4-E2-7α, reacted with DNA. Such a comparison may be valid in this situation as both 11β and E2-7α have identical molecular weights and identical structures, with the exception of the steroid end that, coincidentally, remains intact upon CID. E2-7α also yielded an 813.5 m/z molecular ion and the d4-E2-7α produced a molecular ion of 817.5 m/z. The CID of E2-7α was identical to what was observed with 11β, and the d4-E2-7α had one fragment of identical molecular weight and another of +4 m/z. These ESI-MS results illustrate that the adducts formed with 11β are likely identical to what was previously reported with E2-7α (Mitra et al. 2002), indicating that 11β forms DNA adducts at the N7 position of guanine in a similar manner as to what was previously reported with chlorambucil (Haapala et al. 2001; Povirk and Shuker 1994).

The AR(+) LNCaP cell line was exposed to 11β for 6 hours and the DNA from these cells was isolated, hydrolyzed, and analyzed by ESI-MS. The results illustrate that the same 11β-guanine adducts that formed *in vitro* also form in LNCaP cells. The

formation of these adducts indicates that the molecule is not rapidly degraded through hydrolysis of the bis-2-chloroethyl arms. The importance of this discovery lies in the fact that the molecule crossed two bio-physical membranes in order to reach the intended DNA target.

The permeability of 11β in crossing two biomembranes was quantitatively derived by using an HPLC methodology for calculating its log P. 11β had a log P value of 5.05 and a log D of 2.00 as calculated using an equation derived by Horvath, et al (Horváth, Melánder, and Molnár 1977). These values in addition to the fact that 11β contains fewer than 10 hydrogen bond acceptors and fewer than 5 hydrogen bond donors satisfy 3 of the 4 "rules of 5" that Lipinski has proposed (Lipinski et al. 1997). Molecules that comply with Lipinski's "rule of 5" generally have favorable aqueous solubility and permeability across biomembranes. The one criteria that does not satisfy Lipinski's rule is the molecular weight of 11β is in excess of 500 Da (11β has a molecular weight of 716 Da). The low log D suggests that the compound may have favorable pharmacokinetics (as will be discussed in Chapter 7) and, as evident with the results from the formation of DNA adducts in LNCaP cells, cellular permeability.

John Marquis, of the Essigmann Laboratory, further investigated the permeability and also the toxicity of 11β by exposing the AR(+) LNCaP cells with 0-10 μM doses in culture. In an effort to gain insight into possible mechanistic aspects of the compound, the AR(-) PC-3 and DU-145 cell lines were also exposed to 0-10 μM concentrations of 11β. Chlorambucil was used as a control in all three cell lines. The results shown in Figure 6.8A illustrate that a 10 μM dose of 11β for a brief 2 hour exposure to LNCaP cells is much more toxic than the same dose in PC-3 and DU-145 cells. Furthermore, the alkylating agent, chlorambucil, was no more toxic to any one cell line and the overall toxicity of chlorambucil is much less than what was observed for 11β (Fig 6.8B). These results are consistent with our intended mechanism of action in which cells that express the AR would be selectively more toxic than cell lines that do not, possibly as a result of the repair shielding and transcription factor hijacking hypotheses.

To further address the possible mechanism(s) of 11β, John Marquis and Bob Croy treated the AR(+) LNCaP cells with 11β, 11β-dimethoxy, or chlorambucil. Cells treated with 11β displayed dramatic cytoplasmic contraction and detachment from the culture

dish within 6 hours, whereas chlorambucil treated cells did not. Treatment with 11β-dimethoxy produced a less dramatic and transient change in cell morphology. The cells remained attached to the culture dish and recovered to their pretreatment shapes by 24 hours. Only the cells treated with 11β underwent apoptosis as characterized by Annexin V staining, DNA laddering, and poly-ADP ribose polymerase (PARP) cleavage (Fig 6.9 A-C, respectively). These results suggest that 11β is effective in overcoming the roadblocks in LNCaP cells that prevent other alkylating agents, such as chlorambucil, from activating apoptosis (Marquis et al. 2005).

Although 11β-dimethoxy was unable to initiate an apoptotic response, LNCaP cells treated with the compound arrested in the G1 phase of the cell cycle. These results led us to investigate the expression of the G1 cell cycle checkpoint proteins, specifically the cyclin-dependent kinase (CDK) inhibitors, p21^{Cip1} and p27^{Kip1}. The expression level of p21 constantly increased over time in LNCaP cells treated with chlorambucil. However, in cells treated with 11β and 11β-dimethoxy, the level of p21 was initially suppressed, but was then restored to basal levels in cells treated with 11β-dimethoxy and eventually elevated by several fold in cells treated with 11β (Marquis et al. 2005). See Figure 6.10A. p21 plays an essential role in growth arrest after DNA damage (Gartel and Tyner 2002b). Our findings suggest that p21 expression is modulated by DNA damage produced by the reactive compounds, most likely through activation of the p53 pathway. LNCaP cells express wild-type, functional p53 (Isaacs 2000), which is a major regulator of p21 transcription in response to DNA damage (el-Deiry et al. 1993). There are several reports indicating that increased expression of p21 protects prostate cancer cells as well as other cell types against apoptosis induced by a variety of different anticancer agents (Gartel and Tyner 2002a; Martinez et al. 2002). These findings suggest significance to the different patterns of p21 induction that we observed in LNCaP cells treated with chlorambucil or 11β-dichloro. While chlorambucil produced a rapid increase in the level of p21, the 11β-dichloro compound initially decreased levels of p21 in LNCaP cells. Since the initial reduction of p21 levels also occurred with the unreactive 11β-dimethoxy analog, other features of our compounds, unrelated to DNA damage, are likely involved in this response.

The expression of the other CDK we investigated, p27, was unchanged by chlorambucil but elevated in cells treated with either of the 11β compounds (Marquis et al. 2005). See Figure 6.10A. This result could be explained by a direct interaction of our compounds with the AR. The effects of androgens on the proliferation of LNCaP cells are well characterized. Low concentrations of androgens such as DHT stimulate growth while high concentrations are inhibitory (Kim et al. 1996; Lee et al. 1995). Treatment of growing LNCaP cells with a high dose of DHT (100 nM) results in the accumulation of p27 and growth arrest within 24 h (Tsihlias et al. 2000).

In addition, p27 accumulation during androgen-induced growth arrest has been linked to decreased expression of the p45^{SKP2} subunit of the ubiquitin E3 ligase SCF^{SKP2} (Lu, Schulz, and Wolf 2002b). The direct binding of the Skp2 subunit to the cyclin kinase subunit CKS1 directs the ubiquitination and subsequent proteolysis of p27 (Ganoth et al. 2001; Spruck et al. 2001). Therefore, the levels of p27 can be regulated by its ubiquitin-dependent degradation through the ubiquitin E3 ligase SCF^{Skp2} (Skp2) (Carrano et al. 1999; Lu, Schulz, and Wolf 2002a). Both 11β compounds decreased the expression of Skp2 as seen in Figure 6.10B (Marquis et al. 2005). The decreases in Skp2 expression correlate well with the relative levels of increase in expression of p27 as expected with the involvement of Skp2 in the turnover of p27. Unlike the 11β-dimethoxy compound, which temporarily arrests cells in the G1 phase of the cell cycle, 11β does not arrest LNCaP cells in G1, but instead rapidly induces apoptosis. These results may be explained by the unique nature of 11β-dichloro in that the AR can be attracted to the site of DNA adducts and thus disrupt cellular signaling events, perhaps through the transcription factor hijacking mechanism.

Conclusion

Based upon mechanistic studies of the anticancer agent cisplatin, we have designed a single molecule that can form DNA adducts and attract tumor specific proteins to the site of the lesions. Using the work described in Chapters 2-5 as a model, we have incorporated a new steroid moiety which provided a molecule that could be used to treat AR(+) prostate cancers. This new molecule, 11β, has features derived from E2-

7α – a DNA reactive warhead based on the aniline mustard chlorambucil, a stable linker, and a steroid that has a good affinity for the AR.

The work described here illustrates several important features of this molecule that demonstrate its potential as a chemotherapeutic agent. I have shown that 11β has good aqueous solubility as described by its low log D. 11β forms DNA adducts, and these adducts have been identified as mono-guanine adducts after reaction with DNA *in vitro* and isolated from the DNA of LNCaP cells exposed to 11β for 6 hours. Furthermore, 11β has a good affinity for the AR both alone and when adducted to DNA, and it displays increased toxicity towards the AR(+) LNCaP cell line over the AR(-) PC-3 and DU-145 cell lines. The differences in the expression levels of the cell cycle regulatory proteins, p21, p27, and Skp2, after LNCaP cells were treated with chlorambucil, 11β-dimethoxy, or 11β, illustrate the unique nature of 11β. Only 11β was capable of inducing apoptosis in this cell line. These results indicate features in addition to DNA adduction are responsible for the cytotoxicity of 11β. Therefore, a molecule such as 11β, that combines several different mechanisms into a single agent, may have a unique place in the pharmacopoeia of anticancer agents.

The results here illustrate a unique response of LNCaP cells exposed to 11β. These promising results have given us confidence in further exploring the properties of 11β to address its usefulness as a drug. In the subsequent chapters, I shall discuss experiments designed to evaluate the pharmacokinetics, acute and chronic toxicity, and (antitumor) therapeutic potential.

Future Directions

The results from this chapter illustrate several key features of 11β: a log D indicative of good permeability and absorption, the formation of DNA adducts with guanine *in vitro* and in LNCaP cells in culture, a good affinity for the AR, the induction of apoptosis in LNCaP cells, and altered expression levels of cell cycle checkpoint proteins. These experiments indicate that 11β is unique from other alkylating agents that do not induce apoptosis in a prostate cancer cell line. Furthermore, the ability of 11β, but not 11β-dimethoxy, to induce apoptosis indicates that the role of DNA damage is

essential. It is the combination of DNA damage and the disruption of cellular pathways that enable 11β to achieve its cytotoxic effects.

The work described here illustrates some differences between chlorambucil, 11β, and 11β-dimethoxy. However, these experiments are not conclusive in proving the repair shielding, transcription factor hijacking, or other unknown mechanism(s) of action by which 11β acts. Therefore, considerable efforts must be made in identifying the molecular mechanisms involved. For example, LNCaP cells treated with chlorambucil arrest in S phase. This arrest is likely elicited through the capacity of p21 to halt cell cycle progression by inhibiting CDKs and interacting with the proliferating cell nuclear antigen (PCNA), thereby stopping DNA synthesis (Waga and Stillman 1998). In contrast, LNCaP cells treated with 11β result in a decrease in the number of cells in S phase. The early elimination and delayed increase in the expression of p21 in cells treated with 11β, as described above, may disable a key checkpoint that arrests cell growth in S phase allowing for the repair of damage and sensitizing cells to apoptosis. However, it will require further investigation to identify the mechanism(s) underlying the reduction of p21 and the role it plays in the cytotoxic effects of our compounds.

The results here were accomplished using the AR(+) LNCaP cell line. The AR(-) PC-3 and DU-145 cell line displayed lower toxicity when treated with our compound. The differential toxicity between the lines also needs to be addressed. As initial experiments, it would be of interest to monitor the response of the cell cycle checkpoint proteins of these cells to treatments with chlorambucil, 11β, and 11β-dimethoxy. Since they lack the AR, differences in p27 expression level from what was observed with the LNCaP cells may indicate that the increased levels after treatment with either 11β compound was indeed a result of a direct interaction with the AR.

Finally, the work with the AMS technology described in Chapter 5 can be translated to the 11β compound. A comparison in the rates of DNA adduct formation and repair in the AR(+) LNCaP to that in either the AR(-) PC-3 or DU-145 cell line could provide important evidence in favor of the repair shielding hypothesis. If the rate of repair in the LNCaP cell line is significantly slower than what is observed in one of the AR(-) cell lines, it would imply DNA adducts formed by 11β are indeed attracting the AR to the site of the lesion and inhibiting repair. Further support of this hypothesis would be

provided if the rates of repair were identical for a traditional alkylating agent such as chlorambucil or melphalan.

Reference List

Berrevoets, C.A., Umar, A., and Brinkmann, A.O. Antiandrogens: selective androgen receptor modulators. *Mol. Cell Endocrinol.* **198**, 97-103 (2002)

Brix, H.P., Berger, M.R., Schneider, M.R. et al. Androgen-linked alkylating agents: biological activity in methylnitrosourea-induced rat mammary carcinoma. *J. Cancer Res. Clin. Oncol.* **116**, 538-549 (1990)

Carrano, A.C., Eytan, E., Hershko, A., and Pagano, M. SKP2 is required for ubiquitin-mediated degradation of the CDK inhibitor p27. *Nat. Cell Biol.* **1**, 193-199 (1999)

Denmeade, S.R., Lin, X.S., Tombal, B., and Isaacs, J.T. Inhibition of caspase activity does not prevent the signaling phase of apoptosis in prostate cancer cells. *Prostate* **39**, 269-279 (1999)

Donovan, S.F. and Pescatore, M.C. Method for measuring the logarithm of the octanol-water partition coefficient by using short octadecyl-poly(vinyl alcohol) high-performance liquid chromatography columns. *J. Chromatogr. A* **952**, 47-61 (2002)

Eisenbrand, G., Berger, M.R., Brix, H.P. et al. Nitrosoureas. Modes of action and perspectives in the use of hormone receptor affinity carrier molecules. *Acta Oncol.* **28**, 203-211 (1989)

el-Deiry, W.S., Tokino, T., Velculescu, V.E. et al. WAF1, a potential mediator of p53 tumor suppression. *Cell* **75**, 817-825 (1993)

Ganoth, D., Bornstein, G., Ko, T.K. et al. The cell-cycle regulatory protein Cks1 is required for SCF(Skp2)-mediated ubiquitinylation of p27. *Nat. Cell Biol.* **3**, 321-324 (2001)

Gartel, A.L. and Tyner, A.L. The role of the cyclin-dependent kinase inhibitor p21 in apoptosis. *Mol. Cancer Ther.* **1**, 639-649 (2002b)

Gartel, A.L. and Tyner, A.L. The role of the cyclin-dependent kinase inhibitor p21 in apoptosis. *Mol. Cancer Ther.* **1**, 639-649 (2002a)

Gioeli, D. Signal transduction in prostate cancer progression. *Clin. Sci. (Lond)* ., 2004)

Haapala, E., Hakala, K., Jokipelto, E. et al. Reactions of N,N-bis(2-chloroethyl)-p-aminophenylbutyric acid (chlorambucil) with 2'-deoxyguanosine. *Chem. Res. Toxicol.* **14**, 988-995 (2001)

Horváth, Cs., Melánder, W., and Molnár, I. Liquid chromatography of ionogenic substances with nonpolar stationary phases. *Anal. Chem.* **49**, 142-154 (1977)

Hurley, L.H. DNA and its associated processes as targets for cancer therapy. *Nature Rev. Cancer* **2**, 188-200 (2002)

Isaacs, J.T. Apoptosis: translating theory to therapy for prostate cancer. *J. Natl. Cancer Inst.* **92**, 1367-1369 (2000)

Kim, I.Y., Kim, J.H., Zelner, D.J. et al. Transforming growth factor-beta1 is a mediator of androgen-regulated growth arrest in an androgen-responsive prostatic cancer cell line, LNCaP. *Endocrinology* **137**, 991-999 (1996)

Kish, J.A., Bukkapatnam, R., and Palazzo, F. The treatment challenge of hormone-refractory prostate cancer. *Cancer Control* **8**, 487-495 (2001)

Knebel, N. and von, A.E. Platinum complexes with binding affinity for the estrogen receptor. *J. Med. Chem.* **31**, 1675-1679 (1988)

Lebedeva, I., Rando, R., Ojwang, J. et al. Bcl-xL in prostate cancer cells: effects of overexpression and down- regulation on chemosensitivity. *Cancer Res.* **60**, 6052-6060 (2000)

Lee, C., Sutkowski, D.M., Sensibar, J.A. et al. Regulation of proliferation and production of prostate-specific antigen in androgen-sensitive prostatic cancer cells, LNCaP, by dihydrotestosterone. *Endocrinology* **136**, 796-803 (1995)

Lipinski, C.A., Lombardo, F., Dominy, B.W., and Feeney, P.J. Experimental and computational approaches to estimate solubility and permeability in drug discovery and developmental settings. *Adv. Drug Del. Rev.* **23**, 3-25 (1997)

Lu, L., Schulz, H., and Wolf, D.A. The F-box protein SKP2 mediates androgen control of p27 stability in LNCaP human prostate cancer cells. *BMC. Cell Biol.* **3**, 22-2002a)

Lu, L., Schulz, H., and Wolf, D.A. The F-box protein SKP2 mediates androgen control of p27 stability in LNCaP human prostate cancer cells. *BMC. Cell Biol.* **3**, 22-2002b)

Marcelli, M., Marani, M., Li, X. et al. Heterogeneous apoptotic responses of prostate cancer cell lines identify an association between sensitivity to staurosporine-

induced apoptosis, expression of Bcl-2 family members, and caspase activation. *Prostate* **42**, 260-273 (2000)

Marquis, J.C., Hillier, S.M., Dinaut, A.N. et al. A bisalkylating DNA damaging agent tethered to a ligand for the androgen receptor reduces SKP2 activity and induces apoptosis in prostate cancer cells. (*Submitted to Chemistry and Biology* 2005)

Martel, C.L., Gumerlock, P.H., Meyers, F.J., and Lara, P.N. Current strategies in the management of hormone refractory prostate cancer. *Cancer Treat. Rev.* **29**, 171-187 (2003)

Martinez, L.A., Yang, J., Vazquez, E.S. et al. p21 modulates threshold of apoptosis induced by DNA-damage and growth factor withdrawal in prostate cancer cells. *Carcinogenesis* **23**, 1289-1296 (2002)

Masters, J.R. and Koberle, B. Curing metastatic cancer: lessons from testicular germ-cell tumours. *Nat. Rev. Cancer* **3**, 517-525 (2003)

Mitra, K., Marquis, J.C., Hillier, S.M. et al. A rationally designed genotoxin that selectively destroys estrogen receptor-positive breast cancer cells. *J. Amer. Chem. Soc.* **124**, 1862-1863 (2002)

Morris, M.J. and Scher, H.I. Clinical approaches to osseous metastases in prostate cancer. *Oncologist.* **8**, 161-173 (2003)

Morris, M.J. and Scher, H.I. Novel strategies and therapeutics for the treatment of prostate carcinoma. *Cancer* **89**, 1329-1348 (2000)

Muddana, S.S., Price, A.M., MacBride, M.M., and Peterson, B.R. 11beta-alkyl-Delta9-19-nortestosterone derivatives: high-affinity ligands and potent partial agonists of the androgen receptor. *J. Med. Chem.* **47**, 4985-4988 (2004)

Povirk, L.F. and Shuker, D.E. DNA damage and mutagenesis induced by nitrogen mustards. *Mutat. Res.* **318**, 205-226 (1994)

Raffo, A.J., Perlman, H., Chen, M.W. et al. Overexpression of bcl-2 protects prostate cancer cells from apoptosis in vitro and confers resistance to androgen depletion in vivo. *Cancer Res.* **55**, 4438-4445 (1995)

Rink, S.M., Yarema, K.J., Solomon, M.S. et al. Synthesis and biological activity of DNA damaging agents that form decoy binding sites for the estrogen receptor. *Proc. Natl. Acad. Sci. U. S. A* **93**, 15063-15068 (1996)

Sack, J.S., Kish, K.F., Wang, C. et al. Crystallographic structures of the ligand-binding
domains of the androgen receptor and its T877A mutant complexed with the
natural agonist dihydrotestosterone. *Proc. Natl. Acad. Sci. U. S. A* **98**, 4904-4909
(2001)

Sharma, U., Marquis, J.C., Nicole, D.A. et al. Design, synthesis, and evaluation of
estradiol-linked genotoxicants as anti-cancer agents. *Bioorg. Med. Chem. Lett.* **14**,
3829-3833 (2004)

Singer, B. and Grunberger, D. Molecular Biology of Mutagens and Carcinogens. Plenum
Publishing Corp. New York (1983)

Spruck, C., Strohmaier, H., Watson, M. et al. A CDK-independent function of
mammalian Cks1: targeting of SCF(Skp2) to the CDK inhibitor p27Kip1. *Mol.
Cell* **7**, 639-650 (2001)

Sunters, A., Springer, C.J., Bagshawe, K.D. et al. The cytotoxicity, DNA crosslinking
ability and DNA sequence selectivity of the aniline mustards melphalan,
chlorambucil and 4-[bis(2-chloroethyl)amino] benzoic acid. *Biochem. Pharmacol.*
44, 59-64 (1992)

Teicher, B.A. Cancer Principles and Practice. Antitumor alkylating agents 5, 405-417
(1997)

Tsihlias, J., Zhang, W., Bhattacharya, N. et al. Involvement of p27Kip1 in G1 arrest by
high dose 5 alpha-dihydrotestosterone in LNCaP human prostate cancer cells.
Oncogene **19**, 670-679 (2000)

van Zeeland, A.A. Molecular dosimetry of chemical mutagens. Relationship between
DNA adduct formation and genetic changes analyzed at the molecular level.
Mutat. Res. **353**, 123-150 (1996)

Vlietstra, R.J., van Alewijk, D.C., Hermans, K.G. et al. Frequent inactivation of PTEN in
prostate cancer cell lines and xenografts. *Cancer Res.* **58**, 2720-2723 (1998)

Waga, S. and Stillman, B. Cyclin-dependent kinase inhibitor p21 modulates the DNA
primer-template recognition complex. *Mol. Cell Biol.* **18**, 4177-4187 (1998)

Walsh, P.C. Docetaxel plus prednisone or mitoxantrone plus prednisone for advanced
prostate cancer. *J. Urol.* **173**, 456-2005)

Wang, J.D., Takahara, S., Nonomura, N. et al. Early induction of apoptosis in androgen-independent prostate cancer cell line by FTY720 requires caspase-3 activation. *Prostate* **40**, 50-55 (1999)

Wang, L.G., Ossowski, L., and Ferrari, A.C. Androgen receptor level controlled by a suppressor complex lost in an androgen-independent prostate cancer cell line. *Oncogene* **23**, 5175-5184 (2004)

Zhao, X.Y., Boyle, B., Krishnan, A.V. et al. Two mutations identified in the androgen receptor of the new human prostate cancer cell line MDA PCa 2a. *J. Urol.* **162**, 2192-2199 (1999)

Equations Used to Calculate the Log P and Log D

$$\log P_{unk} = \frac{(\log P_{tol} - \log P_{triph}) * t_{unk} + t_{tol} * \log P_{triph} - t_{triph} * \log P_{tol}}{t_{tol} - t_{triph}}$$

Equation 6.1 t is the retention time as determined by HPLC (tol = toluene, triph = triphenylene, unk = unknown). The log P of toluene and triphenylene were 2.61 and 6.27 respectively as previously reported.

$$\log D = \log (P * 10^{pKa} + P_i * 10^{pH}) - \log(10^{pKa} + 10^{pH})$$

Equation 6.2 P is the partition coefficient for the neutral molecule (as determined by HPLC), P_i is the partition coefficient for the ion (not measured but assumed the log P_i was 3.15 less than the log P of the neutral molecule), K_a is the equilibrium constant for acids.

Structures of 11β Compounds
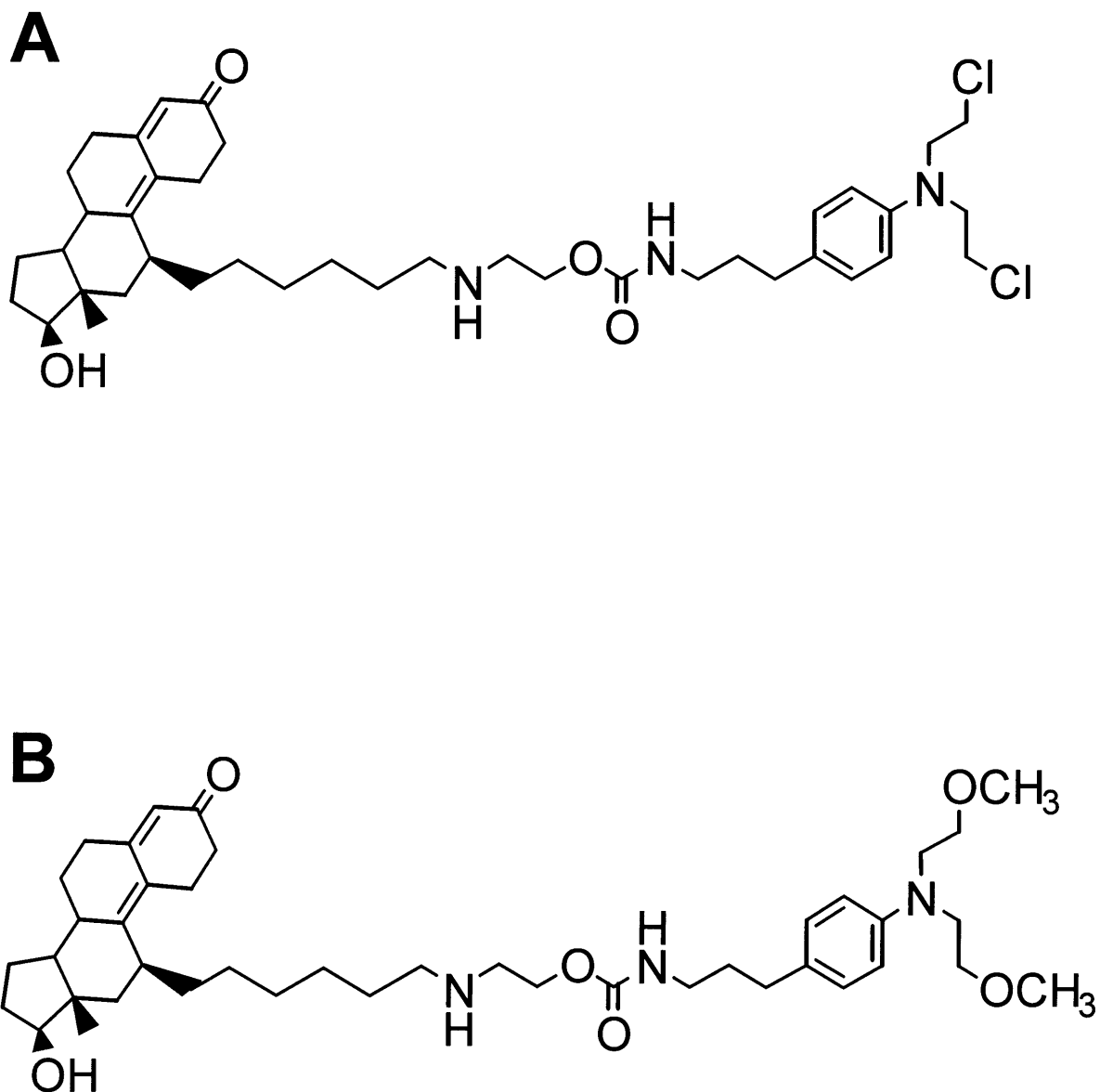
Fig 6.1 Chemical structures of **A.** 11β and **B.** 11β-dimethoxy.

Isolation of 11β DNA Adducts by HPLC
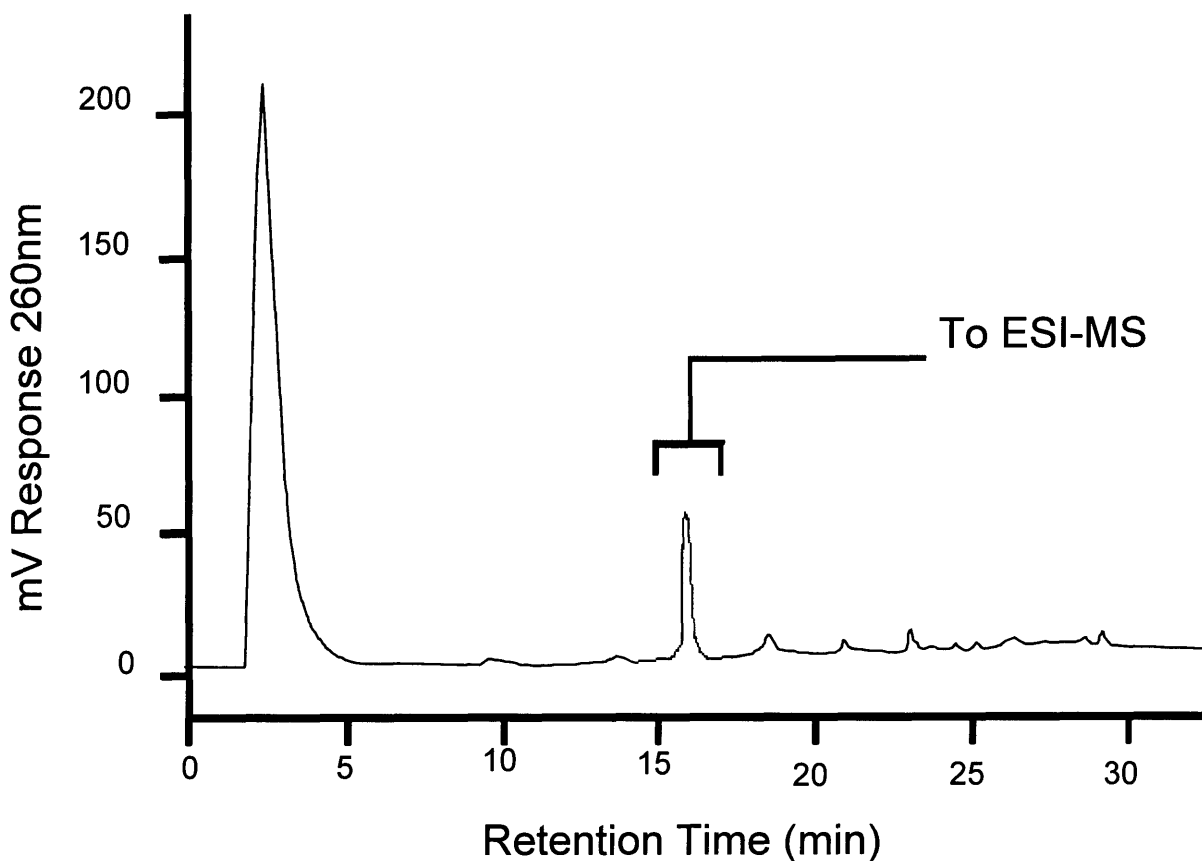
Fig 6.2 HPLC chromatogram of the hydrolysis products from 11β treated DNA. The peak at 16 min was collected and analyzed by ESI-MS for adduct identification.

Characterization and Analysis of 11β DNA Adducts by ESI-MS

A
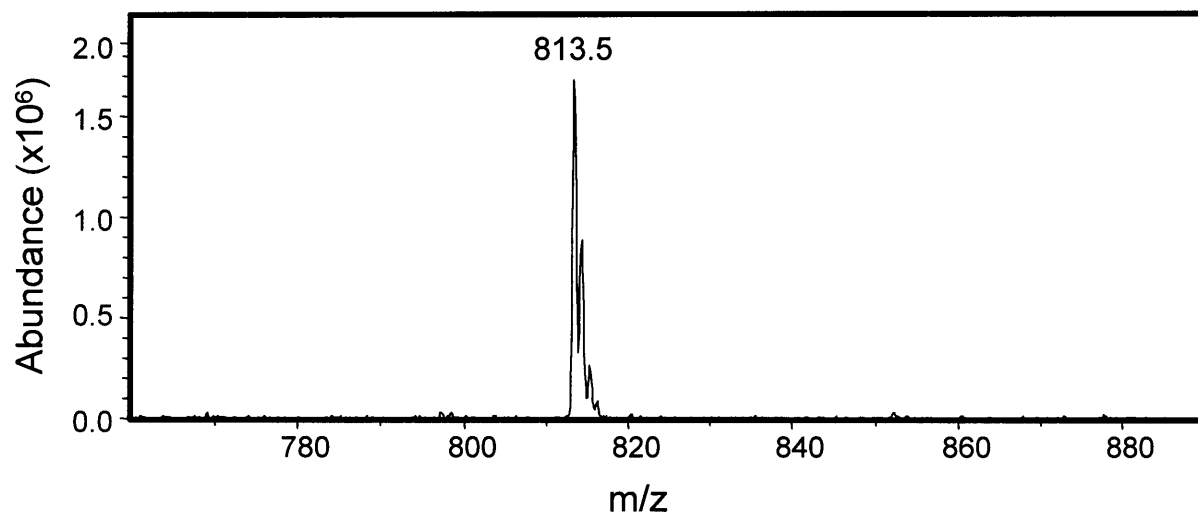
B
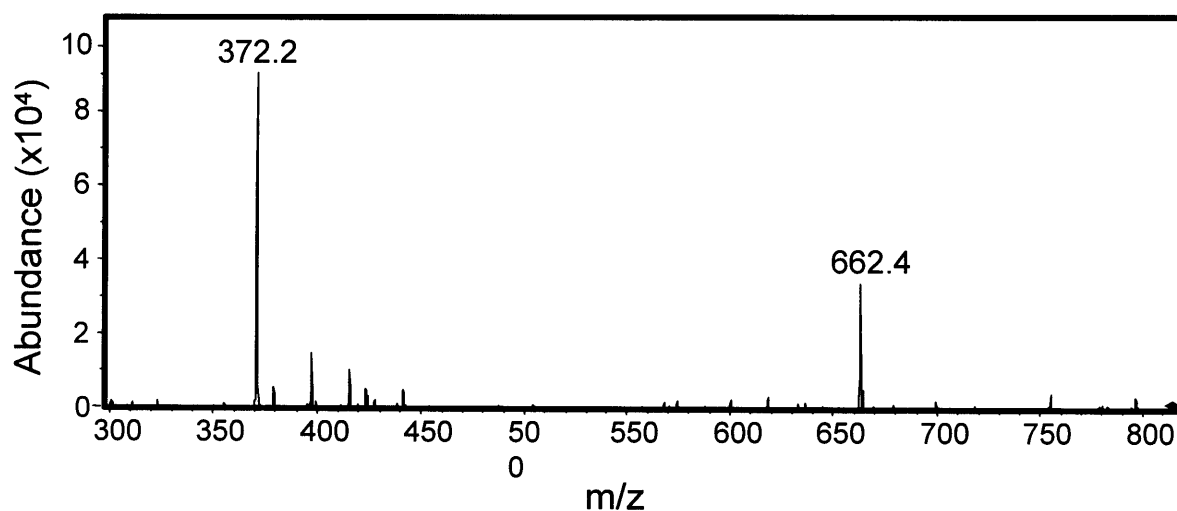
Fig 6.3 A. ESI-MS analysis of the 16 min peak collected on HPLC produces a molecular ion of 813.5 m/z. **B.** CID of the 813.5 m/z ion produces two daughter ions of 372.2 m/z and 662.4 m/z.

Probable Structures of 11β Fragmentation Pattern after Collision Induced Decay Mass Spectrometry

$C_{40}H_{60}N_3O_5$
m/z 662.4

$C_{24}H_{36}NO_2$
m/z 372.2

$C_{40}H_{56}D_4N_3O_5$
m/z 666.5

$C_{24}H_{36}NO_2$
m/z 372.1

$C_{45}H_{64}N_8O_6$
m/z 813.5

$C_{45}H_{60}D_4N_8O_6$
m/z 817.5
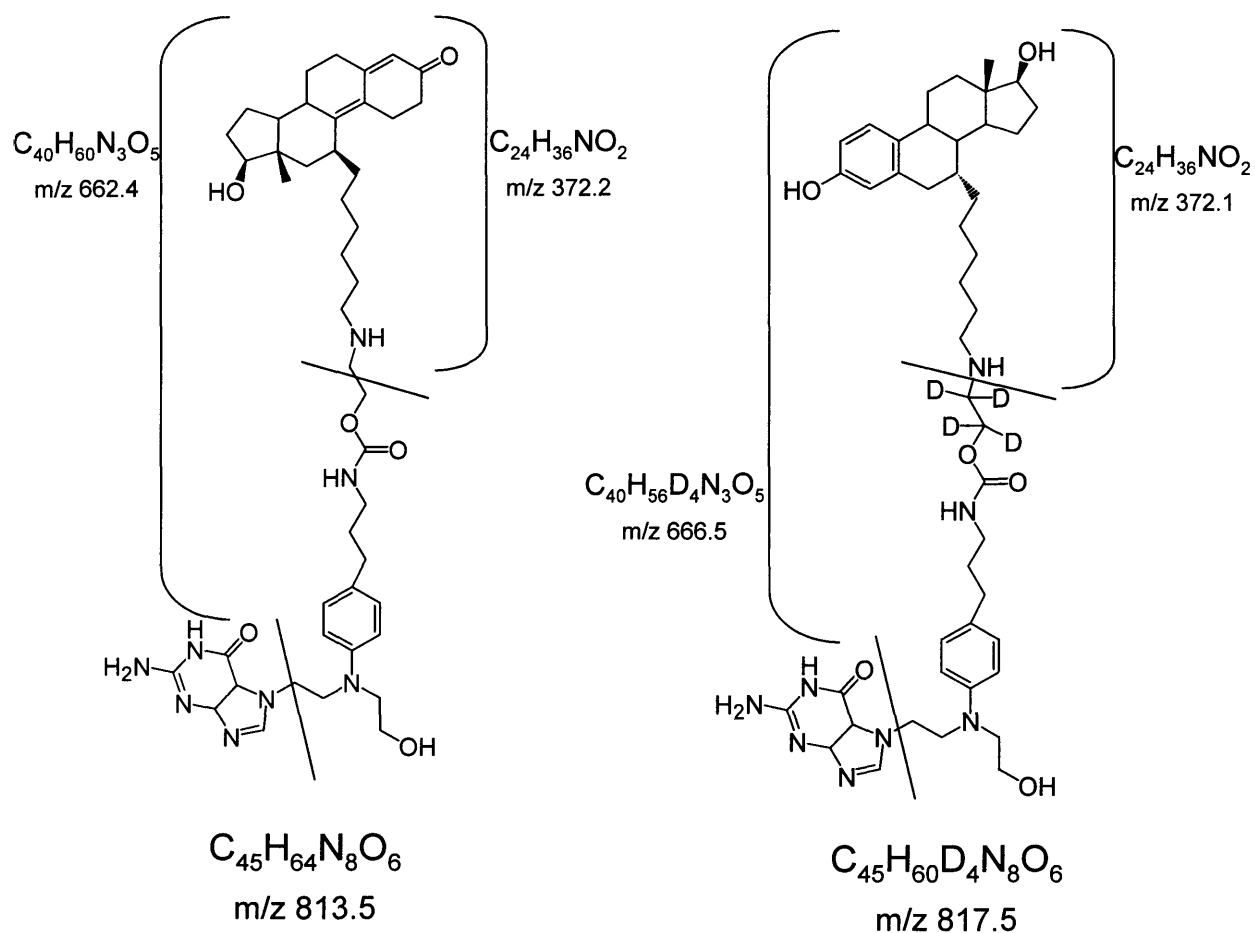
Fig 6.4 CID of the 813.5 m/z ion produced by the reaction of 11β with DNA **(left)**. This fragmentation is the same as what was described in Chapter 2 with E2-7α and as a comparison the fragmentation pattern after the reaction of d4-E2-7α with DNA is also shown **(right)**. The notable difference is in the 662.4 / 666.4 m/z molecular ion in which the latter contains the tetradeuterated linker. This result supports the structure and fragmentation pattern proposed for the non-deuterated 11β compound.

Identification of 11β DNA Adducts from LNCaP Cells
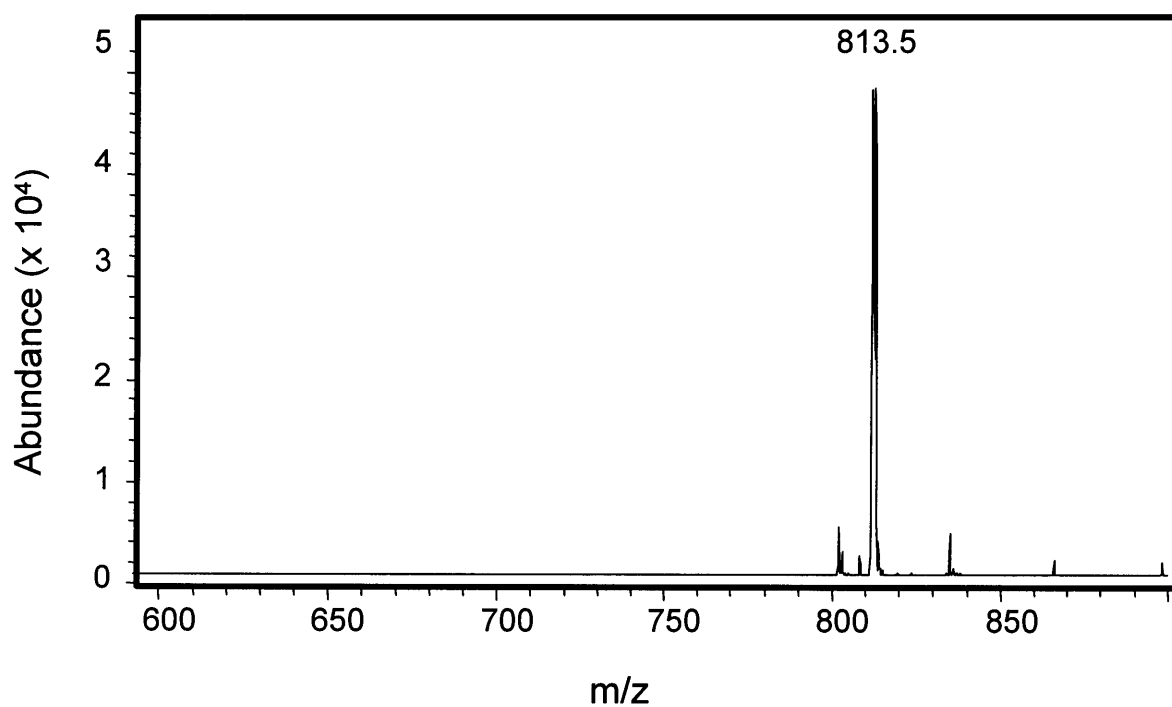
Fig 6.5 ESI-MS analysis of DNA isolated from LNCaP cells following treatment with 11β. A molecular ion with an m/z of 813.5 was identified corresponding to an 11β-guanine adduct.

HPLC Chromatogram used to Determine the Log P of 11β
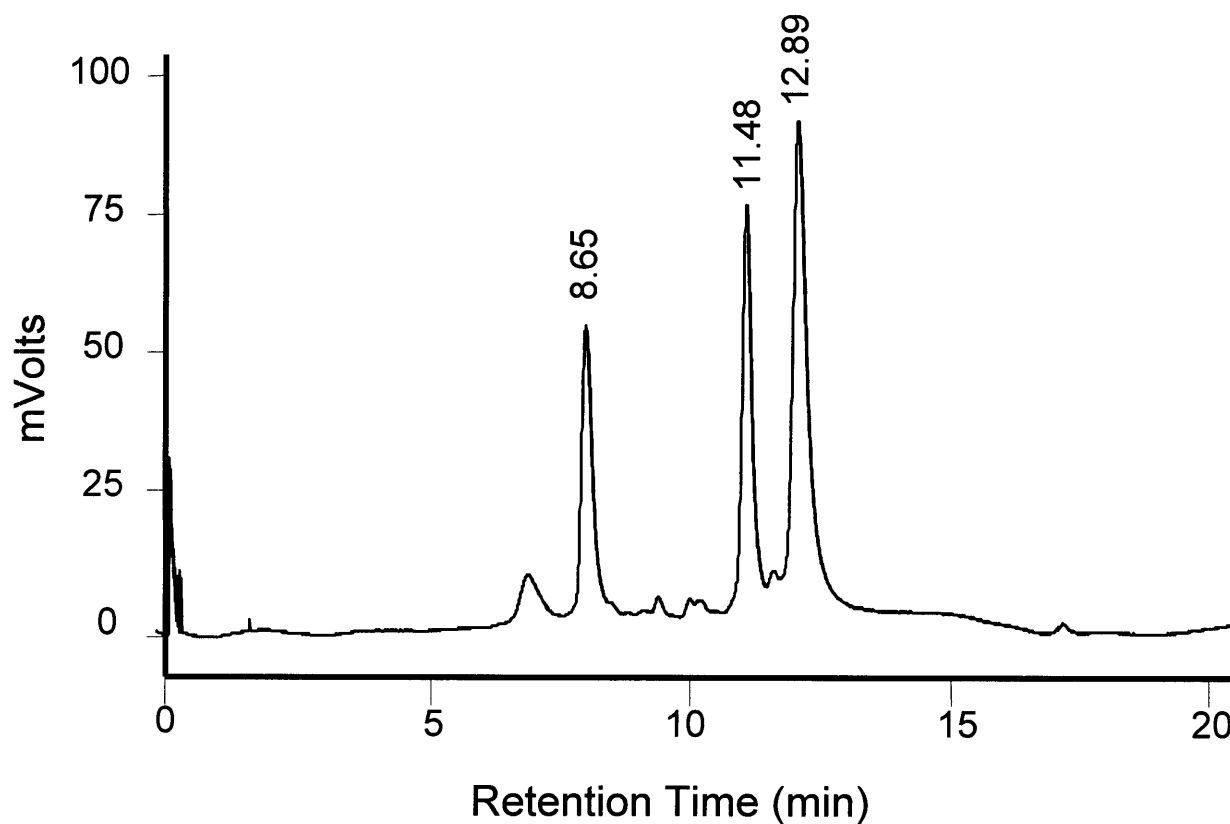
Fig 6.6 HPLC chromatogram of 11β co-injected with the log P standard. The peak at 8.65 min is toluene, 11.48 min is E2-7α, and at 12.89 min is triphenylene. The log P of 11β in this run was determined to be 5.05.

11β and 11β-dimethoxy have Good Affinity for the Androgen Receptor
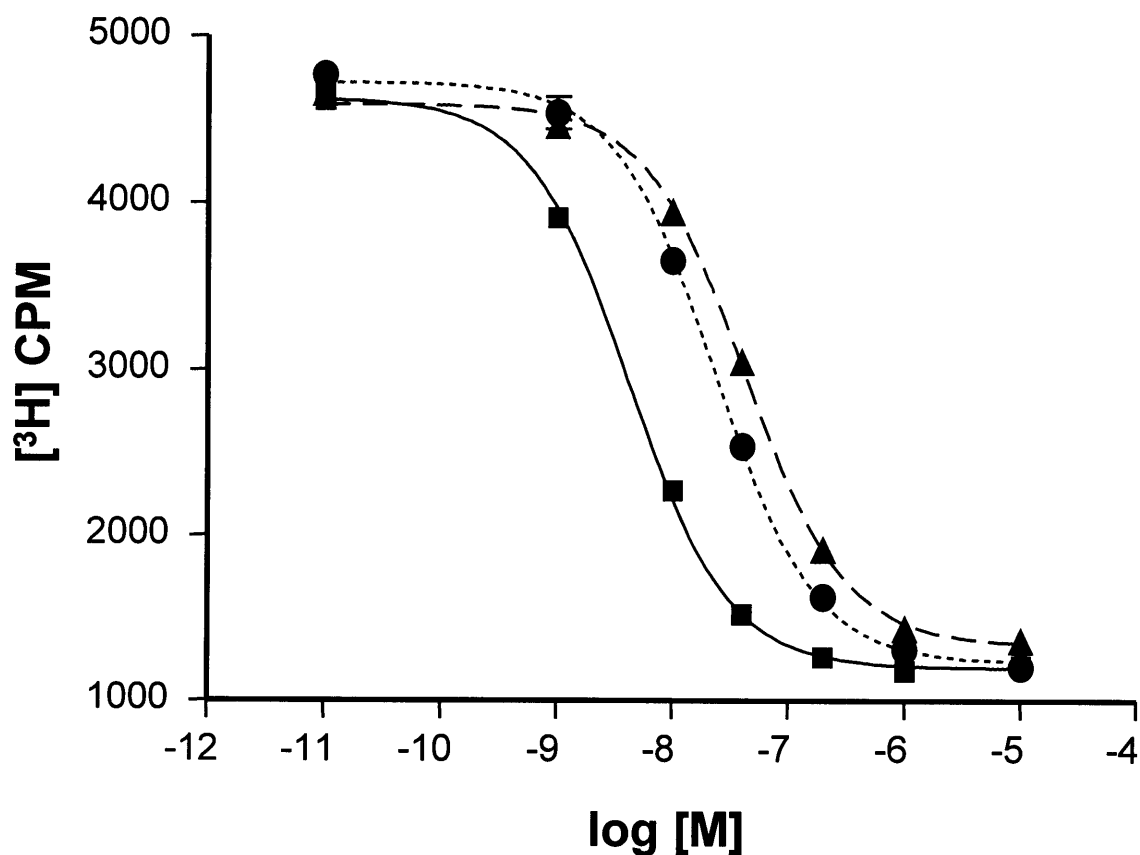
Fig 6.7 Relative binding affinity for the AR. The affinity of 11β
(−▲−) and 11β-dimethoxy (··●··) is compared to the synthetic
androgen R1881 (−■−). Both 11β compounds have roughly
the same affinity for the receptor.

AR (+) LNCaP Cells are More Toxic to 11β than AR (-) Prostate Cancer Cell Lines

A

B
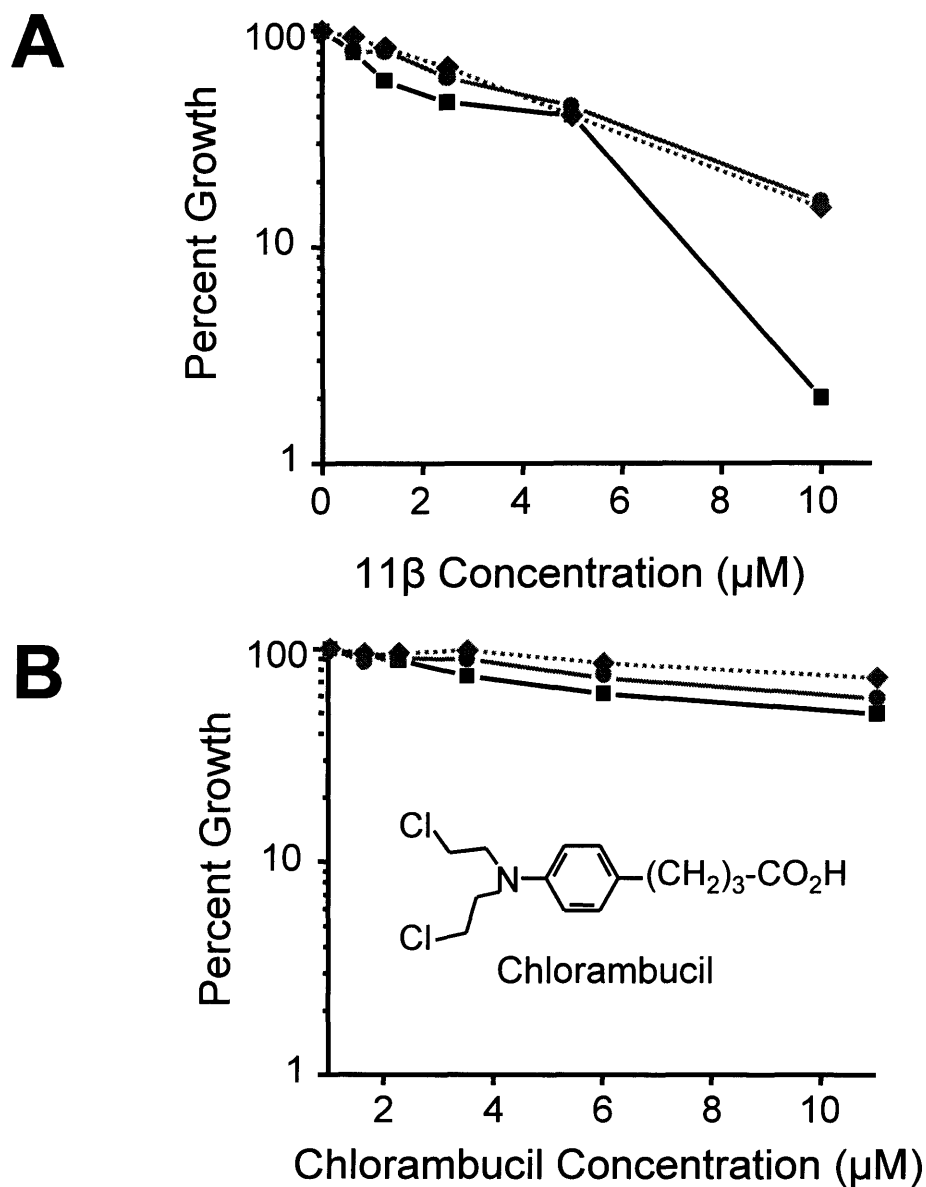
Chlorambucil

Fig 6.8 Prostate cancer cells exposed to increasing doses of 11β **(A)** or chlorambucil **(B)**. The AR (+) LNCaP cell line (—■—) is the most sensitive to a 10 μM dose of 11β. The PC-3 (—●—) and the DU-145 (··◆··) AR (-) cell lines are much less toxic to a 10 μM dose of 11β. Furthermore, all cell lines are equally resistant to doses as high as 10 μM of chlorambucil.

11β Rapidly Induces Apoptosis in LNCaP Cells

A

B

C
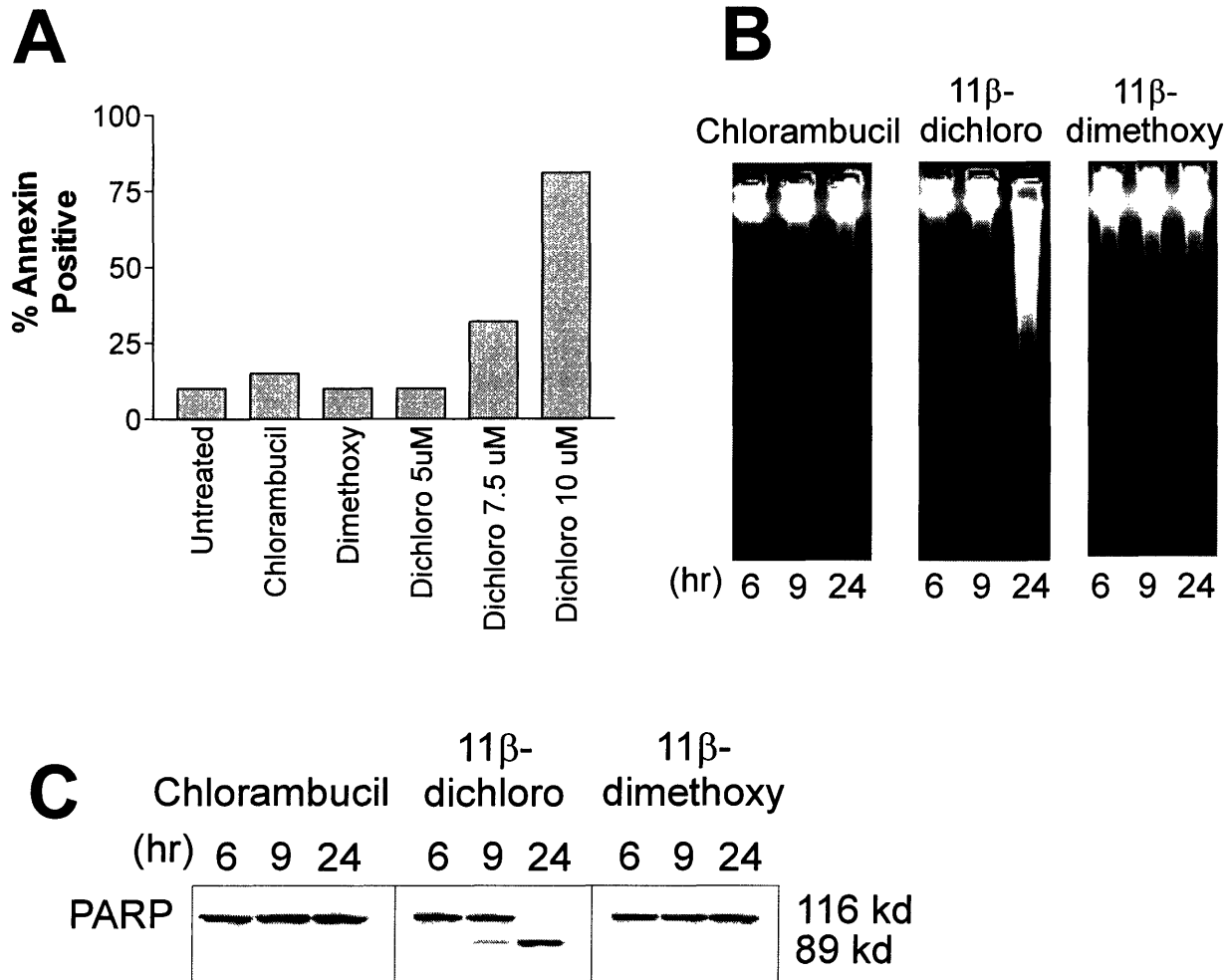
Fig 6.9 Markers of apoptosis. 11β treated LNCaP cells show several characteristic markers indicative of programmed cell death: **A.** Positive staining for Annexin V after 15 hours of treatment, **B.** DNA laddering, and **C.** PARP cleavage. LNCaP cells were exposed to chlorambucil (20 µM), 11β (10 µM), or 11β-dimethoxy (10 µM).

11β Disrupts Cell Signaling Proteins in LNCaP Cells

A

B
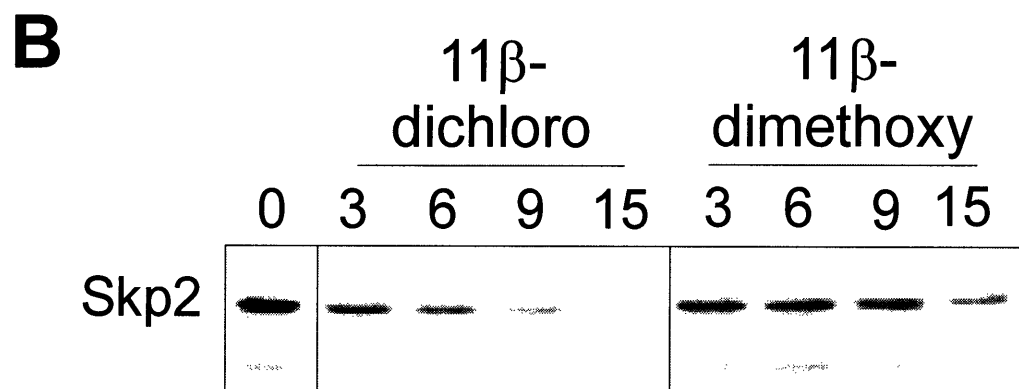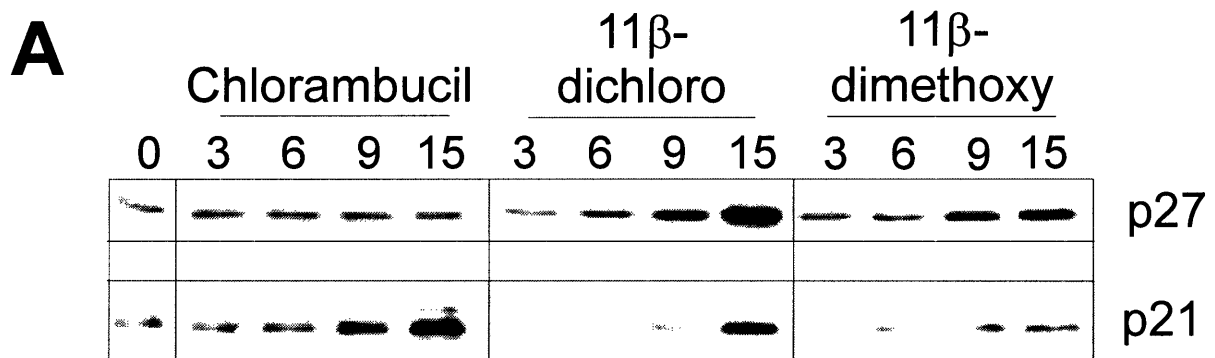
Fig 6.10 Expression levels of cell cycle regulatory proteins in LNCaP cells. Levels of p21 and p27 **(A)** and Skp2 **(B)** in extracts from cells that were treated with chlorambucil (20 μM), 11β (10 μM), or 11β-dimethoxy (10 μM).

Chapter 7

Probing the Biochemical Mechanism of
11β *In Vivo:*

Pharmacokinetics, Toxicity, and Adduct Identification

Introduction

Prostate cancer is the second most commonly diagnosed cancer and the fourth leading cause of cancer death among men in developed countries (Weir et al. 2003). Most prostate cancers are dependent on the presence of androgens for their growth, and therefore chemical or surgical castration is often an adjuvant therapy (following the surgical removal of the tumor) resulting in the apoptotic death of androgen-sensitive cells (Bruckheimer, Gjertsen, and McDonnell 1999; Kozlowski, Ellis, and Grayhack 1991; Kreis 1995; Santen 1992). Unfortunately for the patient, these treatments often result in the transition to aggressive and metastatic androgen-independent prostate cancer or hormone-resistant prostate cancer (HRPC). This transition to androgen-independence occurs likely through selection for growth of androgen-independent cells that may have coexisted with an androgen-dependent population prior to the androgen deprivation therapy (Gingrich et al. 1997; Isaacs and Coffey 1981; Kyprianou 1994). Several reports have illustrated that the androgen-refractory prostate cancer cells, although impervious to androgen receptor (AR) antagonism, retain the capacity to undergo apoptosis (Denmeade et al. 1999; Marcelli et al. 2000; Wang et al. 1999). Novel approaches toward HRPC treatment, including anti-angiogenesis agents, cancer vaccines, antisense oligonucleotides, and novel chemotherapeutics, have been proposed, but these therapies are years away from having a clinical impact and may be of limited efficacy (Gulley and Dahut 2003). Furthermore, current therapies have very limited efficacy in HRPC. Therefore, the need exists for new therapies that can attack both androgen-dependent and androgen-independent prostate cancer cells.

In androgen –dependent and –independent prostate cancer, the AR is frequently over-expressed at both the mRNA and the protein level (Gioeli 2005; Gioeli 2004; Wang, Ossowski, and Ferrari 2004). We have taken advantage of this biological effect by designing compounds that have the ability to adduct DNA and attract the AR to the site of the modified DNA. A protein-drug-DNA complex formed in a prostate cancer cell would shield the DNA adduct from repair enzymes, and the persistence of the DNA adduct would be lethal to the cell. Furthermore, an interaction with DNA adducts would likely titrate away the normal transcriptional activities of the AR and result in the disruption of pro-survival cellular signaling events. The combined repair shielding and

transcription factor hijacking effects would likely be very toxic for an AR expressing prostate cancer cell. The dependency on androgen for growth would be irrelevant and therefore our compound could be effective in treating both androgen –dependent and – independent cancers.

In Chapter 6, I reported the results of several experiments describing the *in vitro* activity of our current lead compound, 11β, against prostate cancer. 11β interacts well with the AR (RBA ~36 as compared to testosterone), has a log D indicative of oral administration (2.00), covalently modifies guanine in DNA, is cytotoxic to AR(+) LNCaP cells, and induces apoptosis in these cells. Despite these promising results there are other factors that impact the ability of a molecule to become a potential drug candidate, such as the bio-distribution, pharmacokinetics, toxicity, ability to remain intact, and ability to form DNA adducts *in vivo*. These features of 11β will be discussed in this chapter.

Based on the results seen in Chapter 3 with E2-7α, 11β was formulated in Cremophor-EL (CR-EL) and injected intraperitoneally (IP). (Note: CR-EL is currently part of the formulation for the clinically used Taxol (paclitaxel) in the therapy of ovarian cancer, breast cancer, Kaposi's Sarcoma, and non-small cell lung cancer.) The distribution in mice injected with 11β will be discussed as will the pharmacokinetic parameters derived from these studies.

Additionally, a dose range finding study was performed to address the acute toxicity of 11β. Blood chemistry and hematology reports provided a means of addressing organ specific toxicity. This information is critical in deciding upon a therapeutic dose when initiating a tumor ablation study and in more focused monitoring of the side-effect profile of the treated mice (to be discussed in Chapter 8). I will also discuss the identification of E2-7α DNA adducts isolated from tissue *in vivo*. These results parallel the *in vitro* work discussed in Chapter 6.

Materials and Methods

Animals. Four to six week old NIH Swiss Webster mice were purchased from Charles River Laboratories, Wilmington, MA. NIH Swiss *nu/nu* athymic mice (25g) were purchased from the National Cancer Institute-Frederick Cancer Center (NCI) (Frederick,

MD). The mice were housed under standard conditions in MIT approved facilities with 12 hour light/dark cycles and food and water *ad libitum*. All protocols were performed in compliance with the regulations of the Animal Care Committee at MIT.

Bio-Distribution. 11β (45 mg/kg) spiked with 5 μCi of ^{14}C-11β was dissolved in 50 μL of a CR-EL based solution (43% CR-EL, 30% saline, 27% ethanol) and injected IP. Mice were sacrificed by carbon dioxide asphyxiation at 0.25, 1, 2, 4, 6, and 24 hours post injection. Blood was obtained by cardiac puncture. The following tissues were removed surgically: lung, liver, spleen, kidney, GI, feces, and in some instances adipose, heart, and skeletal muscle. Approximately 100 mg of each tissue (10 μL of whole blood) were isolated for liquid scintillation counting. To each tissue sample was added 1 mL of Solvable (Packard Biosciences, Meriden, CT) and heated to 65°C for 3 hours or until the tissue was completely dissolved. Two 100 μL aliquots of 30% hydrogen peroxide were added to the cooled off solution to decolorize. Approximately 15 mL of Hionic Flour scintillation fluid (Packard Biosciences, Meriden, CT), which is compatible with Solvable, was added and counted in a Beckman LS1801 Liquid Scintillation Counter. The data are calculated as % injected dose per gram of tissue (% ID/g).

Pharmacokinetic Analysis. Pharmacokinetic parameters after administration of 11β were calculated by standard noncompartmental methods with GraphPad Prism version 3.00 for Windows (GraphPad Software, San Diego California USA). The area under the blood concentration vs. time curve (AUC) was calculated by the linear trapezoidal rule. The systemic clearance (CL) was calculated by dividing the dose by the AUC. The volume of distribution (V_d) was calculated by dividing the dose by the extrapolated concentration of drug in the blood at time equals zero hour. Since the drug concentration (post-peak) declined nearly exponentially, the half-life ($t_{1/2}$) was determined by nonlinear regression analysis using a single phase exponential decay model. C_{max} and t_{max} were read directly from the data.

Plasma Analysis. Whole blood was collected by cardiac puncture from the mice after ^{14}C-11β injection. The plasma was isolated by adding two volumes of acetonitrile to one

volume of whole blood to precipitate the red blood cells and plasma proteins. The colloidal suspension was centrifuged for 5 min at 13,000 × G, and the supernatant was collected and separated into two aliquots. One aliquot was used to determine the amount of protein binding, and the other aliquot was used to determine the concentration of 11β in the plasma.

The aliquot used to determine the amount of protein binding was isolated, combined with scintillation fluid, and counted on a Beckman LS1801 Liquid Scintillation Counter. Additionally, the pellet obtained from the acetonitrile precipitation was collected, combined with 1 mL of Solvable (Packard Biosciences), and heated overnight at 70°C. Subsequently, two 100 μL aliquots of hydrogen peroxide were added to decolorize the solution, and finally scintillation fluid was added to quantify the radioactivity in the pellet. The percentage of 11β in the plasma was calculated by dividing the amount of radioactivity in the plasma by the sum of the amount in the plasma and the amount in the pellet.

In order to determine the concentration of 11β in the plasma the second aliquot was dried in a speed-vac. The dried residue was reconstituted with 100 μL of acetonitrile and injected onto a Rainin HPLC (Rainin HPXL) with a Rainin UV-1 UV Detector monitored at 260 nm and an in-line Packard Flow Scintillation Analyzer Model 150TR. The analyses were performed using a Beckman ODS 4.6 x 250 mm Ultrasphere column eluted at 1 mL/min using 0.1 M ammonium acetate/10% acetonitrile in water and methanol as solvents. A 20 min linear gradient of 50% methanol to 100% methanol was used. Only the radioactive ^{14}C-11β parent peak was used to determine the concentration of the compound in plasma. A ^{14}C-11β standard was counted on a Beckman LS1801 Liquid Scintillation Counter prior to injection onto the HPLC. It was determined that a peak with an area under the curve (AUC) of 432,000 on HPLC corresponded to 13,300 CPM.

Acute Toxicity. Groups of 3-4 NIH Swiss *nu/nu* athymic mice from the NCI were injected IP with 10-150 mg/kg of 11β formulated in a CR-EL solution (43% CR-EL, 30% saline, 27% ethanol). Additionally, 4 mice were injected with vehicle and 4 others were left untreated as controls. The mice were sacrificed by carbon dioxide asphyxiation 24

hours after the injection. Blood was obtained by cardiac puncture and sent to IDEXX (formerly Tufts Veterinary Diagnostic Laboratory, North Grafton, MA) for hematology and blood chemistry analysis.

Identification of 11β DNA Adducts *in Vivo*. 11β (25 mg/kg, not radiolabeled) was injected into NIH Swiss Webster mice by IP injection. The mice were sacrificed after 4 hours by carbon dioxide asphyxiation. The liver was removed surgically, snap frozen on dry ice, and stored at −80°C until it could be worked up. The liver sample was thawed and homogenized in a Dounce homogenizer on wet ice with 15 mL of cold (4°C) 0.01M Tris (pH 6.9), 0.25M sucrose, 2 mM calcium chloride buffer. The homogenate was filtered through a coarse and then a fine nylon mesh to remove all connective tissue. To the filtrate was added 25% Triton X-100 to make a final concentration of 5%. The solution was briefly vortexed and then centrifuged at 1000 × G in a Sorvall RC-2B Centrifuge with a GSA rotor at 4°C for 20 min The supernatant was removed by aspiration, and the nuclear pellet was resuspended in 2.5 mL of buffer. To this solution was added 5 % sodium dodecyl sulfate (SDS) and 5 M sodium chloride (NaCl) to make a solution with a final concentration of 1% SDS and 1 M NaCl. An equal volume of chloroform:isoamyl alcohol (24:1) was then added, and the biphasic mixture was shaken vigorously for 15 min The mixture was then centrifuged at 7000 × G for 15 min at 4°C. The aqueous phase was collected and re-extracted with another volume of chloroform:isoamyl alcohol, shaken, and centrifuged. The aqueous phase was then collected, and the nucleic acids were precipitated with 3 volumes of ice cold ethanol, chilled at -20°C for 20-30 min, and subsequently pelleted by centrifugation at 7000 × G for 15 min at 4°C. The nucleic acids were washed 2 times with cold ethanol and then dried *in vacuo*. The dried pellet was reconstituted with 2 mL of 0.05 M Tris (pH 7.5), 0.1 M NaCl on ice. In order to remove any contaminating RNA, 0.5 mg of RNAse A was added and the solution incubated at 37°C for 10 min. The reaction was stopped by cooling on ice. The NaCl concentration was adjusted to 0.9 M, and the DNA was extracted by subsequent additions of chloroform:isoamyl alcohol as indicated above. The aqueous phase from the second extraction was isolated, and the DNA was precipitated with 3 volumes of ice cold ethanol, centrifuged, and washed 2 times as above. The DNA

was finally hydrolyzed in 0.1 N HCl for 30 min at 70°C. The solution was neutralized with 1N NaOH and adjusted to 20 mM Tris-HCl (pH 7.4), 10% methanol. The hydrolyzed DNA was loaded onto a C18 Sep-Pak ® (Waters Co. Milford, MA) column and eluted sequentially with 10 mL of 10% and 50% aqueous methanol solutions and finally with 100% methanol. The 100% methanol fraction was reduced *in vacuo* and analyzed by HPLC and mass spectrometry. HPLC analyses were performed as described in the Plasma Analysis section. Aliquots of samples obtained from HPLC fractionation were analyzed by electrospray ionization mass spectrometry (ESI-MS) in positive ion mode using flow injection (0.2 mL/min) in methanol:water:acetontrile (50:45:5).

Results

Bio-Distribution and Pharmacokinetics. 11β was injected into mice in order to obtain pharmacologically relevant information about the compound. Based on the results discussed in Chapter 3, 11β was formulated in a CR-EL based vehicle (43% CR-EL, 30% saline, 27% ethanol) and administered IP. The results of this experiment are summarized in Table 1 and expressed in terms of percent injected dose per gram of tissue (% ID/g). 11β is quickly absorbed in the mouse. At the 15 minute time point, the highest concentration of E2-7α could be found in the blood (5% ID/g). The organs with the most accumulation at all time points include the liver, intestines, and kidneys. Surprisingly, very little 11β accumulated in the feces until the 6 hour time point, when it contained approximately 9% ID/g.

The concentration of 11β in whole blood was determined by liquid scintillation counting. However, the concentration of 11β in plasma was determined by precipitating the red blood cells and proteins from the plasma and injecting the serum only onto an HPLC. The concentration of 11β in plasma was derived from the integration of the AUC of the 25 min peak on the HPLC. The 15 min, 1 hour, and 4 hour time points are shown in Figure 7.1 A-C. At the 15 min time point, the only radioactive peak that is present corresponds to intact 11β. However, the 1 and 4 hour time points have smaller peaks eluting at 4 and 13 min which are likely metabolic breakdown products.

The concentration of 11β in whole blood and in plasma is shown in Figure 7.2 A and B, respectively. Only the AUC of the 25 min peak was used to calculate the plasma

curve shown in Figure 7.2B. 11β has a peak concentration in whole blood of 128 μM and 190 μM in plasma. These results indicate that 11β is likely not bound to proteins in blood nor does it accumulate in erythrocytes. This hypothesis was confirmed by the experimental evidence shown in Figure 7.3 in which > 87% of the radioactivity in the blood was in the plasma compartment and not associated with erythrocytes or covalently bound to proteins for the first 6 hours after administration of 11β. At 24 hours nearly 60% of the radioactivity in the blood was still in the plasma compartment.

The pharmacological parameters of 11β after IP administration with the CR-EL based vehicle were also calculated. Table 2 compares the following pharmacological parameters: AUC: area under the plasma concentration-vs.-time curve; $t_{1/2}$: half-life; CL: clearance; V_d: volume of distribution; C_{max}: maximum concentration in blood; t_{max}: time at which C_{max} was achieved. The t_{max} at 15 minutes indicates that 11β is rapidly absorbed by the body even though it was administered IP. The low apparent V_d (0.49 L/kg) indicates that 11β distributes into total body water (Jang, Harris, and Lau 2001).

Acute Toxicity. The acute toxicity of 11β was determined by injecting 3-4 NIH Swiss Nude mice with 0-150 mg/kg of 11β IP. The mice were sacrificed 24 hours post-injection and their blood was obtained for hematology and blood chemistry analysis. The results of these findings are summarized in Table 7.3 and Table 7.4, respectively. Values that are abnormally high or low are shown in bold italics and all values are expressed in terms of measurable units with the exception of neutrophils, lymphocytes, monocytes, and eosinophils, which are expressed in relative terms as % of total white blood cells. Hematological abnormalities included an increase in the total number of white blood cells at the highest doses of 100 and 150 mg/kg and an increase in the ratio of neutrophils to lymphocytes as compared to the control mice. The most notable result, however, is the hepatotoxicity which is first evident at the 50 mg/kg dose with elevated levels of aminotransferase (AST), alanine aminotransferase (ALT), amylase, and lipase. Renal toxicity is apparent at doses of 75 mg/kg and above with increased blood urea nitrogen (BUN) levels as well as increased creatinine and phosphorous and decreased calcium at the 100 and 150 mg/kg doses. Possible cardiac toxicity is evident at the 75 mg/kg dose and above given the elevated creatinine kinase (CK). The LD_{50} was determined to be

between 100-150 mg/kg since the dose was lethal to 50% of the mice within 24 hours after treatment in both groups.

11β Forms DNA Adducts with Guanine Residues *in Vivo*. In order to assess the ability of 11β to adduct DNA *in vivo*, mice were injected with 25 mg/kg of 11β. The bio-distribution results indicated that more of the dose was absorbed by the liver than by any other organ. Therefore, the liver was harvested and homogenized in order to isolate 11β DNA adducts that had formed *in vivo*. The DNA was isolated, hydrolyzed, and analyzed by ESI-MS. Figure 7.4A shows the main molecular ion is at 813.5 m/z. This is the same mass as the ion observed when 11β was reacted with DNA *in vitro* as discussed in Chapter 6. CID of the 813.5 m/z peak resulted in the same 662.5 m/z and 372.1 m/z fragmentation as observed previously with the *in vitro* adducts (Fig 7.4B). The proposed structures of the daughter ions are shown in Fig 7.4C. The daughter ions are the same as what has been seen for 11β adducts *in vitro* (as described in Chapter 6) and for E2-7α *in vitro* and *in vivo* (as reported in Chapter 2 and 3 and in Mitra et al) (Mitra et al. 2002). Unfortunately, a deuterated derivative of 11β has not yet been synthesized. However, E2-7α and 11β have the same exact molecular weight, and therefore it is reasonable to extrapolate the deuterated and undeuterated results with E2-7α to 11β. This provides us with confidence that the 813.5 m/z molecular ion was indeed an 11β-guanine adduct in which one arm was hydrolyzed.

Discussion

11β was formulated in a CR-EL based vehicle and injected IP in order to obtain information regarding the distribution and pharmacokinetics of the compound. 11β was rapidly absorbed by the body and distributed to all major organs. A large fraction of 11β accumulated in the liver, indicating that the liver is likely the major route of metabolism with excretion through the feces. Paclitaxel and docetaxel, both formulated in a CR-EL solution, are also predominantly excreted by the liver and into the feces (Bissery et al. 1995; Sparreboom et al. 1997; Sparreboom et al. 1998; Sparreboom et al. 1996). At the earliest time points the feces contained less than 3% ID/g of 11β, and not until the 6 hour time point did any significant accumulation occur (9% ID/g). The rate of excretion of

11β is slower than what has been reported for paclitaxel, possibly implying more favorable therapeutic efficacy (Klecker et al. 1994; Sparreboom et al. 1996).

Other organs with high accumulations of 11β included the intestines and kidneys. Perhaps one reason the intestines had a high concentration of compound was because of the route of administration and/or the vehicle used. However, a Caco-2 permeability study would be needed in order to confirm this hypothesis. The concentration of 11β in the kidneys increases with time until it reaches a peak concentration at 4 hours. This could be the result of renal absorption or excretion of 11β and/or its metabolic breakdown products. Unfortunately metabolic cages were not used in this experiment and therefore future experiments would be needed to analyze concentrations in the urine and to better understand the excretion of 11β.

11β was rapidly absorbed in the mouse with peak concentrations in the blood of 128 μM and 190 μM in the plasma (C_{max}) at the 15 minute time point (t_{max}). The higher concentration of 11β in plasma compared to that in whole blood indicates that the compound is almost entirely in the plasma compartment of whole blood and very little 11β accumulates in erythrocytes or is covalently bound to plasma proteins. The protein adduction curve provides additional experimental evidence in that >87% of the drug in whole blood was found in plasma, not taken up by erythrocytes or covalently adducted to plasma proteins for the first 6 hours after IP administration (Fig 7.3). However, 11β could still be associated with plasma proteins non-covalently. Chlorambucil has been shown to be 99 % (non-covalently) bound to proteins in mouse plasma (Lee, Coe, and Workman 1986).

Nakai et al, showed that various conventional antitumor drugs can be grouped into two types with respect to cytotoxic action *in vitro*: cell cycle phase nonspecific (type I) and specific (type II) drugs. The cytotoxic activity of type I drugs, which includes alkylating agents and antitumor antibiotics, is AUC specific. However, the cytotoxic activity of type II drugs, which include antimetabolites and vinca alkaloids, is time dependent. Therefore, not only the AUC in the target organ, but also the exposure time is an important factor for evaluating the efficiency of any delivery system for antitumor drugs (Nakai et al. 1996). 11β is an alkylating agent, and therefore the cytotoxicity of the compound should correlate with the AUC. Pharmacokinetic data from Newell et al,

show the AUC of chlorambucil is 22 μg × hr/mL when a therapeutic dose of 10 mg/kg was administered sub-cutaneously in rats (Newell, Shepherd, and Harrap 1981). The AUC of 11β was found to be 402 μg × hr/mL when a 45 mg/kg dose was administered IP in mice. Assuming linear pharmacokinetics, a 10 mg/kg dose of 11β would yield an AUC of 89 μg × hr/mL, 4-fold greater than the AUC found for chlorambucil. Furthermore, the exposure necessary for 11β to be therapeutically active could be much less than what is needed for chlorambucil if the repair shielding and transcription factor hijacking hypotheses are valid. In either case, 11β would be selectively retained in tumor tissue and therefore potentially a lower number of DNA adducts would be required for tumor lethality. This evidence illustrates the potential of 11β as an effective anticancer agent.

To assess further the likelihood of 11β as a chemotherapeutic agent, blood chemistry and hematological analyses were performed in order to gauge organ specific toxicity after an acute dose of 11β in mice. No toxicity was evident at doses at or below 30 mg/kg. At all doses of 11β, a slight alteration in the ratio of lymphocytes to neutrophils was observed, such that the ratio of neutrophils increased -- 50% of the white blood cells were neutrophils while 50% were lymphocytes, whereas in the control group 80% of the white blood cells were lymphocytes and only 20% were neutrophils. Despite the alteration in the ratio of lymphocytes to neutrophils, the total number of leukocytes increased slightly with dose until it reached a maximum at 150 mg/kg (although the number of WBCs after a 150 mg/kg dose is still in the normal range provided by Taconic). This fact is rather surprising as many anticancer agents, including chlorambucil and melphalan, induce myelosuppression (according to their respective package inserts). The dose limiting toxicity of chlorambucil is, in fact, neutropenia, or a decrease in neutrophils (Blumenreich et al. 1988; Inoue et al. 1987). 11β seemingly does not induce myelosuppression but rather stimulates neutrophil proliferation or inhibits the production of lymphocytes so as to alter their respective ratios.

Alternatively, the elevation of neutrophils and suppression of lymphocytes may indicate that 11β is interacting with the glucocorticoid receptor (GR). The GR is a member of the same class of nuclear hormone receptors as the ER and AR. Corticosteroids, the natural ligands for the GR, have profound effects on lymphocytes

and neutrophils. Corticosteroids actually induce the apoptosis of lymphocytes, (Di et al. 2000; Negoescu et al. 1998) whereas they inhibit the death of neutrophils *in vitro* (Cox and Austin 1997; Liles et al. 1996). The mechanisms by which human lymphocyte and neutrophil apoptotic responses to glucocorticoids differ are unknown. However, glucocorticoid action is mediated through the GR and therefore these apoptotic differences may arise from downstream targets of the GR (O'Malley 1971; Strickland et al. 2001; Wenzel et al. 1997). An off-target interaction of 11β with the GR may mediate the responses seen in the alteration in the ratio of neutrophils to lymphocytes. In fact Nicole Dinaut, a former post-doctoral associate in the Essigmann Laboratory, has shown the RBA of 11β for the GR to be 2. Although this is not a tight interaction, it may be sufficient in decreasing lymphocyte count and increasing neutrophil count as we have seen here.

The blood chemistry profile of an acute dose of 11β also shows apparent toxicity. Most significantly, hepatotoxicity is evident at doses of 50 mg/kg and above as evident by increased ALT, AST, amylase, and lipase. These enzymes are all involved in liver function and therefore an increase in the levels of these enzymes signifies hepatotoxicity. Hepatotoxicity has also been documented in patients treated with chlorambucil (Blumenreich et al. 1988).

The evidence of renal toxicity is evident by the alterations in blood urea nitrogen (BUN), creatinine, phosphorous, and calcium at doses of 100 and 150 mg/kg (there is also some indication of renal toxicity at the 75 mg/kg dose as BUN is elevated). Amino acids are catabolized by the liver to produce ammonia. The ammonia is combined with bicarbonate to form urea, which is transported to the kidneys for excretion. Therefore, an increase in BUN is indicative of renal toxicity as a result of a decreased rate in glomerular filtration. Creatinine is also excreted by the kidneys, and an elevated level confirms a decrease in the glomerular filtration rate and therefore renal toxicity. Finally, increased phosphorous and decreased calcium levels further indicate renal toxicity. All of the above conditions are satisfied at doses of 11β above 100 mg/kg.

CK, a sensitive indicator of myocardial injury and muscle damage, was also found to be elevated at doses of 75 mg/kg and above. CK is found primarily in the heart, skeletal muscle, and brain and catalyzes the phosphorylation reaction of ADP by

creatinine. Acute liver damage has no effect on CK, so the elevated level seen in the mice treated with 11β is likely related to muscle damage. Further tests would be needed to determine if 11β has a deleterious effect on cardiac muscle or skeletal muscle. For example, lactate dehydrogenase and troponins are both elevated following cardiac injury. An elevation in these proteins would further suggest cardiac toxicity.

In Chapter 6, the identification of 11β DNA adducts formed *in vitro* was discussed. Using ESI-MS techniques, we illustrated that 11β covalently modified guanine, most likely at the N7 position. The identification of these adducts was remarkable considering the related nitrogen mustard, chlorambucil, has a relatively short half-life of only 18 minutes in a non-nucleophilic 0.2 M cacodylic acid solution at 37°C (Haapala et al. 2001). The rapid decomposition of chlorambucil is a result of an intramolecular, rate-determining attack of the unprotonated nitrogen atom to form an aziridinium ion intermediate followed by attack of an external nucleophile (such as water) (Chatterji, Yeager, and Gallelli 1982; Kundu, Schullek, and Wilson 1994; Owen and Stewart 1979). Hence, chlorambucil (and other nitrogen mustards) is a reactive compound that decomposes rapidly in aqueous solutions and forms covalent bonds with other nucleophiles.

In blood, where the chloride ion concentration approximates 100 mM, chlorambucil has a much longer half-life of 2.4 hours (Newell, Shepherd, and Harrap 1981). With the half-life of chlorambucil in mind, we chose the 4 hour time point to monitor the formation of 11β DNA adducts. We believed 4 hours would be ample time for 11β to covalently modify DNA and form stable adducts prior to being repaired or metabolized. Furthermore, the pharmacokinetic analysis revealed that the highest amount of drug accumulated in the liver, approximately 10% ID/g between 2 and 4 hours. Therefore, liver tissue was analyzed for the presence of DNA adducts.

As in Chapter 6, a molecular ion with a mass of 813.5 m/z was found. This is consistent with one arm of the nitrogen mustard adducted to guanine whereas the second arm had been hydrolyzed. Unfortunately, there is no way of telling when the second, non-reacting arm of the nitrogen mustard warhead underwent hydrolysis. It is possible that the second arm remained chlorinated *in vivo* and only in the procedure used to isolate the DNA adducts did the chloroethyl arm convert to hydroxyethyl. However this may be

an unlikely scenario as the half-life of the related nitrogen mustards, chlorambucil and melphalan, were found to be 2.4 hours and 1.5 hours, respectively, in plasma (Honess et al. 1985; Newell, Shepherd, and Harrap 1981). Currently, we do not have any data on the hydrolysis rate of 11β *in vivo*.

The identification of 11β DNA adducts *in vivo* is extremely encouraging even though the adducts were found in non-target tissue. This data illustrates that 11β can be injected into a mouse, distribute throughout the body, and form DNA adducts while remaining intact. The repair shielding and transcription factor hijacking hypotheses require 11β to form DNA adducts in target tissues and attract tumor specific proteins. In non-target tissues we expect the adducts to be repaired since the tissue would lack the tumor specific protein for which the molecule was designed to attract. Therefore, the formation of DNA adducts in non-target tissues is expected, and in this case it serves as an illustration of the robustness of the molecule: 11β was administered to mice, distributed throughout the body, remained intact, and covalently modified DNA.

Conclusion

11β has previously been shown to contain properties favorable to our intended mechanisms of action: it has a high RBA (36) for the AR, it is capable of covalently modifying DNA, its log D (2.00) indicates it should have favorable pharmacokinetics, and it displays significant toxicity towards the AR(+) LNCaP cell line. These results have been described in Chapter 6. Based on its log D, and other properties making it an attractive chemotherapeutic agent, we have continued to investigate the compound by monitoring its pharmacokinetics, acute toxicity, and ability to adduct DNA *in vivo*.

11β, when formulated with a CR-EL based vehicle and injected IP, illustrates good overall distribution into tissues. At 45 mg/kg, the peak plasma concentration was 190 μM (19-fold higher than what was necessary to kill AR(+) LNCaP cells in culture) and remained greater than 10 μM for nearly 6 hours. Indicators of hepato-, renal, and possible cardiotoxicity were first evident at a dose of 75 mg/kg following an acute dose. However, this observation is not surprising as anticancer agents generally have significant toxicity profiles and a narrow therapeutic index. The LD_{50} was found to be between 100 and 150 mg/kg. Finally, 11β formed DNA adducts *in vivo* indicating the

compound is relatively stable and is not rapidly metabolized or excreted. The DNA adducts identified were the same as those found *in vitro* and described in Chapter 6: a mono-guanine adduct with the other arm of the nitrogen mustard having undergone hydrolysis.

In summary, these results further support the notion of 11β as a potential drug candidate. Following the encouraging pharmacokinetic results, we have continued to use the CR-EL based vehicle for tumor ablation studies. Chapter 8 shall describe the effectiveness of 11β as an anticancer agent using xenograft animal models. I will also quantify the penetrance of 11β into xenograft tumor tissue and describe the toxicity to mice after a therapeutic dose of 11β.

Future Work

CR-EL has provided us with a means of administering 11β into mice; however, as noted in Chapter 3, it is by no means an ideal delivery vehicle. The literature is inundated with reports on the toxic side effects of CR-EL. A number of studies have reported that CR-EL induced side effects such as hypersensitivity, neurotoxicity, nephrotoxicity, and the extraction of plasticizers from intravenous infusion lines (Cheon et al. 2003; Gregory and DeLisa 1993; Mazzo et al. 1997; Onetto et al. 1993). We acknowledge the limitations of CR-EL and therefore we have begun a collaboration with the Sasisekharan Laboratory at MIT in an effort to formulate 11β using liposomes. We have conducted a pilot experiment in which we injected a liposomal solution into two mice. Blood was drawn over time and the percent of the dose in blood over a 24 hour period is shown in Fig 7.5. The data show the liposomes circulate in plasma for a considerable period of time -- as much as 80% of the drug was still circulating in blood 24 hours later. (I do note however, that the theoretical recovery is over 100% in one of the mice. Even still, the amount of compound circulating at 24 hours in this mouse is 50% of that in the blood at 15 min In the second mouse 80% of the dose is still circulating at 24 hours as compared to what was recovered at the 15 min time point.) Unfortunately, a full bio-distribution experiment was not able to confirm these results. Figure 7.6 illustrates that the concentration of 11β in whole blood after a CR-EL or liposomal administration is nearly identical. The results seen with the full bio-

distribution of 11β formulated in liposomes contradicts the results seen in the pilot experiment. The most likely reason for this result was the unfortunate oxidation of the lipids used to prepare the liposomes (something we did not realize at the time of the bio-distribution). The collaboration is still ongoing and we anticipate promising results in the near future. Any new delivery agent would have to undergo the same rigorous experiments described in this chapter: bio-distribution, pharmacokinetic analysis, and acute toxicity. However, the work here sets a foundation for which alternative delivery agents can be measured. If, however, a suitable alternative delivery agent cannot be found, it is possible to continue the use with CR-EL since Taxol is formulated as a concentrated solution of 6 mg per mL of CR-EL:dehydrated ethanol (1:1 v/v) which must be further diluted 5 to 20-fold with saline prior to IV administration (Goldspiel 1994).

Charles Morton and I have begun work using human liver microsomes to address the metabolic fate of 11β. Initial experiments have been relatively unsuccessful; however, a recent search of the literature indicates that we may have been using too much drug for the assay and thus saturated the system. We are confident that in the near future we will be able to identify the metabolites of 11β and also the P450s likely responsible for its breakdown.

Reference List

Bissery, M.C., Nohynek, G., Sanderink, G.J., and Lavelle, F. Docetaxel (Taxotere): a
 review of preclinical and clinical experience. Part I: Preclinical experience.
 Anticancer Drugs **6**, 339-8 (1995)

Blumenreich, M.S., Woodcock, T.M., Sherrill, E.J. et al. A phase I trial of chlorambucil
 administered in short pulses in patients with advanced malignancies. *Cancer
 Invest* **6**, 371-375 (1988)

Bruckheimer, E.M., Gjertsen, B.T., and McDonnell, T.J. Implications of cell death
 regulation in the pathogenesis and treatment of prostate cancer. *Semin. Oncol.* **26**,
 382-398 (1999)

Chatterji, D.C., Yeager, R.L., and Gallelli, J.F. Kinetics of chlorambucil hydrolysis using
 high-pressure liquid chromatography. *J. Pharm. Sci.* **71**, 50-54 (1982)

Cheon, L.S., Kim, C., Chan, K., I et al. Polymeric micelles of poly(2-ethyl-2-oxazoline)-
 block-poly(epsilon-caprolactone) copolymer as a carrier for paclitaxel. *J. Control
 Release* **89**, 437-446 (2003)

Cox, G. and Austin, R.C. Dexamethasone-induced suppression of apoptosis in human
 neutrophils requires continuous stimulation of new protein synthesis. *J. Leukoc.
 Biol.* **61**, 224-230 (1997)

Denmeade, S.R., Lin, X.S., Tombal, B., and Isaacs, J.T. Inhibition of caspase activity
 does not prevent the signaling phase of apoptosis in prostate cancer cells. *Prostate*
 39, 269-279 (1999)

Di, B.A., Secchiero, P., Grilli, A. et al. Morphological features of apoptosis in
 hematopoietic cells belonging to the T-lymphoid and myeloid lineages. *Cell Mol.
 Biol. (Noisy. -le-grand)* **46**, 153-161 (2000)

Gingrich, J.R., Barrios, R.J., Kattan, M.W. et al. Androgen-independent prostate cancer
 progression in the TRAMP model. *Cancer Res.* **57**, 4687-4691 (1997)

Gioeli, D. Signal transduction in prostrate cancer progression. *Clin. Sci. (Lond)* ., 2004)

Gioeli, D. Signal transduction in prostate cancer progression. *Clin. Sci. (Lond)* **108**, 293-
 308 (2005)

Goldspiel, B.R. Pharmaceutical issues: preparation, administration, stability, and
compatibility with other medications. *Ann. Pharmacother.* **28**, S23-S26 (1994)

Gregory, R.E. and DeLisa, A.F. Paclitaxel: a new antineoplastic agent for refractory
ovarian cancer. *Clin. Pharm.* **12**, 401-415 (1993)

Gulley, J. and Dahut, W.L. Novel approaches to treating the asymptomatic hormone-
refractory prostate cancer patient. *Urology* **62**, 147-154 (2003)

Haapala, E., Hakala, K., Jokipelto, E. et al. Reactions of N,N-bis(2-chloroethyl)-p-
aminophenylbutyric acid (chlorambucil) with 2'-deoxyguanosine. *Chem. Res.
Toxicol.* **14**, 988-995 (2001)

Honess, D.J., Donaldson, J., Workman, P., and Bleehen, N.M. The effect of systemic
hyperthermia on melphalan pharmacokinetics in mice. *Br. J. Cancer* **51**, 77-84
(1985)

Inoue, K., Ogawa, M., Horikoshi, N. et al. [Phase II study of chlorambucil in patients
with hematological malignancies]. *Gan To Kagaku Ryoho* **14**, 2672-2675 (1987)

Isaacs, J.T. and Coffey, D.S. Adaptation versus selection as the mechanism responsible
for the relapse of prostatic cancer to androgen ablation therapy as studied in the
Dunning R-3327-H adenocarcinoma. *Cancer Res.* **41**, 5070-5075 (1981)

Jang, G.R., Harris, R.Z., and Lau, D.T. Pharmacokinetics and its role in small molecule
drug discovery research. *Med. Res. Rev.* **21**, 382-396 (2001)

Klecker, R.W., Jamis-Dow, C.A., Egorin, M.J. et al. Effect of cimetidine, probenecid,
and ketoconazole on the distribution, biliary secretion, and metabolism of
[3H]taxol in the Sprague-Dawley rat. *Drug Metab Dispos.* **22**, 254-258 (1994)

Kozlowski, J.M., Ellis, W.J., and Grayhack, J.T. Advanced prostatic carcinoma. Early
versus late endocrine therapy. *Urol. Clin. North Am.* **18**, 15-24 (1991)

Kreis, W. Current chemotherapy and future directions in research for the treatment of
advanced hormone-refractory prostate cancer. *Cancer Invest* **13**, 296-312 (1995)

Kundu, G.C., Schullek, J.R., and Wilson, I.B. The alkylating properties of chlorambucil.
Pharmacol. Biochem. Behav. **49**, 621-624 (1994)

Kyprianou, N. Apoptosis: therapeutic significance in the treatment of androgen-
dependent and androgen-independent prostate cancer. *World J. Urol.* **12**, 299-303
(1994)

Lee, F.Y., Coe, P., and Workman, P. Pharmacokinetic basis for the comparative antitumour activity and toxicity of chlorambucil, phenylacetic acid mustard and beta, beta-difluorochlorambucil (CB 7103) in mice. *Cancer Chemother. Pharmacol.* **17**, 21-29 (1986)

Liles, W.C., Kiener, P.A., Ledbetter, J.A. et al. Differential expression of Fas (CD95) and Fas ligand on normal human phagocytes: implications for the regulation of apoptosis in neutrophils. *J. Exp. Med.* **184**, 429-440 (1996)

Marcelli, M., Marani, M., Li, X. et al. Heterogeneous apoptotic responses of prostate cancer cell lines identify an association between sensitivity to staurosporine-induced apoptosis, expression of Bcl-2 family members, and caspase activation. *Prostate* **42**, 260-273 (2000)

Mazzo, D.J., Nguyen-Huu, J.J., Pagniez, S., and Denis, P. Compatibility of docetaxel and paclitaxel in intravenous solutions with polyvinyl chloride infusion materials. *Am. J. Health Syst. Pharm.* **54**, 566-569 (1997)

Mitra, K., Marquis, J.C., Hillier, S.M. et al. A rationally designed genotoxin that selectively destroys estrogen receptor-positive breast cancer cells. *J. Amer. Chem. Soc.* **124**, 1862-1863 (2002)

Nakai, D., Fuse, E., Suzuki, H. et al. Evaluation of the efficiency of targeting of antitumor drugs: simulation analysis based on pharmacokinetic/pharmacodynamic considerations. *J. Drug Target* **3**, 443-453 (1996)

Negoescu, A., Guillermet, C., Lorimier, P. et al. Importance of DNA fragmentation in apoptosis with regard to TUNEL specificity. *Biomed. Pharmacother.* **52**, 252-258 (1998)

Newell, D.R., Shepherd, C.R., and Harrap, K.R. The pharmacokinetics of prednimustine and chlorambucil in the rat. *Cancer Chemother. Pharmacol.* **6**, 85-91 (1981)

O'Malley, B.W. Mechanisms of action of steroid hormones. *N. Engl. J. Med.* **284**, 370-377 (1971)

Onetto, N., Canetta, R., Winograd, B. et al. Overview of Taxol safety. *J. Natl. Cancer Inst. Monogr* 131-139 (1993)

Owen, W.R. and Stewart, P.J. Kinetics and mechanism of chlorambucil hydrolysis. *J. Pharm. Sci.* **68**, 992-996 (1979)

Santen, R.J. Clinical review 37: Endocrine treatment of prostate cancer. *J. Clin. Endocrinol. Metab* **75**, 685-689 (1992)

Sparreboom, A., van, A.J., Mayer, U. et al. Limited oral bioavailability and active epithelial excretion of paclitaxel (Taxol) caused by P-glycoprotein in the intestine. *Proc. Natl. Acad. Sci. U. S. A* **94**, 2031-2035 (1997)

Sparreboom, A., van, T.O., Nooijen, W.J., and Beijnen, J.H. Tissue distribution, metabolism and excretion of paclitaxel in mice. *Anticancer Drugs* **7**, 78-86 (1996)

Sparreboom, A., van, T.O., Nooijen, W.J., and Beijnen, J.H. Preclinical pharmacokinetics of paclitaxel and docetaxel. *Anticancer Drugs* **9**, 1-17 (1998)

Strickland, I., Kisich, K., Hauk, P.J. et al. High constitutive glucocorticoid receptor beta in human neutrophils enables them to reduce their spontaneous rate of cell death in response to corticosteroids. *J. Exp. Med.* **193**, 585-593 (2001)

Wang, J.D., Takahara, S., Nonomura, N. et al. Early induction of apoptosis in androgen-independent prostate cancer cell line by FTY720 requires caspase-3 activation. *Prostate* **40**, 50-55 (1999)

Wang, L.G., Ossowski, L., and Ferrari, A.C. Androgen receptor level controlled by a suppressor complex lost in an androgen-independent prostate cancer cell line. *Oncogene* **23**, 5175-5184 (2004)

Weir, H.K., Thun, M.J., Hankey, B.F. et al. Annual report to the nation on the status of cancer, 1975-2000, featuring the uses of surveillance data for cancer prevention and control. *J. Natl. Cancer Inst.* **95**, 1276-1299 (2003)

Wenzel, S.E., Szefler, S.J., Leung, D.Y. et al. Bronchoscopic evaluation of severe asthma. Persistent inflammation associated with high dose glucocorticoids. *Am. J. Respir. Crit Care Med.* **156**, 737-743 (1997)

Distribution of 11β in Mouse Tissue with a Cremophor-EL Based Vehicle

	0.25 hr.	1 hr.	2 hr.	4 hr.	6 hr.	24 hr.
Blood	4.90 ± 0.23	1.40 ± 0.25	2.09 ± 1.3	1.28 ± 0.45	0.70 ± 0.04	0.41 ± 0.11
Heart	0.23 ± 0.04	0.83 ± 0.23	1.26 ± 0.71	2.02 ± 0.06	0.98 ± 0.04	0.21 ± 0.05
Lung	0.67 ± 0.34	1.84 ± 1.32	3.76 ± 0.64	4.29 ± 0.27	3.38 ± 0.14	0.66 ± 0.20
Liver	3.82 ± 1.74	6.62 ± 1.47	9.41 ± 0.79	11.10 ± 0.95	4.61 ± 0.97	1.81 ± 0.15
Spleen	1.15 ± 0.05	2.62 ± 0.19	3.64 ± 0.55	4.20 ± 0.92	2.42 ± 0.22	0.79 ± 0.02
Kidney	0.49 ± 0.12	2.42 ± 0.15	4.08 ± 0.37	5.59 ± 0.39	4.31 ± 0.01	1.08 ± 0.02
GI	2.54 ± 0.23	3.81 ± 0.04	7.15 ± 4.55	3.87 ± 0.74	2.54 ± 0.05	1.00 ± 0.01
Feces	0.27 ± 0.10	1.78 ± 0.31	2.93 ± 1.78	1.94 ± 0.36	8.78 ± 2.24	2.49 ± 0.37
Sk. Muscle	0.13 ± 0.06	0.25 ± 0.08	0.23 ± 0.06	0.39 ± 0.02	0.33 ± 0.00	0.08 ± 0.01
Adipose	4.63 ± 1.11	2.22 ± 1.01	2.71 ± 0.76	2.53 ± 0.71	1.25 ± 0.35	0.54 ± 0.17

Table 7.1 Mice were injected IP with 5 µCi of ^{14}C-11β dissolved in 43 % CR-EL, 30 % saline, 27 % ethanol. They were sacrificed at 0.25, 1, 2, 4, 6, or 24 hours after the injection. The results are reported as the mean percent injected dose per gram (of each organ) ± standard deviation.

Pharmacokinetic Parameters of 11β

Parameter	DMSO IV
AUC^{a} (μg x hr/mL)	403
$t_{1/2}^{b}$ (hr)	1.3
CL^{c} (mL/hr)	4.7
V_{d}^{d} (L/kg)	0.49
C_{max}^{e} (μM)	190
t_{max}^{f} (hr)	0.25

Table 7.2 Pharmacokinetic parameters following the administration of 11β IP with a CR-EL based vehicle. [a] area under the blood concentration-Vs-time curve, [b] half-life, [c] clearance, [d] volume of distribution, [e] maximum concentration in blood, [f] time at which C_{max} was achieved.

Acute Toxicity of 11β: Hematology

Test	Control N = 4	Vehicle N = 3	10 mg/kg N = 3	30 mg/kg N = 3	50 mg/kg N = 4	75 mg/kg N = 4	100 mg/kg N =2	150 mg/kg N = 2	Taconic Nude
WBC (x mm³)	5.4	8.2	6.6	7.3	7.5	10.2	10.0	*13.5*	4.3-13.5
RBC (x 10⁶ mm3)	10.1	10.0	9.8	8.8	10.4	9.8	12.0	12.4	6.9-8.52
Hgb (g/dL)	14.8	14.6	14.9	13.5	15.4	14.7	16.8	17.6	7.5-15.2
HCT (%)	53.7	52.4	53.4	47.6	53.5	54.6	63.2	64.1	39.4-43.5
Neutrophils (%)	19.8	17.0	*54.5*	*49.7*	*55.0*	*48.8*	*42.0*	*50.0*	7.0-39
Lymphs (%)	76.8	80.3	*45.0*	*48.7*	*42.8*	*48.5*	*54.0*	*47.5*	56-92
Monos (%)	3.0	3.0	1.0	1.3	2.3	2.5	4.0	2.5	0-7
Eos (%)		2.0		1.0	1.0	1.0			0-4
Platelets (10³/μL)	1177	1263	1214	1226	1442	1462	934	900	790-1014
MCV (fL)	53.1	52.5	55.0	53.8	51.9	56.0	52.7	51.8	51.1-53.4
MCH (pg)	14.7	14.6	15.3	15.2	14.8	15.0	14.2	14.2	17.6-19.1
MCHC (g/dL)	27.6	27.8	27.8	28.4	28.8	26.8	27.1	27.5	34.3-36.1

Table 7.3 Hematology report for mice injected with 11β. Values in bold represent abnormally elevated or suppressed levels. The ratio of neutrophils to lymphocytes is altered at all doses of 11β. Additionally, the hemoglobin is elevated in the 100 mg/kg dose and both the hemoglobin and WBC are elevated in the 150 mg/kg dose.

(Note: Since the test groups contained relatively few mice, the abnormal levels are deviations from the normal range and do not necessarily reflect statistical significance.)

Acute Toxicity of 11β: Blood Chemistry

Test	Control N = 4	Vehicle N = 3	10 mg/kg N = 3	30 mg/kg N = 3	50 mg/kg N = 4	75 mg/kg N = 4	100 mg/kg N = 1	150 mg/kg N = 2	Taconic Nude
Alk. Phosphatase (IU/L)	101	90	72	77	59	69	117	83	96-117
ALT (SGPT) (IU/L)	40	41	50	47	*509*	*2109*	*1482*	*1544*	
AST (SGOT) (IU/L)	73	99	201	105	*594*	*3581*	*2904*	*3879*	61-119
CK (IU/L)	191	321	651	290	552	*53580*	79308	159453	
GGT (IU/L)	0.0	<3	<3	0.0	<3	<3	*3.0*	*9.0*	
Albumin (g/dL)	3.3	3.3	2.9	2.6	3.0	2.6	2.1	1.8	3.4-4.1
Total Protein (g/dL)	5.9	5.7	5.5	4.8	6.1	4.9	*3.6*	*3.0*	4.8-5.6
Globulin (g/dL)	2.6	2.4	2.5	2.2	3.1	2.3	*1.5*	*1.2*	1.1-1.6
Total Bilirubin (mg/dL)	0.1	0.2	<.3	0.1	0.2	0.4	0.3	0.3	0.3-0.8
Direct Bilirubin (mg/dL)	0.0	<.3	<.3	0.0	0.1	0.3	<.3	<.3	
BUN (mg/dL)	25.0	20.7	25.7	25.7	35.8	*76.8*	*117.0*	*108.0*	30-37
Creatinine (mg/dL)	0.3	<.3	<.3	0.2	<.3	<.3	*0.6*	*0.8*	0.5-0.7
Cholesterol (mg/dL)	226	202	156	134	218	135	144	75	116-155
Glucose (mg/dL)	334	295	270	258	220	170	957	336	173-288
Calcium (mg/dL)	10.9	11.5	10.8	10.3	11.3	10.4	*6.6*	*6.6*	10.0-12.0
Phosphorous (mg/dL)	8.7	11.0	10.8	11.2	11.1	11.9	*29.4*	*34.5*	12.3-16.1
Bicarbonate (mEq/L)	19.8	15.7	19.0	25.0	25.5	31.0	*6.0*	*42.0*	
Chloride (mEq/L)	102	<180	101	105	<180	<140	<180	<180	118-124
Potassium (mEq/L)	8.2	11.5	*37.5*	8.6	9.1	8.9	11.4	10.8	13.8-16.7
Sodium (mEq/L)	151	158	155	154	154	171	147	150	157-163
A/G Ratio	1.3	1.4	1.1	1.2	1.0	1.1	1.4	1.5	
B/C Ratio	104	>80	>80	128	245	>341	195	151	
Indirect Bilirubin (mg/dL)	0.1	<.3	<.3	0.1	<.3	<.3	<.3	<.3	
Na/K Ratio	19.0	15.5	18.0	18.3	18.3	20.0			
Anion Gap (mEq/L)	37.8	49.5	41.0	26.3	31.0	25.0			
Amylase (IU/L)	1373	1456	1352	1231	*3307*	*3948*	*12096*	*>9000*	
Lipase (IU/L)	99	108	268	130	*1104*	*1665*	*>1650*	*>1650*	

Table 7.4 Blood Chemistry report for mice injected with 11β. Values in bold represent abnormally elevated or suppressed levels. Hepatotoxicity is evident starting at a 50 mg/kg dose. Also renal and cardiac toxicity is evident at doses of 75 mg/kg and above.

(Note: Since the test groups contained relatively few mice, the abnormal levels are deviations from the normal range and do not necessarily reflect statistical significance.)
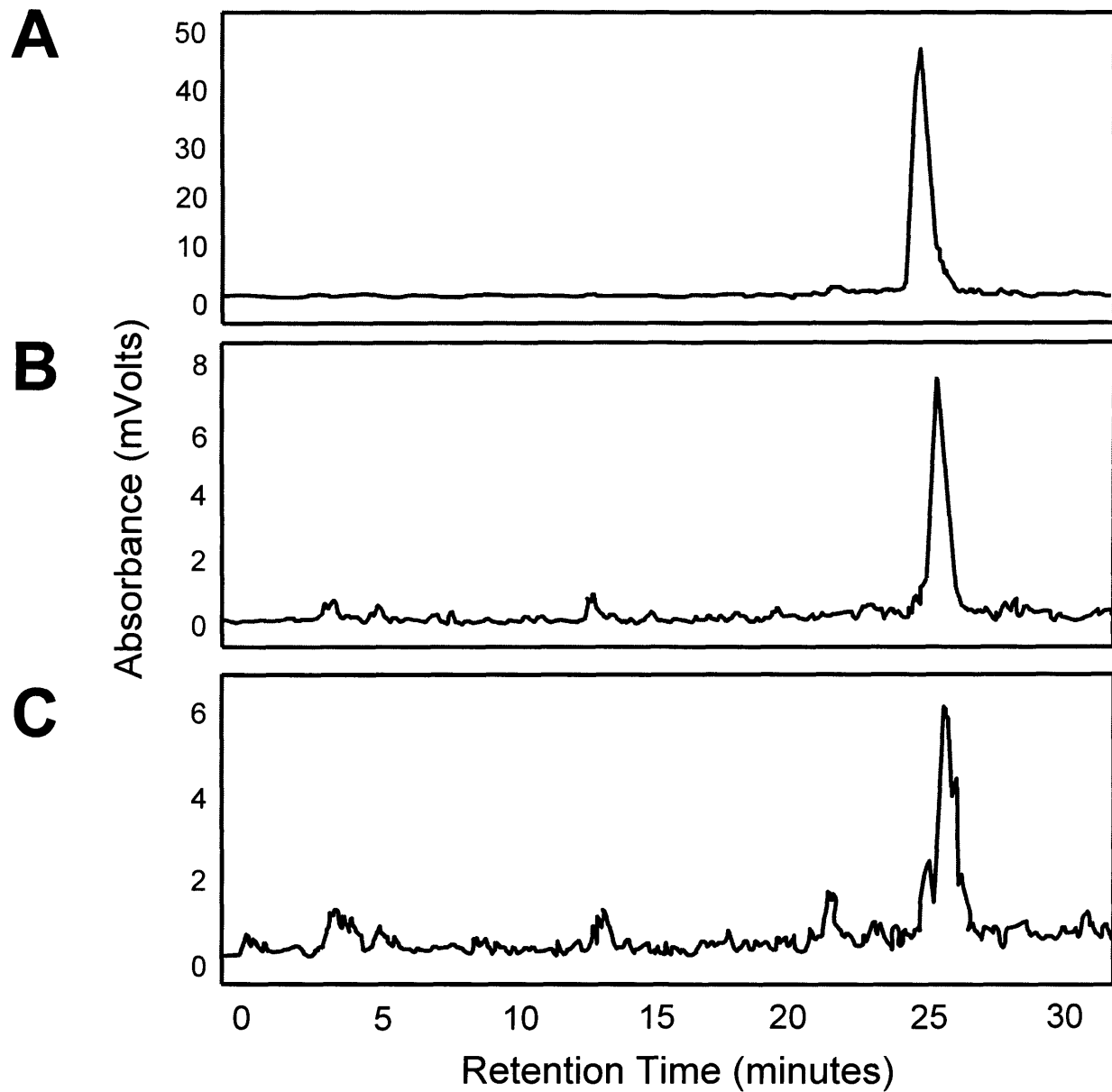
HPLC Chromatograms of 11β in Mouse Plasma

Fig 7.1 HPLC chromatograms of intact 11β in plasma **A.** 15 min. **B.** 1 hour. **C.** 4 hour. Plasma was isolated from whole blood, precipitated with acetonitrile and injected onto HPLC. The peak at 25 min is intact 11β. The peak at 13 min and 4 min in **B** and **C** are likely metabolic breakdown products.

Distribution of 11β in Blood and Plasma
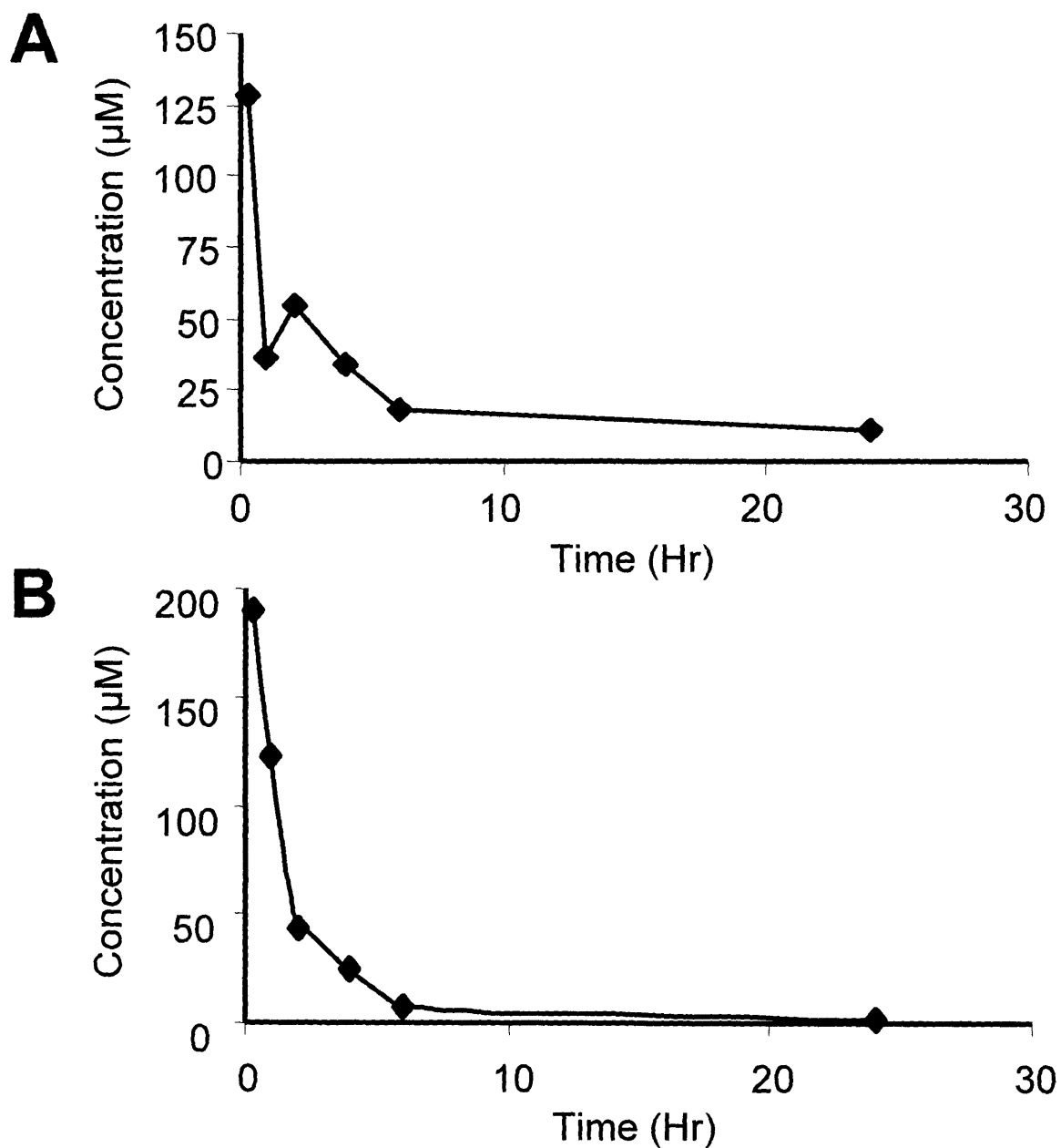
Fig 7.2 11β Blood Curve **(A)** and Plasma Curve **(B)**. 11β was administered to mice and the concentration in whole blood and plasma was determined. The peak concentration is 128 μM in whole blood and 190 μM in plasma, both at the 15 minute time point.

11β is Mainly Unbound to Proteins in Plasma
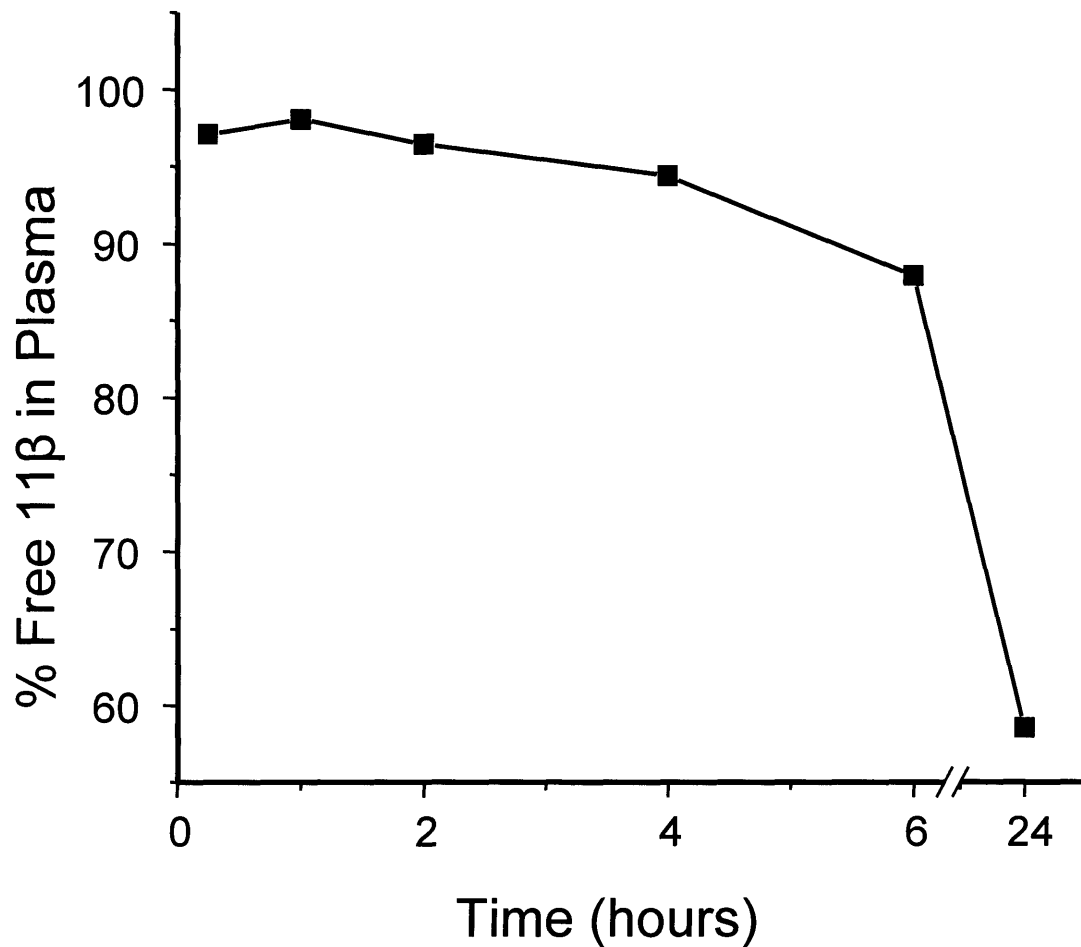
Fig 7.3 Percentage of ^{14}C-11β in the plasma. Greater than 87% of ^{14}C-11β is in the plasma compartment of whole blood for the first 6 hours after administration of the drug.

Identification of 11β DNA Adducts in Mouse Liver Tissue
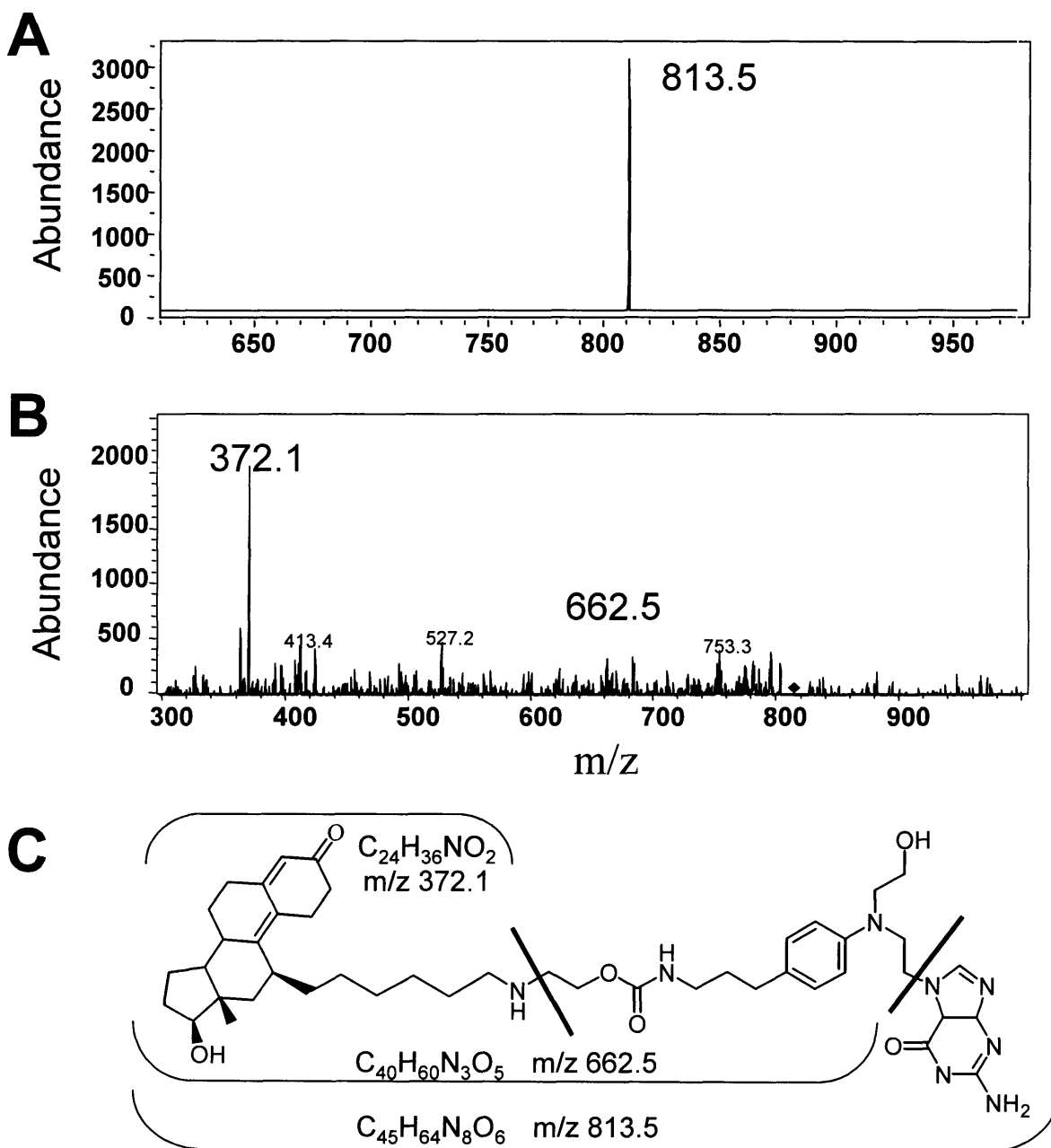
Fig 7.4 A. ESI-MS of an 11β-guanine adduct from liver tissue. **B.** CID of the 813.5 m/z ion results in two daughter ions of 662.5 and 372.1 m/z. **C.** The proposed structure of the 662.5 and 372.1 m/z daughter ions.

Distribution of 11β in Blood using a Liposomes Based Delivery Vehicle
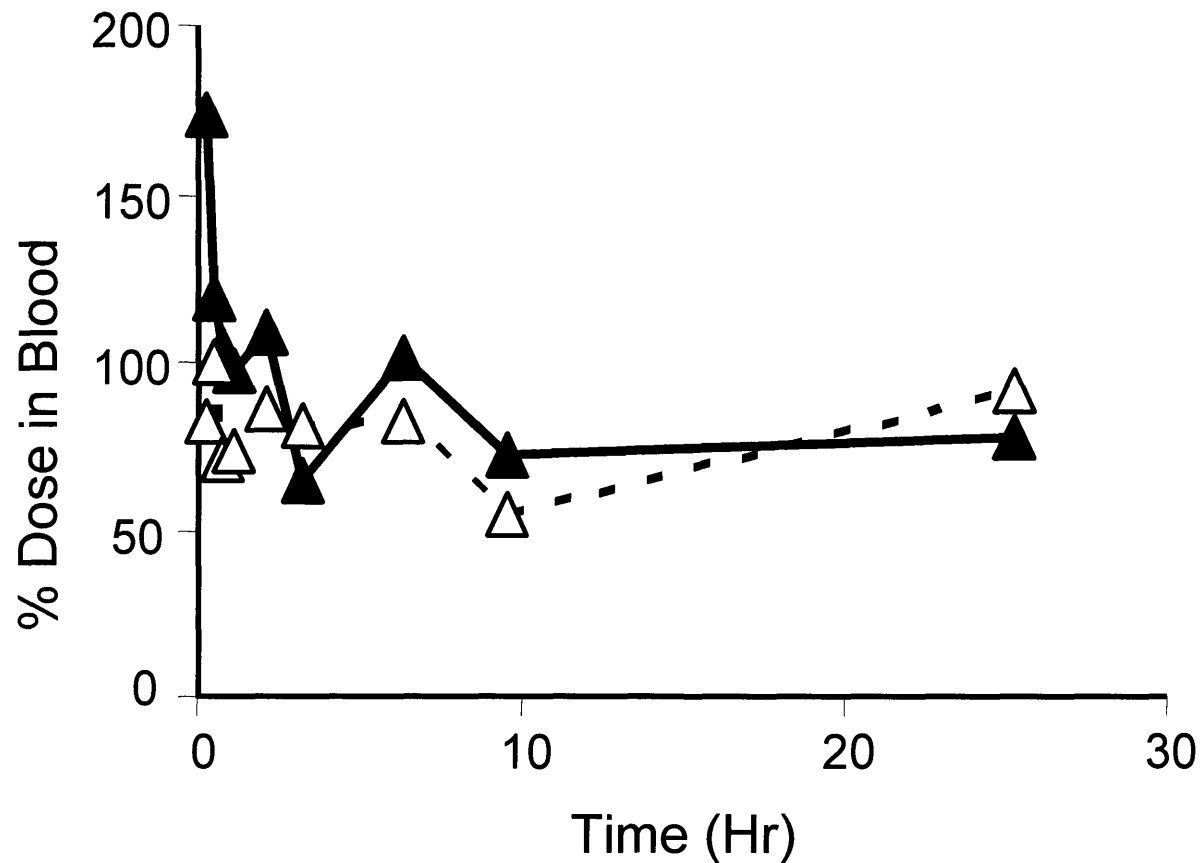
Fig 7.5 Percent of ^{14}C-11β in blood. Two mice (▲ and △) were injected IV with ^{14}C-11β formulated in liposomes. At 24 hours 80% of the dose remained circulating in the blood in one of the mice.

Comparison of Liposomal and Cremophor-EL Based Vehicles in the Distribution of 11β in Mouse Blood
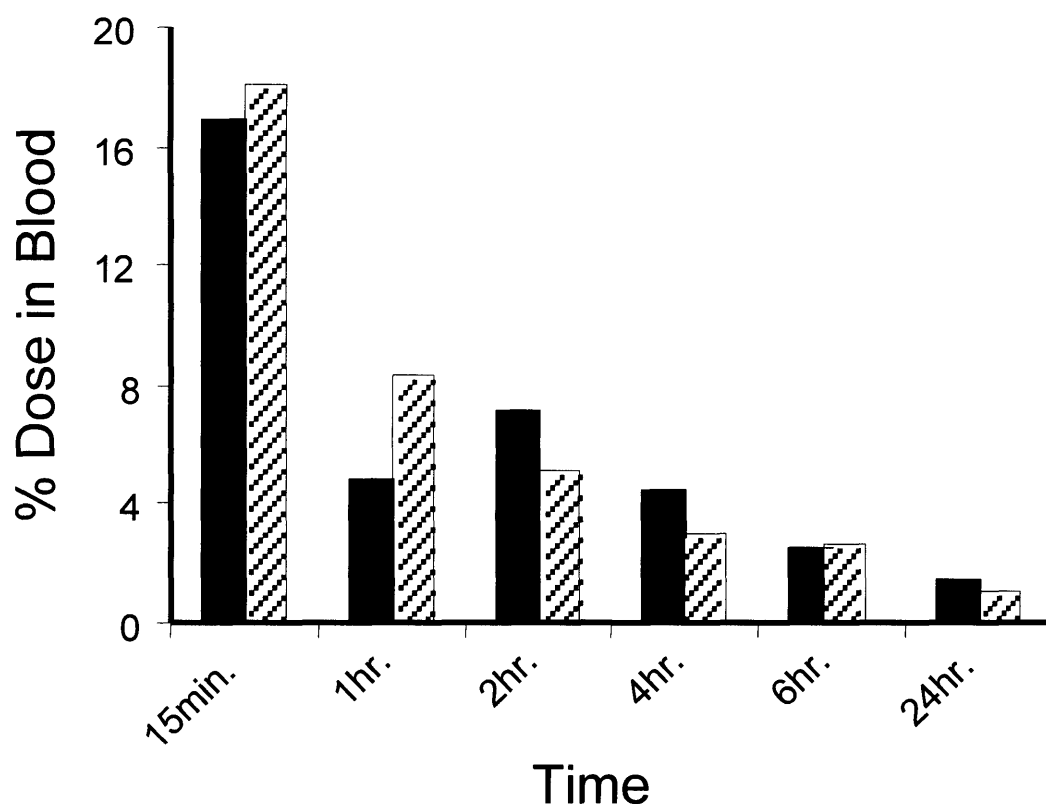
Fig 7.6 Comparison of CR-El (■)and liposomal (▨) formulated ^{14}C-11β in blood. ^{14}C-11β was administered to mice and the concentration in blood was determined. This graph illustrates that the concentration of 11β in blood is nearly identical for either formulation, contradictory to what was seen in Fig 7.5.

Chapter 8

Probing the Biochemical Mechanism of 11β *in Vivo:*

Efficacy against AR(+) Tumors, DNA Adduct Levels and Chronic Toxicity

Introduction

Prostate cancer is the most frequently diagnosed cancer among males in the U.S. with an incidence of 170.1 cases per 100,000 men and a death rate of 32.9 per 100,000 men (Weir et al. 2003). In its earliest stages prostate cancer is curable through surgical intervention and/or radiation therapy. However, in more aggressive forms of the disease and in men diagnosed at a later stage, the cancer can advance to stages characterized by local invasion of the seminal vesicles, followed by metastasis primarily to the bone (Abate-Shen and Shen 2000). The transition to metastatic disease is generally followed by a shift from androgen-dependence to androgen-independence, which is often provoked by androgen-ablation therapy. Androgen ablation therapy is no longer effective in treating androgen-independent, or hormone refractory, prostate cancer (HRPC). Oncologists adjust the therapeutic regimen by introducing chemotherapeutics alone or in combination to try to stop metastases. Unfortunately, chemotherapeutics are not very effective, in part because several anti-apoptotic factors are present in malignant prostate cells (Lebedeva et al. 2000; Raffo et al. 1995; Vlietstra et al. 1998). Some clinical oncologists debate that doing nothing at all may be the right course of action as some HRPC prostate metastases are slow growing and the quality of life of the patient outweighs the potential benefits of chemotherapy (Bhatnagar et al. 2004; Gulley and Dahut 2003).

For many patients, the HRPC is aggressive and requires further intervention. The androgen receptor (AR) is expressed at high levels in both androgen-dependent and – independent cancers at both the primary and metastatic sites and therefore has represented an obvious chemotherapeutic target (Hobisch et al. 1995; Marcelli and Cunningham 1999). However, mutations in the AR along with the aberrant expression of co-activator proteins can induce transcriptional activation in response to antiandrogens and endogenous hormones leading to cancer progression and therapeutic resistance (Buchanan et al. 2001; Heinlein and Chang 2002). Therefore, new modalities are needed not only for HRPC, but also in the treatment of primary prostate cancer prior to metastasis and androgen-independence.

Towards this end, we have designed a multi-functional molecule which incorporates several mechanisms of action into a single anticancer agent. Our molecule

produces covalent DNA adducts that have high affinity for the AR, a protein essential for tumor growth and survival. The attraction of the AR to the sites of damaged DNA would camouflage the adducts from repair enzymes and prevent the AR from performing its transcriptional activities necessary for tumor growth and survival. We believe the sum of these mechanisms of action – DNA damage, repair shielding, and transcription factor hijacking – could lead to increased efficacy in the treatment of prostate cancers.

In the previous two chapters I have described many of the properties which indicate our lead compound, 11β, to be a potentially effective anticancer agent. In Chapter 6, I discussed the results of several *in vitro* experiments, which indicated that 11β has a high affinity for the AR, a low log D, and differential toxicity in favor of killing AR expressing cell lines in culture. In Chapter 7, I discussed the results of *in vivo* experiments in which I illustrated the favorable pharmacokinetics, bio-distribution, and low toxicity of 11β. Here I will discuss the potential of 11β as a chemotherapeutic in the treatment of LNCaP xenografts as well as the toxicity to mice treated with several cycles of this agent. Furthermore, I shall discuss the results of several experiments in which I have quantified the number of DNA adducts formed in cells treated in culture and in liver and tumor tissue from mice treated with 11β. I believe these experiments will indicate the potential therapeutic benefit for patients with prostate cancer.

Materials and Methods

Animals. Four to six week old NIH Swiss *nu/nu* athymic mice (25 g) were purchased from the National Cancer Institute-Frederick Cancer Center (NCI), (Frederick, MD). The mice were housed under standard conditions in MIT approved facilities with 12 hour light/dark cycles and food and water *ad libitum.* All protocols were performed in compliance with the regulations of the Animal Care Committee at MIT.

Cell Culture. The human prostate cell lines, LNCaP and T-47D, the human cervical cancer cell line, HeLa, and the human colon cancer cell line, DLD-1, were obtained from the American Type Culture Collection (Rockville, MD). The LNCaP cell line was maintained in RPMI 1640 supplemented with 2.5 mg/ml glucose, 10% fetal bovine serum (FBS; Hyclone, Salt Lake City, UT), 2 mM glutamax (Gibco), 1 mM sodium pyruvate

and 100 mM HEPES. The T-47D line was maintained in MEM-alpha medium containing 10% FBS (Hyclone), 0.1 mM non-essential amino acids (Invitrogen), 100 mM HEPES, 2 ug/ml bovine insulin, and 1 ng/ml human epidermal growth factor. The HeLa cell line was maintained in DMEM with glutamax (Gibco) supplemented with 10% fetal bovine serum. Cells were grown in a humidified 5% CO_2/air atmosphere at $37^\square$C. When the cells were used for injection into mice, the cells were grown in a P-150 plate to 50-70% confluence. The cells were trypsinized, washed, and pelleted.

Tumor Ablation Therapy. LNCaP, HeLa, and DLD-1 cells were collected and suspended in 50% saline, 50% Matrigel (Becton Dickinson, Franklin Lakes, NJ) and diluted to a concentration of 1 X 10^7 cells/mL. Into the right hind flank of each mouse was injected 0.25 mL of the cell suspension. Additionally, the DLD-1 cells, which are an extremely rapidly growing cell line, were administered into the peritoneal cavity and therapy commenced 3 days after the injection of the cells. Therapy commenced in all other cell lines when a palpable tumor of approximately 4 x 4 mm formed (5-7 days for HeLa cells, 1-2 months for LNCaP cells, and 4-5 days for DLD-1 cells). 11β was formulated in 43% CR-EL, 30% saline, and 27% ethanol and administered IP at a dose of 30 mg/kg. Chlorambucil was dissolved in the same vehicle and injected at an equi-molar dose of 12 mg/kg. Tumor dimensions were measured five times per week with vernier calipers. Tumor volumes were calculated using the formula of an elipse: π/6 x (smaller diameter)^2 x larger diameter. Statistical analyses were performed using a paired t-test. Mice with HeLa xenografts were treated with 3 cycles of 5 days on and 2 days off, mice with LNCaP xenografts were treated with 6.5 cycles, mice with DLD-1 xenografts were treated with 2 cycles, and mice with DLD-1 cells injected intraperitoneally were treated for 1 cycle.

Assessment of Chronic Exposure of 11β. At the end of the LNCaP tumor therapy study, mice were euthanized by CO_2 asphyxiation. Blood was obtained by cardiac puncture and sent to IDEXX (formerly Tufts Veterinary Diagnostic Laboratory, North Grafton, MA) for hematology and blood chemistry analysis.

Quantification of DNA Adducts in cells. LNCaP and T-47D cells were exposed to a 10, 5, 2.5 or 0 μM dose of ^{14}C-11β (specific activity 5 μCi/μmol) dissolved in DMSO for 4 hours. At the end of the incubation the cells were scraped, pelleted, and washed with phosphate buffered saline (PBS). The cells were resuspended in 2 mL of cold (4°C) 0.01 M Tris (pH 6.9), 0.25 M sucrose, 2 mM calcium chloride buffer. Triton X-100 (25% solution) was added to make a final concentration of 5%. The solution was briefly vortexed and then centrifuged at 1000G in a Sorvall RC-2B Centrifuge with a GSA rotor at 4°C for 20 min. The supernatant was removed by aspiration and the nuclear pellet was resuspended in 1 mL of buffer. Sodium dodecyl sulfate (SDS) (5%) and 5 M sodium chloride (NaCl) was added to make a solution with a final concentration of 1% SDS and 1 M NaCl. An equal volume of chloroform:isoamyl alcohol (24:1) was then added and the biphasic mixture was shaken vigorously for 15 min. The mixture was then centrifuged at 7000G for 15 min at 4°C. The aqueous phase was collected and re-extracted with another volume of chloroform:isoamyl alcohol, shaken and centrifuged. The aqueous phase was then collected and the nucleic acids were precipitated with 3 volumes of ice cold ethanol and chilled at -20°C for 20-30 min and subsequently pelleted by centrifugation at 7000G for 15 min at 4°C. The nucleic acids were washed 2 times with cold ethanol and then dried *in vacuo*. The dried pellet was reconstituted with 0.5 mL of 0.05 M Tris (pH 7.5), 0.1 M NaCl on ice. In order to remove any contaminating RNA, 0.2 mg of RNAse A was added and incubated at 37°C for 10 min. The reaction was stopped by cooling on ice, the NaCl concentration was adjusted to 0.9 M, and the DNA was extracted by subsequent additions of chloroform:isoamyl alcohol as indicated above. The aqueous phase from the second extraction was isolated and the DNA was precipitated with 3 volumes of ice cold ethanol, centrifuged, and washed 2 times as above. The concentration of the DNA was obtained by measuring the absorbance at 260 nm. The DNA was dissolved in 0.1-0.5 mL of water, depending on the DNA concentration, and then given to Paul Skipper and Rosa Liberman, both in the Tannenbaum laboratory at MIT, for analysis by AMS as described in Liberman, et al. (Liberman et al. 2004).

Kinetics of 11β DNA adduction in LNCaP cells. LNCaP cells were exposed to a 10 μM concentration of ^{14}C-11β (specific activity 10 μCi/μmol) for 0, 3, 6, 9, 15, and 24 hours. At the end of each incubation period, the cells were scraped, pelleted, and washed with PBS. The DNA was isolated using the above procedure.

Repair of 11β DNA adducts in LNCaP cells. LNCaP cells were exposed to a 2.5 μM dose of ^{14}C-11β (specific activity 27 μCi/μmol) for 2 hours. At the end of the treatment, the media was removed, the cells were washed 3 times with PBS, and fresh media was added. Repair of the DNA adducts was monitored by harvesting cells at 0, 1, 3, 6, 9, 15, and 24 hours after the removal of ^{14}C-11β. The DNA was then isolated as indicated above.

Quantification of DNA Adducts in Tissue. NIH Swiss *nu/nu* mice with LNCaP xenografts were injected with ^{14}C-11β in order to quantify the number of DNA adducts formed in the tumors. 11β was administered intraperitoneally (IP) at a dose of 50 mg/kg spiked with 1 μCi of ^{14}C-11β. The mice were sacrificed after 4 hours by carbon dioxide asphyxiation. The liver was surgically removed, snap frozen on dry ice, and stored at -80 °C until it could be worked up. The DNA was obtained by a similar procedure as described in the "Quantification of DNA adducts in cells" section with a few noted changes. The liver and tumor samples were thawed and homogenized in a Dounce homogenizer on wet ice with 15 mL of cold (4°C) 0.01M Tris (pH 6.9), 0.25 M sucrose, 2 mM calcium chloride buffer. The homogenate was filtered through coarse and then a fine nylon mesh to remove all connective tissue. Triton X-100 (25%) was added to make a final concentration of 5 %. The solution was briefly vortexed and then centrifuged at 1000G in a Sorvall RC-2B Centrifuge with a GSA rotor at 4°C for 20 min. The supernatant was removed by aspiration and the nuclear pellet was resuspended in 2.5 mL of buffer. Sodium dodecyl sulfate (SDS) (5%) and 5 M sodium chloride (NaCl) was added to make a solution with a final concentration of 1% SDS and 1 M NaCl. The nucleic acids were isolated as above and the dried pellet was reconstituted with 2 mL of 0.05 M Tris (pH 7.5), 0.1 M NaCl on ice. In order to remove any contaminating RNA, 0.5 mg of RNAse A was added and incubated at 37°C for 10 min. The DNA was

extracted and the concentration was determined by the same procedures as indicated above. Rosa Liberman and Paul Skipper analyzed the samples.

Results

11β Inhibits the Growth of Xenografts. The cytotoxicity of 11β towards LNCaP cells in culture prompted us to investigate its antitumor properties in a xenograft mouse model. 11β was administered to mice for 6.5 weekly 5-day cycles with a dose of 30 mg/kg and administered IP. As shown in Figure 8.1, this regimen resulted in a 90% growth inhibition of the LNCaP xenografts as assessed on the 45th day of therapy (mean tumor volume of the 11β treated group versus the mean tumor volume of the vehicle only group; P<0.0001). During the course of this regimen, mice in the treated group lost an average of 10 % of their body weight, indicating the treatment was well tolerated by the mice (Fig 8.2). Pictures of representative mice from the 11β treated and vehicle group are shown in Figure 8.3A and B, respectively. The LNCaP tumors are very well vascularized as evident by the blue nodular tumor in Figure 8.3B. Even though there is no tumor evident in the mouse shown in Figure 8.3A, upon removal of 11β the tumor eventually grew back. This indicates that the 45 day regimen was not sufficient in killing 100% of the tumor cells.

In a second experiment with LNCaP xenografts, we compared the efficacy of 11β to chlorambucil at equi-mole doses (30 mg/kg for 11β and 12.6 mg/kg for chlorambucil). Chlorambucil is a clinically used alkylating agent that the DNA damaging portion of 11β was designed after. As shown in Figure 8.4, chlorambucil is more effective in inhibiting the growth of LNCaP xenografts and actually shrinks the tumors, unlike 11β which only inhibits their growth as compared to the vehicle group. In both cases, a paired t-test indicated that P<0.0001 as compared to the vehicle group (error bars were omitted for clarity sake). Despite its increased toxicity towards the LNCaP xenografts, a 12.6 mg/kg dose of chlorambucil was also toxic to the mice as illustrated in Figure 8.5. Mice treated with chlorambucil lost up to 30% of their body weight while 11β was better tolerated , reducing body weight by only 7%. Furthermore, only one chlorambucil treated mouse survived the 45-day treatment regimen, but this lone survivor died 6 days after the

therapy ceased (Fig 8.6). Therefore, at this dose level it seems that the toxicity of chlorambucil to the tumors was also overwhelming to the mice.

11β has also shown toxicity to other cell lines in culture that do not express the AR for reasons yet unknown but possibly unrelated to, or in addition to, the proposed repair shielding and transcription factor hijacking models. (These additional mechanisms were discussed in Chapter 6) Therefore, 11β was administered to mice containing HeLa xenografts to assess its potential as a broader chemotherapeutic agent. Figure 8.7 shows the results of the treatment of the mice after 3 weekly 5 –day cycles of 30 mg/kg administered IP. As evident in the graph, 11β had a significant effect on the xenografts (P<0.0001) as it inhibited their growth by 80% as assessed on the final day of the study (mean tumor volume of treated versus mean tumor volume of the control on day 18). The dose was well tolerated as evident by the modest weight loss in the treated group of 10% (Fig 8.8). Representative examples of the mice treated with 11β and or vehicle alone are illustrated in Fig 8.9A and B, respectively. Unlike the LNCaP tumors, HeLa tumors are not as well vascularized and grow to large, white, nodular tumors. These data indicate that 11β inhibits the growth of the HeLa xenografts and is well tolerated by the mice at this therapeutic dose.

A second cell line that does not express the AR is the colon cancer derived cell line, DLD-1. Cells were injected either as xenografts in the right hind flank of the mice or into the peritoneal cavity. 11β did not have a therapeutic effect on the DLD-1 xenografts that were injected into the flank of mice (data not shown). However, 11β did inhibit the growth of the DLD-1 cells injected into the peritoneal cavity as shown in Figure 8.10A. As a comparison a mouse treated with vehicle only had larger and a greater number of tumors in its abdomen (Fig 8.10B). Unfortunately, the toxicity to the mice in both groups was rather substantial after only 7 days of therapy. Upon necropsy both the vehicle treated and 11β treated mice had adhesions in their abdomen, usually intestinal-to-intestinal but occasionally skeletal muscle or adipose tissue-to-intestinal. The fusing of tissue to a segment of intestines inhibited peristalsis, caused the abdomen of the mice to swell, inhibited the excretion of feces, and caused the mice to lose weight. These data illustrate that 11β is effective against LNCaP and HeLa xenografts but not against DLD-1 xenografts. Although it was also effective against DLD-1 cells injected

into the peritoneal space, this model is not deemed to be very useful as a result of the formation of adhesions in both the treated and vehicle control groups.

Chronic Doses of 11β are Well Tolerated by Mice. The chronic toxicity of 11β was addressed following the administration of 6.5 cycles of 11β to the LNCaP bearing xenograft mice. As indicated above, weight loss was limited to 10 % in treated animals. The hematology report (Table 8.1) indicated that leukopenia was the major toxicological side effect. Additionally, an alteration in the ratio of neutrophils to lymphocytes was observed in both the treated and vehicle control groups, indicating the vehicle may play a role in toxicity. The blood chemistry report did not reveal any significant toxicity (Table 8.2). Creatinine kinase (CK), an indicator of muscle and cardiac toxicity, was elevated slightly in all mice bearing a tumor. This elevation is likely unrelated to 11β. Finally, gamma glutamyl transpeptidase (GGT) was depressed in the mice treated with 11β, perhaps indicative of hypothyroidism, hypothalamic malfunction, or low magnesium level. Overall, the results after a 45 day regimen of 11β at a dose of 30 mg/kg are extremely encouraging as toxicity seemed to be relatively mild.

Quantification of DNA Adduct Formation in Tissues and Cells. 11β has been shown to be an effective agent in the therapy of LNCaP xenografts with minimal unwanted toxicity. The efficacy of 11β is likely related to the formation of DNA adducts. Therefore, we wanted to obtain information regarding the number of DNA adducts formed in tumor tissue after a therapeutic dose of 11β as well as in LNCaP cells *in vitro*. An understanding of the rate of DNA adduction and the rate of repair of these adducts when LNCaP cells are exposed to 11β in culture could assist us in increasing the efficacy of 11β towards xenograft tumors and in the development of new therapeutic regimens. Furthermore, the work here will establish a groundwork for which future generations of compounds or vehicles can be assessed.

In an initial effort to gauge the number of DNA adducts formed by a treatment of 11β we treated LNCaP and T-47D cells with a 10, 5, or 2.5 μM dose. (Note: T-47D cells also express the AR). As shown in Figure 8.11, DNA adduct formation is dose dependent with roughly a 4:2:1 ratio of adducts at the three dose levels. T-47D cells

acquired 13,500 DNA adducts after a 4 hour exposure time to 10 µM 11β. In LNCaP cells however, 11β only formed 5,400 DNA adducts at the same dose. In fact, at all dose levels T-47D cells acquired greater than 2-fold more DNA adducts than did LNCaP cells. Interestingly, work by John Marquis of the Essigmann Laboratory has shown that the two cell lines are essentially equi-sensitive to exposures of 11β -- a 7.5 to 10 µM dose of 11β in either cell line is enough to kill essentially 100% of all the cells on a culture dish.

The rate of DNA adduction over time was then assessed in LNCaP cells treated with a 10 µM dose of 11β. 11β adducted DNA in these cells in a linear manner for 24 hours at a rate of 1500 adducts/hour (R^2 = 0.98). These results, shown in Figure 8.12, are consistent with those displayed in Figure 8.11, as a 10 µM dose of 11β produces 6,000 and 5,400 DNA adducts, respectively, after a 4 hour exposure in both experiments.

In order to monitor the repair of DNA adducts over time, LNCaP cells were exposed to a sub-lethal dose of 11β (2.5 µM) for a brief 2 hour period. The compound was then removed and the cells were washed several times to remove any drug not already incorporated within the cells. As seen in Figure 8.13, the rate of DNA adduction was greater than the rate of repair for the first 9 hours as evident in the increasing number of DNA adducts to this point (550 adducts/hour). However, subsequent to the 9 hour time point, DNA repair overwhelmed the rate of DNA adduction and removal of adducts was seen at a rate of 260 adducts/hour.

Finally, the number of DNA adducts formed *in vivo* was addressed. Three LNCaP xenograft mice were administered a 50 mg/kg dose of 11β. Based on the results described for the bio-distribution experiment described in the previous chapter, the liver was harvested due to the high concentrations of compound that accumulated in the liver at all time points in addition to tumor tissue. The 4 hour time point was chosen since the bio-distribution results show peak accumulation in the liver and most other organs 4 hours after dosing. Not surprisingly, given the route of administration and the bio-distribution results, the liver had significantly higher accumulation of 11β than did the tumor tissue in all three mice. In fact, the liver accumulated almost 10-fold more adducts than tumor tissue, an average of 12,500 adducts in liver tissue as compared to only 1,600 in tumor tissue (Fig 8.14). These results may give credence to the repair shielding and transcription factor hijacking models as 11β inhibited the growth of the LNCaP tumors

while remaining essentially non-toxic to the mouse. With such a high level of DNA adducts in the liver, it is rather surprising that more toxicity was not evident. The rate of repair of these liver adducts may have been greater than in the tumor tissue. Alternatively, a heretofore unidentified biochemical feature of the tumor cells makes these cells hyper-sensitive to 11β.

Discussion

There is accumulating evidence that antihormones, chemotherapeutics, and other cancer therapies, such as radiation, induce apoptosis in their tumor targets. Disruption of the apoptotic cell death pathway may therefore lead to drug resistance (El Etreby et al. 1998; El Etreby et al. 2000; McConkey, Greene, and Pettaway 1996). Suppression of apoptosis may also contribute to tumor progression and metastasis. The possibility that the disruption of the apoptotic pathway may contribute to androgen-independent progression and tumor metastasis has been suggested in a recent study using nonmetastatic and metastatic variants of the LNCaP cell line (McConkey, Greene, and Pettaway 1996). The emergence of androgen-independent clones of cells that do not respond to traditional androgen ablation therapy may involve the acquisition of intrinsic apoptosis resistance (Gingrich et al. 1997; Isaacs and Coffey 1981; Kyprianou 1994; McConkey, Greene, and Pettaway 1996). A single compound that can induce cell death by several different mechanisms simultaneously may provide a novel therapeutic approach to overcome intrinsic apoptosis resistance in androgen-independent cells. Furthermore, a molecule of this type may also be more effective against primary prostate cancer than current therapies. Towards this end we have designed a single molecule capable of covalently modifying DNA and simultaneously attracting tumor specific proteins to the site of the lesion. A protein-DNA adduct complex could inhibit repair enzymes from accessing the lesion and, if this protein is a transcription factor as is the case with the AR, an association with the DNA adduct could disrupt necessary signaling events. These mechanisms would likely be lethal to a cancerous cell.

In the previous chapters I have reported on the design and features of our lead compound, 11β, that could potentially inhibit tumor growth by the repair shielding and transcription factor hijacking mechanisms. Several experiments were described that

illustrate the potential of 11β to be an effective anticancer agent – it has a high affinity for the AR, displays differential toxicity in favor of AR-expressing prostate cancers, favorable pharmacokinetics, and good overall bio-distribution.

Here I assessed the potential of 11β as an anticancer chemotherapeutic using xenograft mouse models. The results illustrated that a 30 mg/kg dose of 11β administered IP in a CR-EL based vehicle inhibits the growth of LNCaP xenograft tumors by an average of 90 % as compared to the vehicle only group after a 45 day therapy regimen. The toxicity to the mice was relatively modest with a 10% loss in body weight. In a second experiment the therapeutic benefit of 11β was compared directly to chlorambucil. If one were to look only at the growth inhibition of the two compounds, chlorambucil would be obviously superior. However, chlorambucil also caused a reduction in body weight by as much as 30% and also was responsible for the death of all mice in this treated group. The inhibition of growth seen with the LNCaP xenografts was in part a result of the toxicity of chlorambucil to the mouse – as the mouse lost weight, sufficient nourishment was not available for the tumor to grow and therefore the tumor was not able to grow as rapidly. These results indicate that at equi-mole doses, chlorambucil is significantly more toxic than 11β.

Increased therapeutic benefit of chlorambucil as compared to 11β may also be attributed to its aqueous solubility. In Chapter 6, I reported the log P of chlorambucil (1.44 by HPLC but -0.66 in other literature reports) (Greig et al. 1990) and 11β (5.05). Even though 11β would likely be ionized under physiological conditions, the log P clearly illustrates that chlorambucil is much more water soluble than 11β. Therefore, one of the possible reasons why chlorambucil was more effective in reducing the growth of the LNCaP xenografts was increased distribution to the tumor as a result of its increased aqueous solubility.

The results from cell culture work indicated that 11β was cytotoxic to cell lines in addition to the AR(+) LNCaP cells. HeLa cells are a cervical cancer derived cell line that does not express the AR but was found to be sensitive to exposure to 11β. HeLa cells grow much more rapidly than LNCaP cells, and we therefore tested this cell line as a more aggressive cancer in a xenograft mouse model. Mice were treated with a dose of 30 mg/kg and injected 5 days per week for 3 cycles. The rapidly growing HeLa cells formed

palpable xenograft tumors 5-7 days after inoculation of 3 x 10^6 cells (LNCaP required 1-2 months before tumors were evident). The growth of the HeLa xenograft tumors were inhibited by 80% and the toxicity was again limited to only 10% loss in body weight. These results illustrate the effectiveness of 11β as an anticancer agent against a more rapidly growing cell line that does not contain the AR.

DLD-1 cells replicate even more quickly than the HeLa cells, and palpable tumors grew in the hind flank of mice after only 4-5 days after an inoculation of 3 x 10^6 cells. Perhaps as a result of the intensity in proliferation of this cell line, 11β did not display a therapeutic benefit to the xenografts. Although this result was somewhat discouraging, we reasoned there could be many possibilities as to why 11β was ineffective against this cell line: DLD-1 cells do not express the AR, the cells grow extremely quickly, or the therapeutic regimen of one injection per day may not have been sufficient as a result of poor distribution or speed in which the cells divide. In order to address the issue of distribution to the tumor, we inoculated the DLD-1 cells into the peritoneal cavity of mice and began a therapeutic course after only 3 days. As shown in Fig 8.10, 11β did indeed display a therapeutic benefit when compared to the vehicle group.

The results with the HeLa and DLD-1 xenograft experiments indicate that there may be cytotoxic properties unrelated to repair shielding and transcription factor hijacking. These properties (discussed in Chapter 6), possibly unrelated to the attraction of the AR to the sites of DNA damage, may prove 11β to have wider applicability in treating cancers of various origins. We are only now beginning to investigate these possible additional mechanisms and aspects of 11β that may make it a chemotherapeutic with broader applicability.

The mechanism(s) by which 11β has proven to be cytotoxic to malignant cells expressed as xenografts is still not fully understood. However, one aspect of 11β that is clear is its minimal toxicological side effect profile. Overall, 11β is well tolerated by mice injected with a 30 mg/kg therapeutic dose. Weight loss was limited to less than 10 % in all mice treated with 6.5 cycles of 11β. The dose limiting toxicity for tumor ablation therapy seems to be leukopenia as the white blood cell level dropped from 5-7 (x mm^3) to 1 (x mm^3). This fact is not surprising as many anticancer agents, including chlorambucil, induce myelosuppression (Inoue et al. 1987). The dose limiting toxicity of

chlorambucil is, in fact, neutropenia, or a decrease in neutrophils (Blumenreich et al. 1988). As in the acute dose of 11β, the ratio of neutrophils to lymphocytes is altered such that the percent of neutrophils increases as compared to the percentage of lymphocytes. Even though these values are still within the normal range provided by Taconic, it is noted that in both the acute and chronic administrations of 11β the same result is observed. The elevation of neutrophils and suppression of lymphocytes could be the result of an active infection or sensitivity to the vehicle.

Alternatively, the elevation of neutrophils and suppression of lymphocytes may indicate that 11β is interacting with the glucocorticoid receptor (GR). The GR is a member of the same class of nuclear hormone receptors as the ER and AR. Corticosteroids, the natural ligands for the GR, have profound effects on lymphocytes and neutrophils. Corticosteroids actually induce the apoptosis of lymphocytes, (Di et al. 2000; Negoescu et al. 1998) whereas they inhibit the death of neutrophils *in vitro* (Cox and Austin 1997; Liles et al. 1996). The mechanisms by which lymphocyte and neutrophil apoptotic responses to glucocorticoids differ are unknown. However, glucocorticoid action is mediated through the GR and therefore these apoptotic differences may arise from downstream targets of the GR (O'Malley 1971; Strickland et al. 2001; Wenzel et al. 1997). An off-target interaction of 11β with the GR may mediate the responses seen in the alteration in the ratio of neutrophils to lymphocytes. In fact, Nicole Dinaut, a former post-doctoral associate in the Essigmann Laboratory, has shown the RBA of 11β for the GR to be 2 as compared to dexamethasone. Although this is not a strong interaction, it may be sufficient in decreasing the lymphocyte count and increasing the neutrophil count as we have seen here.

The blood chemistry profile after chronic administration of 11β is relatively mild. CK is elevated in all tumor bearing mice and therefore the increased levels are unlikely related to the compound or the vehicle. GGT is involved in the transport of amino acids and peptides into cells as well as in glutathione metabolism. As a liver enzyme it is extremely sensitive to ethanol; however, GGT levels typically increase in alcoholics or in those with liver disease. In mice treated with 11β, GGT decreased. Hepatotoxicity can be ruled out as the other enzymes typically elevated were found to be normal (AST, ALT, amylase, and lipase). The decreased level of GGT could be indicative of hypothyroidism,

hypothalamic function, or low level of magnesium. Further tests would be required to determine why a low level of GGT was observed.

The minimal toxicity that was observed is likely the result of DNA adduction in non-target tissues (Bank 1992; Fox and Scott 1980; van Zeeland 1996). Nitrogen mustards elicit their cytotoxic and anticancer effects through the covalent modification of DNA. The lone pair electrons of the unprotonated nitrogen in agents such as chlorambucil and melphalan attack one of the 2-chloroethyl arms in an intramolecular, rate-determining step to form a positively charged aziridinium ion. The attack of the aziridinium ion by an external nucleophile, such as guanine or adenine, results in the formation of a DNA adduct (Chatterji, Yeager, and Gallelli 1982; Kundu, Schullek, and Wilson 1994; Owen and Stewart 1979). A small portion of these monoadducts go on to form crosslinks as a result of a second alkylation reaction with the other arm of the nitrogen mustard. The formation of crosslinks between the 2 strands of DNA, interstrand crosslinking, is considered to be a critical event, and there is clear evidence that their formation and subsequent persistence correlates with *in vitro* cytotoxicity (O'Connor and Kohn 1990; Sunters et al. 1992). However, the abundance of crosslinks is low because of the slower rate of alkylation for the second arm of a nitrogen mustard (Gould, Nixon, and Tilby 2004; Ross, Ewig, and Kohn 1978) and a comparatively quick rate of repair of a monoadduct. Furthermore, the high water concentration in a cell (55 M) results in a significant number of monoadducts reacting with water rather than a second DNA base. The cytotoxicity of nitrogen mustards is thus related to the number of adducts formed. If a sufficient number of adducts form, the repair capacity of a cell would be saturated and thus result in lethal effects in a tumor. A potential advantage of 11β is its ability to attract the AR. An association between the AR and an 11β monoadduct could provide more time for the formation of a cross-link and thus render an 11β monoadduct more toxic than a monoadduct from other nitrogen mustards.

Although we were unable to measure the formation of crosslinks, we were able to monitor the formation of all DNA adducts after cells or mouse tissues were exposed to 11β using the highly sensitive technique of AMS. As a proof of concept, the AR(+) LNCaP and T-47D cell lines were exposed to increasing doses of 11β. As expected, a

higher dose of 11β resulted in a greater number of DNA adducts and in both cell lines the number of adducts formed was roughly proportional to the dose.

The results in Chapter 6 indicated that a 10 μM dose of 11β was lethal to 98% of LNCaP cells in a culture dish after a brief 2 hour exposure. Of significance is the number of DNA adducts that had formed in these cells after a 10 μM exposure. Therefore, we treated cells for various lengths of time and monitored the formation of DNA adducts. DNA adducts accumulated in LNCaP cells at a rate of 1500 adducts/hour. It is somewhat surprising, however, that 24 hours later 11β was still forming DNA adducts as efficiently as it was at earlier time points. One would think that such long durations in aqueous media would render the compound inactive as a result of the deactivation of the compound through hydrolysis of the bis-chloroethyl arms of the nitrogen mustard, a decrease in effective concentration as a result of this deactivation, and also as a result of the removal of DNA adducts by repair enzymes. Chlorambucil was shown to have a half-life of only 18 minutes in a non-nucleophilic, chloride-free buffer at 37°C (Haapala et al. 2001) and 2.4 hours in blood samples where the chloride concentration approaches 100 mM (Newell, Shepherd, and Harrap 1981). Therefore, it is surprising that 11β was capable of forming DNA adducts at such a consistent rate for such a long period of time. Perhaps its lipophilicity results in initial absorption into lipid compartments, in which it is chemically stable, and from which it is slowly delivered to the aqueous portions of the cell – including those portions containing DNA.

The rate of repair of 11β DNA adducts was also investigated by treating cells for a brief 2 hour incubation period and then replacing the drug containing media with drug free media. DNA adducts continued to form for 9 hours after the drug was removed. This indicates that a substantial fraction of 11β entered the cells and likely was not excreted (or at least not very quickly). Evidence of DNA repair was seen at time points later than 9 hours, as the number of DNA adducts eventually diminished. Interestingly, the number of adducts formed at 24 hours was still greater than that at the earliest time points. The longevity of the DNA adducts may implicate the repair shielding hypothesis. The dose of 11β used was sub-lethal, so any disruption in cellular signaling as a result of transcription factor hijacking was minimal as no toxicity was evident.

The results from the 11β DNA adduct repair experiment may also provide insight as to why the compound is an effective agent in the treatment of LNCaP xenografts. The level of DNA adducts formed 4 hours after the administration of a 50 mg/kg dose of 11β was approximately 1600 adducts per cell. Assuming that the LNCaP xenograft tumors behave as the LNCaP cells in the repair experiment, it is likely that the number of DNA adducts at 24 hours is close to the number of adducts at 4 hours. With the 5-day treatment cycle that we used in the therapy of the xenografts, approximately 8,000 DNA adducts would be present in each LNCaP tumor cell at the end of each cycle. The level of adducts may increase considerably with each subsequent cycle such that after 4 or 5 cycles each tumor cell may contain 20,000-50,000 adducts, a level likely to be toxic to a cell.

It is difficult to compare the DNA adduct levels formed after 11β treatments to mice with other nitrogen mustards like chlorambucil or melphalan, as there is very little literature that quantifies DNA adduct levels. Many reports used a technique known as alkaline elution that can only determine relative abundance of DNA adducts (Gould, Nixon, and Tilby 2004; Rink et al. 1996; Ross, Ewig, and Kohn 1978; Sunters et al. 1992). However, one report indicates that a patient with plasma cell leukemia treated with high doses of melphalan had 160,000 melphalan-DNA adducts (Tilby et al. 1993). This is 100-fold higher than what was observed in LNCaP xenografts treated with 11β, also at a therapeutically beneficial level. Although it is somewhat difficult to directly compare two different compounds (with different pharmacokinetics and aqueous solubility) in two different cell types, such a drastic difference in DNA adduct burden may imply mechanisms other than saturation of the DNA repair machinery may play a role in the cytotoxicity of 11β. Until such a time as a direct comparison of DNA adduct levels achieved by doses of melphalan (or chlorambucil) and 11β in the same cell type can be made, speculation on additional mechanisms, related or unrelated to DNA alkylation, is futile at best. Nonetheless, it remains worthwhile to explore the mechanisms by which 11β was designed to achieve toxicity – repair shielding and transcription factor hijacking.

Conclusion

Currently, the most effective therapy against advanced prostate cancer is the combination of docetaxel with prednisone. This combination results in an improvement in median survival time of a paltry 3 months (Walsh 2005). We believe a way to increase the therapeutic effectiveness of an anticancer agent is by designing a single molecule that can act by several distinct mechanisms simultaneously. We have designed a molecule, 11β that is not only capable of forming DNA adducts, but can also attract tumor specific proteins causing the DNA adducts to be shielded from repair enzymes. Furthermore, if the protein attracted to the site of the DNA damage is a transcription factor, as is the case for the AR which is expressed at high levels in prostate cancers (Hobisch et al. 1995; Marcelli and Cunningham 1999), a protein-DNA adduct complex would likely disrupt necessary signaling events.

In the previous chapters, I have described the results of several experiments indicating that our lead compound, 11β, has many favorable properties of a chemotherapeutic agent. Here I described the results from several tumor inhibition studies using 3 different cell lines. 11β inhibited the growth of AR(+) LNCaP cells implanted as xenografts most efficiently (90% as compared to the growth of xenografts in control mice treated with vehicle only) with very little toxic side-effects. 11β was also found to be effective against two other cell lines, HeLa and DLD-1, implanted as a xenograft or into the peritoneal cavity, respectively. Neither of these cell lines expresses the AR and therefore the results with these two cell lines may indicate mechanisms unrelated to repair shielding and transcription factor hijacking. We are currently investigating these other possible mechanisms.

I also described the results from several experiments in which we monitored the number of DNA adducts that had formed after various doses and times of incubation. These results indicated that the AMS technology is a very sensitive means of monitoring DNA adduct formation. We will continue to use AMS to gain further insight into the dynamics of adduct formation and repair in cells treated with 11β. The results here suggest that the adducts formed by 11β persist for long periods of time, and perhaps the accumulation of these adducts after several days of therapy results in toxicity to the LNCaP xenografts. The relatively low level of adducts formed in the LNCaP xenografts,

as compared to what has been reported for a patient with plasma cell leukemia treated with high doses of melphalan (Tilby et al. 1993), may suggest that 11β is indeed disrupting necessary signaling events in the xenograft tumor. This cellular signaling disruption may be the result of the repair shielding and transcription factor hijacking mechanisms we originally proposed.

Future Directions

In this chapter, I have discussed the results of several xenograft models – LNCaP, HeLa and DLD-1. Of the three, only one is derived from malignant prostatic tissue. In chapter 2, I discussed the results of a differential toxicity experiment in which LNCaP cells were more sensitive to 11β than PC-3 and DU-145 cells, both of which are AR(-) prostatic malignancies. It would be of considerable interest to inject these cell lines into mice and compare the efficacy of 11β against these AR(-) xenografts. If 11β is indeed working by our proposed mechanisms, then it should be less effective against the AR(-) PC-3 and DU-145 cells. Furthermore, quantifying the formation of DNA adducts in these cells, both in culture and in xenografts, could provide additional insight into the role of the AR in cellular toxicity. An equal number of DNA adducts in the three cell lines would imply that the AR may have a role in any differential toxicity observed between the AR(+) and AR(-) cells. Ideally, isogenic clones that express or are deficient in the AR would be used; however, I am unaware of any such clones. For the reasons discussed in the "future work" section of Chapter 4, incorporating the AR into a deficient cell line may result in altered proliferation of the clone and therefore such an approach is unwarranted (Hobisch et al. 1995; Jiang and Jordan 1992; Kushner et al. 1990; Maminta, Molteni, and Rosen 1991; Touitou, Mathieu, and Rochefort 1990; Watts, Parker, and King 1989).

The CWR22 and CWR22R cell lines may also be very useful in isolating the role of the AR in the cytotoxic properties of 11β. CWR22 cells, like LNCaPs, are a prostate cancer cell line that expresses the AR and is hormone dependent (Kochera et al. 1999). The CWR22R cell line was derived from a xenograft that was serially propagated in mice after castration-induced regression and relapse of the CWR22 xenograft. These cell lines

represent models of early stage hormone-dependent and late stage hormone-independent prostate cancer. Both the CWR22 and CWR22R xenografts have responses to antitumor agents that are representative of patient tumors (Chen et al. 1998), making them excellent models with which we can further evaluate 11β.

Additionally, more work with the T47-D cells could also be informative. T47-D, like LNCaP cells, express the AR. Comparing the rates of DNA adduction and repair of the cell lines to that of the AR(-) PC-3 and DU-145 cell lines would likely provide further insight into the repair shielding and transcription factor hijacking hypotheses. Since these cell lines were derived from actual cancer patients, each cell line has different mutational spectra in addition to their differences in AR expression. By using several cell lines, it may be easier to parse out differences related to AR expression rather than to other mutations that could cause one cell line to be more sensitive than the others for reasons other than AR expression.

For some time we were limited in our experiments by not having a control compound by which we could compare DNA adduct levels. We have used chlorambucil as a control compound in many of our *in vitro* studies; however, ^{14}C-chlorambucil is prohibitively expensive. Recently, however, we found a supplier of ^{14}C-melphalan and we have begun using it in order to assess a toxicological effect with DNA adduct burden. Our results thus far have been in MCF-7 and MDA-MB231 cells and the comparison has been with E2-7α (described in Chapter 5). We will begin treating prostate cancer cells with ^{14}C-melphalan in order to assess toxicity in relation to the number of DNA adducts that form. If melphalan forms a greater number of DNA adducts at the LD_{50} than does 11β, it would suggest that mechanisms other than DNA adduction were involved in the toxicity of 11β. Furthermore, if the rates of repair of the two molecules differed significantly, it may imply the repair shielding and transcription factor hijacking hypotheses are valid. Other mechanisms unrelated to DNA adduction could not be ruled out, however. Furthermore, these experiments could also be carried out in xenograft tissue to compare the number of DNA adducts formed after therapeutic doses of each compound. Again, these experiments could provide insight into mechanism.

We have received a grant from the National Cancer Institute for the continued development in transitioning 11β from the benches at MIT to clinical medical centers

throughout the country. They are in the process of testing the effects of 11β in a 60 cell line screen. These 60 cell lines represent a diverse array of cancers ranging from solid tumors such as prostate, breast and lung, to hematological cancers. The results from this screen will indicate certain cell lines that are sensitive to 11β while also providing us with cell lines that are resistant (should they exist). Sensitive cell lines will be analyzed for mechanisms related to or unrelated to AR expression. Using the AMS technology we would like to assess the contribution of DNA adduction to the cytotoxic properties of 11β.

The experiments proposed above will be combined with biochemical studies that will ascertain the cellular responses after treatment with 11β. Not only will we be able to monitor the consequences of DNA adduction by cellular toxicity, but we will also monitor changes in protein expression. For example, others in the Essigmann Laboratory have shown that treatment of LNCaP cells with 11β results in increased expression of the cyclin-dependent kinase (CDK) inhibitors, p27 and p21. Skp2 is reported to be a key factor in regulating CDK expression levels in many malignancies (Gstaiger et al. 2001) including prostate cancer (Lu, Schulz, and Wolf 2002) and helps tag p27 for proteolytic degradation. The induction of p27 led us to investigate the fate of Skp2. 11β rapidly decreases the expression of Skp2. Therefore, the increased expression of p27 is likely a result of the decreased expression of Skp2. Although we have only recently begun to investigate the biochemical changes associated with 11β treatment of cells, we are enthusiastic about having a means of directly comparing DNA adduct burden with biochemical and physiological changes.

Finally, the results obtained with both the acute (Chapter 7) and chronic toxicity experiments reveal an interesting phenomenon with respect to the ratio of neutrophils to lymphocytes after a dose of 11β. In both toxicity experiments, the percent of white blood cells that were neutrophils increased as compared to the percent that were lymphocytes. One possible explanation involves the glucocorticoid receptor. Evidence has implicated corticosteroids, the natural ligands for the GR, actually induce the apoptosis of lymphocytes, (Di et al. 2000; Negoescu et al. 1998) whereas they inhibit the death of neutrophils *in vitro* (Cox and Austin 1997; Liles et al. 1996). Nicole Dinaut has shown that the GR has a low, but finite, affinity for 11β (RBA ~2, as compared to

dexamethasone). This may imply that 11β is acting as a corticosteroid and inducing apoptosis in lymphocyte cells and stimulating neutrophil proliferation. A more direct way to investigate the effect of 11β on lymphocytes and neutrophils would be to expose both cell types to 11β *in culture*. Since 11β is a reactive nitrogen mustard and may actually be toxic to both cell lines for its DNA damaging properties, a "defanged" version could be made by replacing the chloride atoms with hydroxyl or methoxyl substituents. These unreactive molecules would not be able to damage DNA and therefore may be capable of stimulating neutrophil proliferation through interactions with the GR while leaving genomic DNA unscathed.

Reference List

Abate-Shen, C. and Shen, M.M. Molecular genetics of prostate cancer. *Genes Dev.* **14**, 2410-2434 (2000)

Bank, B.B. Studies of chlorambucil-DNA adducts. *Biochem. Pharmacol.* **44**, 571-575 (1992)

Bhatnagar, V., Stewart, S.T., Bonney, W.W., and Kaplan, R.M. Treatment options for localized prostate cancer: quality-adjusted life years and the effects of lead-time. *Urology* **63**, 103-109 (2004)

Blumenreich, M.S., Woodcock, T.M., Sherrill, E.J. et al. A phase I trial of chlorambucil administered in short pulses in patients with advanced malignancies. *Cancer Invest* **6**, 371-375 (1988)

Buchanan, G., Irvine, R.A., Coetzee, G.A., and Tilley, W.D. Contribution of the androgen receptor to prostate cancer predisposition and progression. *Cancer Metastasis Rev.* **20**, 207-223 (2001)

Chatterji, D.C., Yeager, R.L., and Gallelli, J.F. Kinetics of chlorambucil hydrolysis using high-pressure liquid chromatography. *J. Pharm. Sci.* **71**, 50-54 (1982)

Chen, C.T., Gan, Y., Au, J.L., and Wientjes, M.G. Androgen-dependent and -independent human prostate xenograft tumors as models for drug activity evaluation. *Cancer Res.* **58**, 2777-2783 (1998)

Cox, G. and Austin, R.C. Dexamethasone-induced suppression of apoptosis in human neutrophils requires continuous stimulation of new protein synthesis. *J. Leukoc. Biol.* **61**, 224-230 (1997)

Di, B.A., Secchiero, P., Grilli, A. et al. Morphological features of apoptosis in hematopoietic cells belonging to the T-lymphoid and myeloid lineages. *Cell Mol. Biol. (Noisy. -le-grand)* **46**, 153-161 (2000)

El Etreby, M.F., Liang, Y., Johnson, M.H., and Lewis, R.W. Antitumor activity of mifepristone in the human LNCaP, LNCaP-C4, and LNCaP-C4-2 prostate cancer models in nude mice. *Prostate* **42**, 99-106 (2000)

El Etreby, M.F., Liang, Y., Wrenn, R.W., and Schoenlein, P.V. Additive effect of mifepristone and tamoxifen on apoptotic pathways in MCF-7 human breast cancer cells. *Breast Cancer Res. Treat.* **51**, 149-168 (1998)

Fox, M. and Scott, D. The genetic toxicology of nitrogen and sulphur mustard. *Mutat. Res.* **75**, 131-168 (1980)

Gingrich, J.R., Barrios, R.J., Kattan, M.W. et al. Androgen-independent prostate cancer progression in the TRAMP model. *Cancer Res.* **57**, 4687-4691 (1997)

Gould, K.A., Nixon, C., and Tilby, M.J. p53 elevation in relation to levels and cytotoxicity of mono- and bifunctional melphalan-DNA adducts. *Mol. Pharmacol.* **66**, 1301-1309 (2004)

Greig, N.H., Genka, S., Daly, E.M. et al. Physicochemical and pharmacokinetic parameters of seven lipophilic chlorambucil esters designed for brain penetration. *Cancer Chemother. Pharmacol.* **25**, 311-319 (1990)

Gstaiger, M., Jordan, R., Lim, M. et al. Skp2 is oncogenic and overexpressed in human cancers. *Proc. Natl. Acad. Sci. U. S. A* **98**, 5043-5048 (2001)

Gulley, J. and Dahut, W.L. Novel approaches to treating the asymptomatic hormone-refractory prostate cancer patient. *Urology* **62**, 147-154 (2003)

Haapala, E., Hakala, K., Jokipelto, E. et al. Reactions of N,N-bis(2-chloroethyl)-p-aminophenylbutyric acid (chlorambucil) with 2'-deoxyguanosine. *Chem. Res. Toxicol.* **14**, 988-995 (2001)

Heinlein, C.A. and Chang, C. Androgen receptor (AR) coregulators: an overview. *Endocr. Rev.* **23**, 175-200 (2002)

Hobisch, A., Culig, Z., Radmayr, C. et al. Distant metastases from prostatic carcinoma express androgen receptor protein. *Cancer Res.* **55**, 3068-3072 (1995)

Inoue, K., Ogawa, M., Horikoshi, N. et al. [Phase II study of chlorambucil in patients with hematological malignancies]. *Gan To Kagaku Ryoho* **14**, 2672-2675 (1987)

Isaacs, J.T. and Coffey, D.S. Adaptation versus selection as the mechanism responsible for the relapse of prostatic cancer to androgen ablation therapy as studied in the Dunning R-3327-H adenocarcinoma. *Cancer Res.* **41**, 5070-5075 (1981)

Jiang, S.Y. and Jordan, V.C. Growth regulation of estrogen receptor-negative breast
    cancer cells transfected with complementary DNAs for estrogen receptor. *J. Natl.
    Cancer Inst.* **84**, 580-591 (1992)

Kochera, M., Depinet, T.W., Pretlow, T.P. et al. Molecular cytogenetic studies of a
    serially transplanted primary prostatic carcinoma xenograft (CWR22) and four
    relapsed tumors. *Prostate* **41**, 7-11 (1999)

Kundu, G.C., Schullek, J.R., and Wilson, I.B. The alkylating properties of chlorambucil.
    Pharmacol. Biochem. Behav. **49**, 621-624 (1994)

Kushner, P.J., Hort, E., Shine, J. et al. Construction of cell lines that express high levels
    of the human estrogen receptor and are killed by estrogens. *Mol. Endocrinol.* **4**,
    1465-1473 (1990)

Kyprianou, N. Apoptosis: therapeutic significance in the treatment of androgen-
    dependent and androgen-independent prostate cancer. *World J. Urol.* **12**, 299-303
    (1994)

Lebedeva, I., Rando, R., Ojwang, J. et al. Bcl-xL in prostate cancer cells: effects of
    overexpression and down- regulation on chemosensitivity. *Cancer Res.* **60**, 6052-
    6060 (2000)

Liberman, R.G., Tannenbaum, S.R., Hughey, B.J. et al. An interface for direct analysis of
    (14)c in nonvolatile samples by accelerator mass spectrometry. *Anal. Chem.* **76**,
    328-334 (2004)

Liles, W.C., Kiener, P.A., Ledbetter, J.A. et al. Differential expression of Fas (CD95) and
    Fas ligand on normal human phagocytes: implications for the regulation of
    apoptosis in neutrophils. *J. Exp. Med.* **184**, 429-440 (1996)

Lu, L., Schulz, H., and Wolf, D.A. The F-box protein SKP2 mediates androgen control of
    p27 stability in LNCaP human prostate cancer cells. *BMC. Cell Biol.* **3**, 22-2002)

Maminta, M.L., Molteni, A., and Rosen, S.T. Stable expression of the human estrogen
    receptor in HeLa cells by infection: effect of estrogen on cell proliferation and c-
    myc expression. *Mol. Cell Endocrinol.* **78**, 61-69 (1991)

Marcelli, M. and Cunningham, G.R. Hormonal signaling in prostatic hyperplasia and
    neoplasia. *J. Clin. Endocrinol. Metab* **84**, 3463-3468 (1999)

McConkey, D.J., Greene, G., and Pettaway, C.A. Apoptosis resistance increases with metastatic potential in cells of the human LNCaP prostate carcinoma line. *Cancer Res.* **56**, 5594-5599 (1996)

Negoescu, A., Guillermet, C., Lorimier, P. et al. Importance of DNA fragmentation in apoptosis with regard to TUNEL specificity. *Biomed. Pharmacother.* **52**, 252-258 (1998)

Newell, D.R., Shepherd, C.R., and Harrap, K.R. The pharmacokinetics of prednimustine and chlorambucil in the rat. *Cancer Chemother. Pharmacol.* **6**, 85-91 (1981)

O'Connor, P.M. and Kohn, K.W. Comparative pharmacokinetics of DNA lesion formation and removal following treatment of L1210 cells with nitrogen mustards. *Cancer Commun.* **2**, 387-394 (1990)

O'Malley, B.W. Mechanisms of action of steroid hormones. *N. Engl. J. Med.* **284**, 370-377 (1971)

Owen, W.R. and Stewart, P.J. Kinetics and mechanism of chlorambucil hydrolysis. *J. Pharm. Sci.* **68**, 992-996 (1979)

Raffo, A.J., Perlman, H., Chen, M.W. et al. Overexpression of bcl-2 protects prostate cancer cells from apoptosis in vitro and confers resistance to androgen depletion in vivo. *Cancer Res.* **55**, 4438-4445 (1995)

Rink, S.M., Yarema, K.J., Solomon, M.S. et al. Synthesis and biological activity of DNA damaging agents that form decoy binding sites for the estrogen receptor. *Proc. Natl. Acad. Sci. U. S. A* **93**, 15063-15068 (1996)

Ross, W.E., Ewig, R.A., and Kohn, K.W. Differences between melphalan and nitrogen mustard in the formation and removal of DNA cross-links. *Cancer Res.* **38**, 1502-1506 (1978)

Strickland, I., Kisich, K., Hauk, P.J. et al. High constitutive glucocorticoid receptor beta in human neutrophils enables them to reduce their spontaneous rate of cell death in response to corticosteroids. *J. Exp. Med.* **193**, 585-593 (2001)

Sunters, A., Springer, C.J., Bagshawe, K.D. et al. The cytotoxicity, DNA crosslinking ability and DNA sequence selectivity of the aniline mustards melphalan, chlorambucil and 4-[bis(2-chloroethyl)amino] benzoic acid. *Biochem. Pharmacol.* **44**, 59-64 (1992)

Tilby, M.J., Newell, D.R., Viner, C. et al. Application of a sensitive immunoassay to the study of DNA adducts formed in peripheral blood mononuclear cells of patients undergoing high-dose melphalan therapy. *Eur. J. Cancer* **29A**, 681-686 (1993)

Touitou, I., Mathieu, M., and Rochefort, H. Stable transfection of the estrogen receptor cDNA into Hela cells induces estrogen responsiveness of endogenous cathepsin D gene but not of cell growth. *Biochem. Biophys. Res. Commun.* **169**, 109-115 (1990)

van Zeeland, A.A. Molecular dosimetry of chemical mutagens. Relationship between DNA adduct formation and genetic changes analyzed at the molecular level. *Mutat. Res.* **353**, 123-150 (1996)

Vlietstra, R.J., van Alewijk, D.C., Hermans, K.G. et al. Frequent inactivation of PTEN in prostate cancer cell lines and xenografts. *Cancer Res.* **58**, 2720-2723 (1998)

Walsh, P.C. Docetaxel plus prednisone or mitoxantrone plus prednisone for advanced prostate cancer. *J. Urol.* **173**, 456-2005)

Watts, C.K., Parker, M.G., and King, R.J. Stable transfection of the oestrogen receptor gene into a human osteosarcoma cell line. *J. Steroid Biochem.* **34**, 483-490 (1989)

Weir, H.K., Thun, M.J., Hankey, B.F. et al. Annual report to the nation on the status of cancer, 1975-2000, featuring the uses of surveillance data for cancer prevention and control. *J. Natl. Cancer Inst.* **95**, 1276-1299 (2003)

Wenzel, S.E., Szefler, S.J., Leung, D.Y. et al. Bronchoscopic evaluation of severe asthma. Persistent inflammation associated with high dose glucocorticoids. *Am. J. Respir. Crit Care Med.* **156**, 737-743 (1997)

The Hematology Profile of Mice Treated Chronically with 11β Indicates the Compound is Well Tolerated

Test	IP N = 3	IP Vehicle N = 3	Tumor Ave N = 4	Norm. Ave N = 4	Taconic Nude
WBC (x mm^3)	*1 ± 0.3*	3.9 ± 0.9	6.9 ± 1.6	5.4 ± 0.4	4.3-13.5
RBC (x 10^6 mm^3)	6.9 ± 2.3	7.5 ± 1.3	8.3 ± 2.1	9.3 ± 0.8	6.9-8.52
Hgb (g/dL)	10.8 ± 4	10.7 ± 1.3	9.3 ± 2.4	11.3 ± 0.3	7.5-15.2
HCT (%)	40.6 ± 14	38.7 ± 5.5	45.1 ± 10.3	50.6 ± 3.3	39.4-43.5
Neutrophils (%)	*73 ± 14*	*64 ± 21*	41.5 ± 11.8	42 ± 8.3	7.0-39
Lymphs (%)	*24 ± 15*	*30 ± 20*	58 ± 12.1	57.8 ± 7.8	56-92
Monos (%)	2 ± 0	1.5 ± 0			0-7
Eos (%)					0-4
Platelets (10^3/µL)	651 ± 340	1111 ± 108	934 ± 542	1101 ± 372	790-1014
MCV (fL)	58.4 ± 3.3	51.8 ± 2.1	54.4 ± 3.6	54.3 ± 1.3	51.1-53.4
MCH (pg)	15.4 ± 0.6	14.4 ± 1	11.2 ± 2	12.2 ± 0.9	17.6-19.1
MCHC (g/dL)	26.5 ± 2	27.7 ± 0.9	20.6 ± 2.5	22.4 ± 1.1	34.3-36.1

Table 8.1 Hematology report for mice injected with 11β. Values in bold represent abnormally elevated or suppressed levels. The most notable toxicity is leukopenia. Additionally the ratio of neutrophils to lymphocytes is altered in both the treated and vehicle group.

(Note: Since the test groups contained relatively few mice, the abnormal levels are deviations from the normal range and do not necessarily reflect statistical significance.)

The Blood Chemistry Profile of Mice Treated Chronically with 11β Indicates the Compound is Well Tolerated

Test	IP N = 3	IP Vehicle N = 3	Tumor Ave N = 4	Norm. Ave N = 4	Taconic Nude
Alk. Phosphatase (IU/L)	44 ± 11	60 ± 5	58 ± 18	65 ± 8	96-117
ALT (SGPT) (IU/L)	28 ± 13	48 ± 10	36 ± 10	26 ± 7	
AST (SGOT) (IU/L)	138 ± 56	119 ± 33	112 ± 46	64 ± 22	61-119
CK (IU/L)	*426 ± 353*	*367 ± 126*	*722 ± 411*	184 ± 146	
GGT (IU/L)	*0 ± 0*	1 ± 1	1.8 ± 0.5	2 ± 0	
Albumin (g/dL)	2.8 ± 0.2	2.5 ± 0.9	2.8 ± 0.7	2.9 ± 0.1	3.4-4.1
Total Protein (g/dL)	5.1 ± 0.3	4.7 ± 0.9	5 ± 0.6	5.4 ± 0.3	4.8-5.6
Globulin (g/dL)	2.3 ± 0.1	2.2 ± 0.2	2.3 ± 0.1	2.6 ± 0.2	1.1-1.6
Total Bilirubin (mg/dL)	0.1 ± 0.1	0.2 ± 0.1	0.2 ± 0	0.1 ± 0.1	0.3-0.8
Direct Bilirubin (mg/dL)	0.1 ± 0	0.1 ± 0.1	0.1 ± 0.1	0 ± 0.1	
BUN (mg/dL)	25.3 ± 1.5	30.3 ± 11.9	20 ± 34.7	18.8 ± 2.2	30-37
Creatinine (mg/dL)	0.2 ± 0.1	0.1 ± 0.1	0.3 ± 0.1	0.3 ± 0.1	0.5-0.7
Cholesterol (mg/dL)	104 ± 21	171 ± 131	215 ± 187	133 ± 11	116-155
Glucose (mg/dL)	240 ± 38	239 ± 40	238 ± 31	253 ± 13	173-288
Calcium (mg/dL)	9.7 ± 0.3	9.1 ± 0.7	10.5 ± 0.4	10.5 ± 0.5	10.0-12.0
Phosphorous (mg/dL)	10.5 ± 0.8	9 ± 1.2	6.4 ± 0.9	9.5 ± 1.8	12.3-16.1
Bicarbonate (mEq/L)	27.7 ± 2.1	27.3 ± 2.5	28 ± 2.4	28.3 ± 2.2	
Chloride (mEq/L)	111 ± 1	111 ± 1	108 ± 2	108 ± 1	118-124
Potassium (mEq/L)	6.6 ± 0.1	6.1 ± 0.6	6.7 ± 1	7 ± 0.7	13.8-16.7
Sodium (mEq/L)	158 ± 2	156 ± 1	152 ± 3	153 ± 2	157-163
A/G Ratio	1.2 ± 0.1	1.2 ± 0.4	1.3 ± 0.3	1.1 ± 0.1	
B/C Ratio	0 ± 0	0 ± 0	0 ± 0	0 ± 0	
Indirect Bilirubin (mg/dL)	24 ± 1	25.7 ± 2.3	23.8 ± 4.3	22.3 ± 2.1	
Na/K Ratio	26.7 ± 1.2	24.7 ± 2.3	21.3 ± 0.5	24 ± 4.2	

Table 8.2 Blood Chemistry report for mice injected with 11β. Values in bold represent abnormally elevated or suppressed levels. The toxicity of 11β is rather mild.

(Note: Since the test groups contained relatively few mice, the abnormal levels are deviations from the normal range and do not necessarily reflect statistical significance.)

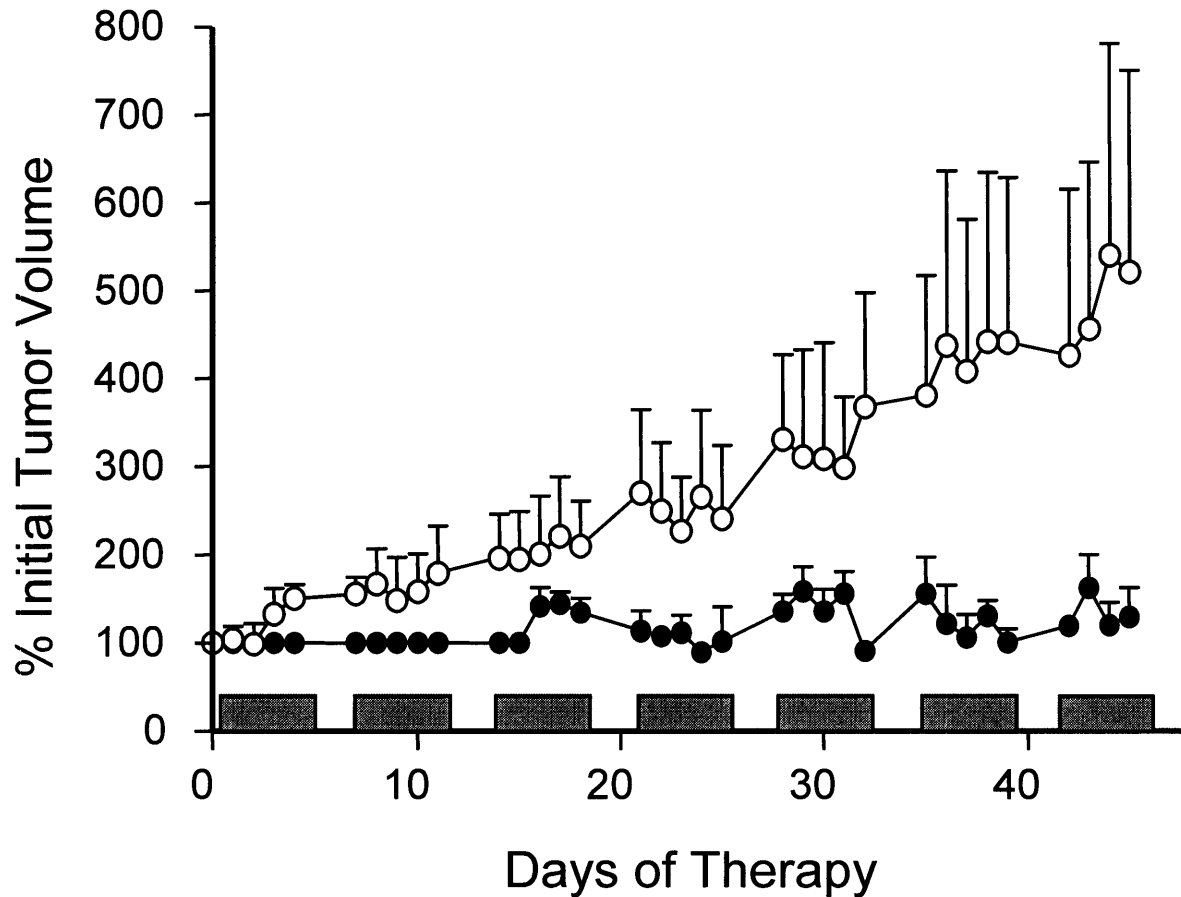# 11β Inhibits the Growth of LNCaP Xenografts.

Fig 8.1 11β therapy of LNCaP xenografts in mice. Groups of 5 mice were injected with 30 mg/kg of 11β (●) or vehicle only (○). Error bars are the standard deviation of the mean and a paired t-test provided a P< 0.0001. The gray bars indicate days of treatment.

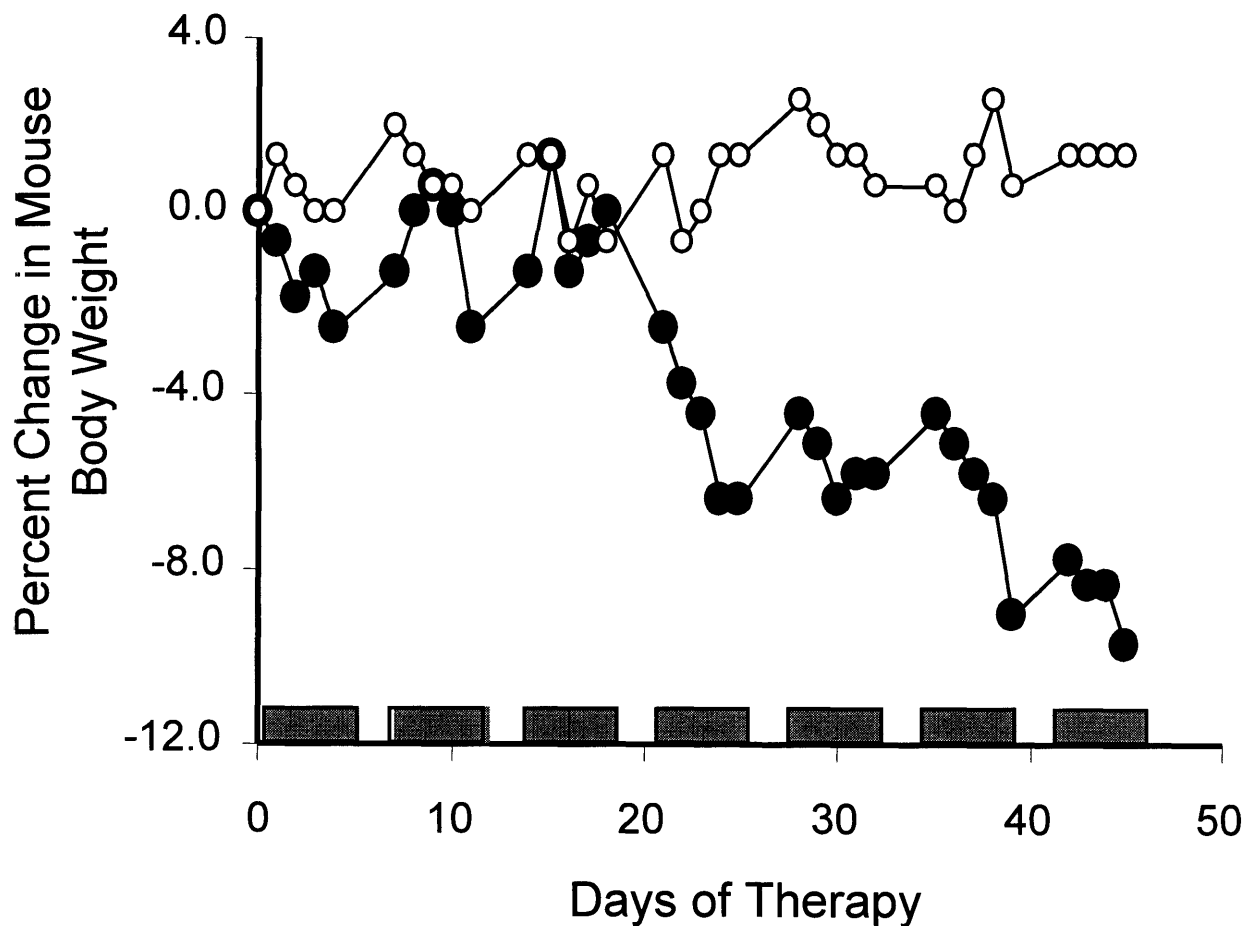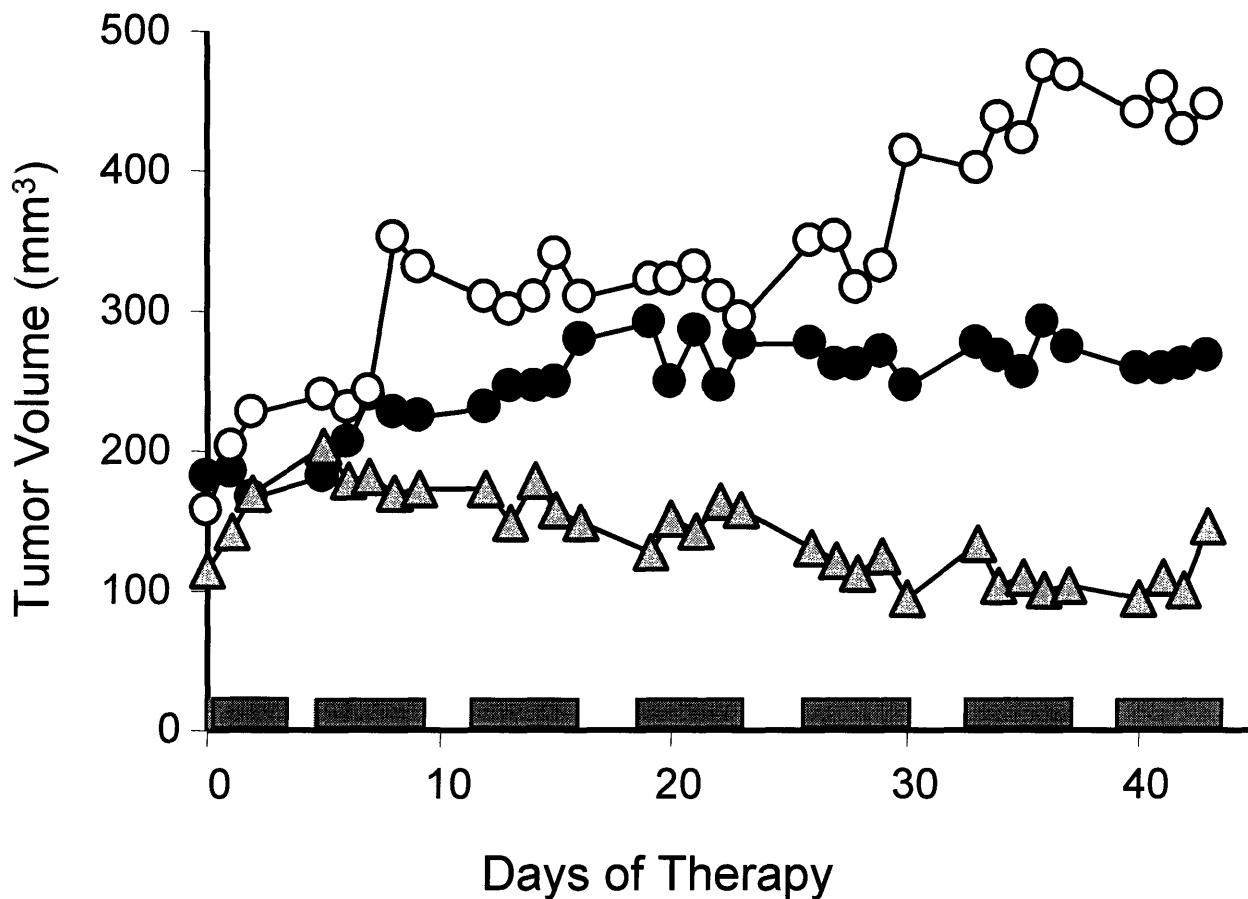# 11β is Well Tolerated by Mice after 6.5 Treatment Cycles as Assessed by Weight Loss

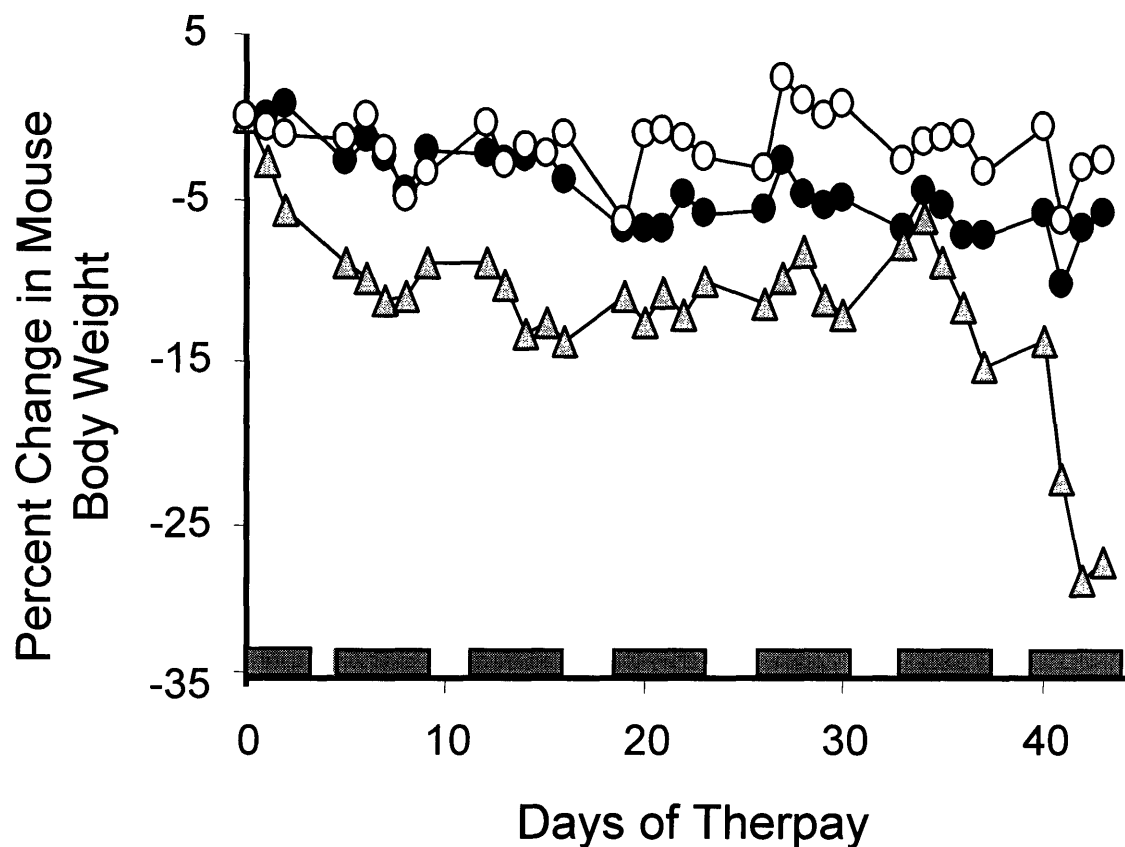**Fig 8.2** 11β therapy of LNCaP xenografts in mice. Groups of 5 mice were injected with 30 mg/kg of 11β (●) or vehicle only (○). After 3 cycles of therapy the average mouse in the 11β treated group lost 10% of its body weight.

A Mouse Treated with 11β does not have a Visible LNCaP Xenograft Tumor

A

B
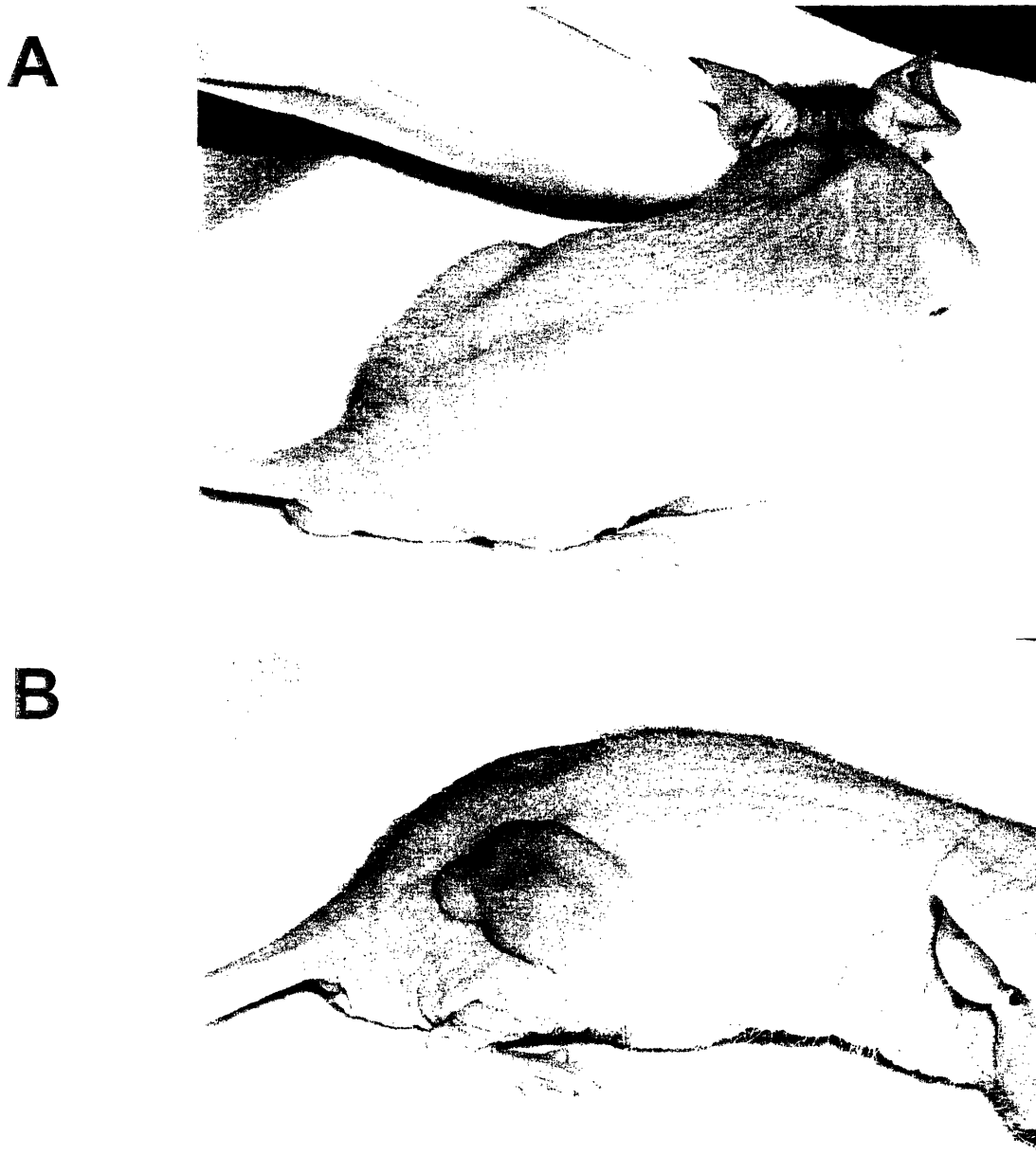
Fig 8.3 Pictures of LNCaP xenograft bearing NIH Swiss Nude mice. **A.** Mouse treated with 7 cycles of 30 mg/kg 11β. **B.** Mouse treated with vehicle alone.

Chlorambucil is Seemingly More Efficacious than 11β Against LNCaP Xenograft Tumors
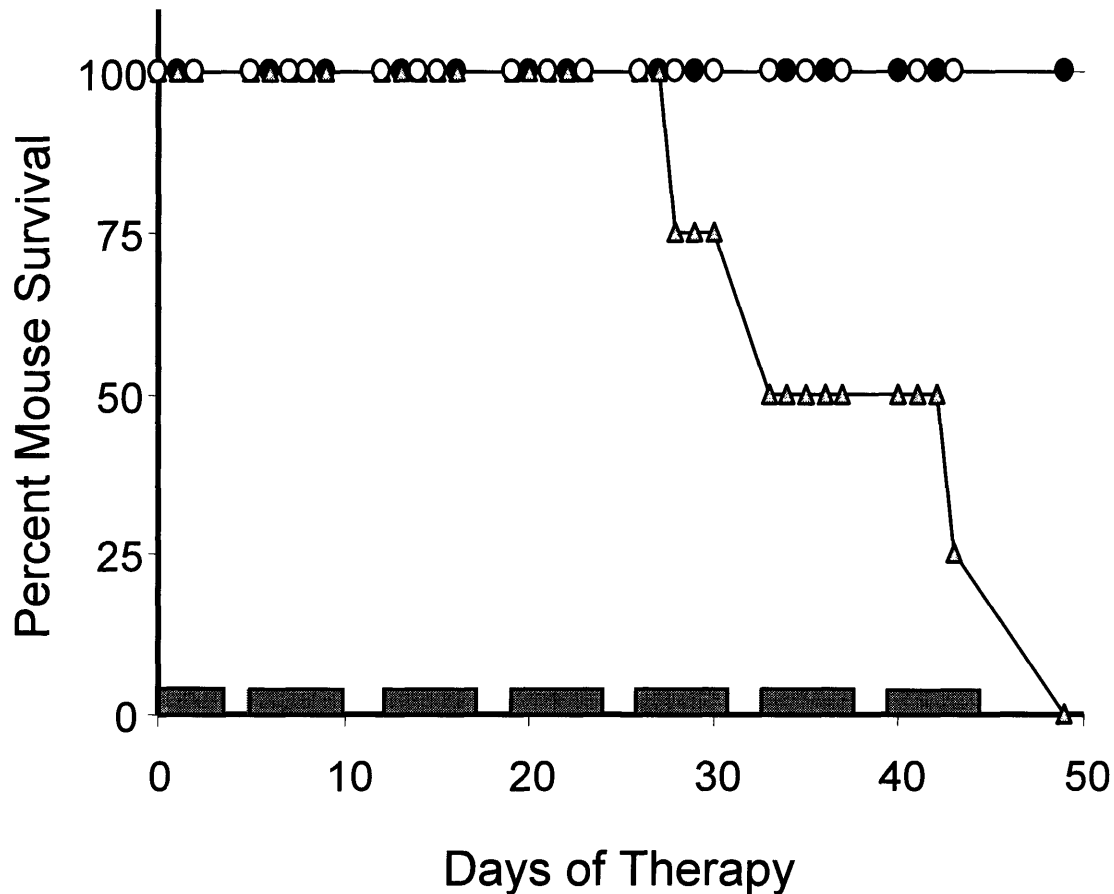
Fig 8.4 Therapy of LNCaP xenografts in mice. Groups of 5 mice were injected with 30 mg/kg of 11β (●), 12 mg/kg of chlorambucil (▲), or vehicle only (○). Error bars are not shown for clarity sake but a paired t-test provided a P< 0.0001 for both 11β and chlorambucil when compared to the vehicle group. The gray bars indicate days of treatment.

Chlorambucil is More Toxic Than 11β as Assessed by Weight Loss in Mice

Fig 8.5 Therapy of LNCaP xenografts in mice. Groups of 5 mice were injected with 30 mg/kg of 11β (●), 12 mg/kg of chlorambucil (△), or vehicle only (○). After 7 cycles of treatment mice dosed with 11β lost only 6% of their body weight. However mice treated with chlorambucil (at an equi-mole dose) lost up to 30% of their body weight.

The Toxicity of Chlorambucil is too Great to Overcome as All Mice Eventually Die

Fig 8.6 Therapy of LNCaP xenografts in mice. Groups of 5 mice were injected with 30 mg/kg of 11β (●), 12 mg/kg of chlorambucil (▲), or vehicle only (○). All of the mice treated with chlorambucil were dead 6 days after the termination of the 7 cycle tumor therapy study. However, all of the mice treated with 11β survived the therapy.
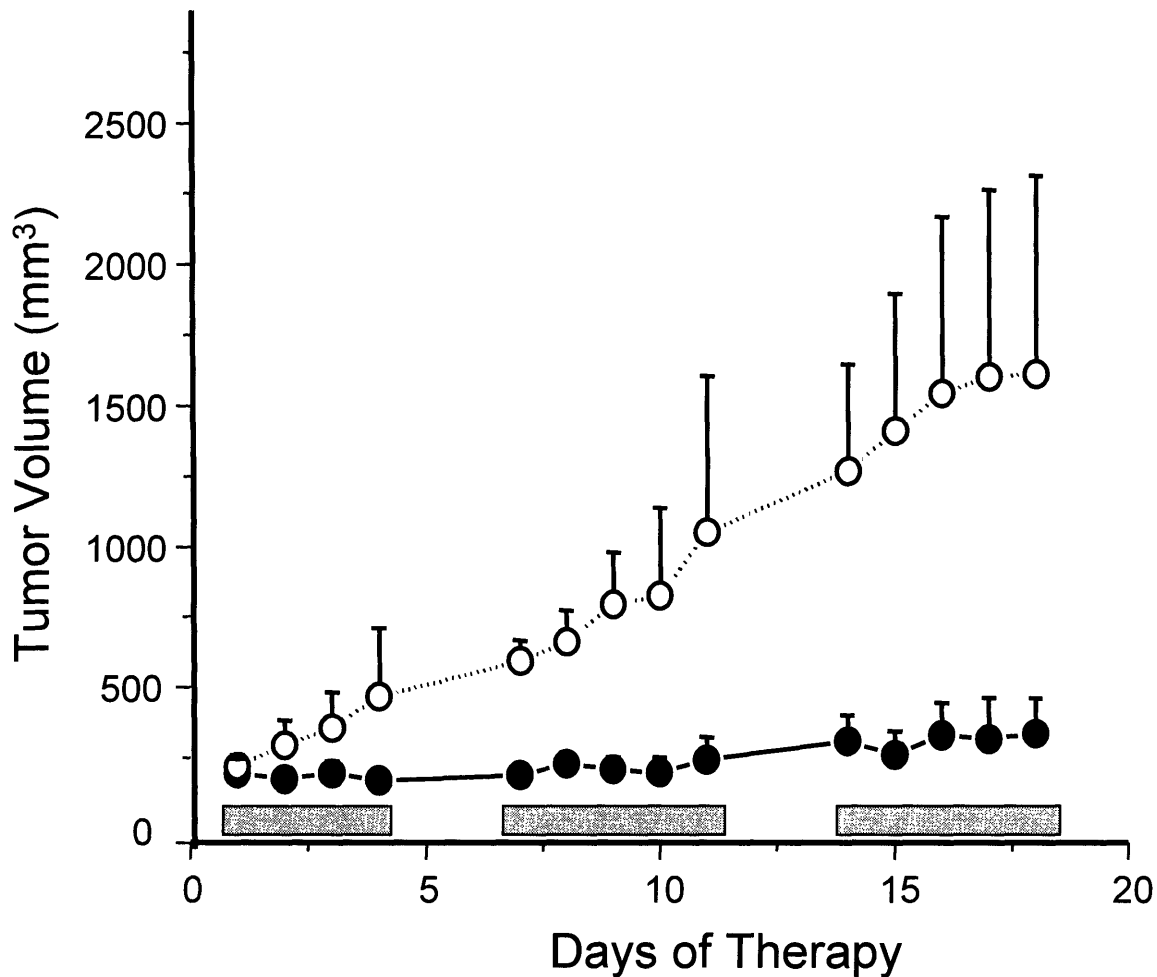
11β is also Efficacious Against HeLa Xenograft Tumors

Fig 8.7 11β therapy of HeLa xenografts in mice. Groups of 5 mice were injected with 30 mg/kg of 11β (●) or vehicle only (○). Error bars are the standard deviation of the mean and a paired t-test provided a P< 0.0001. The gray bars indicate days of treatment.

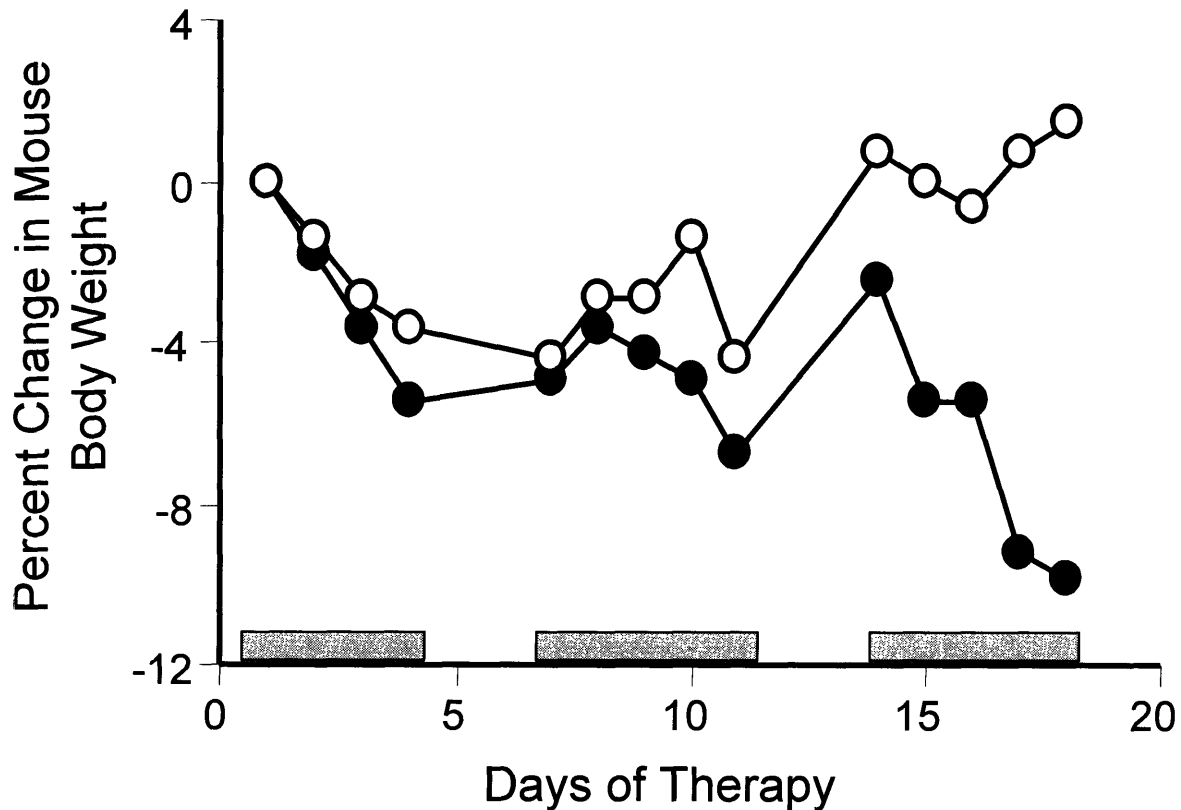# 11β is Well Tolerated by Mice after 3 Treatment Cycles as Assessed by Weight Loss

Fig 8.8 11β therapy of HeLa xenografts in mice. Groups of 5 mice were injected with 30 mg/kg of 11β (●) or vehicle only (○). After 3 cycles of therapy the average mouse in the 11β treated group lost 10% of its body weight.

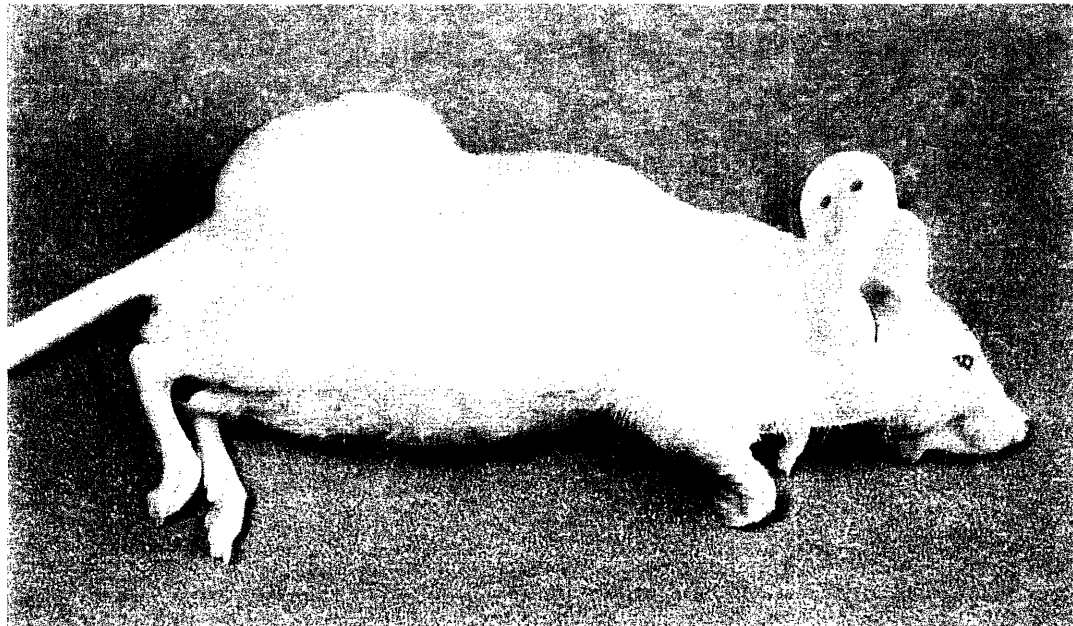# Mice Treated with 11β Have Smaller HeLa Xenografts than Mice Treated with Vehicle
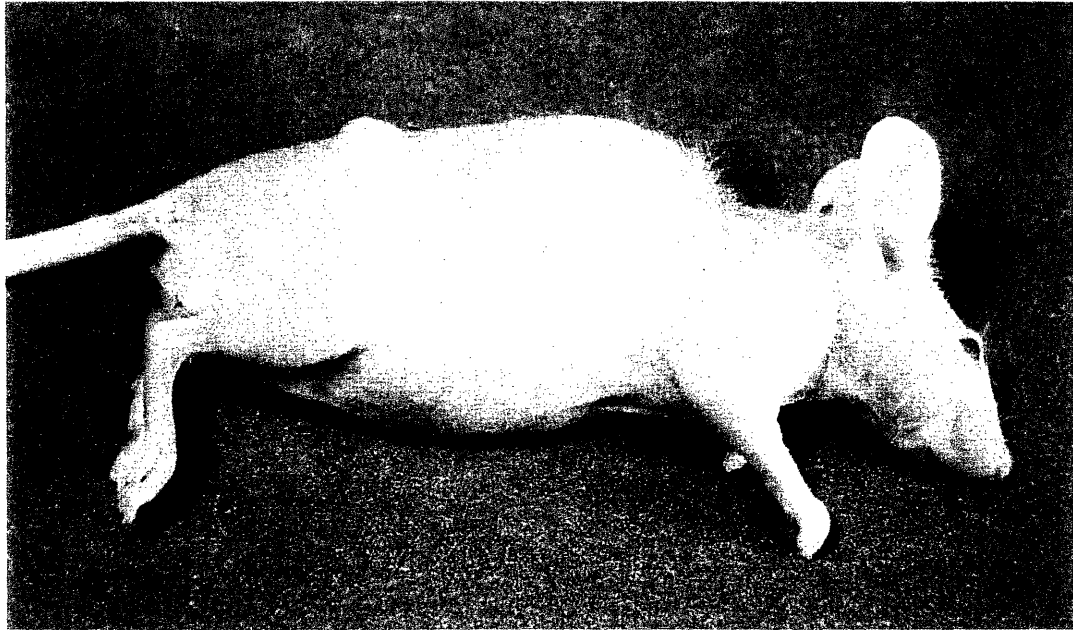
Fig 8.9 Pictures of HeLa xenograft bearing NIH Swiss Nude mice. **A.** Mouse treated with 3 cycles of 30 mg/kg 11β. **B.** Mouse treated with vehicle alone.

11β is Efficacious Against DLD-1 Cells Implanted Intraperitoneally
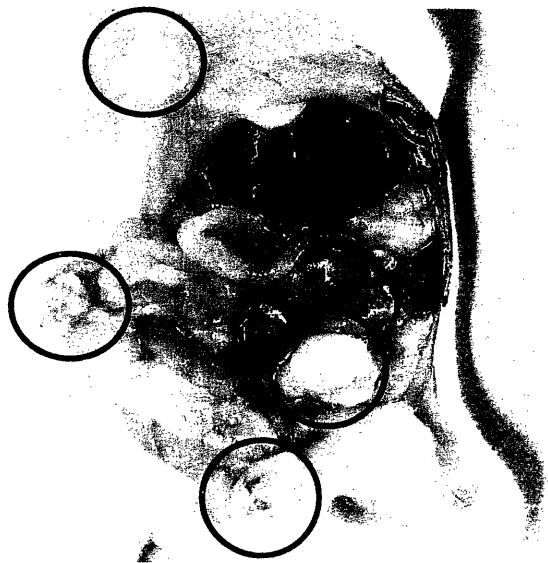
A

B

Fig 8.10 11β therapy of DLD-1 tumors. **A.** A mouse treated with 11β. **B.** A mouse treated with vehicle only. Tumors are white and nodular and are high-lighted by encircling.

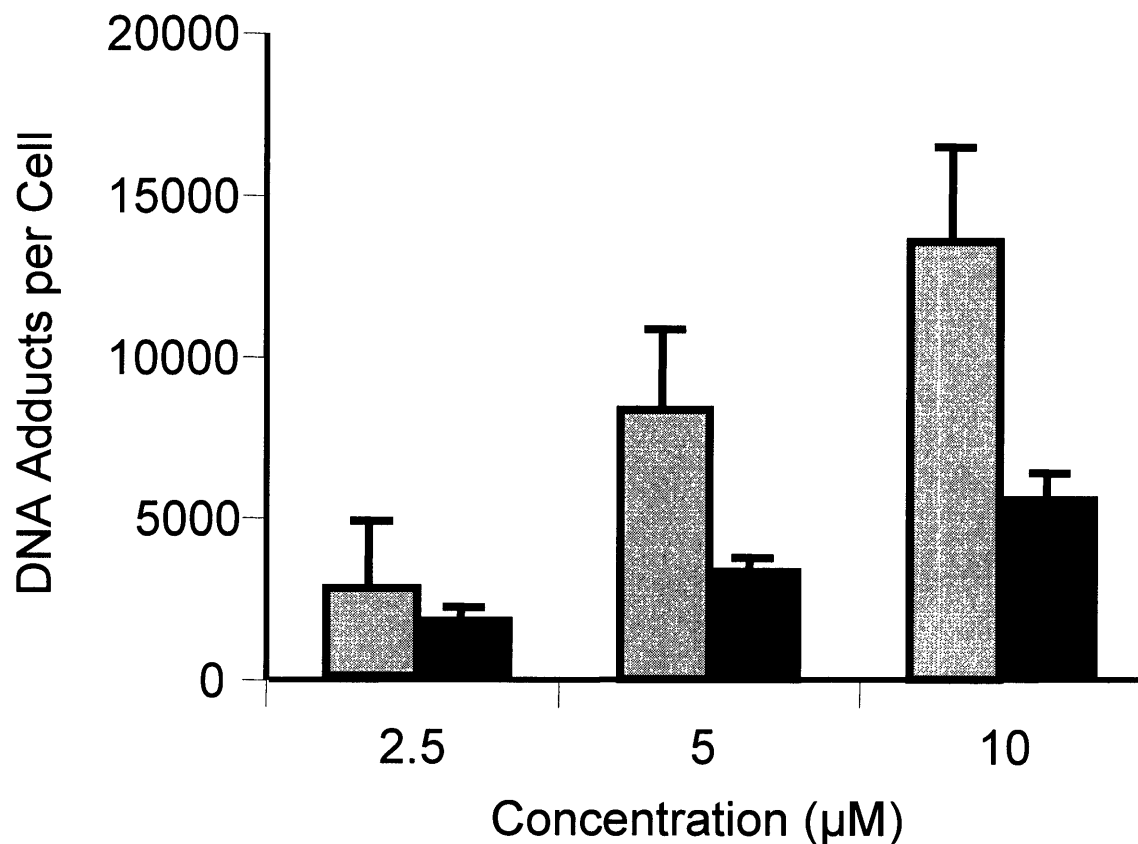# 11β Adducts DNA in T-47D and LNCaP Cells in a Dose-Dependent Manner

Fig 8.11 Quantification of DNA adduct formation. T-47D (▨) and LNCaP (■) cells were exposed to 3 concentrations of 11β for 4 hours. The number of adducts formed is linearly dependent on concentration for both cell lines. Error bars are standard deviation of the mean.
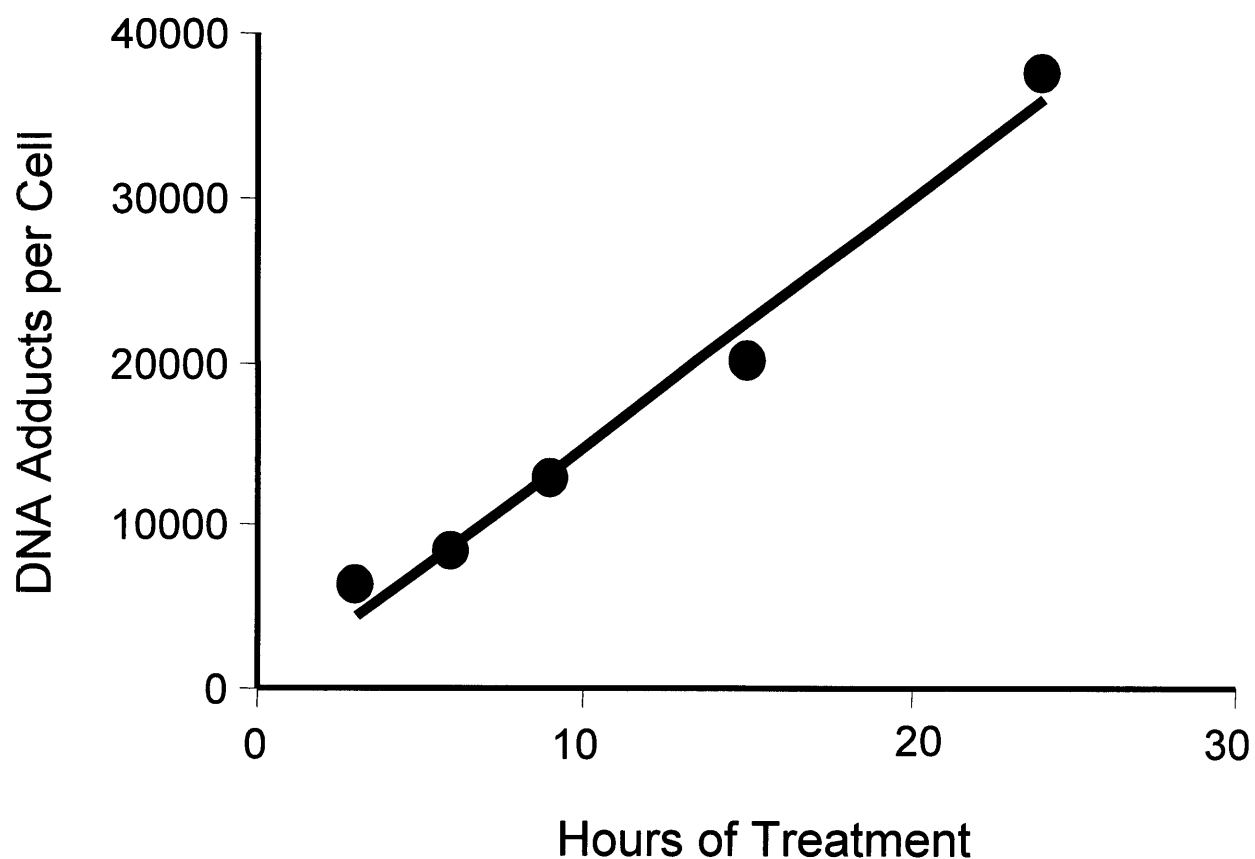
Fig 8.12 Rate of DNA adduct formation in LNCaP cells. LNCaP cells were exposed to 10 μM 11β for 3, 6, 9, 15, and 24 hours. The rate of adduction was 1500 adducts/hour and the R^2 = 0.98.
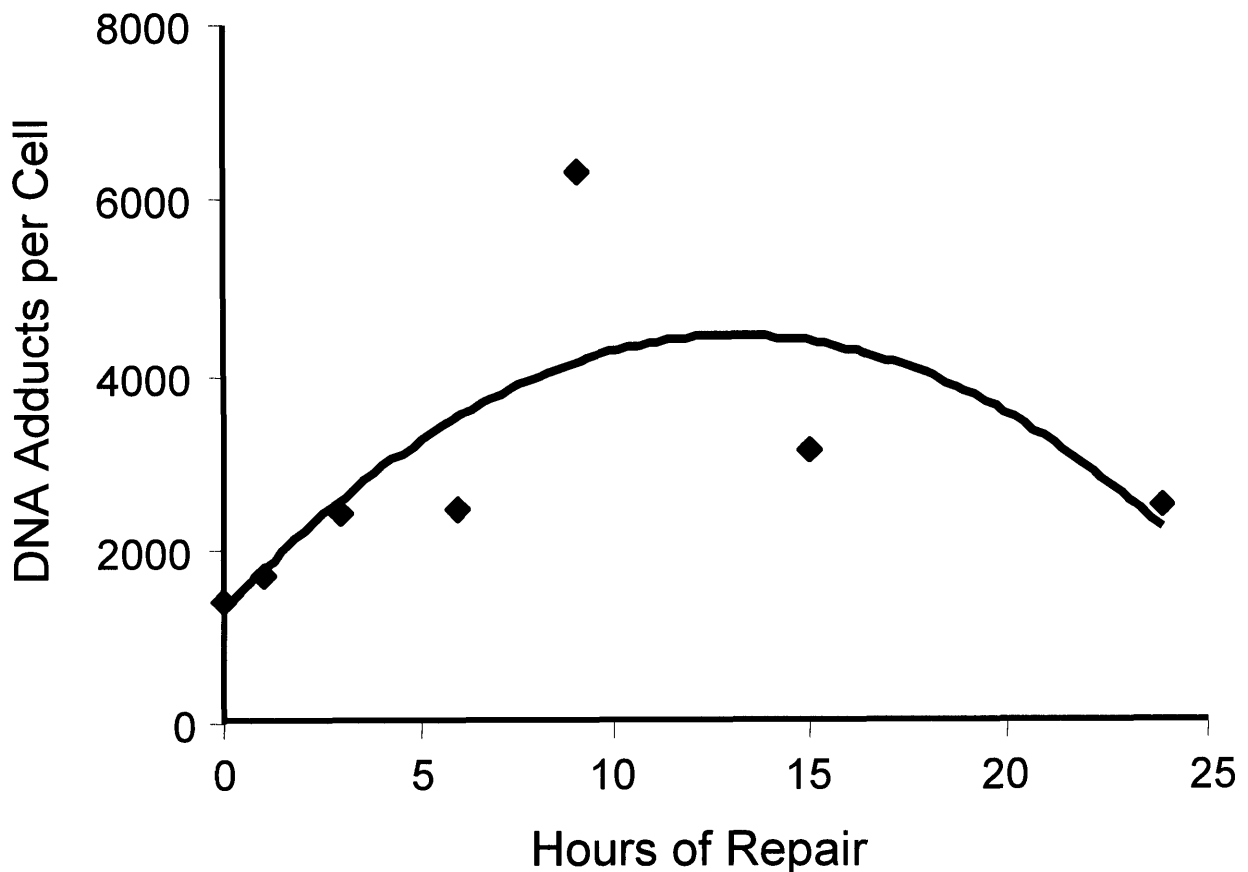
Kinetics of Repair of 11β DNA Adducts

Fig 8.13 Monitoring DNA repair in LNCaP cells. LNCaP cells were treated with a sub-lethal dose of 2.5 µM of 11β for 0, 1, 3, 6, 9, 15, and 24 hours after the removal of the drug. Interestingly, 11β continued to form DNA adducts even after it was removed from the media. DNA repair seems to overwhelm adduct formation at 9 hours, although a significant portion of the adducts remain 24 hours after the removal of the drug.

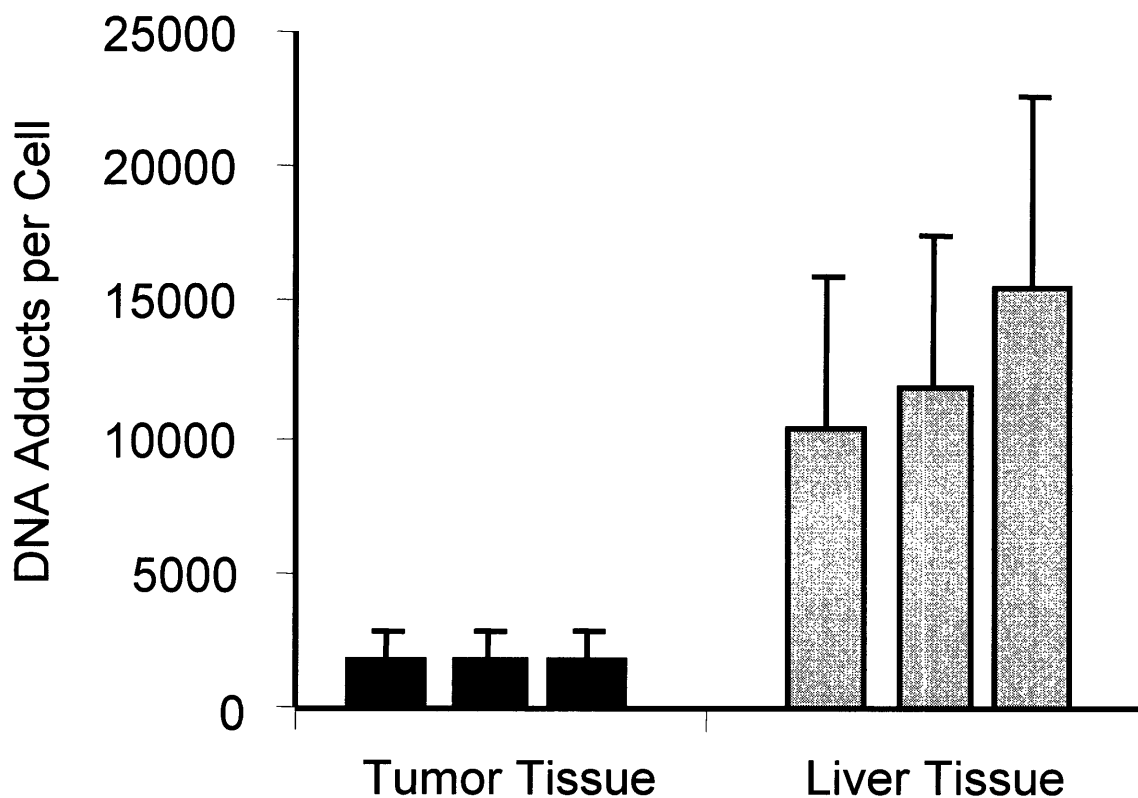# Concentration of 11β DNA Adducts
in Mouse Tissue

Fig 8.14 Quantitation of DNA adducts in tumor (■) and liver (▨) tissues. Three Mice were each injected with a 50 mg/kg dose of 11β and sacrificed 4 hours later. Liver tissue forms 5-10 times more adducts than tumor tissue. Error bars are standard deviation of the mean from replicate injections on the AMS.

Biography

The author was born on December 16, 1975 to William and Joyce Hillier in New Bedford, Massachusetts. He was raised in the neighboring town of Acushnet with his brother, Adam. After graduating from New Bedford High School, he attended the College of the Holy Cross in Worcester, Massachusetts where he studied Chemistry. The author conducted independent research under the advisement of Professor Paul McMaster on the "Synthesis of novel derivatives of the antiarrythmic agent, apridine-1". After graduating in 1997, he worked at Massachusetts General Hospital in the Department of Radiology Division of Nuclear Medicine in the laboratory of Dr. Alan Fischman and under the direct supervision of Dr. John Babich. His work focused on the development of novel diagnostic imaging agents focused on the early detection of Parkinson's disease, the detection of bacterial infections, and on monitoring cardiac viability. One of the compounds that he evaluated is currently in clinical trials. In 1997, he pursued a Ph.D. in Chemistry at Massachusetts Institute of Technology. He joined the laboratory of Professor John M. Essigmann and wrote his dissertation on "Novel genotoxins that target estrogen receptor- and androgen receptor- positive cancers: identification of DNA adducts, pharmacokinetics, and mechanism". During his Ph.D. career he married Kristen Boudrot, whom he met while working at Massachusetts General Hospital, and they expanded their family with the birth of their son, Ryan Antonio, on October 1, 2005.

Shawn M. Hillier

55Ash St. /Danvers, MA 01923
(617) 253-6207
Email: hillier@mit.edu

EDUCATION

Massachusetts Institute of Technology, Cambridge, MA   1999-2005
    Ph.D. in Chemistry, June 2005   Cumulative GPA 4.7 / 5.0

College of the Holy Cross, Worcester, MA   1993-1997
    Bachelor of Arts in Chemistry May 1997   Cumulative GPA 3.4 / 4.0

EXPERIENCE

Massachusetts Institute of Technology, Cambridge, MA   1999-2005
Graduate Student, Department of Chemistry
Thesis under John M. Essigmann: "The Rational Design of Genotoxins that Selectively Target Hormone Receptor-Positive Breast and Prostate Cancers: DNA Adduction, Repair, and Mechanism."
- Quantify the number of DNA adducts formed *in vitro* and *in vivo* by accelerator mass spectrometry.
- Monitor repair of DNA adducts using an *in vitro* whole cell extract system.
- Develop xenograft animal models for tumor ablation therapy.
- Evaluate pharmacokinetic profile after administration of compounds I.P. and I.V.
- Determine the major metabolites of our compounds using human liver microsomes.
- Analyze the toxicity profile by determining the LD_{50} and monitoring serum chemistries.
- Identify DNA adducts in cell and tissue samples by mass spectrometry.

Massachusetts General Hospital, Boston, MA   1997-present
Consultant, Department of Radiology, Division of Nuclear Medicine   1999-present
Employed part time (3-6 hrs/wk) to diagnose and solve instrumentation problems, interview and train new laboratory technicians, address interpersonal issues, and assist in daily tasks of research technicians.
Laboratory Supervisor,   1998-1999
Coordinated all research studies (5-10/wk); hired, trained and oversaw 1-2 laboratory technicians; assisted in submission of grants and manuscripts; developed new protocols; assisted in daily tasks of research technicians.
Laboratory Technician,   1997-1998
- Biological studies including: drug metabolism analysis in human and monkey blood samples, bio-distributions and pharmacokinetic analysis, toxicity profiles in rats and rabbits.
- Radiochemistry and radiolabeling with frequent handling of ^{99m}Tc, ^{125}I, ^{111}In, ^{67}Ga, ^{11}C, ^{18}F.
- Administered: anesthesia, I.V. injections, and I.M. infections.
- Sterile cell culture techniques including the maintenance of cancerous human cell lines (SK-OV, SK-BR).

Massachusetts Institute of Technology, Cambridge, MA   1999-2000
Teaching Assistant, Department of Chemistry, Conducted recitation sections of freshman-level general chemistry course, graded exams, held office hours.

College of the Holy Cross, Worcester, MA   1996 - 1997
Independent Research, Department of Chemistry, Synthesis of new derivatives of the antiarrythmic agent aprindine-1.

UMASS Medical Center, Worcester, MA   Jan. - May 1997
Academic Internship, Department of Organ Transplantation, Assisted in liver transplant research project using porcine xenografts; shadowed the renal transplant team during clinic and on rounds; monitored vital signs (blood pressure, temperature, etc.)

ChemDesign Corporation, Fitchburg, MA, summer 1996
Quality Control Laboratory Technician, Accurately analyzed batch chemical samples and troubleshot instrumentation errors.

College of the Holy Cross, Worcester, MA, 1995-1997
Organic Chemistry Laboratory Teaching Assistant, Aided in supervising chemistry laboratories, graded lab reports.

INSTRUMENTATION
chromatography (gas, liquid, thin layer), atomic absorption, spectroscopy (UV-VIS, IR, mass, flourometric, nuclear magnetic), gamma camera, gamma counter, pH meters, electrophoresis.

AWARDS AND PROFESSIONAL MEMBERSHIPS
Aspen Cancer Conference Fellow, Aspen Cancer Conference, Aspen, Colorado, July 20-23, 2003
Edward A Smuckler Award, best abstract, 2003 Pathobiology of Cancer, AACR Workshop in Cancer Research, Keystone, CO, July 13-20, 2003 Bifunctional Genotoxins that Target Hormone Receptor Positive Breast and Prostate Cancers: Selectivity, DNA Adduction, and Mechanism.
Best poster award, Toxicology Division, 222nd ACS National Meeting, Chicago, IL, August 26-30, 2001 Synthesis, biochemical properties, and pharmacokinetic profiles of DNA-damaging genotoxins with selective toxicity towards estrogen receptor-positive breast cancer cells and androgen receptor-positive prostate cancer cells.
Member, American Association of Cancer Researchers, 2002-2003
Member, American Chemical Society, 2001-2003
Member, International Society for the Study of Xenobiotics, 2003

PUBLICATIONS
Papisov M, Yurkovetskiy A, Hiller A, Yin M, Barzana M, **Hillier S,** and Fischman AJ. Semi-synthetic hydrophilic polyals. Under review, J. Biomed. Mater. Res. 2005

Sharma U, Marquis JC, Nicole Dinaut A, **Hillier SM,** Fedeles B, Rye PT, Essigmann JM, Croy RG. Design, synthesis, and evaluation of estradiol-linked genotoxicants as anti-cancer agents. Bioorg. Med. Chem. Lett. 2004 Jul 16;14(14):3829-3833.

Mitra K, Marquis JC, **Hillier SM,** Rye PT, Zayas B, Lee AS, Essigmann JM, Croy RG.
A rationally designed genotoxin that selectively destroys estrogen receptor-positive breast cancer cells.
J Am. Chem. Soc. 2002 Mar 6;124(9):1862-3.

Rose D, Zubieta J, Graham W, **Hillier S,** Babich J. The synthesis and structural characterization of the neutral ^{111}In (III) thiolate species In(SCH$_2$CH$_2$)$_3$N. Inorganic Chemistry Communications May 1998; 1:164-173

SELECTED PRESENTATIONS
Hillier SM, Marquis JC, Mitra KK, Rye PT, Dinaut AN, Sharma U, Rodrigues DC, Liberman RG, Skipper PL, Wishnok JS, Tannenbaum SR, Essigmann JM, Croy RG. The Rational Design of Genotoxins that Selectively Destroy Hormone Receptor-Positive Breast and Prostate Cancers. Aspen Cancer Conference, Aspen, Colorado, July 20-23, 2003

Hillier S, Zayas B, Park H-J, Wishnok J, Wogan G, Essigmann J, Croy RG. Novel genotoxins that target ER+ breast cancers: identification of DNA adducts, mechanism, and pharmacokinetics. Abstract of Papers, 92nd American Association of Cancer Researchers, New Orleans, Louisiana, March 24-28, 2001

Carter EA, Tompkins RG, Graham W, Barzana M, **Hillier S,** Babich JW, Fischman AJ. Accumulation of a Tc-99m Chemotactic Peptide and FDG by Sterile Inflammation in Rats. The Society of Nuclear Medicine 45th Annual Meeting in Toronto, June 7-June 11, 1998